

COP9 signalosome subunit knockdown in K562
provides novel insight into the function and potential regulation of
the CSN

by

Claire Pearce

A thesis submitted to
The University of Birmingham
for the degree of
DOCTOR OF PHILOSOPHY

School of Biosciences
The University of Birmingham
September 2009

UNIVERSITY OF
BIRMINGHAM

University of Birmingham Research Archive

e-theses repository

This unpublished thesis/dissertation is copyright of the author and/or third parties. The intellectual property rights of the author or third parties in respect of this work are as defined by The Copyright Designs and Patents Act 1988 or as modified by any successor legislation.

Any use made of information contained in this thesis/dissertation must be in accordance with that legislation and must be properly acknowledged. Further distribution or reproduction in any format is prohibited without the permission of the copyright holder.

Dedicated to my parents, Steve and Kim, for their
boundless support and belief in me.

Acknowledgements

I can say with certainty that during my PhD I have been fortunate enough to have had relatively few lows and will always look back on my PhD with only good memories. This would not have been the case without excellent colleagues, family and friends, to all of whom I am thankful.

In particular I would like to thank Chris Bunce who afforded me both my initial opportunity to experience scientific research and a PhD position in his lab. From the outset Chris, a group leader, colleague and friend, has provided fantastic support and guidance whilst also allowing me to be independent, for all of which I will always be grateful. I would like to extend my thanks to Farhat Khanim, for everything she has done for me, and whose infectious enthusiasm and passion for scientific research significantly influenced my decision to do a PhD.

I would also like to thank Rachel Hayden. Her help and support as a scientist has contributed to my thesis and as a friend she has made the few tough times bearable and the copious good times even better. Thanks also to Nick Davies for invaluable advice and support, and other members of the Bunce group including Jane Birtwistle and Karen Exley who have also become good friends.

My family and friends, including Sarah Thomas and Sarah Stevenson, have been an unfailing support during my PhD whilst also providing much appreciated light relief. I would also like to take the opportunity to thank my oldest friend Deborah Makin who, without exception, has always been there, thank you Deb.

Also, I would like to acknowledge the unfaltering support and understanding I have received from my fiancé Stephen Hughes.

Finally, I would like to thank Robin May for all his help and guidance, and both the BBSRC and LRF who's funding made the project possible.

Abstract

The co-ordinated degradation of proteins is vital to all aspects of cellular activity. The main mechanism of intracellular protein degradation is the ubiquitin proteasome system (UPS) which labels target proteins with ubiquitin, thereby marking them for degradation by the 26S proteasome. Protein ubiquitination is mediated by three enzymes; E1, E2, E3. The largest family of E3's is the cullin-RING E3 ubiquitin ligases (CRLs). CRLs require the cyclic addition and removal of a ubiquitin-like protein called NEDD8 to and from the cullin subunit. Removal of NEDD8 (deneddylation) is mediated by the eight subunit COP9 signalosome (CSN; CSN1-8). Cullin deneddylation by the CSN has been demonstrated to prevent the autocatalytic degradation of the substrate recognition subunit (SRS) of CRLs. The CSN has also been shown to associate with deubiquitinase and kinase activity and has thus been identified as a highly conserved key regulator of protein degradation. CSN subcomplexes have also been identified which function in protein degradation, and a direct role for the CSN complex in transcriptional regulation has been posited. Although the COP9 signalosome (CSN) has been studied in human cells, little is known of its role in haematopoietic cells or of any potential contribution to leukaemogenesis.

In this study the deneddylase catalytic subunit CSN5 and the non-catalytic subunit CSN2 were knocked down in the human haematopoietic cell line and chronic myeloid leukemia model, K562. Both knockdowns had similar consequences for CRL activity whilst having divergent effects on the levels of SRS mRNA. Knockdown of either subunit also

resulted in a common sequential proteasome-dependent loss of SRS proteins, an observation that had not been previously described. Although both knockdowns resulted in reduced cell proliferation followed by significant cell death, the cellular phenotypes and mechanisms of cell death were distinct. CSN5 knockdown was associated with mitotic defects, G2/M arrest, and culminated in apoptosis. In contrast, CSN2 knockdown resulted in autophagy inhibition and non-apoptotic cell death. This is the first time the CSN has been associated with autophagy. CSN2 and CSN5 knockdowns also had divergent effects on the intact CSN complex. CSN2 loss resulted in significant reduction of the intact CSN whilst, for the first time, the intact CSN complex was shown to be retained in CSN5 knockdown cells with loss of only monomeric CSN5. The common effect on CRL activity by either knockdown suggests a common loss of deneddylase activity, which was explained in CSN2 knockdowns with the loss of the intact CSN complex. However, in the case of CSN5 knockdown, in which the intact complex remained, the reason for loss of deneddylase activity is less easy to explain. The results of this study may indicate for the first time that sustained deneddylase activity is dependent on a novel mechanism requiring a pool of CSN5 monomer. Finally, the significance of monomeric CSN5 function loss to the differential phenotype of CSN5 knockdown cells to cells lacking CSN2 was tested by re-expression of both wild type and deneddylase dead CSN5 in a CSN5 knockdown background. Importantly, both approaches rescued the cellular phenotype to the same extent. Overall, the findings of this study provide novel insight into both the function and potential regulation of the CSN complex, whilst further suggesting that the CSN may be a target worthy of investigation in the treatment of chronic myeloid leukaemia.

Contents

1. General Introduction	1
1.1 Intracellular protein degradation	2
1.1.1 Autophagy	2
1.1.2 The ubiquitin-proteasome system	4
1.1.3 Protein ubiquitination	4
1.2 The Cullin-RING E3 ubiquitin ligase (CRL) family	7
1.2.1 The CRLs and their component subunits	7
1.2.2 CRL function	11
1.2.3 CRL regulation via cullin modification	14
1.3 The COP9 signalosome (CSN) complex	18
1.4 Regulation of CRLs by the CSN complex	25
1.4.1 Deneddylation of CRLs by the CSN complex	25
1.4.2 Deubiquitination of CRLs by the CSN complex	29
1.4.3 A third function for the CSN complex in CRL regulation?	31
1.4.4 Consequences of CSN impairment on CRL function	33
1.5 Other functions of the CSN complex	36
1.5.1 The CSN and protein phosphorylation	36
1.5.2 The CSN and deubiquitination	38
1.5.3 The CSN and transcriptional regulation	39
1.5.4 CSN subcomplexes	41
1.5.5 The CSN as an alternative lid for the proteasome?	44
1.6 The regulation of CSN activity	46
1.7 CSN independent functions of CSN subunits	50
1.7.1 CSN2	50
1.7.2 CSN5	52
1.8 The CSN and leukaemia	55
1.9 Chronic myeloid leukaemia	58
1.10 Project aims	60
2. Materials and Methods	62
2.1 Cell culture and treatments	63
2.1.1 Maintenance of cell lines	63
2.1.2 Storage of cell lines in liquid nitrogen	63
2.1.3 Recovery of cell lines from liquid nitrogen	63
2.1.4 Treatment of cells with MG132	64
2.1.5 Treatment of cells with 3-methyladenine	64
2.1.6 Treatment of cells with Bafilomycin A1	65
2.1.7 Treatment of cells with rapamycin	65
2.2 shRNA construct production	66
2.2.1 shRNA sequence design	66
2.2.2 Oligonucleotide annealing	67
2.2.3 Vector preparation	67
2.2.4 Ligation of linear vector and shRNA insert	68
2.2.5 Bacterial transformation with plasmid DNA	69

2.2.6	<i>Amplification of plasmid DNA</i>	70
2.2.7	<i>Isolation of plasmid DNA</i>	70
2.2.8	<i>Quantification of plasmid DNA</i>	71
2.2.9	<i>Plasmid sequencing</i>	71
2.3	<i>CSN5 protein expression construct production</i>	72
2.3.1	<i>CSN5 coding sequence primer design</i>	72
2.3.2	<i>CSN5 coding sequence amplification</i>	72
2.3.3	<i>CSN5 coding sequence PCR product digestion</i>	73
2.3.4	<i>pcDNA3.1 plasmid digestion</i>	73
2.3.5	<i>Ligation of CSN5 coding sequence with pcDNA 3.1</i>	74
2.3.6	<i>CSN5 shRNA/deneddylase mutation primer design</i>	74
2.3.7	<i>CSN5 expression plasmid mutation</i>	75
2.3.8	<i>Mutated CSN5 expression plasmid transformation into XL10-Gold cells</i>	75
2.4	<i>Co-transfection of cell lines</i>	77
2.4.1	<i>Cell preparation</i>	77
2.4.2	<i>Cell transfection</i>	77
2.4.3	<i>Analysis of transfection efficiency</i>	78
2.4.4	<i>Cell sorting</i>	78
2.5	<i>Assessment of cell proliferation and death</i>	81
2.5.1	<i>Cumulative cell growth</i>	81
2.5.2	<i>Cell cycle analysis</i>	81
2.5.3	<i>Thymidine incorporation assay</i>	82
2.5.4	<i>Annexin V</i>	82
2.6	<i>Morphological analysis of cells</i>	84
2.6.1	<i>Cytospins</i>	84
2.6.2	<i>Jenner-Giemsa staining</i>	84
2.6.3	<i>Immunofluorescent staining</i>	85
2.6.4	<i>Monodansylcadaverine staining</i>	86
2.6.5	<i>Visualisation of propidium iodide retention in cells</i>	86
2.7	<i>Protein analysis: Western blotting and Blue Native gels</i>	87
2.7.1	<i>Protein extraction and quantification</i>	87
2.7.2	<i>Calculating the amount of protein per cell</i>	88
2.7.3	<i>Sample preparation and protein separation by SDS PAGE</i>	88
2.7.4	<i>Protein transfer</i>	89
2.7.5	<i>Immunodetection of proteins</i>	90
2.7.6	<i>Western blot densitometry</i>	91
2.7.7	<i>Blue native gels</i>	91
2.7.8	<i>2-Dimensional blue native gels</i>	92
2.7.9	<i>2-Dimensional blue native gel densitometry</i>	94
2.8	<i>mRNA analysis: Quantitative real-time polymerase chain reaction (QRT-PCR)</i>	95
2.8.1	<i>RNA extraction</i>	95
2.8.2	<i>RNA quantification</i>	96
2.8.3	<i>Reverse transcriptase PCR</i>	96
2.8.4	<i>β-actin PCR</i>	97

2.8.5 Neomycin PCR	98
2.8.6 QRT-PCR primer and probe design and verification	99
2.8.7 Optimisation of primers and probe for QRT-PCR	100
2.8.8 Verifying primers and probe can be multiplexed with 18S internal control	101
2.8.9 TAQMAN based QRT-PCR	103
2.8.10 SYBR-Green based QRT-PCR	105
2.8.11 QRT-PCR data analysis	106
2.9 Statistical Analysis of data	107
3. Analysis of the molecular and cellular effects of CSN2 knockdown	108
3.1 Introduction	109
3.2 Results	110
3.2.1 Construction of plasmid encoding CSN subunit specific shRNA	110
3.2.2 Determination of transfection efficiency and verification of co-transfection	113
3.2.3 Assessment of cDNA quality and optimisation of primers and probe for QRT-PCR	115
3.2.4 Assessment of target mRNA knockdown	118
3.2.5 Assessment of target protein knockdown	120
3.2.6 Assessment of the effect of CSN2 knockdown in K562 cells on SCF components and activity	120
3.2.7 Assessment of the effect of CSN2 knockdown on the level of F-box proteins	124
3.2.8 Assessment of the effect of CSN2 knockdown on F-box protein mRNA	127
3.2.9 Assessment of the effect of CSN2 knockdown on cell growth and death	130
3.2.10 Determination of the mechanism of CSN2 knockdown induced cell death	133
3.2.11 Morphological analyses of CSN2 knockdown in K562 cells	138
3.2.12 Autophagy inhibition recapitulates shCSN2 cell growth, morphology and LC3-II accumulation	141
3.2.13 Analysis of the effect of a vector control scramble sequence	147
4. Analysis of the molecular and cellular effects of CSN5 knockdown	155
4.1 Introduction	156
4.2 Results	157
4.2.1 Assessment of target mRNA knockdown	157
4.2.2 Assessment of target protein knockdown	157
4.2.3 Assessment of the effect of CSN5 knockdown on SCF components and activity	159
4.2.4 Assessment of the effect of CSN5 knockdown on the level of F-box proteins	162

4.2.5 <i>Assessment of the effect of CSN5 knockdown on F-box mRNA</i>	165
4.2.6 <i>Assessment of the effect of CSN5 knockdown on cell growth and death</i>	165
4.2.7 <i>Determination of the mechanism of CSN5 knockdown induced cell death</i>	171
5. Analysis of the effect of CSN2 and CSN5 knockdown on CSN complex integrity	178
5.1 <i>Introduction</i>	179
5.2 <i>Results</i>	180
5.2.1 <i>Optimisation of the 2-Dimensional NativePAGE/SDS-PAGE gel electrophoresis protocol</i>	180
5.2.2 <i>Determination of the effect of CSN2 knockdown on CSN complex integrity</i>	182
5.2.3 <i>Assessment of the effect of CSN2/CSN5 double knockdown on CSN subcomplex formation and the occurrence of autophagy</i>	186
5.2.4 <i>Determination of the effect of CSN5 knockdown on CSN complex integrity</i>	191
6. Expression of wild-type and deneddylase dead CSN5 in shCSN5 expressing cells	199
6.1 <i>Introduction</i>	200
6.2 <i>Results</i>	201
6.2.1 <i>Preparation of plasmids</i>	201
6.2.2 <i>Assessment of CSN5 protein levels</i>	205
6.2.3 <i>Assessment of the cumulative growth of cells expressing CSN5 in a shCSN5 background</i>	205
6.2.4 <i>Assessment of the morphology of cells expressing CSN5 in a shCSN5 background</i>	208
6.2.5 <i>Assessment of the effect of CSN5 protein expression in a shCSN5 background on SCF^{Skp2} activity</i>	210
7. General discussion	216
7.1 <i>CSN subunit knockdown results in aberrant CRL activity</i>	217
7.2 <i>Targeting the CSN results in the sequential loss of F-box proteins</i>	218
7.3 <i>The CSN and F-box protein/CSN subunit transcription</i>	219
7.4 <i>CSN2 knockdown</i>	221
7.5 <i>CSN5 knockdown</i>	223
7.6 <i>CSN5 re-expression results in partial rescue of the shCSN5 phenotype</i>	226
7.7 <i>ddCSN5 expression rescues Skp2 protein levels</i>	227
7.8 <i>A novel mechanism of CSN deneddylase activity regulation?</i>	227
7.9 <i>The CSN and CML</i>	228
References	229
Manuscript	245

Figure List

1. General Introduction

Figure 1. The autophagy mechanism of protein degradation	3
Figure 2. The ubiquitin proteasome system	5
Figure 3. The Skp1, CUL1, F-box protein complex	8
Figure 4. CRL constituents	10
Figure 5. Summary of alternative CSN nomenclature	19
Figure 6. Recently proposed subunit topology of the human CSN complex	22
Figure 7. The cycling model of CRL regulation	28
Figure 8. A modified cycling model of CRL regulation	30
Figure 9. An alternative model of CRL regulation	32

2. Materials and Methods

Figure 10. Schematic of the co-transfection and cell sorting techniques	79
Figure 11. The NativePAGE/SDS PAGE 2-D gel analysis technique	93

3. Analysis of the molecular and cellular effects of CSN2 knockdown

Figure 12. Schematic diagram of plasmids and short hairpin structure	111
Figure 13. Short hairpin vector preparation and validation	112
Figure 14. Validation of K562 cell co-transfection	114
Figure 15. Assessment of cDNA quality using β -actin PCR	116
Figure 16. Validation and optimisation of QRT-PCR primers and probe	117
Figure 17. Determination of CSN2 mRNA and protein knockdown	119
Figure 18. CSN2 knockdown results in accumulation of neddylated Cul1, loss of the F-box protein Skp2 and accumulation of p27	122
Figure 19. CSN2 knockdown results in significant loss of Cul1 protein	123
Figure 20. CSN2 knockdown results in a significant decrease in the Cul3:Nedd8 Cul3 ratio and loss of Cul3 protein	125
Figure 21. CSN2 knockdown results in the sequential loss of F-box proteins	126
Figure 22. F-box protein loss in CSN2 knockdowns is rescued with the addition of the proteasome inhibitor MG132	128
Figure 23. CSN2 knockdown results in significant alteration to the level of F-box mRNA	129
Figure 24. CSN2 knockdown results in significantly reduced cell growth	131
Figure 25. CSN2 knockdown results in significantly reduced thymidine incorporation into cellular DNA	132
Figure 26. CSN2 knockdown has no significant effect on the cell cycle	134
Figure 27. CSN2 knockdown has no effect on caspase-9 activation	135
Figure 28. CSN2 knockdown results in a significant increase in annexin V positivity	137
Figure 29. CSN2 knockdown results in a significant increase in the proportion of propidium iodide+ve:annexin V-ve cells, not caused by propidium iodide retention within vacuoles	139
Figure 30. CSN2 knockdown cells contain autophagosomes	140

Figure 31. CSN2 knockdown results in accumulation of the autophagy marker protein LC3-II	142
Figure 32. Treatment of vector control cells with 3-methyladenine recapitulates the cell growth pattern of CSN2 knockdown cells, whilst having little effect on cells lacking CSN2	144
Figure 33. Dose titration of bafilomycin A1	145
Figure 34. Treatment of vector control cells with bafilomycin A1 recapitulates the vacuolar morphology and LC3-II accumulation observed in shCSN2 cells	146
Figure 35. Treatment of K562 cells with the autophagy inducer rapamycin does not recapitulate the LC3-II accumulation observed in shCSN2 cells	148
Figure 36. CSN2 knockdown results in a significant increase in total cellular protein	149
Figure 37. A vector control scramble sequence has no significant effect on the level of CSN2 or CSN5 protein or mRNA	150
Figure 38. A vector control scramble sequence has no significant effect on cell growth	153
Figure 39. A vector control scramble sequence has no effect on the SCF or the SCF target p27	154

4. Analysis of the molecular and cellular effects of CSN5 knockdown

Figure 40. Determination of CSN5 mRNA and protein knockdown	158
Figure 41. CSN5 knockdown results in accumulation of neddylated Cul1, loss of Skp2 and accumulation of p27	160
Figure 42. CSN5 knockdown results in the significant accumulation of neddylated Cul3 protein and loss of Cul3 protein	161
Figure 43. CSN5 knockdown results in the sequential loss of F-box proteins	163
Figure 44. F-box protein loss in CSN5 knockdowns is rescued with the addition of the proteasome inhibitor MG132	164
Figure 45. CSN5 knockdown results in significant alteration to the level of F-box mRNA	166
Figure 46. CSN5 knockdown results in significantly reduced cell growth	167
Figure 47. CSN5 knockdown results in significantly reduced thymidine incorporation into cellular DNA	169
Figure 48. CSN5 knockdown results in significant changes in cell cycle	170
Figure 49. CSN5 knockdown results in altered cell morphology and aberrant mitotic spindle formation	172
Figure 50. CSN5 knockdown results in caspase-9 activation	173
Figure 51. CSN5 knockdown results in a significant increase in annexin V positivity	175
Figure 52. CSN5 knockdown has no significant effect on propidium iodide+ve:annexin V-ve staining	176
Figure 53. CSN5 knockdown has no effect on the level of the autophagy marker protein LC3-II	177

5. Analysis of the effect of CSN2 and CSN5 knockdown on CSN complex integrity

Figure 54. Optimisation of the 2-Dimensional NativePAGE gel protocol	181
Figure 55. CSN2 knockdown results in a significant loss of CSN2 from the CSN complex	183
Figure 56. CSN2 knockdown results in a significant loss of CSN5 from the CSN complex	184
Figure 57. CSN2 knockdown results in a significant reduction of both CSN5 protein and mRNA	185
Figure 58. CSN2 knockdown results in the formation of a CSN5 containing CSN subcomplex	187
Figure 59. Determination of CSN2 and CSN5 mRNA knockdown in double knockdown cells	188
Figure 60. Cells lacking both CSN2 and CSN5 do not form CSN5 containing subcomplexes but do have a mixed phenotype associated with the loss of these subunits	190
Figure 61. CSN5 knockdown has no significant effect on CSN5 within the intact CSN complex	192
Figure 62. CSN2 knockdown results in a significant reduction of the intact CSN complex, whilst CSN5 knockdown has no significant effect on the intact CSN complex	193
Figure 63. CSN5 knockdown results in loss of the free form of CSN5	194
Figure 64. RIPA buffer does not extract the entire cellular CSN5 pool	196
Figure 65. CSN5 knockdown has no significant effect on CSN2 integration into the CSN complex	197
Figure 66. CSN5 knockdown has no significant effect on the level of CSN2 protein or mRNA	198

6. Expression of wild-type and deneddylase dead CSN5 in shCSN5 expressing cells

Figure 67. Amplification of CSN5 coding sequence	202
Figure 68. CSN5 re-expression plasmid preparation and validation	203
Figure 69. Determination of CSN5 re-expression plasmid shRNA sequence and deneddylase dead mutations	204
Figure 70. CSN5 protein expression in a shCSN5 background	206
Figure 71. Expression of either wild-type or deneddylase dead CSN5 partially rescues cell growth	207
Figure 72. Expression of either wild-type or deneddylase dead CSN5 reduces the proportion of cells with disorganised, fragmented DNA	209
Figure 73. Expression of wild-type CSN5, but not deneddylase dead CSN5, restores Cull1 deneddylation	211
Figure 74. Expression of either wild-type or deneddylase dead CSN5 rescues Skp2 protein day 3 post transfection	213
Figure 75. Expression of wild-type, but not deneddylase dead, CSN5 rescues Skp2 protein day 7 post transfection	214
Figure 76. Expression of either wild-type or deneddylase dead CSN5 fails to	215

restore the basal level of p27 protein

7. General discussion

Figure 77. Diagram depicting the possible consequences of CSN2 or CSN5 loss for the functions of the intact CSN complex 222

Abbreviation list

3-MA	3-methyladenine
5/6-kinase	inositol 1,3,4-trisphosphate 5/6-kinase
APS	ammonium persulphate
Baf A1	bafilomycin A1
β -ME	β -mercaptoethanol
β -TrCP	beta-transducin repeat containing protein
BSA	bovine serum albumin
BTB	broad complex, tramtrack, bric-a-brac
CAND1	cullin-associated and deneddylation-dissociated 1
Cdc4	cell division cycle gene 4
CDK	cyclin dependant kinase
cDNA	complementary DNA
cds	coding sequence
ChIP	chromatin immunoprecipitation
CML	chronic myeloid leukaemia
COP	constitutive photomorphogenesis
CRL	Cullin-RING E3 ubiquitin ligase
CSA	Cockayne syndrome protein A
CSN	COP9 signalosome
Ct	cycle threshold
Cullin1-5	Cul1-5
Dab1	Disabled-1
dd CSN5	denedylase dead CSN5
DDB1	DNA damage binding protein 1
DDB2	damage-specific DNA binding protein 2
DMSO	dimethyl sulfoxide
DNA	deoxyribonucleic acid
dNTP	deoxynucleotide triphosphate
dUTP	deoxyuridine triphosphate
EB1	microtubule end-binding protein 1
ERalpha	estrogen receptor alpha
FBS	foetal bovine serum
Fbx7	F-box protein 7
FBXW8	F-box and WD repeat domain containing 8
FWD-1	F-box/WD40-repeat containing protein 1
GGR	global genome repair
HDAC	histone deacetylase
HECT	homologous to E6-associated protein C-terminus
HIF	hypoxia inducible factor
HKK	pMACS K ^k .II plasmid
HRP	horseradish peroxidase
HSP70	heat shock protein 70
ICSBP	interferon consensus sequence-binding protein
I κ B α	inhibitor of NF- κ B alpha

Jab1	Jun activator domain binding protein 1
JAMM	Jab1/MPN domain metalloenzyme
Keap1	Kelch-like ECH-associated protein 1
KLHL13	Kelch-like protein 13
KLHL9	Kelch-like protein 9
LC3	light chain 3
LHR	lutropin/choriogonadotropin receptor
LMB	leptomycin B
MDC	monodansylcadaverine
MEF	mouse embryonic fibroblast
MHC	major histocompatibility
MIF	macrophage inhibitory factor
MLF1	myeloid leukaemia factor 1
MPN	Mpr1p Pad1p N-terminal
mRNA	messenger RNA
MS	mass spectrometry
NAP1	nucleosome assembly protein 1
Nedd8	neural precursor cell expressed, developmentally down-regulated 8
NER	nucleotide excision repair
NES	nuclear export signal
NF- κ B	nuclear factor kappa-light-chain-enhancer of activated B cells
NPM	nucleophosmin
Nrf2	NF-E2-related factor-2
PCI	Proteasome, Cop9, Initiation factor 3
PCR	polymerase chain reaction
PI	propidium iodide
PKD	protein kinase D
QRT-PCR	quantitative real-time PCR
RING	really interesting new gene
RNA	ribonucleic acid
SCF	Skp1, Cul1, F-box protein
SDS	sodium dodecyl sulphate
shCSN2	short hairpin RNA targeting CSN2
shCSN5	short hairpin RNA targeting CSN5
shRNA	short hairpin RNA
shVC	vector control
Skp1	S-phase kinase-associated protein 1
Skp2	S-phase kinase-associated protein 2
SOCS	suppressor of cytokine signaling
SRS	substrate recognition subunit
TCR	transcription-coupled repair
TCR	T cell antigen receptor
TIR1	transport inhibitor response protein 1
TR	thyroid hormone receptor
UNG	uracil-DNA glycosylase
UPS	ubiquitin proteasome system

USP15
VEGF
VHL
WNVCp
WT CSN5

ubiquitin specific protease 15
vascular endothelial growth factor
von Hippel-Lindau
West Nile virus capsid
wild-type CSN5

Chapter 1.0:
General Introduction

1.1 Intracellular protein degradation

The concentration of any protein within the cell at any given time is tightly regulated. This regulation is of primary biological importance and is mediated at multiple levels, including via gene transcription, mRNA translation and protein degradation. This project is concerned with the process of intracellular protein degradation, of which there are two key mechanisms within the cell, autophagy and the ubiquitin-proteasome system. These systems differentially degrade long-lived and short-lived proteins within cells.

1.1.1 Autophagy

Autophagy is the main mechanism of degradation of long-lived proteins within the cell (Doherty and Mayer, 1992, Levine and Klionsky, 2004). Protein degradation by autophagy culminates in proteolysis within the (autophago)lysosome, a single membrane vesicular structure which contains proteases active at the low pH of the lysosomal lumen (Doherty and Mayer, 1992). Macroautophagy, which has been the focus of the majority of autophagy research, involves the formation of a double membrane structure around cytosolic proteins which, when completed, forms a structure called the autophagosome (Levine and Klionsky, 2004). The outer membrane of the autophagosome fuses with the lysosome membrane resulting in the formation of a single membrane autophagic body within the lumen of the lysosome (figure 1) (Levine and Klionsky, 2004). In the final stage of autophagy the single membrane of the autophagic body is broken down and the

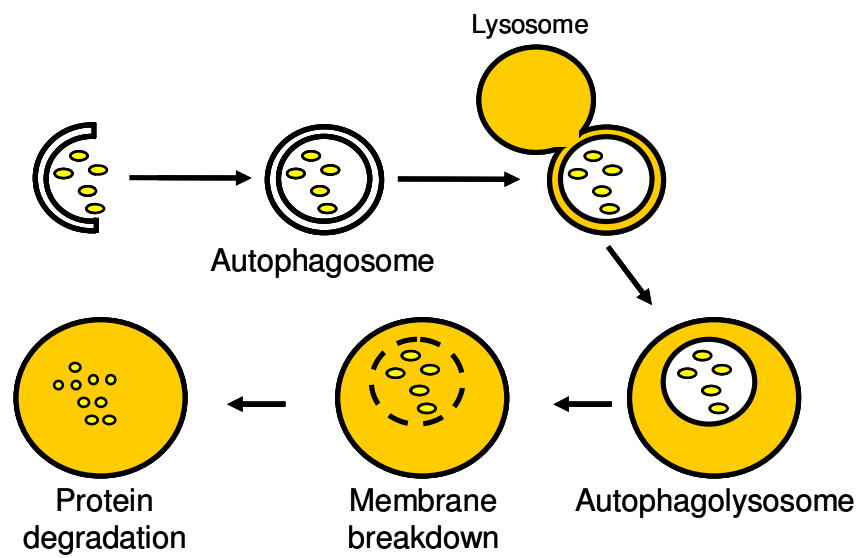


Figure 1. The autophagy mechanism of protein degradation.

Schematic depicting the process of macroautophagy. In macroautophagy target proteins are surrounded by a double membrane structure called an autophagosome, the outer membrane of which fuses with the lysosome membrane to yield an autophagolysosome. The inner membrane is then broken down, enabling lysosomal protease mediated protein degradation.

protein contents degraded by proteases within the lumen of the lysosome (figure 1) (Doherty and Mayer, 1992, Levine and Klionsky, 2004).

1.1.2 The ubiquitin-proteasome system

The ubiquitin-proteasome system (UPS) is the main mechanism of degradation of short-lived proteins within the cell (Doherty and Mayer, 1992, Levine and Klionsky, 2004). Proteolysis is carried out by a multicatalytic protease, the 26S proteasome, present in both the cytoplasm and nucleus (Doherty and Mayer, 1992). The proteasome consists of a 20S core particle and two 19S regulatory particles (figure 2). The core particle is a hollow cylinder whilst the regulatory particles form caps at either end of the core particle (figure 2), with proteins being degraded in the hollow compartment which is formed (Alberts, 2002). Proteins are recognised by the 19S cap and delivered to the 20S core for degradation (Alberts, 2002). Unlike autophagy, which tends to carry out bulk protein degradation, the UPS carries out specific protein degradation. The specificity of the UPS is conferred through specific target labelling with ubiquitin, a signal which is recognised by the 19S particle of the proteasome (Alberts, 2002, Doherty and Mayer, 1992).

1.1.3 Protein ubiquitination

Simpson demonstrated the requirement for ATP in protein degradation in 1953 (Simpson, 1953). Hershko and co-workers later identified a heat-stable polypeptide which was essential for ATP-dependent proteolysis in rabbit reticulocytes (Ciehanover et al., 1978).

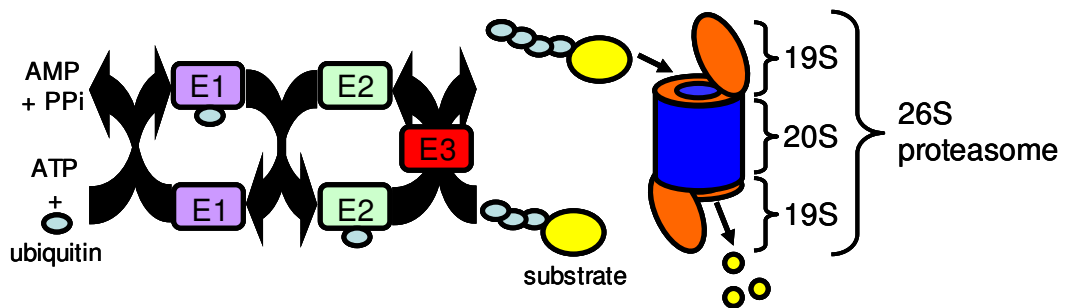


Figure 2. The ubiquitin proteasome system.

Schematic depicting the ubiquitin proteasome system. Initially, ubiquitin is activated by binding to E1 enzyme via a thiol ester linkage, a reaction dependant upon ATP. Ubiquitin is then transferred to an E2 ubiquitin conjugating enzyme. A specific E3 ubiquitin ligase then mediates the transfer of ubiquitin from E2 to a specific target protein. Protein ubiquitination signals for protein degradation by the 26S proteasome. Target proteins are initially deubiquitinated by the lid of the proteasome and the ubiquitin recycled. The protein is then partially unfolded before translocation into the proteasome core where it is degraded.

They then determined that this polypeptide was conjugated to proteins in an ATP-dependent manner (Ciechanover et al., 1980), and that polypeptide conjugation to proteins resulted in their degradation (Hershko et al., 1984). This polypeptide, which was determined to be ubiquitin (Wilkinson et al., 1980), was shown to be activated by an E1 ubiquitin activating enzyme, a process requiring ATP (Ciechanover et al., 1981, Haas et al., 1982). Following this, three enzymes required for ubiquitin conjugation to proteins were isolated; E1 as above, E2 ubiquitin conjugating enzyme which was shown to mediate the transfer of E1 activated ubiquitin to the target protein, and E3 which was primarily shown to function in the final, ligation step of ubiquitin conjugation (Hershko et al., 1983), and was later shown to be the substrate binding component of the ubiquitin conjugating system (Hershko et al., 1986). With this the ubiquitin proteasome system was identified, responsible for the majority of protein degradation (Bosch and Kipreos, 2008), in which proteins are targeted for 26S proteasome mediated degradation by a three step mechanism which covalently attaches ubiquitin molecules to target proteins (figure 2).

As the E3 enzyme interacts with the substrate protein, the E3 is also responsible for conferring target specificity to the ubiquitin proteasome system. Two main classes of E3 ubiquitin ligase have been identified; homologous to E6-associated protein C-terminus (HECT) domain and really interesting new gene (RING) ligases. The Cullin-RING E3 ubiquitin ligases form the largest class of E3 ubiquitin ligases identified to date and specifically regulate the degradation of many proteins (Petroski and Deshaies, 2005). In the following section, the literature regarding the structure, function and regulation of the Cullin-RING E3 ubiquitin ligase family is reviewed.

1.2 The Cullin-RING E3 ubiquitin ligase (CRL) family

1.2.1 The CRLs and their component subunits

Cullin-RING E3 ubiquitin ligases (CRLs) comprise multiple subunits including a cullin, a RING finger protein and an adaptor protein which binds both the cullin and the variable, substrate specific CRL subunit, the substrate recognition subunit (SRS) (Bosu and Kipreos, 2008). Nayak *et al* have demonstrated, using phylogenetic analysis, that there are five metazoan cullin families (Cul1-Cul5) (Nayak et al., 2002).

The most studied CRL is that containing Cul1 which, along with the RING finger protein Roc1, the adaptor protein S-phase kinase-associated protein 1 (Skp1) and an SRS known as an F-box protein, forms an SCF (Skp1, Cul1, F-box protein) complex (Petroski and Deshaies, 2005). The crystal structure of the SCF complex demonstrates that Cul1 acts as a scaffold for complex formation, binding Roc1 at its C-terminus and Skp1 at its N-terminus (Zheng et al., 2002b). Roc1 recruits the E2 ubiquitin conjugating enzyme and Skp1 binds the F-box protein through an F-box motif. The F-box protein recruits a substrate through a substrate interaction motif, bringing the target protein into close proximity with the activated ubiquitin molecule (Petroski and Deshaies, 2005) (figure 3). The F-box protein is therefore responsible for conferring target specificity to the SCF complex. As humans have been shown to have approximately 70 F-box proteins (Jin et al., 2004), there is the potential for the formation of multiple SCF complexes with the Roc1/Cul1/Skp1 base in order to facilitate the degradation of a diverse array of specific

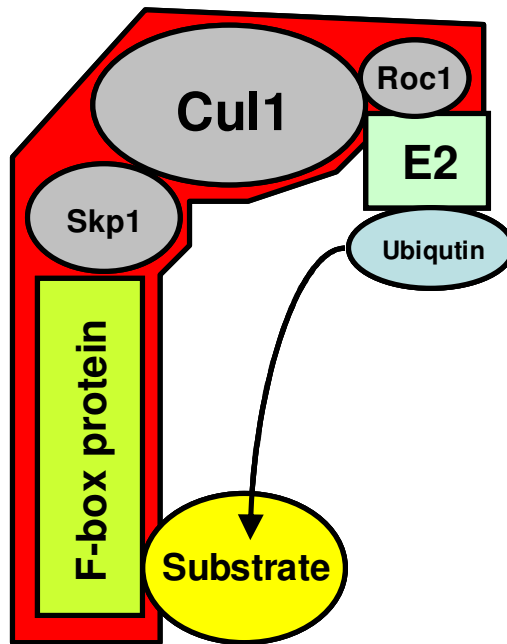


Figure 3. The Skp1, CUL1, F-box protein complex.

Illustration depicting SCF component interactions and indicating how recruitment of ubiquitin charged E2 and substrate by this complex enables substrate ubiquitination.

target proteins. Indeed, multiple SCF complexes have been identified which target distinct proteins for degradation. These will be reviewed in the following section which looks at CRL function.

CRLs containing Cul2 have a structure comparable to that of the SCF complex, with Roc1 also binding to the C-terminus of Cul2 and an adaptor binding to the N-terminus (Kamura et al., 1999, Pause et al., 1999). However, in the case of Cul2 based CRLs, the adaptor is a heterodimer of Elongin B and Elongin C and the SRS is a von Hippel-Lindau (VHL)-box protein which is recruited to the CRL by Elongin C through a VHL-box motif (Bosu and Kipreos, 2008) (figure 4).

Cul5 containing CRLs have a structure and composition very similar to that of Cul2 based CRLs, with Cul5 also binding an Elongin B/C heterodimer as an adaptor (Bosu and Kipreos, 2008). However, Cul5 recruits target proteins via a suppressor of cytokine signaling (SOCS)-box protein which binds to Elongin C through a SOCS-box motif, as opposed to the VHL-box protein utilised by Cul2 containing CRLs (Kamura et al., 2004). Furthermore, instead of Roc1, Cul5 based CRLs interact with the RING finger protein Roc2 (Petroski and Deshaies, 2005) (figure 4).

Cul4 based CRLs continue the generic structure and composition of CRLs, with the binding of a Roc protein (Roc1) to Cul4 and the recruitment of an SRS via an adaptor protein (Bosu and Kipreos, 2008), although the adaptor has also been shown to recruit substrates directly (McCall et al., 2005). The adaptor protein in Cul4 based CRLs is DNA

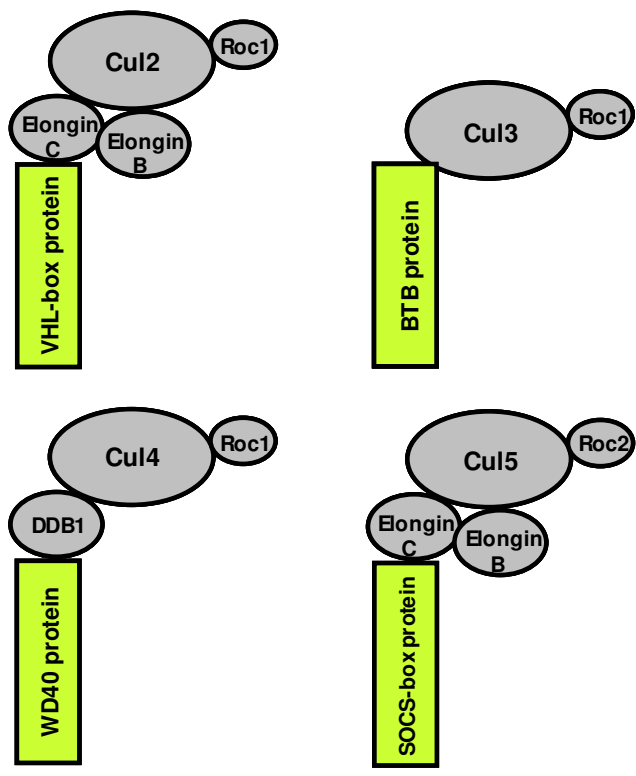


Figure 4. CRL constituents.

Illustration to show the constituent subunits of Cul2-Cul5 CRL complexes and subunit interactions.

damage binding protein 1 (DDB1), which recruits WD40 proteins (Angers et al., 2006, He et al., 2006) (figure 4).

As with the majority of CRLs, CRLs which contain Cul3 utilise Roc1. However, they differ from all other cullin containing E3 ligases as they do not require a separate adaptor protein and SRS. Rather, SRSs called BTB (broad complex, tramtrack, bric-a-brac) proteins both interact directly with Cul3 and recruit target proteins (Geyer et al., 2003, Xu et al., 2003) (figure 4).

More recently, a further cullin, Cul7, has been identified and found to form a complex with Roc1, Skp1 and the F-box protein Fbx29 (also called FBXW8; F-box and WD repeat domain containing 8) (Dias et al., 2002). However, research regarding Cul7 is relatively scant and Cul7 is yet to be shown to interact with any other F-box proteins. Nonetheless, Tsunematso *et al*, 2006 have suggested that the abnormalities observed in CUL7^{-/-} mice which are not observed in mice lacking Fbx29 are indicative of Fbx29 independent functions of the Cul7 containing CRL complex (Tsunematsu et al., 2006), suggesting that this cullin also interacts with other SRSs.

1.2.2 CRL function

The SCF has been shown to mediate the degradation of multiple cell cycle associated proteins, with the SCF complex containing the F-box protein Skp2 (S-phase kinase-associated protein 2; SCF^{Skp2}) regulating the cell cycle inhibitors p21 (Yu et al., 1998)

and p27 (Tsvetkov et al., 1999). In addition, SCF^{Cdc4} (containing the F-box protein Cdc4; cell division cycle gene 4) facilitates the degradation of cyclin E, a mediator of the G1 to S phase transition of the cell cycle (Koepp et al., 2001), and the cell proliferation promoter, c-Myc (Yada et al., 2004). SCF ^{β -TrCP} (containing the F-box protein β -TrCP; beta-transducin repeat containing protein) has been shown to ubiquitinate I κ B α , an inhibitor of the transcription factor NF- κ B (nuclear factor kappa-light-chain-enhancer of activated B cells), in the presence of E1, E2 and ATP (Yaron et al., 1998). As NF- κ B is a major regulator of the immune and inflammatory responses, such findings implicate this SCF complex in the regulation of both of these processes (Maniatis, 1999).

VHL protein, in complex with elonginB/C, has been identified as a Cul2 interacting protein (Pause et al., 1997). This Cul2 based CRL has been shown to mediate the ubiquitination and degradation of the alpha subunit of the hypoxia inducible factor (HIF) complex in normoxic conditions (Leung and Ohh, 2002). The HIF complex is an integral oxygen dependent transcriptional regulator which, in response to conditions of low oxygen, activates the transcription of hypoxia inducible genes, including the angiogenic protein vascular endothelial growth factor (VEGF) (Leung and Ohh, 2002). Thus, the Cul2/VHL CRL is implicated in the regulation of angiogenesis.

Four groups have independently demonstrated the potential function of Cul3 based CRLs in regulating oxidative and xenobiotic stress response via Nrf2 (NF-E2-related factor-2) degradation (Cullinan et al., 2004, Furukawa and Xiong, 2005, Kobayashi et al., 2004, Zhang et al., 2004). Kobayashi *et al*, 2004 showed that the oxidative stress sensing BTB

protein Keap1 (Kelch-like ECH-associated protein 1) binds to both Cul3 and the target protein Nrf2 and directly promotes Nrf2 ubiquitination and degradation (Kobayashi et al., 2004), thereby determining Keap1 and Nrf2 as a Cul3 based CRL SRS and target, respectively.

Cul3 based CRLs have also been shown to regulate mitotic processes, including mitotic spindle assembly (Pintard et al., 2004), and chromosome alignment in metaphase and completion of cytokinesis (Sumara et al., 2007). In *C. elegans*, the BTB protein MEL-26 functions as an SRS and is required in a complex with Cul3 for ubiquitin mediated degradation of the microtubule severing protein MEI-1 for assembly of the mitotic spindle (Pintard *et al*, 2004). Cul3 knockdown in HeLa cells was demonstrated to result in chromosome misalignment, disorganized anaphase spindles and failure to complete cytokinesis (Sumara et al., 2007). Furthermore, the BTB proteins KLHL9 and KLHL13 (Kelch-like protein 9 and 13) were shown to interact with Cul3 and mediate ubiquitination of Aurora B protein, a protein which functions in the attachment of the mitotic spindle to the centromere, potentially accounting for the mitotic defects observed in cells lacking a component of the Cul3/KLHL9/KLHL13 based CRL (Sumara et al., 2007).

Cul4 based CRLs have been implicated in the maintenance of DNA integrity, with the identification of the nucleotide excision repair (NER) proteins DDB2 (damage-specific DNA binding protein 2) and CSA (Cockayne syndrome protein A) as SRSs in Cul4 ligase complexes (Groisman et al., 2003). Groisman *et al* demonstrated that the WD40 proteins

DDB2 and CSA, which function in global genome repair (GGR) and transcription-coupled repair (TCR) respectively, are associated with the same protein complex (including Cul4, Roc1 and DDB1) via interaction with DDB1. In addition, the DDB2 and CSA containing complexes were shown to possess ubiquitin ligase activity and were further demonstrated to rescue the GGR and TCR deficient phenotypes, respectively, when microinjected into corresponding mutant cells (Groisman et al., 2003).

Cul5 has been demonstrated to function in neuron positioning during cortical development by regulation of Disabled-1 (Dab1) protein levels (Feng et al., 2007). The authors observed that SOCS proteins can bind specifically to Dab1 protein and that expression of SOCS1, SOCS2 or SOCS3 protein induces Dab1 degradation. Furthermore, transfection of embryonic cortical neurons with Cul5 shRNA protects Dab1 from degradation. This observation was also made *in vivo* using *in utero* microinjection and electroporation of the lateral ventricles of day 14.5 mouse embryos, with concomitant neuron displacement which could be rescued by Dab1 knockdown (Feng et al., 2007). Cullin 5 based CRLs have therefore been identified as a regulator of cortical neuron migration via, at least in part, degradation of Dab1.

1.2.3 CRL regulation via cullin modification

All of the human cullins analysed so far (Cul1, 2, 3, 4A, 4B and 5 i.e. all except Cul7) have been shown to be modified by the addition of a ubiquitin-like protein, Nedd8 (neural precursor cell expressed, developmentally down-regulated 8) (Hori et al., 1999).

The neddylation process requires an E1 to activate Nedd8 and an E2 (UBC12 or UBE2F) that transfers Nedd8 to the cullin (Gong and Yeh, 1999, Liakopoulos et al., 1998, Huang et al., 2009). Furthermore, the E2 recruiting subunit of CRLs, Roc1, has been shown to be required for cullin neddylation (Kamura et al., 1999). More recently, cullin neddylation has also been shown to be upregulated by an E3 ligase, Dcn1, which promotes neddylation by binding to both the cullin target and UBC12 (Kurz et al., 2008, Kurz et al., 2005), thereby bringing the neddylation target into close proximity with the active Nedd8; suggesting a scaffold function for Dcn1 comparable to that of cullin based E3 ubiquitin ligases.

The neddylation of CRLs increases ubiquitin ligase activity *in vitro*, with groups demonstrating the requirement for cullin neddylation in the ubiquitination of I κ B α (Read et al., 2000, Wu et al., 2000) and others determining cullin neddylation as a promoter of p27 ubiquitination (Morimoto et al., 2000, Podust et al., 2000). Moreover, neddylation has been shown to be required for CRL function *in vivo*, including mammalian cells (Ohh et al., 2002). The mechanisms behind Nedd8 promotion of CRL mediated protein ubiquitination have been investigated. Cullin neddylation has been shown to increase ubiquitin bound E2 binding to the E3 (Kawakami et al., 2001). Further, Nedd8 has been shown to directly interact with E2 ubiquitin conjugating enzyme and thereby recruit the E2 to cullin based E3 ligases, possibly in co-operation with Roc1 (Sakata et al., 2007). In addition, cullin neddylation has been shown to result in significant conformational alterations in the structure of Cul5 C-terminal domain (Cul5^{ctd})-Roc1 complex and Cul1^{ctd}-Roc1 complex, resulting in the release of the Roc1 RING domain from a cullin

subdomain and allowing conformational flexibility within these complexes (Duda et al., 2008). These Nedd8 induced conformational changes and increased flexibility are required for CRL activity (Duda et al., 2008), and may enhance E2 binding as above but may also bridge the predicted $\sim 60\text{\AA}$ gap between the E2 and substrate binding site (Duda et al., 2008), thereby enhancing CRL mediated protein ubiquitination.

In addition to promoting CRL activity, cullin neddylation also prevents the binding of cullins to CAND1 (cullin-associated and deneddylation-dissociated 1) (Zheng et al., 2002a), possibly by blocking a CAND1 binding site (Duda et al., 2008). CAND1 is an inhibitor protein which, in the absence of neddylation, binds to all cullins (Min et al., 2003); although Cul7 has yet to be tested (Petroski and Deshaies, 2005). CAND1 has been shown to interact with the Cul1-Roc1 complex by wrapping around the cullin, with the N-terminus of CAND1 interacting with the C-terminal of the cullin and the C-terminus of the inhibitor binding to the N-terminal of the cullin, blocking both the neddylation and Skp1 interaction sites (Goldenberg et al., 2004). Furthermore, increasing CAND1 in an *in vitro* system has been shown to result in a decreased association of Skp1 with Cul1 and a concomitant decrease in I κ B α ubiquitination (Min et al., 2003), thereby directly demonstrating the negative regulatory effect of CAND1 on CRL activity *in vitro*. In addition, a more recent manuscript presents data to suggest that a CAND1 paralogue, CAND2, found in mouse cardiac and skeletal muscle, accelerates myogenic differentiation of mouse myoblast C2C12 cells by inhibition of Cul1 mediated myogenin ubiquitination and subsequent proteasomal degradation (Shiraishi et al., 2007).

Overall, cullin neddylation appears to have a positive regulatory role on CRL activity, with neddylation promoting CRL activity and preventing interaction with the inhibitor CAND. However, as is discussed in the following sections, this is not the full story of cullin modification. The neddylation of cullins is reversible, with deneddylation being carried out by the COP9 signalosome (CSN) complex.

1.3 The COP9 signalosome (CSN) complex

Initial studies by Wei and Deng identified a mutation in the COP9 (constitutive photomorphogenesis 9) gene (later identified as the gene encoding CSN8) in *Arabidopsis thaliana*, which resulted in constitutive photomorphogenesis in the absence of light (Wei and Deng, 1992). COP9 (CSN8) was then found to be a component of a complex (initially called the COP9 complex) identified in *A. thaliana* as a regulator of light controlled development (Wei et al., 1994). The eight subunit ~500kDa complex, now termed the COP9 signalosome (CSN), is highly conserved amongst eukaryotes and has been studied in a diverse array of organisms including humans (Seeger et al., 1998), mice (Lykke-Andersen et al., 2003), *Drosophila melanogaster* (Freilich et al., 1999, Oren-Giladi et al., 2008), *Aspergillus nidulans* (Busch et al., 2003), *Dictyostelium discoideum* (Rosel and Kimmel, 2006), *Schizosaccharomyces pombe* (Mundt et al., 1999), *Caenorhabditis elegans* (Pintard et al., 2003) and *Brassica oleracea* (Chamovitz et al., 1996). The study of this complex in such a wide variety of organisms resulted in a confusing array of names for the complex and its subunits such as COPS in mice, Sgn in humans and DCH in *Drosophila*. A unified nomenclature was thus determined in which COP9 signalosome was abbreviated to CSN and the subunits were designated CSN1-8 according to their decreasing molecular mass (Deng et al., 2000a, Deng et al., 2000b) (figure 5).

The CSN complex has been shown to be essential for the development of multiple organisms. *Arabidopsis* homozygous for the COP9 (CSN8) mutation do not survive past

CSN subunit	Other names
CSN1	COP11, FUS6, Sgn1, GPS1, COPS1, Mfh, DCH1, Caa1, CsnA
CSN2	Subunit 2, Sgn2, TRIP15, ALIEN, COPS2, DCH2, CsnB
CSN3	Subunit 3, Sgn3, COPS3, DCH3, CsnC
CSN4	COP8, FUS4, Sgn4, COPS4, DCH4, CsnD
CSN5	AJH1, AJH2, Sgn5, JAB1, DCH5, CsnE
CSN6	Subunit 6, Sgn6, hYIP, COPS6, DCH6, CsnF
CSN7	FUS5, Sgn7, COPS7a, COPS7b, DCH7, CsnG
CSN8	COP9, Sgn8, COPS8, DCH8, CsnH

Figure 5. Summary of alternative CSN nomenclature.

A table to summarise the alternative names for CSN subunits in *Arabidopsis*, human, mouse, *Drosophila*, *S.pombe* and *A. nidulans*. Adapted from Deng *et al*, 2000.

five weeks and do not undergo reproductive development (Wei and Deng, 1992). Similarly, homozygous CSN5 gene deletion or P-element insertion in *Drosophila*, both of which result in the loss of CSN5 protein, are lethal, with developmental retardation at the third larval or pupal stage (Freilich et al., 1999). *Dictyostelium* cell lines null for either CSN2 or CSN5 could not be recovered, suggesting that loss of the CSN complex in this organism is also lethal and that the CSN complex is vital for *Dictyostelium* development (Rosel and Kimmel, 2006). In addition, CSN2, CSN3 or CSN5 knockout in mice is associated with developmental defects and early embryonic lethality (Lykke-Andersen et al., 2003, Tomoda et al., 2004, Yan et al., 2003). Finally, although not lethal, CSN subunit gene deletion in *A. nidulans* and CSN5 knockdown by RNAi in *C. elegans* result in a block in sexual development and sterility of the organism, respectively (Busch et al., 2003, Smith et al., 2002, Busch et al., 2007), again indicating the essential function of the CSN complex in developmental processes.

Cell proliferation has been shown to be regulated by the CSN complex in several organisms. Disruption of CSN2 or CSN5 in mice results in deficient cell proliferation, increased levels of cyclin E and accumulation of p53 (Lykke-Andersen et al., 2003, Tomoda et al., 2004). In addition, CSN8 has been shown to be essential for antigen receptor-induced murine T-cell entry into the cell cycle from quiescence (Menon et al., 2007). Reduction of CSN subunits 1-6 in *C. elegans* by RNAi all result in a similar phenotype of impaired microtubule function and defective spindle formation and orientation, with failure of cytokinesis (Pintard et al., 2003). In addition, Rosel and Kimmel demonstrated, using CSN5 RNAi, that reduction of the CSN severely effects the

proliferation of *Dictyostelium* (Rosel and Kimmel, 2006), whilst a function for the CSN complex in the regulation of *S. pombe* proliferation has been demonstrated, with the finding that a deletion mutant of CSN1 results in accumulation of cells in S phase (Mundt et al., 1999). More recently, the CSN complex has been shown to be integral for progression through the G2 phase of the cell cycle in *Arabidopsis* (Dohmann et al., 2008). Finally, the CSN complex has been implicated in the positive regulation of human cell (HEK293T and HeLa) proliferation, with reduction of either CSN4 or CSN5 in human cells resulting in p27 accumulation and a significant reduction in cell proliferation (Denti et al., 2006).

Although studies have investigated the subunit-subunit interactions in the CSN complex using yeast two-hybrid and filter-binding assays (Kapelari et al., 2000, Rosel and Kimmel, 2006, Wei and Deng, 2003), and low resolution electron microscopy images of the CSN have been generated (Kapelari et al., 2000), the precise structure of the CSN complex remains to be determined. The most recent progress in CSN structure delineation used mass spectrometry (MS), tandem MS and the algorithm SUMMIT to generate a CSN subunit topology model (figure 6) (Sharon et al., 2009). This model, generated from 35 identified subcomplexes, depicts the CSN complex as two symmetrical modules containing CSN1, 2, 3 and 8 and CSN4, 5, 6 and 7 which are connected through interaction between CSN1 and CSN6 (figure 6A). CSN1 and CSN6 appear to be the core subunits, each forming interactions with four other subunits, whilst CSN2 and CSN5 are peripheral and were found to be the most readily dissociable subunits of the complex (figure 6A) (Sharon et al., 2009). The authors suggest that

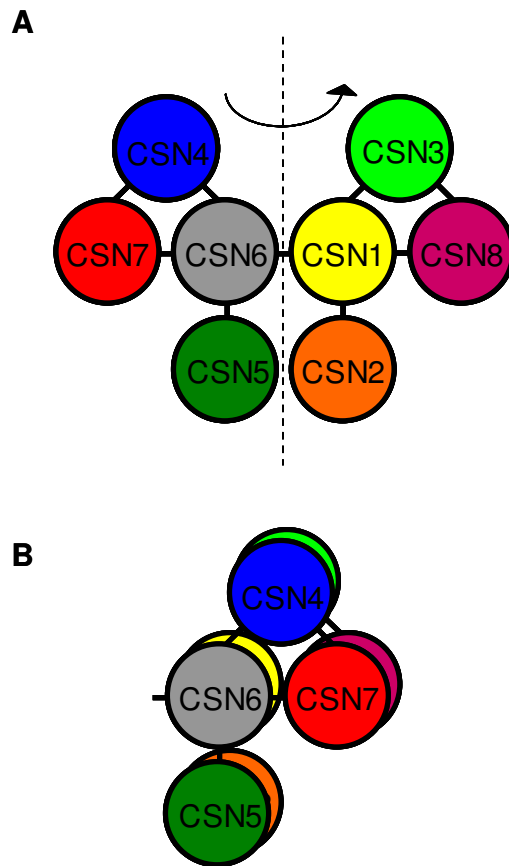


Figure 6. Recently proposed subunit topology of the human CSN complex.

Mass spectrometry (MS) and tandem MS identified a total of 35 CSN subcomplexes. This data was applied to the network inference algorithm SUMMIT to generate the above interaction network. **(A)** The interaction network shows two symmetrical modules connected by an interaction between CSN1 and CSN6. **(B)** Additional interactions may occur between the distinct modules if they were to rotate through the CSN1/CSN6 interaction plane. Image adapted from Sharon *et al*, 2009.

further interactions may occur between the two 4 subunit modules (in accordance with earlier findings of yeast two-hybrid studies) if the two units were to rotate as shown in figure 6B (Sharon et al., 2009). The authors further suggest that the CSN complex, of which the constituent subunits add up to a mass of 321kDa, fractionates at the larger size of ~500kDa as a result of the irregular bi-modular shape of the complex (Sharon et al., 2009). However, the association of the complex with other proteins or post-translational modification of CSN subunits may also be contributing factors to this phenomenon.

Although the precise structure of the CSN complex remains undetermined, the contribution of each of the subunits to complex stability has been demonstrated. A mutation in *Arabidopsis* CSN1 results in CSN complex destabilisation as measured by comparative gel filtration analysis of CSN4, 5, 7 and 8 subunits from wild-type and CSN1 mutant seedling extracts (Wang et al., 2002). In addition, CSN3 knockout mice lack CSN8, implicating CSN3 in CSN complex stability (Yan et al., 2003). Furthermore, genetic mutations of CSN subunits 2, 4, 7 and 8 in *Arabidopsis* were shown to prevent CSN5 incorporation into the complex (Kwok et al., 1998). More recently, CSN5 and CSN6 have also been shown to be vital for CSN complex integrity in *Arabidopsis* (Gusmaroli et al., 2007). The requirement of all subunits for CSN complex integrity and function is also reflected in the finding that different CSN subunit knockout or mutation can result in similar phenotypes. For example, gene deletion of CSN1, 2, 4 or 5 in *A. nidulans* results in identical blocks in fungal fruit body formation (Busch et al., 2007) and multiple CSN subunit mutants result in the constitutive photomorphogenic phenotype in *Arabidopsis* (Schwechheimer, 2004, Dohmann et al., 2005).

Interestingly, it should be noted that CSN5 has been shown not to be integral for CSN complex integrity, both *in vitro* (Sharon et al., 2009) and in the model organisms *Arabidopsis* (Dohmann et al., 2005) and *Drosophila* (Oron et al., 2002) and the human cell line HeLa (Peth et al., 2007a), with CSN5 mutation or knockdown having no effect on the remaining CSN complex lacking CSN5 (Dohmann et al., 2005, Oron et al., 2002, Peth et al., 2007a). These data suggest that rather than CSN complex integrity, CSN5 harbors the fundamental catalytic activity of the CSN complex. Indeed the cullin deneddylase activity of the CSN has been shown to reside within a particular domain of CSN5 (see next section).

The fact that CSN5 cannot function in deneddylation as a monomer (Cope et al., 2002), together with the finding that CSN subunit deficiency in *Arabidopsis* and human cells result in accumulation of neddylated cullins (Denti et al., 2006, Dohmann et al., 2005, Schwechheimer et al., 2001) suggests that the phenotypes observed in CSN deficient organisms may be attributable to defects in CSN complex mediated CRL regulation. Indeed, connections have been made between CSN deficiency associated phenotypes such as reduced cell proliferation (Denti et al., 2006, Pintard et al., 2003), auxin resistance (Stuttman et al., 2009) and a block in fungal fruit body formation (Busch et al., 2007), and the role of the CSN complex in CRL regulation (Denti et al., 2006, Pintard et al., 2003, Stuttman et al., 2009, Busch et al., 2007).

1.4 Regulation of CRLs by the CSN complex

1.4.1 Deneddylation of CRLs by the CSN complex

Lyapina *et al.*, 2001 first demonstrated the cullin deneddylation capability of the CSN complex. The authors clearly showed that the CSN associates with cullins (Cul1-3), and that disruption of the CSN complex results in accumulation of neddylated Cul1 in *S. pombe* (Lyapina *et al.*, 2001). Furthermore, they demonstrated that purified CSN isolated from pig spleen, which deneddylates immunopurified neddylated Cul1, can restore Cul1 deneddylation in CSN deficient *S. pombe* cell extracts (Lyapina *et al.*, 2001). CSN5 was then shown to contain the deneddylase activity of the CSN complex, with the zinc binding Jab1 (Jun activator domain binding protein 1)/MPN (Mpr1p Pad1p N-terminal) domain metalloenzyme (JAMM) motif of CSN5 determined to be integral to cullin deneddylation (Cope *et al.*, 2002). The addition of the metal chelator ethylene diamine tetraacetic acid to *S. pombe* lysates resulted in the accumulation of neddylated Cul1, and mutation in the JAMM motif of CSN5 in *S. pombe*, although not detrimental to CSN complex formation, abolished cullin deneddylation (Cope *et al.*, 2002).

The finding that neddylation enhances CRL activity suggested that deneddylation would have an opposing effect. However, studies regarding the effect of CSN mediated CRL deneddylation on CRL activity produced contradictory models of cullin regulation, with at least two reports suggesting a negative regulatory role for deneddylation and many groups reporting a positive function for cullin deneddylation in CRL activity. At least two

in vitro studies have presented data which implicate the CSN complex in the negative regulation of CRLs. For example, CSA and DDB2-containing CRL complexes lack ubiquitin ligase activity when complexed with the CSN complex (Groisman et al., 2003), and addition of the CSN complex to an *in vitro* degradation system results in inhibition of SCF mediated p27 ubiquitination and degradation (Yang et al., 2002). However, the vast majority of data is indicative of a positive regulatory role for deneddylation in CRL activity. For example, deletion of CSN5 in temperature sensitive *S. cerevisiae* SCF mutant strains exacerbated SCF mediated defects such as Sic1 protein turnover (Cope et al., 2002), whilst in *C. elegans* disruption of the CSN complex by RNA interference resulted in hyperneddylated Cul3 and accumulation of the Cul3 target protein, MEI-1 (Pintard et al., 2003). Furthermore, in *A. thaliana*, the E3 ubiquitin ligases SCF^{TIR1}, SCF^{COII} and SCF^{UFO} have been shown to interact with, and be positively regulated by, the COP9 signalosome complex (Feng et al., 2003, Schwechheimer et al., 2001, Wang et al., 2003).

The above data led to the proposal of a cycling model of CRL regulation *in vivo*, in which cycles of neddylation and deneddylation are required for optimal CRL activity. In an initial model, cullin neddylation was suggested to result in the recruitment of a ubiquitin loaded E2 enzyme whilst deneddylation was thought to release the non-ubiquitin charged E2 and thereby enable the “refreshment” of the CRL complex with another ubiquitin loaded E2 (Pintard et al., 2003). However, given that the SCF can ubiquitinate target protein in the absence of the CSN *in vitro* (Petroski and Deshaies, 2003) this cycling model was suggested to be unlikely (Cope and Deshaies, 2003). An alternative cycling

model was thus proposed by Cope and Deshaies, given the findings that CAND1 also functions in the positive regulation of CRLs (Zheng et al., 2002a) and that cullin neddylation results in CAND1 dissociation (Liu et al., 2002) and prevents CAND1 binding to cullin (Zheng et al., 2002a). Unlike the initial model, this model does not implicate the CSN in the direct facilitation of protein ubiquitination *per se*. Rather, this model incorporates both cullin neddylation/deneylation and CAND1 binding as requirements for the efficient recycling of CRLs (figure 7). In this model, deneylation inactivates the CRL allowing for CAND1 displacement of Skp1 and the F-box protein. Cullin neddylation then occurs, allowing for CAND1 displacement and Skp1 and F-box protein recruitment, and enabling another round of substrate ubiquitination prior to cullin deneylation (Cope and Deshaies, 2003) (figure 7). However, it should be noted that, with the findings that the deneylating activity of the CSN complex facilitates CRL activity by preventing the autocatalytic degradation of F-box proteins (Galan and Peter, 1999, Wee et al., 2005), and that cullin neddylation can only occur upon Skp1-F-box protein mediated CAND1-cullin dissociation (Bornstein et al., 2006), this cycling model could be modified as shown in figure 8.

Interestingly, an alternative model of CRL regulation has been proposed more recently in which, rather than a cycle, CRL activity is regulated by two reversible processes; the dissociation of CAND1 from the cullin subunit and cullin neddylation (figure 9) (Bornstein et al., 2006). In this model, CAND1 dissociation is mediated by the F-box protein/adaptor complex allowing for subsequent cullin neddylation (figure 9) (Bornstein et al., 2006). Further, the presence of substrate inhibits the deneylase activity of the

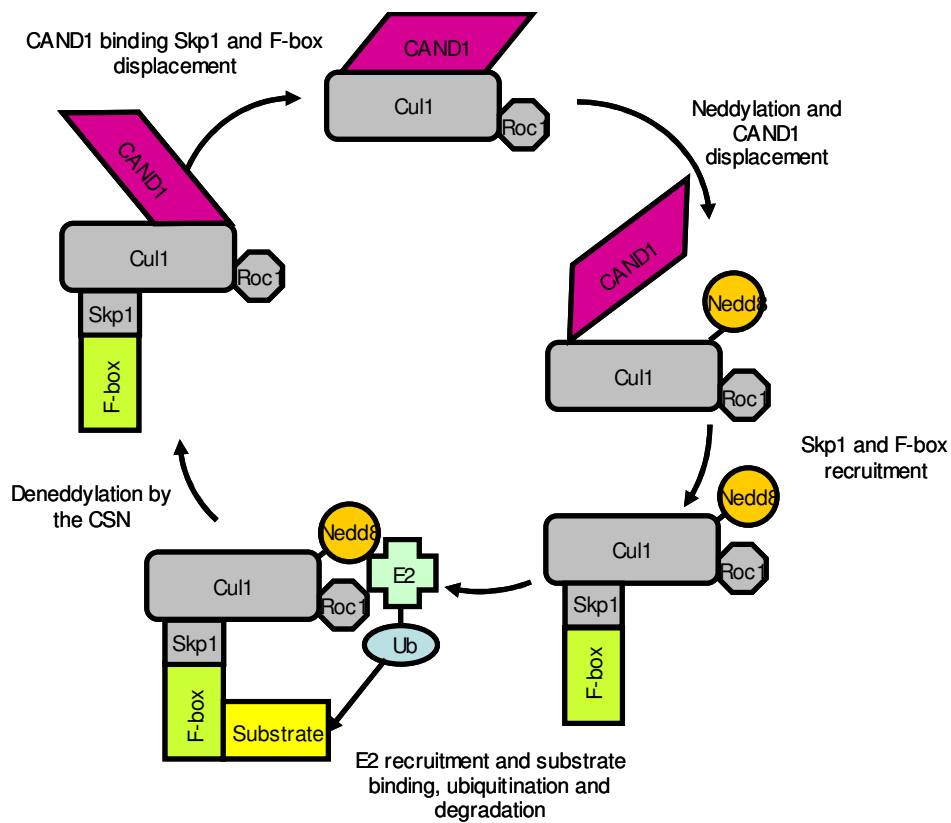


Figure 7. The cycling model of CRL regulation.

Schematic of the cycling model of CRL regulation in which both cycles of cullin neddylation/deneddylation and CAND1 binding are required for efficient CRL activity with respect to F-box protein recycling. In this model, neddylation results in CAND1 displacement, allowing for F-box protein-adaptor binding. Protein degradation takes place within this active complex whilst cullin deneddylation by the CSN complex enables CAND1 binding and F-box protein-adaptor displacement, yielding an inactive complex. Modified from Cope and Deshaies, 2003.

CSN complex (figure 9) (Bornstein et al., 2006) presumably allowing for efficient substrate degradation, upon which the CSN complex deneddylates the cullin subunit in order to protect F-box proteins from degradation, and enabling CAND1 binding to the cullin.

1.4.2 Deubiquitination of CRLs by the CSN complex

F-box proteins have been shown to be unstable, and degraded in a ubiquitin proteasome system dependent manner by an autocatalytic mechanism within their cognate SCF complex (Galan and Peter, 1999). Furthermore, the CSN complex has been shown to recruit the deubiquitinating enzyme Ubp12 in *S. pombe*, and stabilize F-box proteins. Initially, the deubiquitinating activity of CSN-Ubp12 was shown to inhibit *S. pombe* Cul1 and Cul3 based CRL activity *in vitro* as measured by ubiquitin ligase activity assays (Zhou et al., 2003). However, also documented in this report was the stabilization of the *S. pombe* F-box protein, Pop1, by CSN-Ubp12, as determined by the decreased half-life of Pop1 in CSN5 and Ubp12 mutants (Zhou et al., 2003). Subsequently, Wee *et al*, 2005 also demonstrated the destabilization of Pop1 in *S. pombe* CSN5 and Ubp12 mutants and further showed that this destabilization resulted in the increased half-life of the Pop1 target protein Rum1. In addition, ubiquitination and destabilisation of the Cul3 adaptor protein Btb3 was also observed in CSN-Ubp12 deficient cells (Wee et al., 2005). Altogether, these data suggest that, although CSN-Ubp12 has been associated with CRL inhibition *in vitro*, the deubiquitinating activity of CSN-Ubp12 facilitates CRL function *in vivo* by counteracting autocatalytic adaptor instability. Thus, cumulatively, data

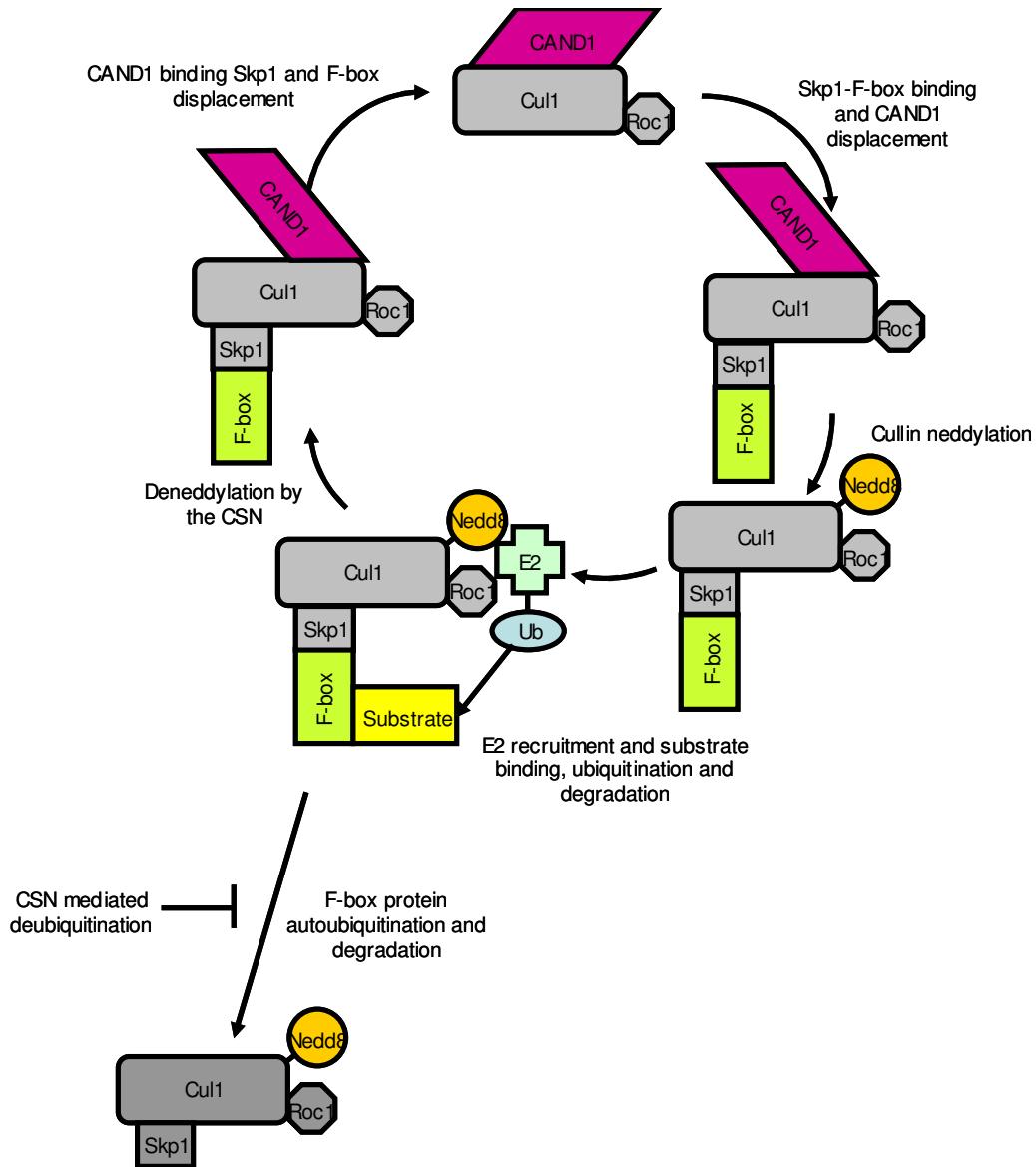


Figure 8. A modified cycling model of CRL regulation.

Schematic of a modified cycling model of CRL regulation in which the more recent findings of CAND1 displacement by F-box protein-adaptor and CRL function facilitation by the prevention of F-box protein degradation are included. In this model, both cycles of cullin neddylation/deneddylation and CAND1 binding are required for the efficient functioning of CRLs and prevention of F-box protein autocatalytic degradation. Also shown is the CSN mediated deubiquitination of F-box proteins, the second mechanism by which the CSN prevents F-box autocatalytic degradation.

indicates that both the deneddylation and deubiquitination activities of the CSN complex function to facilitate CRL activity *in vivo* by stabilising CRL substrate adaptor proteins and enabling adaptor protein recycling or switching (figure 8).

It is also noteworthy that the human homolog of Ubp12, USP15, has been shown to associate with the CSN complex from human erythrocytes (Hetfeld et al., 2005). However, although CSN-USP15 has been shown to deubiquitinate the CRL substrate I κ B α (Schweitzer et al., 2007), CSN-USP15 mediated stabilisation of F-box proteins is yet to be directly determined in human cells.

1.4.3 A third function for the CSN complex in CRL regulation?

Recently, a novel function of the CSN complex in the regulation of CRLs has been proposed. This mechanism involves the facilitation of CRL activity via CSN mediated dissociation of ubiquitinated substrate from the CRL, allowing for the binding of non-ubiquitinated substrate (Miyauchi et al., 2008). The data presented suggests that the activity of the Cul2/elonginB/C/VHL CRL is enhanced by the CSN complex independently of both the deneddylating and USP15 deubiquitinating activities of the CSN. Furthermore, they demonstrate that the CSN complex causes the dissociation of ubiquitinated substrate from Cul2/elonginB/C/VHL and that CSN knockdown in human cells impairs the degradation of the Cul2/elonginB/C/VHL substrate HIF-1 α , potentially as a result of an increased association between HIF-1 α and the Cul2 based CRL complex (Miyauchi et al., 2008). However, the contribution of this function of the CSN complex

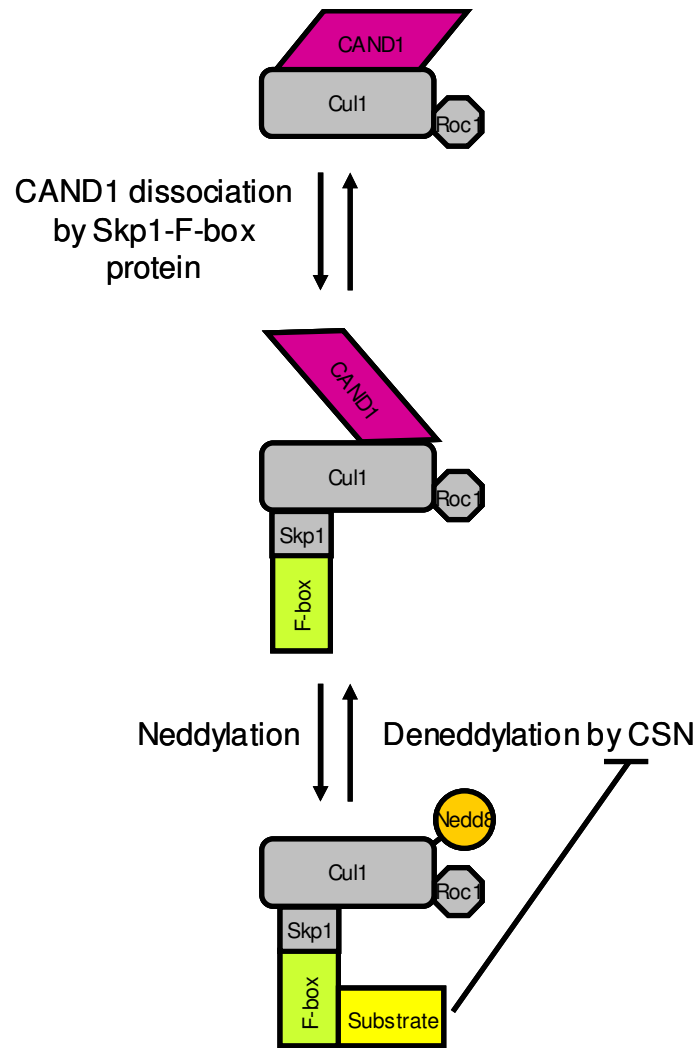


Figure 9. An alternative model of CRL regulation.

A series of reversible protein interactions/modifications has been implicated in the regulation of CRLs. In this model, Skp1-F-box protein binding to the cullin dissociates CAND1 from the cullin and neddylation follows this. Substrate binding ensues and inhibits cullin deneddylation, presumably enabling efficient breakdown of substrate, upon which deneddylation can occur to protect the F-box protein from autocatalytic degradation. Image adapted from Bornstein *et al*, 2006.

to the regulation of other CRLs remains to be determined. Further, given that proteins can be efficiently ubiquitinated both *in vitro* (Cope and Deshaies, 2003, Miyauchi et al., 2008) and *in vivo* (Miyauchi et al., 2008) in the absence of CSN, with the addition of the CSN complex having a relatively small effect (Miyauchi et al., 2008), the physiological relevance of CSN in the direct facilitation of protein ubiquitination remains to be determined.

1.4.4 Consequences of CSN impairment on CRL function

Consistent with the cycling model, impairment of CSN function results in the loss of F-box proteins. For example, disruption of CSN2 in *Neurospora* results in the loss of the F-box protein FWD-1, the β -TrCP homolog (He et al., 2005). This loss is prevented by mutation of the F-box motif, through which the F-box protein is recruited into the SCF complex. Furthermore, a CSN2 mutant *A. thaliana* has been identified in which the F-box protein TIR1 (transport inhibitor response protein 1) is unstable; an instability dependent on the proteasome (Stuttman et al., 2009). These findings are consistent with the cycling model in which the CSN complex facilitates SCF function by preventing autocatalytic F-box protein degradation within its cognate SCF complex. The proteasome dependent degradation of F-box proteins in the absence of CSN activity has also been demonstrated in human cells by multiple laboratories. Cumulatively, CSN5 knockdown has been shown to result in the loss of the F-box proteins Skp2, Cyclin F, Cdc4 and Fbx7 (F-box protein 7), with the addition of the proteasome inhibitor MG132 inhibiting CSN5 knockdown mediated F-box protein loss (Cope and Deshaies, 2006, Denti et al., 2006).

Furthermore, as a consequence of the loss of the F-box proteins Skp2 and Cdc4, the target proteins p27, cyclin E and c-myc have been shown to accumulate in cells lacking CSN5 (Cope and Deshaies, 2006, Denti et al., 2006).

In addition to the loss of F-box proteins, the stability of other components of the SCF complex has been shown to be affected by the loss of CSN function. For example, CSN2 knockout in *Neurospora* results in the loss of the adaptor protein Skp1 which links the F-box protein to the cullin subunit (He et al., 2005). Furthermore, the instability of the cullin subunit of the CRL has been observed in cells lacking a CSN subunit. In addition to cullin hyperneddylation, knockout of either CSN4 or CSN5 in *Drosophila* resulted in the loss of cullin protein; Cul1 protein was lost in CSN4 knockouts whilst Cul1, Cul3 and Cul4 protein was lost as a result of CSN5 knockout (Wu et al., 2005). Interestingly, cullin stability was found to be restored with a double knockdown of CSN5 and Nedd8, indicating that the intrinsic instability of cullins is conferred by the attachment of Nedd8 (Wu et al., 2005), and further demonstrating the function of CSN deneddylase activity in the stability and recycling of cullins. The instability of Cul1 has also been demonstrated in a *Neurospora* CSN2 knockout (He et al., 2005), whereas a study in human cells concluded that there was no effect of CSN knockdown on cullin stability (Cope and Deshaies, 2006). However, although there was no reduction in the levels of either Cul1 or Cul3 protein in HEK293 cells lacking CSN5 reported in this manuscript, it could be argued that the loss of Cul2 observed is indeed significant, particularly if densitometry was used to analyse this data set. Finally, loss of the RING finger protein Roc1/Rbx1, responsible for E2 recruitment to the E3 ligase, has been reported in HeLa cells lacking

CSN5 (Peth et al., 2007a). Cumulatively, data suggests that the CSN complex is not only required for the protection of F-box proteins from autocatalytic degradation, but may also be fundamental, in a cell type and organism dependent manner, to the stability of all CRL components.

1.5 Other functions of the CSN complex

1.5.1 The CSN and protein phosphorylation

The CSN complex isolated from human erythrocytes has been demonstrated to mediate protein phosphorylation (Seeger et al., 1998). As none of the CSN subunits contain a defined kinase domain, this kinase activity was referred to as a CSN associated kinase activity (Naumann et al., 1999). The CSN complex was subsequently shown to co-purify with inositol 1,3,4-trisphosphate 5/6-kinase (5/6-kinase) from calf brain (Wilson et al., 2001); an association later identified in human cells (Sun et al., 2002) and *Arabidopsis* (Qin et al., 2005). Further, the protein kinases CK2 and protein kinase D (PKD) have been shown to co-purify with the CSN complex from human erythrocytes (Uhle et al., 2003). These three kinases have been shown to phosphorylate previously described targets of CSN associated kinases (Bech-Otschir et al., 2001, Seeger et al., 1998, Sun et al., 2002, Uhle et al., 2003), and to be inhibited by curcumin (Sun et al., 2002, Uhle et al., 2003), the yellow pigment in turmeric which is known to inhibit CSN associated kinases (Henke et al., 1999). These data verify that these kinases are indeed CSN associated kinases, although they do not rule out the possibility that there are other kinases that associate with the CSN complex which remain to be identified.

CSN associated kinase activity has been demonstrated to regulate the function or stability of several proteins. For example, c-jun (Naumann et al., 1999, Uhle et al., 2003) and microtubule end-binding protein 1 (EB1) (Peth et al., 2007b) phosphorylation by CSN

associated kinases results in stabilisation of these proteins and protection from ubiquitin-proteasome mediated degradation, whilst CSN mediated phosphorylation of p53 and estrogen receptor alpha (ERalpha) signals these proteins for degradation (Bech-Otschir et al., 2001, Callige et al., 2005). Additionally, Cohen and colleagues have provided data to suggest that CSN mediated phosphorylation of interferon consensus sequence-binding protein (ICSBP) at serine 260 facilitates the transcriptional repressor activity of ICSBP (Cohen et al., 2000).

Multiple observations collectively appear to implicate the requirement of the intact CSN complex for kinase activity. Firstly, the CSN associated kinases identified to date, CK2, PKD and 5/6-kinase, interact with CSN3/7, CSN3 (Uhle et al., 2003) and CSN1 (Sun et al., 2002), respectively. Secondly, p27 (Tomoda et al., 1999), c-jun (Claret et al., 1996), p53 (Bech-Otschir et al., 2001), EB1 (Peth et al., 2007b) and ERalpha (Callige et al., 2005) have been shown to interact with the CSN via CSN5, whilst ICSBP interacts with CSN2 (Cohen et al., 2000). Finally, CSN5 expression in a siCSN5 background which seems to have no significant effect on the remaining CSN complex rescues c-jun protein levels (Peth et al., 2007a), whilst CSN5 expression in a siCSN1 background which has a reduced level of intact CSN complex (Peth et al., 2007b) fails to rescue c-jun protein (Peth et al., 2007a). It is also noteworthy that the kinase activity of the CSN complex has been shown to be independent of CSN deneddylase activity, with the expression of the D151N deneddylase dead CSN5 in a siCSN5 background retaining the ability to rescue c-jun protein (Peth et al., 2007a).

1.5.2 The CSN and deubiquitination

The CSN complex has been associated with deubiquitinase activity (Groisman et al., 2003, Zhou et al., 2003). The CSN complex has also been shown to associate with the deubiquitinase Ubp12p in *S. pombe* (Zhou et al., 2003) and the human ortholog, ubiquitin specific protease 15 (USP15) (Hetfeld et al., 2005). Ubp12p has been demonstrated to depolymerise polyubiquitin chains *in vitro* (Zhou et al., 2003), whilst USP15 associated CSN purified from human erythrocytes was shown to both depolymerise polyubiquitin and cleave ubiquitin from a model substrate of the 26S proteasome (Hetfeld et al., 2005). In accordance with this, the human CSN complex was shown to deubiquitinate polyubiquitinated Cul4A *in vitro* to yield non-ubiquitinated Cul4A (Groisman et al., 2003), suggesting that the CSN mediates both depolymerisation of polyubiquitin and cleavage of mono/polyubiquitin from protein substrates.

Interestingly, a deneddylase dead CSN complex, although retaining the ability to depolymerise polyubiquitinated Cul4A, failed to cleave monoubiquitin from Cul4A *in vitro* (Groisman et al., 2003). These data suggest that the CSN complex is associated with two separate deubiquitinase activities, and further indicate that the metalloprotease domain of CSN5, responsible for deneddylation, may also deubiquitinate target proteins by a similar mechanism. Similar findings were made *in vivo*, with an increase in ubiquitinated exosomal heat shock protein 70 (HSP70) protein being demonstrated in a human cell line transfected with mutant CSN5 expressing plasmid relative to cells expressing wild-type CSN5 (Liu et al., 2009). It is noteworthy that this study also

determined the requirement for the intact CSN complex for deubiquitination, with the addition of CSN5 to an *in vitro* deubiquitination assay yielding no effect on the level of ubiquitinated HSP70 protein (Liu et al., 2009). Although a direct function of the CSN complex in protein deubiquitination via the metalloprotease domain of CSN5 has been suggested, further work would have to be carried out in order to rule out the possibility that a yet unidentified deubiquitinase associates with the CSN complex through this domain. Nonetheless, the CSN complex has been demonstrated to deubiquitinate multiple protein targets, including CRL substrate adapter proteins (Wee et al., 2005) and I κ B α (Schweitzer et al., 2007), both of which are protected from degradation by deubiquitination (Schweitzer et al., 2007, Wee et al., 2005), and HSP70 (Liu et al., 2009).

More recently, the CSN complex has been shown to associate with a lysine 63 (K63) specific deubiquitinase, Brcc36 (Cooper et al., 2009). Whilst K48 linked ubiquitin chains signal for protein degradation (Pickart, 2004), K63 linked ubiquitin chains have non-proteolytic functions (Cooper et al., 2009). This association is therefore indicative of a role for the CSN associated deubiquitinase activity not only in the regulation of protein degradation but also in the modulation of protein function.

1.5.3 The CSN and transcriptional regulation

As a regulator of the function and/or stability of a myriad of proteins, including transcription factors, the finding that the CSN complex regulates transcription

(Chamovitz, 2009, Su et al., 2009) is not surprising. However, the question remains as to whether the nuclear CSN complex can regulate transcription directly (Chamovitz, 2009).

The CSN has been shown in multiple systems to associate with chromatin (Groisman et al., 2003, Menon et al., 2007, Ullah et al., 2007), implying a potential direct role for the CSN in regulating transcription. In two of these systems the CSN likely functions at chromatin to regulate protein function or stability rather than having a direct function in transcriptional regulation (Groisman et al., 2003, Ullah et al., 2007). However, the study by Menon and colleagues suggests a direct role for the CSN complex in transcriptional regulation. CSN8 deficient CD4⁺ T cells failed to accumulate all G1 cyclins and cyclin dependent kinases (CDKs) studied upon T cell antigen receptor (TCR) stimulation (Menon et al., 2007). If this finding were attributable to altered protein degradation in the absence of CSN8 then proteasome inhibition should restore protein levels of cyclins and CDKs. However, this study demonstrated that treatment with the proteasome inhibitor MG132 could not rescue these proteins (Menon et al., 2007), indicating a proteasome independent function of the CSN complex in the regulation of these proteins. Further, given the findings that mRNA levels of cyclins could not be upregulated upon TCR stimulation in CSN8 deficient cells and that both CSN1 and CSN8 (and probably the entire CSN complex) precipitate with a cyclin promoter in chromatin immunoprecipitation (ChIP) assays (Menon et al., 2007), it is probable that the CSN complex can function in the direct regulation of transcription via a proteasome independent mechanism. It is noteworthy that in this instance an indirect function of the CSN complex in transcriptional regulation cannot be completely ruled out. For example,

transcription factor activity modification could occur as a result of CSN associated kinase activity at the promoter. Nonetheless, these data do implicate the CSN complex in the direct regulation of transcription, with the exact mechanism still to be elucidated.

Although CSN subunits have been shown to interact with chromatin, a direct interaction between the CSN complex and DNA has not been demonstrated. Interestingly, however, the recent elucidation of the structure of CSN7 has demonstrated that the winged helix subdomain of the PCI domain has a structure comparable to that of winged helix nucleic acid binding proteins (Chamovitz, 2009, Dessau et al., 2008), whilst modelling shows that this domain of CSN7 has the potential to interact with DNA (Dessau et al., 2008). Although a direct interaction between the CSN complex and DNA remains to be demonstrated experimentally, these data suggest that the CSN complex has the potential to bind DNA with enhanced affinity via its six PCI domains (Dessau et al., 2008) and may therefore directly regulate transcription.

1.5.4 CSN subcomplexes

Although the CSN complex is ~500kDa, a ~100kDa cytoplasmic CSN5 containing complex was identified in mammalian cells. The occurrence of this subcomplex was inhibited by the nuclear export inhibitor leptomycin B (LMB), suggesting that this subcomplex is produced from nuclear COP9 signalosome (Tomoda et al., 2002). Immunoprecipitation of this subcomplex with an antibody specific for the subcomplex bound CSN5 co-immunoprecipitated CSN4, 6, 7 and 8, but not subunits CSN1, 2 or 3

(Tomoda et al., 2002). Several findings implicate this CSN5 containing subcomplex in the nuclear export of p27 protein. First, mutation of the nuclear export signal (NES) of CSN5 resulted in nuclear accumulation of both CSN5 and p27. Second, expression of a dominant negative CSN5 N-terminus (lacking the C-terminus NES), which did not affect the intact CSN complex and fractionated in smaller complexes, also resulted in an increase in nuclear p27 protein (Tomoda et al., 2002). Third, overexpression of components of this subcomplex resulted in reduced p27 protein, and further, CSN7 overexpression was shown to result in the LMB sensitive redistribution of CSN5 to the cytoplasm and loss of nuclear p27 signal (Tomoda et al., 2002). However, it is important to note that this study did not address whether CSN5 interacts with the other CSN subunits together, or in various combinations to produce multiple subcomplexes. The latter is probable as suggested by both the small size of the identified subcomplex/subcomplexes and given the finding that overexpression of CSN4, which co-immunoprecipitated with the CSN5 containing subcomplex, does not affect p27 protein (Tomoda et al., 2002). Further, a more recent report has demonstrated using native-PAGE that CSN subunits occur in multiple distinct subcomplexes (Fukumoto et al., 2005). Collectively, these data implicate a CSN5/6/7/8 ~100kDa containing CSN subcomplex in the nuclear export of p27 and further suggest the occurrence of other CSN subcomplexes with unidentified functions.

A CSN5 containing CSN subcomplex, which negatively regulates p27 protein, has also been identified in both chronic myeloid leukaemia (CML) cell lines and primary CMLs (Tomoda et al., 2005), although the constituent subunits were not identified. Interestingly,

this CSN subcomplex has been shown to be a downstream mediator of BCR-ABL kinase activity (Tomoda et al., 2005); this topic is discussed in section 1.8. These data suggest that the activity of a CSN subcomplex has the potential to contribute to leukaemogenesis.

The function of a CSN subcomplex in regulating the level of p27 protein has also been demonstrated *in vivo*. Embryonic fibroblasts (MEFs) from CSN5 heterozygous mice, in which downstream proteins of the CSN complex including Cul1, Skp2 and p53 were unaffected, contained only 40% of the CSN subcomplex relative to wild-type mice and demonstrated p27 accumulation (Tomoda et al., 2004). In accordance with this, CSN5 heterozygous MEFs grew significantly slower than wild-type MEFs and, at 15 weeks, heterozygous mice were significantly smaller (~15%) than wild-type mice (Tomoda et al., 2004).

Although this is not an exhaustive review of CSN subcomplexes, the above data provides strong evidence for both the occurrence and functionality of CSN subcomplexes. In addition, many substoichiometric complexes were identified in a recent structural study of the CSN complex (Sharon et al., 2009). However, much more work is required to determine the precise function, regulation and physiological relevance of CSN subcomplexes.

The alternative functions of the CSN/CSN subcomplexes discussed above may explain why, in some organisms, different CSN subunit disruption results in divergent phenotypes. For instance, CSN4 and CSN5 null mutations in *Drosophila* result in

different phenotypes, with that of CSN4 mutation appearing more severe (Oron et al., 2002). These differences may be attributable to the fact that these mutations have divergent effects on the stability of the intact CSN complex (Oron et al., 2002), and that in CSN5 mutants, the retained CSN complex lacking CSN5 possibly still functions in deneddylation independent processes such as phosphorylation and deubiquitination. Further, although null mutation in CSN subunits 1, 2, 4 and 5 in *S. pombe* all result in hyperneddylated Cul1, CSN4 and CSN5 mutants do not have the same phenotype as CSN1 and CSN2 mutants (Mundt et al., 2002), suggesting that CSN1 and CSN2 function as a subcomplex independent of CSN4 and CSN5. However, these differences may also be explained by the CSN independent functions of CSN subunits (see section 1.7).

1.5.5 The CSN as an alternative lid for the proteasome?

As already discussed, the 19S regulatory particle of the 26S proteasome is important for substrate recognition and delivery to the 20S core particle where substrates are subsequently degraded. Interestingly, the 19S particle has been shown to be formed from two subcomplexes called the base and the lid (Glickman et al., 1998). The base is sufficient to activate the protein degradation activity of the 20S core particle but ubiquitin mediated protein degradation requires both the base and lid of the regulatory particle (Glickman et al., 1998), with the Rpn11 subunit of the lid being responsible for target protein deubiquitination prior to proteasomal degradation (Sharon et al., 2009, Verma et al., 2002).

The CSN complex displays homology to the lid of the proteasome (Glickman et al., 1998). Further, there is data to suggest that the CSN complex interacts with the proteasome in plant (Peng et al., 2003), human (Seeger et al., 1998) and mouse (Huang et al., 2005) cells. These observations, together with the findings of both CSN associated deubiquitinase activity (see 1.5.2) and a possible competition between the lid and CSN complex for proteasome binding (Huang et al., 2005), have led to the suggestion that the CSN complex may be an alternative lid of the proteasome (Li and Deng, 2003). However, it is important to note that the replacement of the proteasome lid with the CSN complex and any functional significance of this replacement remains to be experimentally determined *in vivo*. Nonetheless, the identified interactions of the CSN complex with the proteasome and CRLs (Huang et al., 2005, Peng et al., 2003) suggest that the CSN may function to bring the processes of protein ubiquitination and degradation into close proximity, thereby increasing the efficiency of ubiquitin mediated protein degradation, whilst also regulating both of these processes via the identified CSN associated deneddylase and deubiquitinase activities.

1.6 The regulation of CSN activity

Given the diverse functions of the CSN complex and the plethora of proteins for which the CSN regulates stability or activity, it would seem extremely probable that the activities of the CSN complex are tightly regulated. However, this topic remains relatively unstudied and subsequently, little is known of the mechanisms of CSN activity regulation.

Several studies have demonstrated the sequestration of CSN5 by protein interaction, suggesting this as a mechanism of CSN activity regulation. CSN5 has been shown by yeast-two hybrid, GST pulldown and co-immunoprecipitation assays to interact with the integrin LFA-1 (Bianchi et al., 2000), the lutropin/choriogonadotropin receptor (LHR) (Li et al., 2000) and the cytokine macrophage inhibitory factor (MIF) (Kleemann et al., 2000). The sequestration of CSN5 at peripheral membranes by unliganded LFA-1 has been demonstrated, whilst CSN5 was redistributed to the nucleus upon LFA-1 stimulation, with a concomitant increase in AP-1 transcriptional activity (Bianchi et al., 2000). In addition, CSN5 interacts with the endoplasmic reticulum localised protein LHR, an interaction which reduces AP-1 promoter driven luciferase reporter activity (Li et al., 2000). Finally, MIF binding to CSN5 in the cytosol has also been shown to reduce c-jun mediated transcriptional activity at AP-1 sites, and further result in reduced c-jun phosphorylation and inhibition of CSN5 dependent p27 protein degradation (Kleemann et al., 2000). Collectively, these data suggest that multiple functions of the CSN and its subunits may be downstream mediators of multiple signalling pathways, and that

cytosolic sequestration of CSN5 may be a mechanism of regulating multiple functions of the CSN complex.

Interestingly, double mutation of CSN5 (a reduction of function mutation generated by T-DNA insertion into a CSN5 intron) and Cul3 in *Arabidopsis* resulted in an increase in the level of CSN5 protein relative to CSN5 mutation alone, and a concomitant increase in deneddylation activity (Gusmaroli et al., 2007). Along with the finding that CSN5/Cul3 double mutation has no significant effect on CSN5 mRNA (Gusmaroli et al., 2007), these data suggest that a Cul3 based E3 ubiquitin ligase may mediate the degradation of CSN5 and thus the activity of the CSN complex. Although this is an interesting possibility, particularly given the prospect of a negative feedback mechanism of CRL regulation, further work is required to exclude any possible indirect effects of Cul3 loss on CSN5 protein level and to determine the specific adapter protein responsible for CSN5 protein degradation.

Overexpression of 1,3,4-trisphosphate 5/6-kinase (5/6-kinase) in HEK293 cells has been shown to result in an increase in CSN5 protein relative to vector control transfected cells by western blot analysis, although a loading control was not shown (Sun et al., 2002). The authors suggest 5/6-kinase induction of CSN5 as a possible regulatory mechanism for CSN5 activity, however much more work would be required to both confirm CSN5 induction by this kinase and to determine the mechanism by which 5/6-kinase increases CSN5 i.e. CSN5 phosphorylation, CSN5 mRNA increase or CSN5 protein stabilisation as examples.

CSN2 and CSN5 appear to be relatively stable outside of the CSN complex (Gusmaroli et al., 2007), are the most readily dissociable subunits of the CSN (Sharon et al., 2009) and have well documented CSN independent functions (see 1.7). Thus, a key mechanism of CSN/CSN subunit function regulation may be dependent upon the level of other CSN subunits and therefore whether CSN2/CSN5 are monomeric or incorporated into the CSN complex. The same can also be said for CSN subcomplexes. Although the occurrence, composition and function of such subcomplexes remains to be elucidated fully, it is plausible that the availability of each of the eight subunits would have great influence on CSN/CSN subcomplex formation and therefore CSN function.

Finally, CSN activity may be regulated by post-translational modification of CSN subunits. For example, the cleavage of CSN6 has been shown to occur upon apoptosis induction in a caspase dependent manner; a modification which increases the deneddylase activity of the CSN complex without affecting CSN mediated protein deubiquitination or phosphorylation (Hetfeld et al., 2008). In addition, CSN2 and CSN7 have been shown to be phosphorylated by CSN associated kinases (Uhle et al., 2003), suggesting another potential mechanism of CSN activity regulation. Further, phosphorylation sites have also been identified in CSN subunits 1, 3 and 8 (Fang et al., 2008). Although the possibility of phosphorylation dependent CSN activity regulation has not been investigated in detail, curcumin treatment has been shown to result in complete loss of the reported CSN subcomplex (Tomoda et al., 2005, Fukumoto et al., 2005) and the collapse of CSN supercomplexes (Fukumoto et al., 2005), implicating the

CSN associated kinases in the regulation of CSN subcomplex/supercomplex formation, possibly via CSN subunit phosphorylation.

1.7 CSN independent functions of CSN subunits

Individual subunits of the CSN complex have been shown to have alternative functions independent of the CSN complex. The discussion here will be of CSN2 and CSN5, as these subunits have been suggested to be relatively stable outside of the CSN complex (Gusmaroli et al., 2007), have recently been shown to be the most readily dissociable, peripheral subunits of the CSN complex (Sharon et al., 2009), and have the most well documented CSN independent functions.

1.7.1 CSN2

Two different splice variants are generated from the CSN2 locus, one encoding the 50kDa CSN2 and the other encoding the ~36kDa Alien protein which consists of the N-terminal 300 amino acids of CSN2 (Chamovitz, 2009, Tenbaum et al., 2003). Interestingly, part of the PCI domain of CSN2 is lacking from Alien (Chamovitz, 2009) and the intracellular distribution of Alien has been shown to be distinct from that of CSN subunits (Eckey et al., 2007), making incorporation of this isoform into the CSN complex unlikely, although not experimentally determined. Any potential CSN independent function of CSN2 remains relatively unstudied, whilst the function of Alien has undergone significant investigation. Given that the amino acid sequence of Alien is identical to the N-terminal of CSN2 and the probable independence of Alien from the CSN, it remains possible that CSN2 and Alien have overlapping functions independent of the CSN complex. The function of Alien is thus worthy of discussion here.

Alien was initially shown to interact with thyroid hormone receptor (TR) by yeast two-hybrid, GST pull-down and co-immunoprecipitation assays; an interaction shown to be thyroid hormone sensitive (Dressel et al., 1999). Further, Alien was shown to enhance TR mediated transcriptional repression in the absence of thyroid hormone, thus identifying Alien as a transcriptional corepressor (Dressel et al., 1999). Alien has since been demonstrated as an interacting partner for multiple nuclear hormone receptors including the ecdysone receptor (Dressel et al., 1999), the vitamin D receptor (Polly et al., 2000), DAX-1 (Altincicek et al., 2000) and the androgen receptor (Moehren et al., 2007). Interestingly, in addition to gene silencing at nuclear hormone receptors, Alien has also been shown to both interact with and repress the transcriptional activation activity of the transcription factor E2F1 (Tenbaum et al., 2007).

The mechanisms by which Alien mediates transcriptional repression have been investigated (Papaioannou et al., 2007). Initially, Alien was shown to interact with a known component of a large histone deacetylase complex, SIN3A, by both yeast two-hybrid and co-immunoprecipitation assays (Dressel et al., 1999) and GST pull-down assay (Moehren et al., 2004). Further, co-expression of SIN3A with Alien resulted in increased transcriptional repression relative to Alien expression alone (Moehren et al., 2004). Together with the finding that Alien also interacts with histone deacetylase (HDAC) proteins (Papaioannou et al., 2007), these data indicate that one mechanism by which Alien mediates transcriptional repression is via recruitment of HDAC machinery. However, addition of a HDAC inhibitor reduced Alien mediated transcriptional repression only partially (Dressel et al., 1999), suggesting at least a second mechanism by

which Alien silences transcription. Indeed, interaction between Alien and nucleosome assembly protein 1 (NAP1) has been demonstrated, with the addition of Alien to a supercoiling assay resulting in a dose dependent increase in NAP1 mediated DNA supercoiling (Eckey et al., 2007). Collectively, these data suggest that Alien mediates transcriptional repression by at least two mechanisms, both HDAC dependent and independent, and both of which rely upon chromatin modification for DNA compaction.

1.7.2 CSN5

CSN5 was identified in a yeast two hybrid screen of a human B lymphocyte cDNA library as a c-jun interacting protein, and this interaction further verified in co-immunoprecipitation assays (Claret et al., 1996). Subsequently, CSN5 was shown to increase DNA binding of the transcription factor c-jun to its cognate AP-1 transcription activation sites, and increase c-jun mediated transcriptional activity (Claret et al., 1996). Similar findings were also made regarding junD, but not v-jun or junB (Claret et al., 1996), indicating that, through selective interaction with members of the jun family of transcription factors, CSN5 (or jun activation domain binding protein 1; JAB1) increases the specificity of transcriptional activation at AP-1 transcription sites. Through this function CSN5 has been implicated in both the integrin LFA-1 (Bianchi et al., 2000) and the cytokine macrophage migration inhibitory factor (MIF) (Kleemann et al., 2000) signalling pathways. In addition to c-jun mediated transcription, CSN5 has also been shown to potentiate the hormone dependent transcriptional activation activity of steroid hormone nuclear receptors (Chauchereau et al., 2000).

CSN5 has been implicated in the nuclear export of proteins such as Smad7 (Kim et al., 2004), p53 (Oh et al., 2006a) and West Nile virus capsid (WNVCP) (Oh et al., 2006b). However, it is important to note with JAB1 associated literature that many publications do not discern between CSN5 monomer function and CSN5 function within the CSN complex. For example, although Oh and colleagues demonstrated that the fragment of CSN5 required for p53 nuclear export does not interact with other CSN subunits, suggesting that CSN5 mediated p53 nuclear export is independent of the CSN complex (Oh et al., 2006a), others have not investigated whether CSN5 mediated protein nuclear export is dependent on the CSN complex/subcomplex rather than monomeric CSN5 (Kim et al., 2004, Oh et al., 2006b). Indeed, a CSN subcomplex is implicated in the nuclear export of p27 protein (Tomoda et al., 2002).

Similar caution should also be used when interpreting data regarding JAB1 function as a transcriptional coactivator. For instance, the increased c-jun dependent AP-1 directed transcriptional activity observed in the presence of CSN5/JAB1 (Claret et al., 1996) could be attributable to a function of CSN5 within the intact CSN complex as opposed to a function of JAB1 monomer. In support of this, the stabilisation of c-jun protein towards the ubiquitin-proteasome system by CSN associated kinase mediated c-jun phosphorylation has been demonstrated (Uhle et al., 2003). Moreover, the observed increase in AP-1 driven luciferase activity in the presence of c-jun and JAB1 (Claret et al., 1996, Wang et al., 2004) was reduced to the level of luciferase activity in the presence of c-jun alone upon treatment with the CSN associated kinase inhibitor curcumin (Wang et al., 2004). Collectively, these data suggest that the positive effect

exerted on c-jun mediated transcriptional activation at AP-1 sites by CSN5 may be mediated through the CSN complex rather than CSN5/JAB1 function as a monomer.

1.8 The CSN and leukaemia

A role for the CSN in cancer is emerging, with aberrant expression of CSN subunits identified in multiple cancers (Richardson and Zundel, 2005, Adler et al., 2008, Patil et al., 2005, Yan et al., 2007). Indeed, the deneddylase activity of the CSN has been shown to be essential for breast epithelial cell transformation and *in vivo* tumour progression (Adler et al., 2008), whilst inhibition of CSN associated kinases resulted in reduced pancreatic cell proliferation (Li et al., 2009). However, to date the links between the CSN complex and leukaemia are limited. Nevertheless, associations are beginning to be made and are therefore of interest for discussion here.

Myeloid leukaemia factor 1 (MLF1) has been shown to regulate the level of p53 via CSN subunit 3 (CSN3) (Yoneda-Kato et al., 2005). The NPM (nucleophosmin)/MLF1 fusion protein, generated by the chromosomal translocation t(3;5)(q25.1;q34) (Yoneda-Kato et al., 1996), is associated with myelodysplastic syndrome, often resulting in progression to acute myeloid leukaemia (Raimondi et al., 1989). Yoneda-Kato *et al*, 2005 demonstrated that MLF1 induces p53 mediated cell cycle arrest via CSN3-directed downregulation of COP1 (an E3 ligase which targets p53 for degradation). They suggest therefore, that the inactivation of MLF1 by formation of the NPM/MLF1 fusion protein would result in potentially tumourigenic dysregulated p53 degradation. These data further suggest a potential role for CSN3 in leukaemogenesis. However, it remains to be determined whether COP1 mediated p53 degradation is regulated via CSN3 alone or as a component of the intact CSN complex.

A small CSN subcomplex has been shown to be a downstream mediator of BCR-ABL kinase activity (Tomoda et al., 2005). BCR-ABL is an oncogenic fusion protein with constitutive tyrosine kinase activity, formed as a result of the Philadelphia chromosome translocation, which is present in 90% of chronic myeloid leukaemia (CML) patients (Rowley, 1980). A 100kDa CSN subcomplex was identified in CML cell lines and primary CML samples which was not detectable in other cell lines or primary cells tested. This complex was found to be upregulated by BCR-ABL, with BCR-ABL kinase inhibition resulting in a reduced level of the CSN subcomplex and a concomitant increase in p27. Furthermore, targeted degradation of CSN5, a component of the CSN subcomplex, resulted in the loss of BCR-ABL mediated p27 degradation (Tomoda et al., 2005). Together, these results suggest that the cytoplasmic shuttling and subsequent degradation of p27 associated with the CSN subcomplex (Tomoda et al., 2002) is a contributing factor to the oncogenic transformation mediated by the BCR-ABL fusion protein in CML.

The above observations, along with the recent association of CSN5 with non-Hodgkin's lymphoma (Qi et al., 2006, Wang et al., 2008), are suggestive of a role for the CSN complex in haematological malignancy, including leukaemia. However, observations to date have been made regarding either a CSN subcomplex or an individual subunit of the CSN. The intact CSN complex has not, therefore, been associated with leukaemia *per se*. Nonetheless, with the plethora of proteins known to be degraded by CRLs and the diverse cellular processes which they regulate, and given the multitude of activities associated

with the CSN complex, it is not difficult to envisage a role for dysregulated CSN complex activity in leukaemia.

1.9 Chronic myeloid leukaemia

Chronic myeloid leukaemia (CML) is a disease of haematopoietic stem cells predominantly arising from a genetic aberration called the Philadelphia chromosome (Hehlmann et al., 2007). The Philadelphia chromosome is formed from the translocation t(9;22)(q34;q11), which results in the production of the BCR-ABL oncogene on chromosome 22. This oncogene encodes the BCR-ABL fusion protein, a tyrosine kinase with aberrant activity (Hehlmann et al., 2007) which is the underlying cause of CML (Weisberg et al., 2007). Therapy targeting the activity of this fusion protein has revolutionised CML treatment. Treatment with imatinib, an ABL kinase inhibitor which competitively binds at the ATP-binding site, yields good responses in patients with early phase, chronic CML (Hehlmann et al., 2007). However, problems have arisen with imatinib treatment including the limited response of later stage blast crisis CML to imatinib (Sawyers et al., 2002), the development of imatinib resistant disease (Gorre et al., 2001) and the insensitivity of CML stem cells to imatinib treatment (Graham et al., 2002). As a result, other inhibitors of BCR-ABL kinase activity have been developed (Weisberg et al., 2007). However, a limited response in blast crisis CML still appears to be a problem, and mutations have also been identified which confer resistance to these inhibitors (Weisberg et al., 2007).

As the above problems with BCR-ABL targeting in the treatment of CML persist, studies have begun into the use of other compounds in combination with imatinib to overcome resistant disease, gain greater responses in blast crisis CML, and target the CML stem

cell. Three key findings suggest the CSN complex may be a viable target in CML. First, one process being targeted in combination with imatinib in CML is intracellular protein degradation (Bellodi et al., 2009, Gatto et al., 2003). Second, a CSN subcomplex has been shown to be a downstream mediator of BCR-ABL kinase activity in CML (Tomoda et al., 2005). Third, ectopic CSN5 expression in mice, shown to incorporate into CSN complexes, resulted in progressive myeloid hyperplasia with overproduction of granulocytes, resembling chronic phase CML (Mori et al., 2008).

1.10 Project aims

As discussed, the CSN is a highly conserved complex with a multitude of functions, and is thus studied in a wide variety of organisms. Studies of the CSN complex in human cells to date are generally limited to the use of cell lines such as HeLa and HEK293. This study aimed to investigate the function of the CSN in a haematological setting and in relation to human leukaemia. This study thus used a cell line model of human blast crisis CML, K562, derived from a 53 year old female with CML that had progressed to blast crisis following splenectomy (Lozzio and Lozzio, 1975).

In order to achieve this aim, first the non-catalytic subunit CSN2 and the deneddylase activity containing subunit CSN5 were knocked down in K562 cells using a short hairpin RNA (shRNA) technique. Once CSN subunit knockdowns were established, studies were carried out in an attempt to answer the following questions:

1. Does CSN subunit knockdown in K562 result in aberrant CRL activity and if so, is this aberrant activity similar to that observed in other organisms and human cell lines?
2. With the emerging function of the CSN in transcriptional regulation, either direct or indirect, does CSN subunit disruption in K562 have any effect on the level of F-box protein or CSN subunit mRNA?
3. Given that CSN subunit loss is lethal in higher eukaryotes and that CSN subunit disruption has been associated with reduced proliferation and cell death, what are

the consequences of CSN subunit knockdown for K562 cell proliferation and death?

4. Are the molecular and cellular effects of CSN2 and CSN5 knockdown in K562 the same, and if not, what may be the cause of any divergence?

Chapter 2.0:
Materials and Methods

2.1 Cell culture and treatments

2.1.1 Maintenance of cell lines

Cell lines were maintained in RPMI 1640 (Invitrogen Gibco, Paisley, U.K.) supplemented with 100U/ml penicillin, 100µg/ml streptomycin and 10% v/v foetal bovine serum (all Invitrogen Gibco). Cultures were maintained at 37°C with 5% CO₂. Cells were diluted one part in three parts media every 48 hours to maintain a cell density between 2x10⁵ and 1x10⁶ cells/ml, to maintain cells in exponential growth.

2.1.2 Storage of cell lines in liquid nitrogen

1x10⁷ cells were harvested by centrifugation at 1500 rpm for 5 minutes (FALCON 6/300, MSE, London, U.K.). The supernatant was discarded, the cell pellet resuspended in 1ml freezing mix (95% FBS, 5% DMSO) and the cell suspension transferred to a cryovial. Cells were slowly frozen by placing the vials in a sealed polystyrene container and incubating this at -20°C for 60 minutes and -80°C overnight. Cells were stored in liquid nitrogen thereafter.

2.1.3 Recovery of cell lines from liquid nitrogen

A vial containing 1x10⁷ cells (see above) was removed from liquid nitrogen and thawed rapidly in water (50°C) for 2-3 minutes. Cells were transferred to a 25ml universal and

0.5, 1, 2, 5 and 10ml aliquots of cold media added drop wise to gradually dilute the freezing mix and prevent apoptotic shock. The cell suspension was centrifuged at 1500 rpm for 5 minutes (FALCON 6/300, MSE) and the supernatant discarded. The cell pellet was resuspended in 2ml cold media, transferred to a 24 well plate and maintained as in 2.1.1.

2.1.4 Treatment of cells with MG132

Transfected cells were set at a density of 3×10^5 cells/ml in a total volume of 4ml and this volume split equally into two wells of a 24 well plate. DMSO (0.2 μ l) was added to the control well and 10 μ M MG132 (BIOMOL, Exeter, U.K.; 0.2 μ l of a 100mM stock in DMSO) added to the other. Cells were cultured for 18 hours with treatment before being harvested for western blot analysis. Time points for MG132 treatment are as indicated in the results sections.

2.1.5 Treatment of cells with 3-methyladenine

3-methyladenine (3-MA, Sigma, Dorset, U.K.) powder was added to media and this mix incubated at 100°C for 10 minutes to give a 1x stock solution (10mM). Control media was also incubated at 100°C for 10 minutes. Day 3 post transfection, 2.4×10^6 transfected cells were pelleted by centrifugation at 1500rpm for 5 minutes (FALCON 6/300, MSE) and the supernatant discarded. Half of the cells were resuspended in 3ml control media (see 2.1.1) and the other half resuspended in 3ml media supplemented with 10mM 3-MA.

Cells were plated in a 12 well plate and all cells/treatments maintained in the same volume and same size culture vessel until they were harvested day 7 post transfection.

2.1.6 Treatment of cells with Bafilomycin A1

To determine optimal concentrations to be used, wild-type K562 cells were plated at 4×10^5 cells/ml in 4ml in a 12 well plate and treated with either DMSO (control), 1nM, 10nM, 100nM or 1 μ M Bafilomycin A1 (Axxora, Nottingham, U.K.; 1mM stock in DMSO). Cells were cultured for 48 hours until harvested for analysis.

In subsequent experiments, day 5 post transfection, transfected cells were plated at 4×10^5 cells/ml in 2ml in a 24 well plate and either DMSO (control) or 1 μ M Bafilomycin A1 (1mM stock in DMSO) added. Cells were cultured for 48 hours until harvested for analysis.

2.1.7 Treatment of cells with rapamycin

Wild-type K562 cells were set at 4×10^5 cells/ml in 6ml in a 25cm² flask and treated with either DMSO (control), 20nM, 50nM or 100nM rapamycin (Sigma; 200 μ M stock in DMSO). Cells were cultured as in 2.1.1 for six days, with rapamycin supplementation into the media as appropriate, and then cells harvested for analysis.

2.2 shRNA construct production

2.2.1 shRNA sequence design

Knockdown sequences were designed using a QIAGEN siRNA tool (<http://www1.qiagen.com/products/genesilencing/customsirna/sirnadesigner.aspx>). These sequences (shown in bold below), flanked by the appropriate hairpin and restriction site sequences were ordered from Sigma Genosys (Sigma).

Vector control scramble: 5'GTACCAAGCGGGATTCAGTAGTTACGTTCAAGAG
ACGTA ACTACTGAATCCCGCTTTTTTTGGAAAT 3' (Forward),

5'CTAGATTTCCAAAAAAGCGGGATTCAGTAGTTACGTCTCTTGAACGTAA
CTACTGAATCCCGCTTG 3' (Reverse),

shCSN2: 5'GTACCAAGCGGCATTAAGCAGTTTCCTTCAAGAGAGGAAACTG
CTTAATGCCGCTTTTTTTGGAAAT 3' (Forward),

5'CTAGATTTCCAAAAAAGCGGCATTAAGCAGTTTCCTCTCTTGAAGGAAA
CTGCTTAATGCCGCTTG 3' (Reverse),

shCSN5: 5'GTACCAAGGGCTACAAACCTCCTGATTTCAAGAGAATCAGGAG
GTTTGTAGCCCTTTTTTTGGAAAT 3' (Forward),

5'CTAGATTTCCAAAAAAGGGCTACAAACCTCCTGATTCTCTTGAATCAG
GAGGTTTGTAGCCCTTG 3' (Reverse).

2.2.2 Oligonucleotide annealing

Lyophilised oligonucleotides (Sigma Genosys, see above) were reconstituted to 100 μ M stock concentration in TE pH8 (10mM Tris HCl pH 8, 1mM EDTA pH 8, in distilled water). An annealed oligonucleotide stock (10 μ M) was produced by mixing 5 μ l of each oligonucleotide with 40 μ l TE pH 8, heating the mix to 70°C for 10 minutes and allowing them to cool slowly by incubating at room temperature for 45 minutes.

2.2.3 Vector preparation

Multi-core buffer (5 μ l) was mixed with 2.5 μ l Acc65I, 2.5 μ l XbaI (all from Promega, Southampton, U.K.), 6 μ g vector DNA (modified pcDNA3.1 vector developed by Heiko Lickert (Kunath et al., 2003) and the volume made up to 50 μ l with DNase RNase free water (Invitrogen Gibco). Vector was digested by 3 hour incubation at 37°C.

Digestion products (40 μ l) were mixed with 10 μ l 5x DNA gel loading buffer (Bioline, London, U.K.) and samples separated by electrophoresis on a 1.5% agarose (Invitrogen, Paisley, U.K.) gel with 0.4 μ g/ml ethidium bromide (Sigma). 5 μ l each of Hyperladder I (Bioline) and Hyperladder IV (Bioline) markers were used and the gel electrophoresed in 1xTBE (89mM Tris, 89mM boric acid and 2mM EDTA pH8 in distilled water) at 70V for 30 minutes. DNA was visualised under UV transillumination with a Geneflash Syngene Bio Imager (GeneFlow, Fradley, U.K.).

The linear vector DNA fragment was excised from the gel and the DNA extracted using a QIAquick gel extraction kit (Qiagen, Crawley, U.K.). Briefly, the gel slice was weighed, three volumes of buffer QG added and the gel slice incubated at 50°C for 10 minutes. One volume of isopropanol was added, the sample mixed and applied to a QIA quick column. The column was centrifuged for 1 minute at 14,000 rpm (Centrifuge 5415C, Eppendorf, Cambridge, U.K.) and the flow through discarded. 0.75ml of buffer PE was added to the column and the column centrifuged as previous. The flow through was discarded and the tube spun as previous. The column was placed into a 1.5ml centrifuge tube, 50µl water applied to the column and the column spun as previous. DNA was quantified as in 2.2.8 and stored at -20°C.

2.2.4 Ligation of linear vector and shRNA insert

The ligation reaction was set up in a final volume of 10µl as follows:

	Vector only	Vector plus insert (annealed oligos)
10x ligase buffer (Invitrogen)	1	1
Vector	5	5
Annealed oligos (10µM)	0	2
DNase RNase free water	3	1
T4 DNA ligase (Invitrogen)	1	1

The reaction mix was incubated overnight at 4°C.

Ligation reactions were monitored by agarose gel electrophoresis. 2µl ligation product was mixed with 0.5µl 5x DNA gel loading buffer and samples separated by electrophoresis on a 1% agarose gel with 0.4µg/ml ethidium bromide. 5µl each of Hyperladder I and Hyperladder IV markers were used and the gel electrophoresed in 1xTBE at 70V for 30 minutes. DNA was visualised under UV transillumination with a Geneflash Syngene Bio Imager.

2.2.5 Bacterial transformation with plasmid DNA

An aliquot of the competent bacterial strain DH5α (50µl, Novogen, Windsor, U.K.) was added to plasmid DNA (100ng), mixed and incubated on ice for an hour. Bacterial cells were heat shocked at 37°C for 20 seconds, transferred to ice for 5 minutes and 1ml L-Broth added (L-Broth; 20.6g LB Broth (Sigma) in 1L distilled water). Cells were incubated at 37°C for 1 hour with shaking (225rpm), centrifuged at 14,000rpm for 1 minute (Centrifuge 5415C, Eppendorf) and the supernatant removed. The pellet was resuspended in 50µl L-Broth and the cells spread onto an ampicillin containing agar plate (Agar; 20.6g LB Broth, 15g Agar technical (Oxoid, Basingstoke, U.K.) in 1L distilled water containing 1ml 1000x stock ampicillin (Sigma) to a final concentration of 100µg/ml) using aseptic technique. Plates were incubated at 37°C overnight.

2.2.6 Amplification of plasmid DNA

A single colony was picked and used to inoculate 3ml LB medium containing ampicillin (100µg/ml) and incubated for 6 hours at 37°C with shaking (225rpm). This starter culture (250µl) was subsequently added to 250ml LB supplemented with 100µg/ml ampicillin in a 2L flask, and incubated overnight at 37°C with shaking (225rpm).

2.2.7 Isolation of plasmid DNA

Cells were harvested by centrifugation at 6000rpm for 15 minutes at 4°C (Mistral 300i, MSE). Isolation of plasmid DNA from bacterial cells was carried out using a QIAfilter Plasmid Purification Kit (Qiagen) according to manufacturer instructions. Briefly, the bacterial pellet was resuspended in 10ml buffer P1, 10ml buffer P2 added, mixed thoroughly and incubated at room temperature for 5 minutes. 10ml chilled buffer P3 was added, the tube inverted vigorously and the lysate poured into the barrel of the QIAfilter cartridge, with incubation at room temperature for 10 minutes. A QIAGEN-tip 100 was equilibrated with the addition of 10ml buffer QBT. The plunger was inserted into the QIAfilter cartridge and the lysate filtered into the pre-equilibrated QIAGEN-tip 100. Once the lysate had cleared the tip was washed with 2 x 30ml buffer QC. The DNA was eluted with the addition of 15ml buffer QF and the DNA precipitated with the addition of 10.5ml isopropanol. After mixing, the mix was centrifuged at 6000g for 30 minutes at 4°C (Mistral 300i, MSE), and the supernatant removed. The pellet was washed with 5ml 70% ethanol and centrifuged at 6000g for 10 minutes (Mistral 300i, MSE). The

supernatant was removed, the pellet air-dried for 10 minutes and the DNA resuspended in 300µl RNase-DNase free water.

2.2.8 Quantification of plasmid DNA

Samples were diluted 1 in 20 with DNase RNase free water in a total of 100µl. The absorbance was determined at both 260 and 280 nm. The purity of the plasmid preparation was determined by dividing the value at 260nm by the value at 280nm. A figure between 1.8 and 2.0 defines a pure plasmid preparation. The concentration of plasmid was determined as follows:

$$\text{Plasmid concentration } (\mu\text{g}/\mu\text{l}) = (\text{OD}_{260} \times \text{dilution factor} \times 50)/1000$$

2.2.9 Plasmid sequencing

0.5µg plasmid DNA and 3.2pmol BGH reverse primer (Alta Bioscience, Birmingham, U.K.) were mixed and made up to 10µl with DNase RNase free water. Sequencing was carried out by the proteomics service at the University of Birmingham. Briefly, Big Dye Terminator Kit V3.1 was added to the DNA/primer mix, the PCR cycle carried out and samples purified for sequencing. Labelled DNA was loaded into the analyser and sequencing carried out using an ABI 3700 sequencer (Applied Biosystems, California, USA). Sequencing data was analysed using Chromas Pro software.

2.3 CSN5 protein expression construct production

2.3.1 CSN5 coding sequence primer design

Webcutter software was used to determine which restriction sites do not occur in CSN5 protein coding sequence and two restriction sites (BamHI and EcoRI) were selected for use in CSN5 protein coding sequence (cds) primer design and subsequent ligation of CSN5 coding sequence with pcDNA3.1 plasmid. Primers used were as follows:

Cap BamHI site First 17 bases of CSN5 cds
5' $\overbrace{\text{GCAGGGATCC}}^{\text{BamHI site}} \overbrace{\text{ATGGCGGCGTCCGGGAG}}^{\text{First 17 bases of CSN5 cds}}$ 3' (Forward)

Cap EcoRI site Rev. Comp. of final 26 bases of CSN5 cds
5' $\overbrace{\text{GCAGGAATTCTTAAGAGATGTTAATTTGATTAAACA}}^{\text{Rev. Comp. of final 26 bases of CSN5 cds}}$ 3' (Reverse)

The melting temperatures of the primers were calculated to determine similarity and sequences ordered from SigmaGenosys.

2.3.2 CSN5 coding sequence amplification

CSN5 coding sequence was amplified from oligo dT cDNA (provided by Dr Farhat Khanim) in a 50 μ l reaction containing 1x Accuzyme buffer (Bioline), 2 μ l cDNA, 400 μ M dNTPs (Bioline), 2mM MgCl₂ (Bioline), 400nM forward primer, 400nM reverse primer

and 5U Accuzyme DNA polymerase (Bioline). The PCR reaction included initial incubation at 94°C for 5 minutes, 10 cycles of 94°C for 30 seconds, 54°C for 30 seconds and 72°C for 1 minute 45 seconds, 30 cycles of 94°C for 30 seconds, 68°C for 30 seconds and 72°C for 1 minute 45 seconds and a final incubation of 72°C for 7 minutes. PCR products were separated by electrophoresis on an agarose gel and the band corresponding to the length of the CSN5 coding sequence was identified, cut out and the DNA extracted, all as in 2.2.3.

2.3.3 CSN5 coding sequence PCR product digestion

The isolated CSN5 coding sequence was digested in a 30µl reaction containing 1x multi-core buffer (Promega), 20µl DNA, 10U BamHI (Fermentas) and 10U EcoRI (Fermentas), and this mix incubated for 2 hours at 37°C.

2.3.4 pcDNA3.1 plasmid digestion

pcDNA3.1 was digested in a 20µl reaction containing 1x multi-core buffer (Promega), 5µl DNA, 10U BamHI (Fermentas) and 10U EcoRI (Fermentas), and this mix incubated for 2 hours at 37°C. Calf intestinal phosphatase (New England Biolabs; 10U) was added for 40 minutes at 37°C and the phosphatase removed using the gel extraction kit as in 2.2.3.

2.3.5 Ligation of CSN5 coding sequence with pcDNA3.1

Ligation was carried out in a 10µl reaction containing 1x ligation buffer (Invitrogen), 1µl T4 DNA ligase (Invitrogen), 3µl digested plasmid and 3µl digested insert, with overnight incubation at 4°C. Ligated plasmid was then transformed into DH5α and plasmid DNA amplified, isolated, quantified and sequenced as in 2.2.5-2.2.9.

2.3.6 CSN5 shRNA/deneddylase mutation primer design

Primers were designed according to QuikChange XL Site-Directed Mutagenesis Kit manufacturer instructions (Stratagene, California, USA). Briefly, selected codons were mutated (shown in bold below) to give a codon with a comparable usage value. This sequence was made up to ~45 bases with extension either side of the mutated region and the sequence checked by blast analysis (http://www.ncbi.nlm.nih.gov/blast/Blast.cgi?PAGE=Nucleotides&PROGRAM=blastn&MEGABLAST=on&BLAST_PROGRAMS=megaBlast&PAGE_TYPE=BlastSearch&SHOW_DEFAULTS=on) to ensure gene specificity. Finally, primer melting temperatures were determined and optimised as per manufacturer instructions and the following sequences (forward and reverse complement) ordered from SigmaGenosys:

shRNA sequence mutation primers: 5' AGGACATACCCAAAGGGATACAAGCCA
CCAGATGAAGGACCTTC 3' (Forward),

5' GAAGGTCCTTCATCTGGTGGCTTGTATCCCTTTGGGTATGTCCT 3' (Reverse complement),

Deneddylase dead mutation primers: 5' CTGCTGGCTTTCTGGGATTAATGTTAG
TACTCAGATGCTC 3' (Forward),
5' GAGCATCTGAGTACTAACATTAATCCCAGAAAGCCAGCAG 3' (Reverse
complement).

2.3.7 CSN5 expression plasmid mutation

Plasmid mutation was carried out according to QuikChange XL Site-Directed Mutagenesis Kit manufacturer instructions (Stratagene). Briefly, plasmid mutation was carried out in a 50µl PCR reaction containing 1x reaction buffer (Stratagene), 5ng plasmid DNA, 125ng forward primer, 125ng reverse primer, 1µl dNTP mix (Stratagene) and 3µl QuikSolution (Stratagene), which was mixed before the addition of 2.5U Pfu Turbo DNA polymerase (Stratagene). The PCR reaction included initial incubation at 95°C for 1 minute, 18 cycles of 95°C for 50 seconds, 60°C for 50 seconds and 68°C for 6 minutes, and a final incubation of 68°C for 7 minutes. The reaction was then incubated on ice for 2 minutes and 10U Dpn1 restriction enzyme (Stratagene) added before mixing and incubation at 37°C for 1 hour.

2.3.8 Mutated CSN5 expression plasmid transformation into XL10-Gold cells

Transformation of XL10-Gold Ultracompetent cells was carried out according to QuikChange XL Site-Directed Mutagenesis Kit manufacturer instructions (Stratagene). Briefly, XL10-Gold Ultracompetent cells (Stratagene; 45µl) were mixed with 2µl β-

mercaptoethanol and incubated on ice for 15 minutes with mixing every 2 minutes. Mutation PCR product (2 μ l) was added and the mix incubated on ice for 30 minutes. The mix was heated to 42°C for 30 seconds and incubated on ice for 2 minutes before the addition of 0.5ml prewarmed NZY⁺ broth. Cells were incubated at 37°C with shaking (225rpm) for 1hour and cells spread onto an ampicillin plate as in 2.2.5. Plasmid DNA was amplified, isolated, quantified and sequenced as in 2.2.6-2.2.9.

2.4 Co-transfection of cell lines

2.4.1 Cell preparation

Three days prior to transfection, cells were counted and set at a density of 2.5×10^5 cells/ml. Cells were diluted 1:1 in media the following day and cells counted and set back to 2.5×10^5 cells/ml the day before transfection.

2.4.2 Cell transfection

A cell count was taken and 5×10^6 cells harvested by centrifugation at 1500rpm for 5 minutes (FALCON 6/300, MSE), and the resultant pellet washed in 1ml PBS and centrifuged as previous. The supernatant was discarded and cells resuspended in 100 μ l Solution V (Amaza, Cologne, Germany). For co-transfection, pMACS K^k.II plasmid (5 μ g) and 10 μ g shVC, shCSN2 or shCSN5 plasmid were aliquotted into an electroporation cuvette (Amaza) and 100 μ l cell suspension added. For double knockdown transfections, 2.5 μ g pMACS K^k.II plasmid was used with either 10 μ g shVC or 5 μ g each of shCSN2 and shCSN5 plasmid. For CSN5 re-expression transfections, 2.5 μ g pMACS K^k.II plasmid was used with either 10 μ g shVC, 10 μ g shCSN5, or 5 μ g each of shCSN5 and wild-type/deneddylase dead CSN5 re-expression plasmid. Cells were electroporated using programme T-16 on Nucleofector I (Amaza). Prewarmed media (0.5ml) was added to the cuvette and the mix transferred to 1.5ml media in a 24

well plate. Four hours post transfection, cells were transferred to a 12 well plate and 2ml media added.

2.4.3 Analysis of transfection efficiency

24 hours post transfection an 80µl aliquot of transfected cells was mixed with 5µl anti-H-2K^k-FITC antibody (Miltenyi Biotec, Surrey, U.K.) and incubated at room temperature for 15 minutes. 3ml PBS was added and cells centrifuged at 1500 rpm for 5 minutes (FALCON 6/300, MSE), the supernatant removed and the cells resuspended in 300µl FACS fix (1% formaldehyde (v/v) and 2% FBS (v/v) in PBS). Staining was analysed by FACS flow cytometry using FACS Calibur and Cell Quest Pro software (Becton Dickinson, Oxford, U.K.) within two weeks.

2.4.4 Cell sorting

A schematic of the co-transfection and cell sorting techniques is shown in figure 10. Transfected cells were sorted 24 hours post transfection using MACSelect microbeads (Miltenyi Biotec) according to manufacturer instructions. Briefly, cells were harvested by centrifugation at 1500 rpm for 5 minutes (FALCON 6/300, MSE) followed by a PBS wash and centrifugation as previous. The pellet was resuspended in 320µl PBE (PBS plus 2mM EDTA) and 80µl MACSelect microbeads added to the suspension. This mix was incubated for 15 minutes on ice and the volume adjusted to 2ml with PBE. A MACS column MS (Miltenyi Biotec) was placed in the magnetic field of a MACS separator

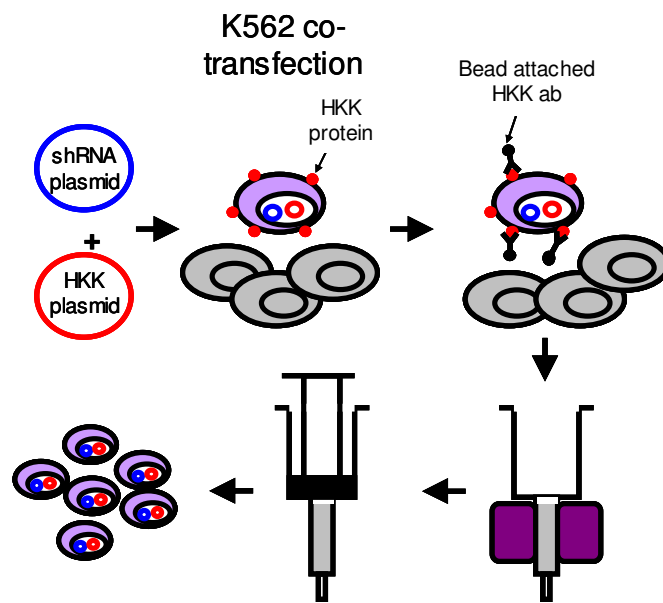


Figure 10. Schematic of the co-transfection and cell sorting techniques.

K562 cells are co-transfected with two plasmids, one encoding the shRNA of interest and the other encoding a truncated murine cell surface protein (HKK). Transfected cells transiently express this protein on the cell surface. An antibody specific for this protein with a bead attached is used to label transfected cells. Cells are then applied to a column placed in a magnet, with the labelled cells being retained and the unlabelled, untransfected cells being washed through the column. The column is then removed from the magnet and the transfected cells eluted.

magnet (Miltenyi Biotec) and 500 μ l PBE applied to the column. The cell suspension was then added to the column and the negative fraction discarded. The column was washed four times with 500 μ l PBE. The column was removed from the magnetic field and placed into a collection tube. 1ml PBE was added to the column, the plunger firmly applied and the positive fraction collected in the tube. A cell count was taken, the cells harvested by centrifugation at 1500 rpm for 5 minutes (FALCON 6/300, MSE) and the cells resuspended in the appropriate volume of media to set the cells at a density of 3×10^5 /ml. Cells were cultured as in 2.1.1 and harvested for analysis at the appropriate time point.

2.5 Assessment of cell proliferation and death

2.5.1 Cumulative cell growth

All co-transfections were maintained in the same size culture vessel and same volume throughout culture. Cell counts were taken and cultures set back to 3×10^5 cells/ml daily. Cumulative cell growth for each time point was determined by multiplying cell count by both culture volume and the cumulative dilution factor. The average cumulative cell growth of three co-transfections and the standard error of this average were calculated using Microsoft Office Excel. The significance of any difference in cumulative cell growth between vector control and knockdown cells was also determined using the t-test function in Microsoft Excel. This data was then plotted using SigmaPlot.

2.5.2 Cell cycle analysis

200 μ l cells were transferred to a FACS tube and 2ml PBS added. Cells were pelleted by centrifugation at 1500rpm for 5 minutes (FALCON 6/300, MSE). The supernatant was removed and cells resuspended in 300 μ l cell cycle buffer (10 μ g/ml propidium iodide, 0.1% triton X100, 0.1mM NaCl, in distilled water). Staining was analysed using a FACS Calibur (Becton Dickinson) within 24 hours (samples were stored at 4°C if staining was analysed the next day) and data evaluated using Cell Quest Pro software (Becton Dickinson).

2.5.3 Thymidine incorporation assay

2×10^4 cells were transferred to a 96 well plate in triplicate wells and the volume made up to 200 μ l with media. Cells were incubated at 37°C with 5% CO₂ for 2 hours prior to the addition of 2 μ Ci/ml tritiated thymidine (20 μ Ci/ml stock in RPMI 1640, Amersham, Buckinghamshire, U.K.). Cells were further incubated for 18 hours and the plate then stored at -20°C. Samples were transferred to a filter mat (Wallac, Massachusetts, USA) using a Skatron cell harvester (Skatron Instruments, Bath, U.K.) and readings taken using a Beta-Plate scintillation counter (Skatron Instruments). The average thymidine incorporation of three co-transfections and the standard error of this average were calculated using Microsoft Office Excel. The significance of any difference between thymidine incorporation in vector control and knockdown cells was also determined using the t-test function in Microsoft Excel. This data was then plotted using SigmaPlot.

2.5.4 Annexin V staining

1×10^5 cells were transferred to a FACS tube and 1ml cold PBS added. Cells were centrifuged for 5 minutes at 1500rpm (FALCON 6/300, MSE). The supernatant was removed and cells were washed again in PBS as previous. Annexin V binding buffer (BD Biosciences, Oxford, U.K.) was diluted 1 in 10 in distilled water and cells resuspended in 100 μ l of this buffer. 5 μ l each of annexin V FITC and Propidium Iodide stain (both BD Biosciences) were added to the cells prior to incubation at room temperature for 15

minutes. Staining was analysed using a FACS Calibur (Becton Dickinson) within 1 hour and data evaluated using Cell Quest Pro software (Becton Dickinson).

2.6 Morphological analysis of cells

2.6.1 Cytospins

Cytospins were produced using a Shandon Cytospin3 (Thermo, Loughborough, U.K.), Shandon filter cards (Thermo) and glass slides (VWR, Lutterworth, U.K.) according to manufacturer instructions. 5×10^4 cells were spun onto a slide by spinning at 500rpm for 3 minutes. Slides were then allowed to dry at room temperature for 15 minutes.

2.6.2 Jenner-Giemsa staining

Slides were fixed in methanol for 5 minutes at room temperature. Giemsa buffer (200mM sodium phosphate pH5.6) was diluted 1 in 25 in distilled water and this diluted buffer used to dilute Jenner stain (VWR) 1 in 3 and Giemsa stain (VWR) 1 in 20. Diluted Jenner stain was applied to the slides and incubated at room temperature for 5 minutes. Jenner stain was washed off with distilled water and Giemsa stain applied to the slides and incubated for 10 minutes at room temperature. Giemsa stain was washed off with distilled water, slides wiped to remove excess liquid and allowed to dry for 15 minutes at room temperature. Slides were mounted with 20 μ l DePeX mounting medium (VWR) and 22mm x 22mm cover slips (VWR). Jenner-Giemsa staining was viewed using an Olympus BX40 microscope (Olympus, Watford, U.K.) and images captured using an Olympus Chameleon digital SLR camera (Olympus).

2.6.3 Immunofluorescent staining

Slides were fixed in 4% paraformaldehyde in PBS for 10 minutes at room temperature. Slides were washed twice in PBS and incubated for 10 minutes in room temperature ammonium chloride (50mM in PBS). Slides were washed twice more in PBS and incubated in 0.1% Triton X-100 in PBS for 4 minutes at room temperature. Cells were rinsed in PBS and staining carried out.

Primary anti-tubulin antibody (Sigma) was diluted 1 in 500 in PBS and 40µl applied to the cell spot. Slides were incubated at room temperature for 1 hour in a humid chamber and then washed three times in PBS. Secondary antibody (FITC conjugated anti-mouse; Jackson Laboratories) was diluted 1 in 500 in PBS and Hoechst (Sigma) added to a final dilution of 1 in 1000 (1mg/ml stock and 1µg/ml final concentration). Excess liquid was removed from slides and 40µl secondary antibody/Hoechst mix applied to the cell spot. Slides were incubated at room temperature for 40 minutes and washed three times in PBS. Excess liquid was removed and slides were allowed to dry for 15 minutes at room temperature, prior to mounting with 5µl Moviol mounting medium (6g glycerol, 2.4g Moviol-4-88, 12ml 0.2M Tris HCl pH8.5, 6ml dH₂O, three p-phenyldiamine crystals) and 22mm x 22mm cover slips (VWR). Immunofluorescent staining was visualised using an Axioskop2 microscope (Zeiss, Hertfordshire, U.K.) and images captured with a Qimaging 12-bit QICAM camera (Media Cybernetics, Bethesda, USA) and Openlab software (Improvision, Coventry, U.K.).

2.6.4 Monodansylcadaverine staining

5×10^4 cells were centrifuged for 15 seconds at 14,000 rpm (Centrifuge 5415C, Eppendorf), resuspended in 300 μ l PBS and incubated with 0.05mM monodansylcadaverine (Sigma; 5mM stock in DMSO) at 37⁰C for 10 minutes. Cells were washed 4 times by centrifugation for 15 seconds at 14,000 rpm (Centrifuge 5415C, Eppendorf) and resuspension in 0.5ml PBS. Cells were resuspended in 100 μ l PBS and cytopspins made as above. Staining was analysed immediately using a DMIRE2 system (Leica, Milton Keynes, U.K.). Analysis of this staining was carried out by Dr Simon Johnston.

2.6.5 Visualisation of propidium iodide retention in cells

1×10^5 cells were transferred to a FACS tube and 1ml cold PBS added. Cells were centrifuged for 5 minutes at 1500rpm (FALCON 6/300, MSE). The supernatant was removed and cells were washed again in PBS as previous. Annexin V binding buffer (BD Biosciences, Oxford, U.K.) was diluted 1 in 10 in distilled water and cells resuspended in 100 μ l of this buffer. 5 μ l of Propidium Iodide stain (BD Biosciences) was added to the cells prior to incubation at room temperature for 15 minutes. Cytospins were then made as in 2.6.1 and propidium iodide retention visualised using a DMIRE2 system (Leica, Milton Keynes, U.K.). Analysis of this staining was carried out by Simon Johnston.

2.7 Protein analysis: Western blotting and Blue Native gels

2.7.1 Protein extraction and quantification

For protein extraction, $1-3 \times 10^6$ cells were resuspended in 50 μ l lysis buffer (10% 10x complete protease inhibitor (Roche diagnostics, West Sussex, U.K.), 90% RIPA buffer (1% v/v NP40, 0.5% w/v sodium deoxycholate, 0.1% w/v SDS in distilled water)). Cells were incubated for 30 minutes on ice, centrifuged at 14,000rpm at 4°C for 10 minutes (Hawk 15/05, Sanyo, Watford, U.K.) and the supernatant transferred to a 1.5ml centrifuge tube (eppendorf).

For protein quantification, the D_c protein assay protocol was followed according to manufacturer instructions (Bio-Rad, Hemel Hempstead, U.K.). Briefly, 5 μ l standards (0, 0.625, 1.25, 2.5, 5 and 10mg/ml BSA in distilled water) were added to duplicate wells and 2 μ l of each protein sample was added to 3 μ l distilled water in replicate wells. 20 μ l reagent S was added to each ml of reagent A required to make solution A', and 25 μ l A' added to each well. 200 μ l reagent B was then added to each well, the wells mixed, and the reaction allowed to develop for 15 minutes before the optical density was measured at 645nm using a plate reader (BIO-TEK, Vermont, USA) and KC4 software (BIO-TEK). These readings were transferred to Microsoft Excel and used to calculate sample protein concentration.

2.7.2 Calculating the amount of protein per cell

The total amount of protein in the extract was determined by multiplying the extraction volume by the protein concentration. The final cell count before cell harvesting was multiplied by the culture volume harvested to determine the total number of cells from which protein was extracted. Total protein was then divided by total cell number to give protein per cell. The average and standard error of the mean of three vector control and three knockdown samples was determined and this data plotted using Sigma Plot. The significance of any difference between protein levels in vector control and knockdown cells was also determined using the t-test function in Microsoft Excel.

2.7.3 Sample preparation and protein separation by SDS PAGE

Protein samples (20-40 μ g) were mixed in a 3:1 ratio with 4x SDS gel loading buffer (62.5mM Tris HCl pH6.8, 25% v/v glycerol, 2% SDS, 5% 2- β -ME, Bromophenol Blue, in distilled water), heated to 100°C for 10 minutes and centrifuged for 15 seconds at 14,000rpm (Centrifuge 5415C, Eppendorf).

Resolving gel mixes (10ml final volume) were prepared as follows:

	10%	12.5%	15%
30% Acrylamide/Bis-Acrylamide 37.5:1 (Geneflow)	3.3ml	4.2ml	5.0ml
1.5M Tris HCl pH8.8	2.5ml	2.5ml	2.5ml
10% Sodium dodecyl sulphate (SDS; Fisher Scientific)	0.1ml	0.1ml	0.1ml
distilled water	4.1ml	3.2ml	2.4ml
10% Ammonium persulphate (APS; Sigma)	60µl	60µl	60µl
TEMED (VWR international)	4.5µl	4.5µl	4.5µl

Once the resolving gel was set a stacking gel was added. The stacking gel consisted of the following:

30 % Bis/Acrylamide	440µl
0.5M Tris HCl pH6.8	830µl
10% SDS	33µl
distilled water	2.03ml
10% APS	16.7µl
TEMED	1.7µl

Protein samples, and 5µl prestained precision blue markers (Bio-Rad) were loaded onto the gel and separated by electrophoresis at 120V with 1x SDS gel running buffer (25mM Tris, 192mM glycine, 3.5mM SDS in distilled water) for 90 minutes.

2.7.4 Protein transfer

PVDF membrane (Millipore, Watford, U.K.) was soaked in methanol for 15 seconds, dH₂O for 2 minutes and equilibrated in transfer buffer (25mM Tris, 192mM glycine, 20%

Methanol in distilled water) for 10 minutes. Then layered onto the black side of the transfer cassette was the following:

Blotting pad

Wet 3mm filter paper

The gel with the stacking gel removed

PVDF membrane

Wet 3mm filter paper

Blotting pad

The transfer was carried out using a Mini-Protean transfer tank (Bio-Rad) at 80V for 1 hour with cooling.

2.7.5 Immunodetection of proteins

The membrane was rinsed in TBS-T (137mM NaCl, 20mM Tris HCl pH 7.6, 0.2% Tween20 in distilled water) and then blocked for 45 minutes in 5% dried milk solution (5% milk powder (Marvel) in TBS-T). Primary antibodies were diluted 1 in 1000 (except for the anti β -actin antibody (Sigma) which was diluted 1 in 10,000) in 5% milk, and the membrane incubated for an hour in this solution at room temperature. The membrane was washed three times in TBS-T, each wash for 5 minutes, the secondary antibody (horseradish peroxidase (HRP) conjugated anti-rabbit, Pierce (Illinois, USA) or HRP conjugated anti-mouse, Sigma) diluted 1 in 1000 (except for when following incubation with anti β -actin antibody when secondary antibody was diluted 1 in 10,000) in 5% milk and the membrane incubated for 45 minutes in this solution at room temperature. The

membrane was washed as above and signal developed using Supersignal West Pico Chemiluminescent substrate (Pierce) and signal detected by exposure to Xomat scientific imaging film (Kodak, Sigma) for 5 minutes. Films were developed using an AGFA CURIX 60 (Agfa, Mortsel, Belgium).

2.7.6 Western blot densitometry

Quantitative analysis of western blots was carried out using Image J software (<http://rsb.info.nih.gov/ij/download.html>) and Microsoft Office Excel. Briefly, the density of each band was measured and background density subtracted. The ratio of protein band density to corresponding β -actin band density was then calculated to give a value corrected for loading. The appropriate ratios of corrected band density in control and treated cells were then calculated, and the average and standard error of the mean of three vector control and three knockdown samples determined. This data was then plotted, along with the standard error of the mean, using Sigma Plot. The significance of any difference between protein levels in vector control and knockdown cells was also determined using the t-test function in Microsoft Excel.

2.7.7 Blue native gels

Blue native gels were carried out using a NativePAGE Novex Bis-Tris Gel System (Invitrogen) according to manufacturer instructions. Briefly, 1×10^6 cells were resuspended in 100 μ l mild lysis buffer (1x NativePAGE sample buffer (Invitrogen), 1%

digitonin (Sigma), 1x protease inhibitor, in distilled water), incubated on ice for 30 minutes, centrifuged for 20 minutes at 14,000 rpm and 4°C (Hawk 15/05, Sanyo), and the supernatant collected. A final concentration of 0.25% NativePAGE 5% G-250 sample additive (Invitrogen) was added to native protein extract, 25µl sample loaded onto a NativePAGE Novex 3-12% Bis-Tris gel (Invitrogen), and 10µl NativeMARK protein markers (Invitrogen) loaded onto the gel. Samples were separated by electrophoresis for 45 minutes at 150V with 1x NativePAGE Anode Buffer (1x NativePAGE Running Buffer (Invitrogen) in distilled water) and dark blue NativePAGE Cathode Buffer (1x NativePAGE Running Buffer (Invitrogen) and 1x NativePAGE Cathode additive (Invitrogen) in distilled water), followed by 45 minutes electrophoresis at 250V with anode buffer as above and light blue NativePAGE Cathode Buffer (1x NativePAGE Running Buffer (Invitrogen) and 0.1x NativePAGE Cathode additive (Invitrogen) in distilled water). The western protocol was then followed from 2.7.4 with the addition of a 10 minute incubation of the membrane in 100% methanol between the transfer and blocking steps to prevent the interference of coomassie with protein immunodetection.

2.7.8 2-Dimensional blue native gels

A schematic of the 2-dimensional NativePAGE/SDS-PAGE technique is shown in figure 11. The first dimension was carried out as in 2.6.9 and the gel cut into individual lanes. The native gel slice was incubated in 1x SDS gel loading buffer (15.6mM Tris HCl pH6.8, 6.25% glycerol, 0.5% SDS, 1.25% 2-β-ME, Bromophenol Blue in distilled water) for 30 minutes at room temperature, the gel slice placed horizontally onto a 12.5% SDS

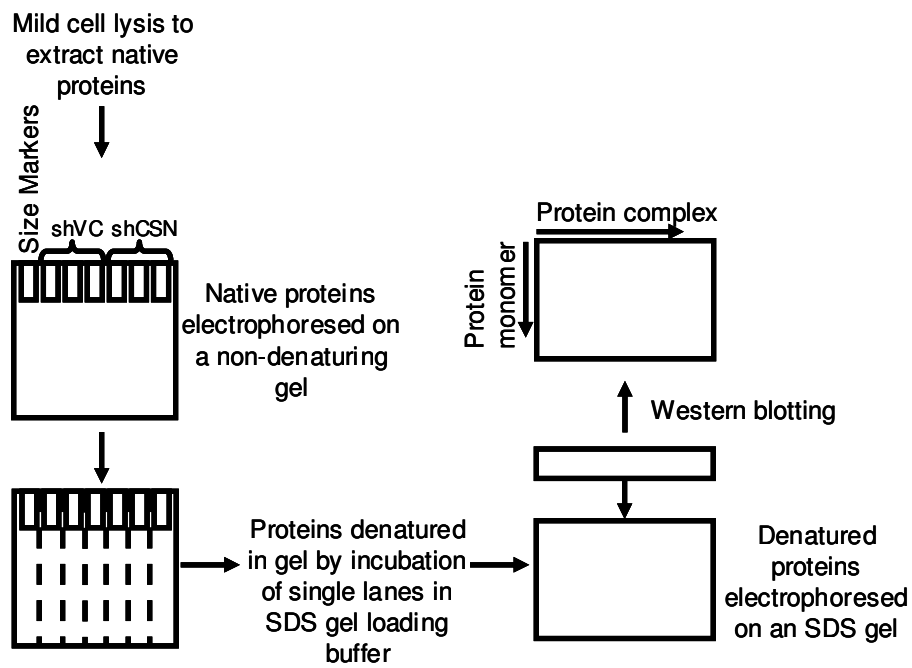


Figure 11. The NativePAGE/SDS PAGE 2-D gel analysis technique.

Native proteins are extracted from cells and electrophoresed on a non-denaturing gel in order to separate proteins on the basis of their complexed, native state in the first dimension. This gel is then cut into individual lanes and proteins denatured. Each individual gel lane is rotated by ninety degrees and lay onto an SDS gel. Proteins are thus electrophoresed in the second dimension based on monomeric size.

gel and overlaid with 1ml 1x SDS gel loading buffer. 5µl prestained precision blue markers (Bio-Rad) were loaded onto the SDS gel, proteins separated by electrophoresis as in 2.7.3 and the western protocol followed from 2.7.4.

The NativeMARK lane of the native gel was coomassie stained. Briefly, the gel was stained with coomassie stain (50% methanol, 0.05% coomassie, 10% acetic acid, in distilled water) for 2 hours at room temperature and incubated in destain (7% acetic acid, 5% methanol, in distilled water) overnight at room temperature.

2.7.9 2-Dimensional blue native gel densitometry

Quantitative analysis of 2-D gels was carried out using Image J software (<http://rsb.info.nih.gov/ij/download.html>) and Microsoft Office Excel. Briefly, the density of each band was measured and background density subtracted. The ratio of protein band density in knockdown cells to that of vector control cells was calculated and this value converted to percent by multiplication by 100. The average and standard error of the mean of three CSN2 and three CSN5 knockdown samples were then determined and data plotted using Sigma Plot. The significance of any difference between protein levels in vector control and knockdown cells was also determined using the t-test function in Microsoft Excel.

2.8 mRNA analysis: Quantitative real-time polymerase chain reaction (QRT-PCR)

2.8.1 RNA extraction

RNA was extracted from a pellet of 2×10^6 cells using a Qiagen RNeasy mini kit according to the manufacturer instructions. Briefly, cells were resuspended in 350 μ l buffer RLT (plus β -mercaptoethanol). The sample was then homogenized using a QIAshredder spin column (Qiagen). One volume of 70% ethanol was added to the homogenized sample and 700 μ l of this mixture added to an RNeasy mini column. The column was centrifuged for 15 seconds at 14,000 rpm (Centrifuge 5415C, Eppendorf). On column DNA removal was carried out using the RNase-Free DNase set (Qiagen). 350 μ l buffer RW1 was added to the column and the column centrifuged for 15 seconds at 14,000 rpm (Centrifuge 5415C, Eppendorf). The DNase I stock solution was added to buffer RDD according to manufacturer instructions and 80 μ l of this mix added to the column and incubated for 15 minutes at room temperature. 350 μ l buffer RW1 was added to the column and the column centrifuged for 15 seconds at 14,000 rpm (Centrifuge 5415C, Eppendorf). Buffer RPE (500 μ l) was added to the column and centrifuged for 15 seconds at 14,000 rpm (Centrifuge 5415C, Eppendorf). Another 500 μ l RPE was applied to the column and the column centrifuged for 2 minutes at 14,000 rpm (Centrifuge 5415C, Eppendorf). The RNeasy column was transferred to a 1.5ml collection tube, RNA eluted with the addition of 30 μ l RNase-free water and centrifugation for 1 minute at 14,000 rpm (Centrifuge 5415C, Eppendorf), and RNA stored at -20°C .

2.8.2 RNA quantification

RNA samples were diluted 1 in 50 in RNase-free water in a total volume of 100 μ l. The absorbance at 260nm was measured using a spectrophotometer and the RNA concentration calculated using the following equation:

$$\text{RNA concentration } (\mu\text{g}/\mu\text{l}) = (\text{OD}_{260} \times 40 \times \text{dilution factor})/1000$$

2.8.3 Reverse transcriptase PCR

cDNA was produced from 1 μ g RNA using reverse transcription. All constituents were obtained from Invitrogen and the procedure carried out as follows: 1 μ l of both random primers (Promega, 500 μ g/ml) and dNTP's (Bioline, 10mM stock) were added to 1 μ g RNA, the volume made up to 12 μ l with DNase RNase free water, and the mix heated to 65°C for 5mins, transferred to ice and centrifuged for 15 seconds at 14,000rpm (Centrifuge 5415C, Eppendorf). A master mix was made as follows:

	1x (μ l)
5xbuffer (Invitrogen)	4
0.1M DTT (Invitrogen)	2
RNase Out (Promega, 40U/ μ l)	1
Superscript (Invitrogen, 200U/ μ l)	1

After centrifugation, 8 μ l of master mix was added to the RNA, primer, dNTP mix. The mix was incubated at 25°C for 10 minutes, 42°C for 90 minutes and 70°C for 15 minutes.

2.8.4 β -actin PCR

All constituents were obtained from Bioline with the exception of the primers which were obtained from Alta Biosciences (The University of Birmingham). The sequence of these primers is as follows:

Forward 5' GTCACCAACTGGGACGACA 3'

Reverse 5' TGGCCATCTCTTGCTCGAA 3'

The reaction mix was set up as follows:

	1x (μ l)
10x Taq buffer	5
Primers (33 μ M)	1
dNTP's (10mM)	1
MgCl ₂ (50mM)	1
DNase RNase free water	40
Taq polymerase (1U/ μ l)	1
cDNA	1

The PCR cycle included an initial denaturation step (95°C for 2 minutes) followed by 38 cycles of 94°C for 20 seconds, 55°C for 30 seconds and 72°C for 60 seconds. The cycle was completed with a final incubation at 72°C for 5 minutes.

β -actin PCR products were separated by electrophoresis on a 1% agarose gel with 0.4 μ g/ml ethidium bromide. The sample (6 μ l) was mixed with 2 μ l 5x DNA gel loading buffer and 8 μ l loaded into the well. Gels were electrophoresed in 1xTBE at 60V for 45

minutes and products visualised under UV transillumination with a Geneflash Syngene Bio Imager.

2.8.5 Neomycin PCR

All constituents were obtained from Bioline with the exception of the primers which were obtained from Alta Biosciences (The University of Birmingham). The sequence of these primers is as follows:

Forward 5' ATGAACTGCAAGACGAGGCAG 3'

Reverse 5' CATTGCATCAGCCATGATGGAT 3'

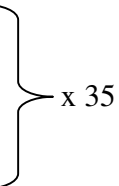
A 50µl reaction was set up as follows:

	1x (µl)
10x Taq buffer	5
Primers (10µM)	2
dNTP's (10mM)	1
MgCl ₂ (50mM)	1
DNase RNase free water	37
Taq polymerase (1U/µl)	1
cDNA	3

The PCR cycle was as follows (temperatures are in °C):

94 – 3mins

94 – 20secs
58 – 20secs
72 – 60secs



x 35

72 – 7mins

4 – hold

Neomycin PCR products were separated by electrophoresis on a 1% agarose gel with 0.4µg/ml ethidium bromide. The sample (6µl) was mixed with 2µl 5x DNA gel loading buffer and 8µl loaded into the well. Gels were electrophoresed in 1xTBE at 60V for 45 minutes and products visualised under UV transillumination with a Geneflash Syngene Bio Imager.

2.8.6 QRT-PCR primer and probe design and verification

QRT-PCR primers and probes were designed using Primer Express software (Applied Biosystems). Briefly, the coding sequence of the gene of interest was copied into Primer Express and potential primer/probe sequences identified. These sequences were checked by blast analysis (http://www.ncbi.nlm.nih.gov/blast/Blast.cgi?PAGE=Nucleotides&PROGRAM=blastn&MEGABLAST=on&BLAST_PROGRAMS=megaBlast&PAGE_TYPE=BlastSearch&SHOW_DEFAULTS=on) to ensure gene specificity, and a set of primers and probe selected which crossed an exon boundary. Primers were ordered from

either Alta Bioscience at the University of Birmingham or Sigma Genosys, and FAM/TAMRA labelled probes were ordered from Eurogentec (Southampton, U.K.).

Primers were tested in the following 20µl reaction:

	1x
2x master mix	10
(Eurogentec, containing dNTP/dUTP, HotGoldStar, UNG, MgCl ₂ , stabilizers and ROX passive reference)	
Forward primer (9µM)	2
Reverse primer (9µM)	2
cDNA	1
DNase RNase free water	5

The PCR cycle included an initial hot start step (50°C for 2 minutes) followed by 95°C for 10 minutes. This was followed by 44 cycles of 95°C for 15 seconds and 60°C for 60 seconds.

Sample (6µl) was mixed with 2µl 5x DNA gel loading buffer and 8µl loaded into the well. Gels were electrophoresed in 1xTBE at 60V for 45 minutes and products visualised under UV transillumination with a Geneflash Syngene Bio Imager.

2.8.7 Optimisation of primers and probe for QRT-PCR

In order to optimise the amount of probe for use in QRT-PCR, reactions were set up as follows:

	1x (μ l)
2x master mix	10
Forward primer (9 μ M)	2
Reverse primer (9 μ M)	2
cDNA	1
μ l probe (1.25 μ M stock)	μ l DNase RNase free water
0	5
0.5	4.5
1	4
1.5	3.5
2	3
2.5	2.5
3	2
3.5	1.5

Each amount of probe was tested in triplicate in a total reaction volume of 20 μ l. The PCR cycle included an initial hot start step (50°C for 2 minutes) followed by 95°C for 10 minutes. This was followed by 44 cycles of 95°C for 15 seconds and 60°C for 60 seconds.

2.8.8 Verifying primers and probe can be multiplexed with 18S internal control

In order to verify primers and probe can be multiplexed with 18S control reactions were set up as follows:

18S alone:

	1x (μ l)
2x master mix	10
18S mix	1

(50nM forward primer, 50nM reverse primer, 200nM probe, Applied Biosystems)

μ l cDNA	μ l DNase RNase free water
0.25	8.75
0.5	8.5
1	8
2	7
3	6
4	5

Gene of interest alone:

	1x (μ l)
2x master mix	10
Forward primer (9 μ M)	2
Reverse primer (9 μ M)	2
Probe (1.25 μ M)	2

μ l cDNA	μ l DNase RNase free water
0.25	3.75
0.5	3.5
1	3
2	2
3	1
4	0

18S and gene of interest combined:

	1x (μ l)
2x master mix	10
Forward primer (9 μ M)	2
Reverse primer (9 μ M)	2
Probe (1.25 μ M)	2
18S mix	1

μ l cDNA	μ l DNase RNase free water
0.25	2.75
0.5	2.5
1	2
2	1
3	0
4	0

Each cDNA amount was carried out in duplicate in a total volume of 20 μ l. The PCR cycle included an initial hot start step (50°C for 2mins) to activate the polymerase, followed by 95°C for 10 minutes to denature DNA. This was followed by 44 cycles of 95°C for 15 seconds and 60°C for 60 seconds, which denature DNA and anneal and extend primers, respectively.

2.8.9 TAQMAN based QRT-PCR

For TAQMAN assays, QRT-PCR was carried out in duplicate 20 μ l reactions containing 1x qPCR Mastermix Plus (Eurogentec), 20-40ng cDNA, 18pmoles each primer and the

optimal concentration of FAM/TAMRA dual labeled probes (see 2.7.7). QRT-PCR was carried out in a 96 well optical plate and a plastic seal used to cover the plate.

QRT-PCR was performed using an ABI Prism 7000 (Applied Biosystems) according to manufacturer instructions. The PCR cycle included incubation at 50°C for 2 minutes followed by incubation at 95°C for 10 minutes. QRT-PCR was completed with 44 cycles of 95°C for 15 seconds and 60°C for 60 seconds.

The following primers (Sigma Genosys) and FAM/TAMRA labeled probes (Eurogentec) were used in TAQMAN QRT-PCR:

CSN2: 5'-CCTCATCCACTGATTATGGGAGT-3' (forward),

5'-CATCATAATTCTTGAAGGCTTCAAAA-3' (reverse),

5'-CCCTCAAGTGCATTTTACCACCACATTCTCT-3' (probe);

CSN5: 5'-ATATCCGCAGGGAAAG-3' (forward),

5'-GGTCCTTCATCAGGAGGTTTGT-3' (reverse),

5'- TGGCGCCTTTAGGACATACCCAAAGG-3' (probe).

Preoptimised primers and probes to 18S ribosomal RNA were used as internal standards in TAQMAN QRT-PCR (Applied Biosystems).

2.8.10 SYBR-Green based QRT-PCR

For SYBR-Green based assays, QRT-PCR was carried out in duplicate 25µl reactions containing 1x Sensimix (Quantace), 20-40ng cDNA, 9pmoles each primer, 1x SYBR-Green solution (Quantace), 4mM MgCl₂ and 0.5 units UNG (Quantace). QRT-PCR was carried out in a 96 well optical plate and a plastic seal used to cover the plate.

QRT-PCR was performed using an ABI Prism 7000 (Applied Biosystems) according to manufacturer instructions. The PCR cycle included incubation at 37°C for 10 minutes followed by incubation at 95°C for 10 minutes. QRT-PCR was completed with 40 cycles of 95°C for 15 seconds, 58°C for 30 seconds and 72°C for 30 seconds.

The following primers (Sigma Genosys) were used in SYBR-Green based QRT-PCR:

Skp2: 5'-CGCTGCCCACGATCATTT-3' (forward),

5'-CCATGTGCTGTACACGAAAAGG-3' (reverse);

Cdc4: 5'-ACGACGCCGAATTACATCTGT-3' (forward),

5'-ACTCCAGCTCTGAAACATTTTTAGC-3' (reverse);

β-TrCP: 5'-GAGGCATTGCCTGTTTGCA-3' (forward)

5'-TGTC CCATAATCTGATAGTGTGTCA-3' (reverse)

18S: 5'-GCCGCTAGAGGTGAAATTCTTG-3' (forward),

5'-CATTCTTGGCAAATGCTTTTCG-3' (reverse).

2.8.11 QRT-PCR data analysis

QRT-PCR data was first analysed using ABI Prism 7000 software (Applied Biosystems) according to manufacturer guidelines. Briefly, cycle threshold (Ct) values were determined for both 18S internal control and gene of interest in each sample by placing a threshold line through the exponential phase of the PCR cycle profiles. This data was then exported to Microsoft Office Excel where the average Ct values were calculated from the duplicates. The 18S internal control value was then subtracted from the value for the gene of interest to give ΔCt values. A control transfection ΔCt value was subtracted from sample ΔCt values to give $\Delta\Delta\text{Ct}$ values. This value was converted to fold change in gene expression relative to control using the equation: $\text{fold change} = 2^{-\Delta\Delta\text{Ct}}$, and fold change converted to percentage expression relative to control via multiplication by 100. The average and standard error of the mean of three vector control and three knockdown samples was calculated and data plotted as a bar chart using Sigma Plot. The significance of any difference between gene expression in vector control and knockdown cells was also determined using the t-test function in Microsoft Excel.

2.9 Statistical Analysis of data

The average and standard error of the mean of n=3 experiments was determined using Microsoft Excel. Data was plotted as the average \pm standard error of the mean using Sigma Plot. The significance of any differences between control and treated cells was determined using the t-test function in Microsoft Excel.

Chapter 3.0:

**Analysis of the molecular and cellular
effects of CSN2 knockdown**

3.1 Introduction

In order to answer the questions set out in the project aims, interfering RNA approaches were used to generate CSN subunit knockdown in the CML cell line K562. However, as K562 cells have a relatively low transfection efficiency, this study began with the generation of highly efficient shRNA mediated CSN subunit knockdown using a co-transfection technique. This chapter describes the development of this procedure and the molecular and cellular consequences of using this approach to knockdown expression of CSN2 in K562 cells.

3.2 Results

3.2.1 Construction of plasmid encoding CSN subunit specific shRNA

Due to the relatively low transfection efficiency of K562 cells a technique was required to permit the isolation of homogenous knockdown populations. To do this a dual transfection approach was used in which shRNAs targeted against either CSN2 or CSN5 were delivered together with the pMACS K^k.II vector. The pMACS K^k.II plasmid produces a truncated murine MHC class I cell surface protein, H-2K^k that is transiently expressed on the cell surface of transfected cells. The cell surface expression of this protein allows for the purification of transfected cells as described in materials and methods.

Figure 12 A & B show representations of the human H1 promoter modified pcDNA3.1 plasmid used to deliver shRNAs and the pMACS K^k.II plasmid (hereafter called HKK) respectively. In order to clone the silencing sequences into pcDNA3.1-H1, shRNA forward and reverse oligonucleotide sequences targeting CSN2 or CSN5 were first designed, incorporating the loop sequence (shown for CSN2 in figure 12C) and flanked by Acc65I and XbaI sites, and the oligonucleotides annealed. pcDNA3.1-H1 (figure 12A) was then digested using the restriction enzymes Acc65I and XbaI, and efficient digestion verified (figure 13A). The annealed targeting oligos and digested vector were ligated and the ligation verified (figure 13B). The plasmid was then transformed into dH5 α and

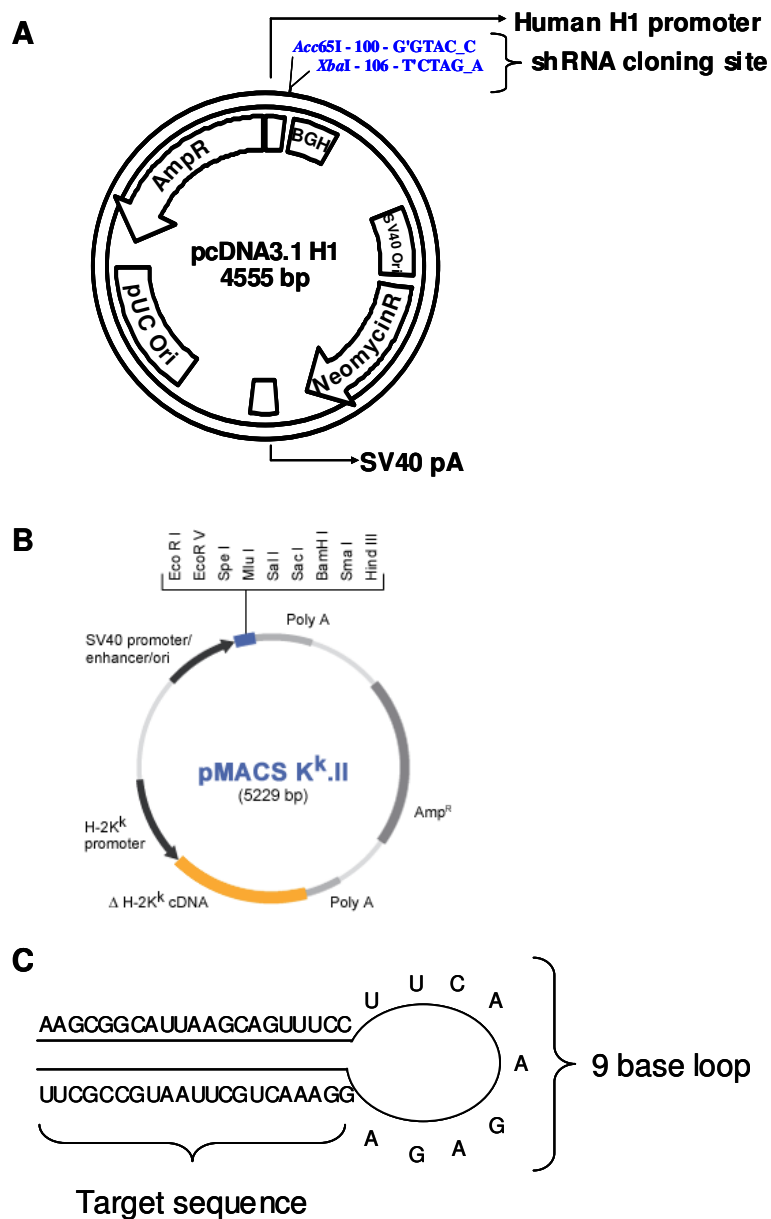


Figure 12. Schematic diagram of plasmids and short hairpin structure.

A, Human H1 promoter modified pcDNA3.1 plasmid into which the required shRNA sequence is cloned at the Acc65I and XbaI restriction sites. Image generated using pDRAW32 software. **B**, pMACS K^k.II plasmid which encodes the truncated H-2K^k cell surface protein. Image obtained from www.miltenyibiotec.com/pid/ProductGroupImageView.aspx?id=26&l=1&opid=16624. **C**, The 9 base sequence which forms the hairpin and an example target sequence specific for CSN2.

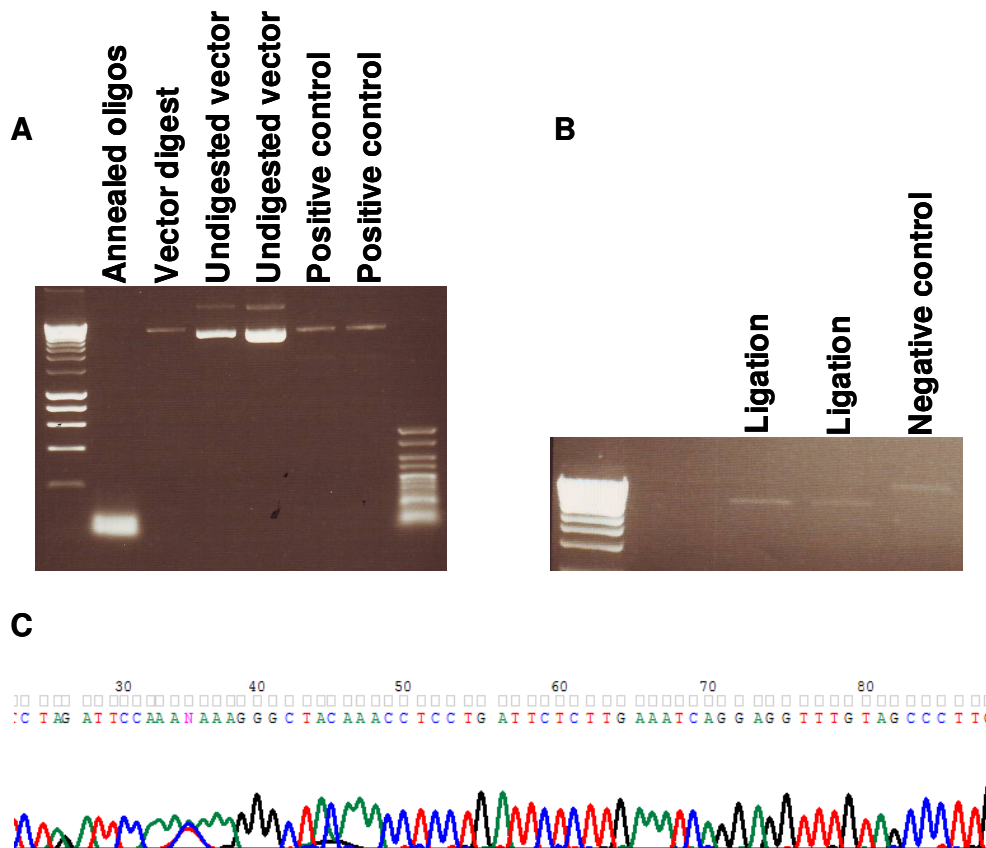


Figure 13. Short hairpin vector preparation and validation.

A, Modified pcDNA3.1 vector was digested and the products separated by electrophoresis on a 1% agarose gel along with positive and negative controls to determine plasmid digestion. **B**, Annealed oligonucleotides and digested vector were ligated and the products separated by electrophoresis on a 1% agarose gel along with a negative control to determine oligo and digested plasmid ligation. **C**, Following amplification of plasmid DNA in DH5 α , plasmid DNA was isolated and sequenced. The shCSN5 plasmid insert sequence is shown. Images shown are representative of several digestions, ligations and sequencing reactions.

colonies screened for correct sequence insertion by sequencing of purified plasmid DNA (figure 13C).

3.2.2 Determination of transfection efficiency and verification of co-transfection

The truncated murine major histocompatibility (MHC) class I cell surface protein, H-2K^k, is transiently expressed on the cell surface of transfected cells between 6 and 48 hours post-transfection with HKK plasmid. The transfection efficiency of K562 cells was therefore determined by flow cytometry following H-2K^k staining of mock transfected and HKK transfected cells 24 hours post transfection. As can be seen in figure 14A, a significant proportion of HKK transfected cells stained positive for the cell surface protein relative to mock transfected cells, demonstrating that, prior to H-2K^k mediated cell sorting, the HKK plasmid was present in around 27% of K562 cells.

As a co-transfection technique was being used, it was important to verify that both plasmids had been efficiently transfected into cells. Post enrichment for H-2K^k positive cells by magnetic bead sorting, cells were harvested, RNA extracted and quantified, and cDNA produced using 1µg RNA. As the pcDNA3.1-H1 plasmid contains the neomycin resistance gene, PCR was carried out in order to detect the presence of this gene in transfected cells. Figure 14B shows that mock transfected cells and cells transfected with HKK alone do not contain the neomycin resistance gene, whereas those cells co-transfected with HKK and pcDNA3.1-H1 are positive for the neomycin resistance PCR

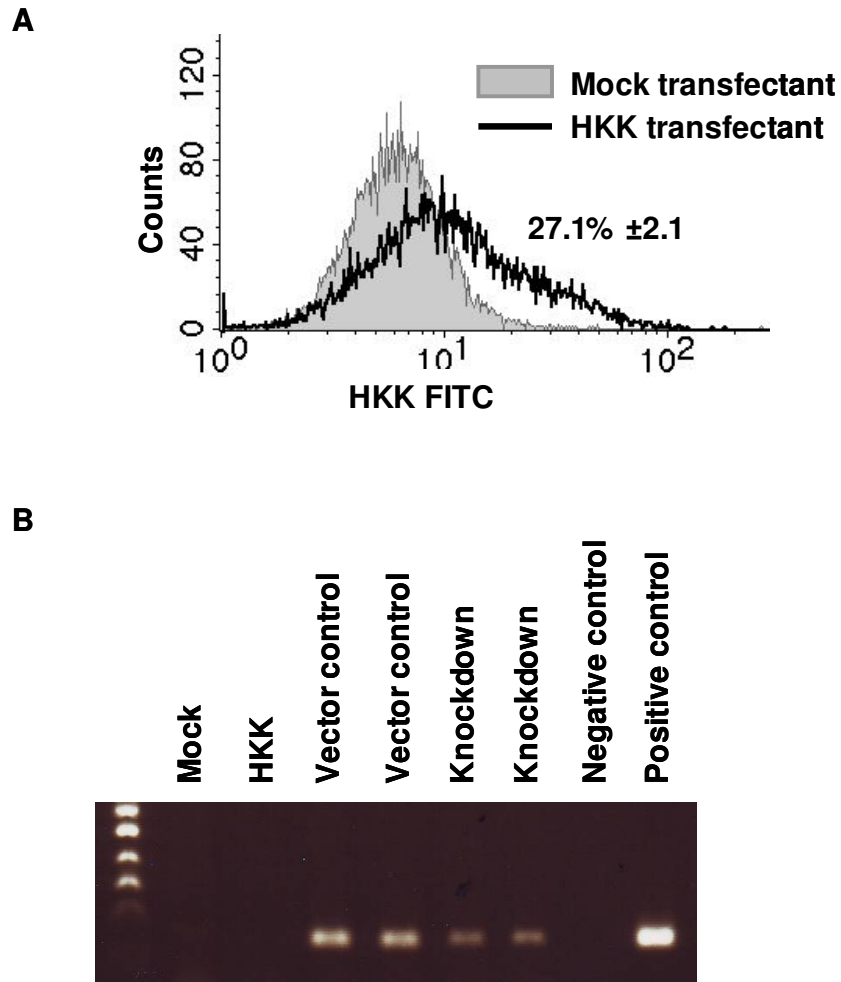


Figure 14. Validation of K562 cell co-transfection.

Data demonstrating how efficient K562 co-transfection was determined. **A**, A representative histogram is shown of flow cytometry data demonstrating the HKK positive staining of K562 cells transfected with HKK plasmid relative to mock transfected cells. Data shown is the average of $n=5$ transfections \pm SEM. **B**, PCR for the neomycin resistance gene was carried out on mock, HKK and co-transfected K562 cells, and products separated by electrophoresis on a 2% agarose gel along with both a positive and negative control. K562 cells co-transfected with the modified pcDNA3.1 plasmid (either vector control or plasmid containing short hairpin insert) were positive for the neomycin resistance gene product. Images shown are representative of $n=5$ transfections.

product, thereby demonstrating successful co-transfection of cells with both the HKK and pcDNA3.1-H1 plasmids.

3.2.3 Assessment of cDNA quality and optimization of primers and probe for QRT-PCR

Prior to mRNA quantification by QRT-PCR, the quality and relative quantities of cDNA in each sample was assessed by performing β -actin PCR. As can be seen in figure 15, the amount of PCR product produced was relatively equal between samples, indicating that cDNA generation had occurred with relatively equal efficiency between samples and that the cDNA was of sufficient quality to continue to QRT-PCR.

QRT-PCR primers and probes were designed, verified and optimised prior to measurement of gene expression in samples. First, the primers were demonstrated to amplify only one specific product of the correct size (figure 16A). Secondly, the optimum amount of probe for use in QRT-PCR was determined. This was achieved by adding increasing amounts of probe to the QRT-PCR mastermix, and plotting cycle threshold (Ct) values against volume of probe. As can be seen in figure 16B, increasing the amount of probe in a QRT-PCR reaction reduced the Ct value obtained. The optimal volume of probe was identified as the point where the graph reaches a plateau. Finally, the effect of multiplexing the gene of interest primer/probe mix with the primer/probe mix for the 18S internal control was determined. The highest accuracy is achieved in QRT-PCR by measuring the expression of the internal control gene and gene of interest in the same reaction mix, known as multiplexing. However, not all primers and probes can be

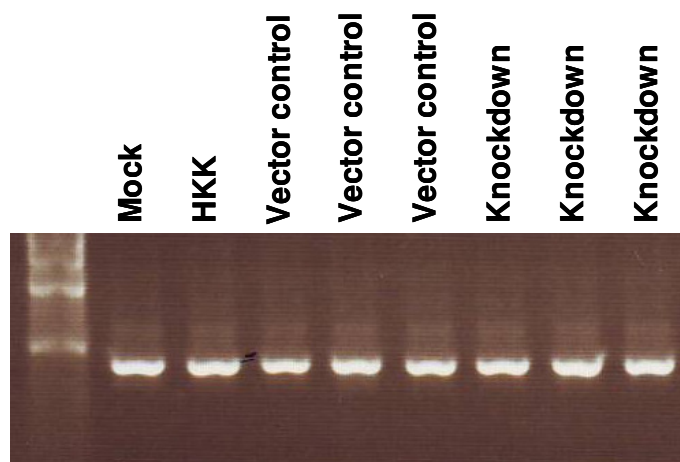


Figure 15. Assessment of cDNA quality using β -actin PCR.

Transfected cells were harvested, RNA extracted, cDNA generated and β -actin PCR carried out. A representative image of β -actin PCR products separated by electrophoresis on a 1% agarose gel is shown.

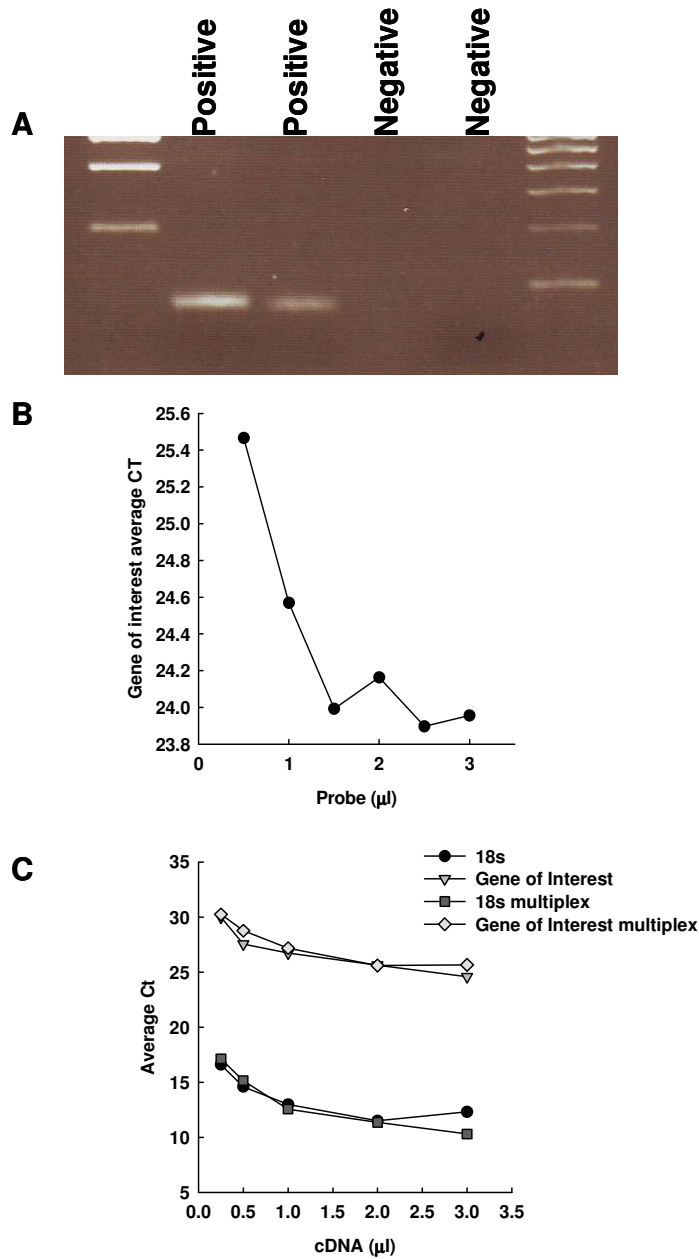


Figure 16. Validation and optimisation of QRT-PCR primers and probe.

A, Primers for the gene of interest were designed, a PCR carried out using these primers and the PCR products separated by electrophoresis on a 2% agarose gel. A representative image is shown. **B**, QRT-PCR was carried out using the pre-validated primers and 0.5, 1, 1.5, 2, 2.5 and 3μl probe and average cycle threshold (CT) values plotted against amount of probe. **C**, QRT-PCR was carried out using the validated primers, the optimised amount of probe and increasing amounts of cDNA. The validated primers/probe and 18S internal control primers/probe mix were tested both individually and in combination and average CT values plotted against amount of cDNA. Representative graphs are shown in B and C.

multiplexed with 18S primers/probe. In order to determine whether a primers/probe mix can be multiplexed, 18S and gene of interest primers and probe were used in both singleplex and multiplex QRT-PCR reactions with increasing amounts of cDNA, and Ct values plotted against volume of cDNA (figure 16C). The incompatibility of a primers/probe set with multiplexing is determined by significant alteration in the multiplex Ct values obtained with increasing cDNA compared to singleplex reactions. As can be seen in figure 16C, no significant changes in Ct values were observed, indicating that the gene of interest primers/probe set can be multiplexed with 18S internal control.

3.2.4 Assessment of target mRNA knockdown

The knockdown plasmids used here produce a specific short hairpin RNA (an example is shown in figure 12C), which is processed in the cell by DICER to remove the loop sequence, and is in turn integrated into the RISC complex where the resulting double stranded RNA sequence targets complementary cellular mRNA sequences for degradation. This degradation subsequently results in the loss of the cellular protein encoded by this mRNA, thereby generating a knockdown. In order to determine CSN2 mRNA levels in mock, vector control and shCSN2 K562 cells, cells were harvested day 6 post transfection, RNA extracted, quantified and cDNA produced using 1µg RNA. Once the quality of the sample cDNA was determined and the QRT-PCR protocol optimised, CSN2 expression was determined. Co-transfection of cells with HKK and empty vector had no significant effect on the expression of CSN2 (figure 17A) relative to expression in mock transfected cells. However, co-transfection with HKK and shCSN2 resulted in a

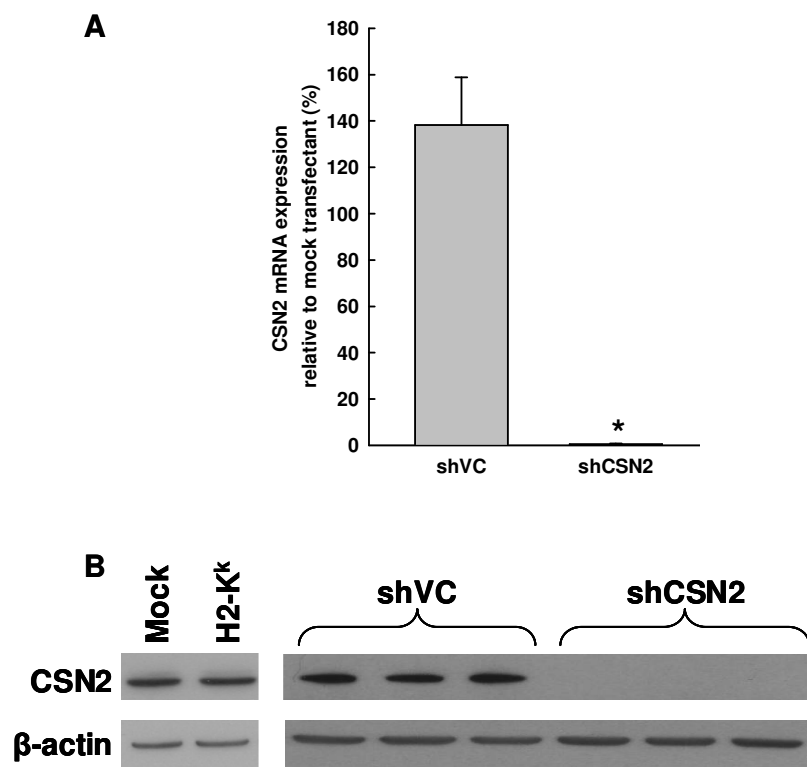


Figure 17. Determination of CSN2 mRNA and protein knockdown.

A, Mock, vector control and CSN2 knockdown transfected cells were harvested day 6 post transfection, RNA extracted, cDNA generated and QRT-PCR carried out. Data shown is the mean CSN2 mRNA expression relative to mock transfected cells of $n=3$ transfections \pm SEM. * indicates $p<0.05$. **B**, Transfected cells were harvested day 6 post transfection, protein extracted and CSN2 protein levels in mock, HKK alone, vector control and CSN2 knockdown cell extracts determined by western blot. Even loading was determined by β -actin western blot. The image shown is representative of five sets of $n=3$ transfections.

significant reduction in the level of CSN2 mRNA (figure 17A; P=0.001), with only 0.5% CSN2 mRNA remaining in CSN2 knockdowns.

3.2.5 Assessment of target protein knockdown

In order to determine CSN2 protein knockdown, shCSN2 cells were harvested day 6 post transfection, protein extracted, quantified, and 20µg used in western blot analyses. Importantly, transfection of cells with HKK alone or co-transfection with HKK and empty vector (shVC) had no effect on the level of CSN2 protein relative to mock transfected cells (figure 17B). However, when cells were co-transfected with HKK and shCSN2, CSN2 protein could not be detected, indicating a highly efficient knockdown at the protein level (figure 17B).

3.2.6 Assessment of the effect of CSN2 knockdown in K562 cells on SCF components and activity

CSN mediated cullin deneddylation has been shown to stabilise F-box proteins and protect them against autocatalytic degradation within their respective SCF complex (Wee et al., 2005). In accordance with this, knockdown of either CSN4 or CSN5 in human cells resulted in an increase in the level of neddylated Cul1, reduction of the F-box protein Skp2 and accumulation of the SCF^{Skp2} target protein p27 (Denti et al., 2006). As CSN2 has been shown to be integral to the integrity of the CSN complex (Kwok et al., 1998), it

was predicted that the CSN2 knockdown achieved in K562 cells would result in similar alterations to SCF^{Skp2} and its target p27.

In order to determine the effect of CSN2 loss on the level of Cul1, Skp2 and p27 proteins, vector control and CSN2 knockdown cells were harvested 6 days post transfection, protein extracted and the level of proteins in these samples determined by western blot analysis. As shown in figure 18A, knockdown of CSN2 caused a marked increase in neddylated Cul1 relative to vector control cells, at the expense of the deneddylated form of Cul1. This was confirmed using densitometry which demonstrated that the Cul1:Neddylated Cul1 ratio in cells lacking CSN2 was significantly less than that of vector controls (figure 18B; P=0.008). Furthermore, western blot analysis of Skp2 protein levels showed apparent total loss of Skp2 in cells lacking CSN2 (figure 18C), whilst p27 western blot analysis demonstrated p27 accumulation in CSN2 knockdown cells relative to vector control cells (figure 18D). This data suggests that loss of CSN2 results in deregulation of Cul1 neddylation and therefore, aberrant SCF^{Skp2} activity in K562 cells.

The stability of cullin proteins has also been shown to be dependent on CSN mediated cullin deneddylation (Wu et al., 2005). The effect of CSN2 loss on the level of both Cul1 and Cul3 protein was therefore studied. In this case transfected cells were harvested at the later time point of day 9 post transfection and the level of Cul1 protein determined by western blot. In accordance with published data, Cul1 protein was significantly decreased in CSN2 knockdown cells relative to vector control cells day 9 post transfection (figure 19). Furthermore, Cul3 protein was also reduced in cells lacking CSN2 compared to

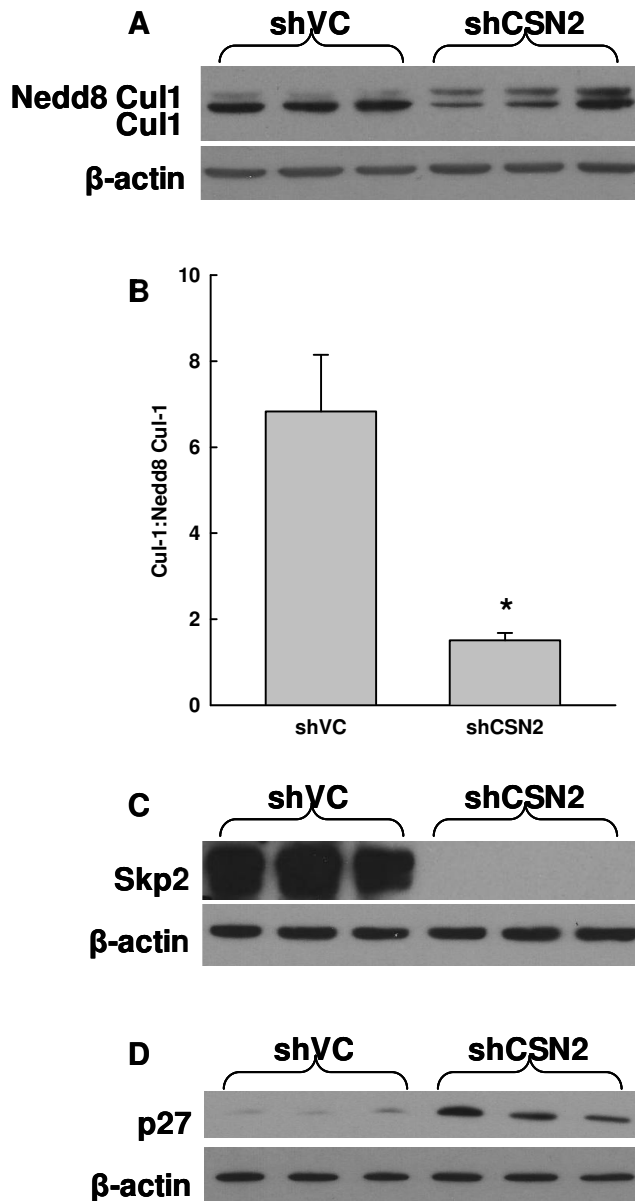


Figure 18. CSN2 knockdown results in accumulation of neddylated Cul1, loss of the F-box protein Skp2 and accumulation of p27.

Transfected cells were harvested day 6 post transfection, protein extracted and Cul1 (A), Skp2 (C) and p27 (D) protein levels in vector control and CSN2 knockdown cell extracts determined by western blot. Even loading was determined by β -actin western blot. The images shown are representative of three sets of n=3 transfections. B, Densitometry was carried out on the Cul-1 western blot and the Cul-1 to neddylated Cul-1 ratios of vector control and CSN2 knockdown cells calculated. Data shown is the average of n=3 transfections \pm SEM. * indicates $p < 0.05$.

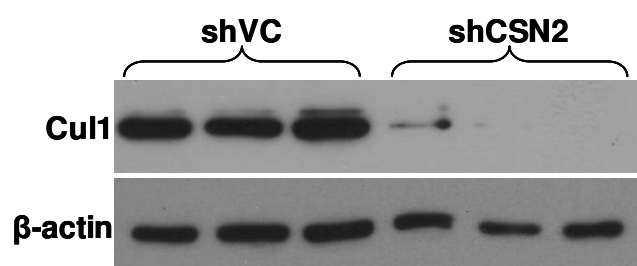


Figure 19. CSN2 knockdown results in significant loss of Cul1 protein.

Transfected cells were harvested day 9 post transfection, protein extracted and Cul1 protein levels in vector control and CSN2 knockdown cell extracts determined by western blot. Even loading was determined by β -actin western blot. The image shown is of three independent vector control and CSN2 knockdown transfections.

vector controls at day 6 post transfection (figure 20A). Densitometry of this western blot demonstrated that this loss in total Cul3 protein is significant (figure 20B; P=0.0007), whilst densitometry also showed that there was a significant reduction in the Cul3:Neddylated Cul3 ratio as observed for Cul1 (figure 20C; P=0.0009). These data confirm that the CSN is vital for cullin protein stability and further suggest that loss of CSN2 affects multiple cullins/CRL complexes and therefore the degradation of a plethora of proteins.

3.2.7 Assessment of the effect of CSN2 knockdown on the level of F-box proteins

There appear to be discrepancies within the literature with respect to the effect of CSN disruption on the level of particular F-box proteins. For example, the stability of the *Neurospora* β -TrCP homolog, FWD-1, has been shown to be dependent on CSN activity, with CSN2 knockout resulting in a significant increase in FWD-1 protein degradation (He et al., 2005), whilst others have reported no effect of CSN disruption on the level of this F-box protein in HEK293 cells (Su et al., 2008). In order to compare the effect of CSN2 knockdown on the level of multiple F-box proteins, protein levels of Skp2, Cdc4 and β -TrCP were determined over time following knockdown of CSN2 in K562 cells. Vector control and CSN2 knockdown cells were harvested 2, 3, 6 and 9 days post transfection, proteins extracted and the levels of F-box proteins determined by western blot analyses. By day 9 post transfection, all three F-box proteins were undetectable in the CSN2 knockdown cells (Figure 21). However, the loss of these F-box proteins was found to occur sequentially. Densitometry was carried out on all F-box protein westerns

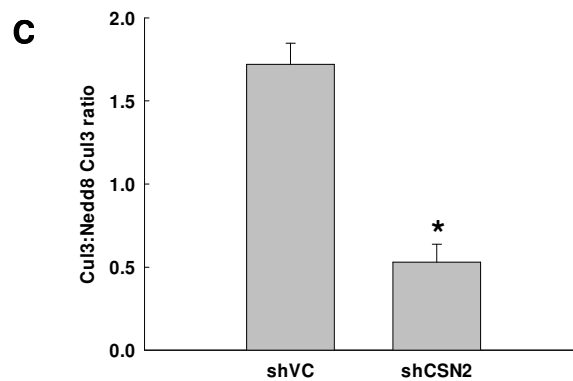
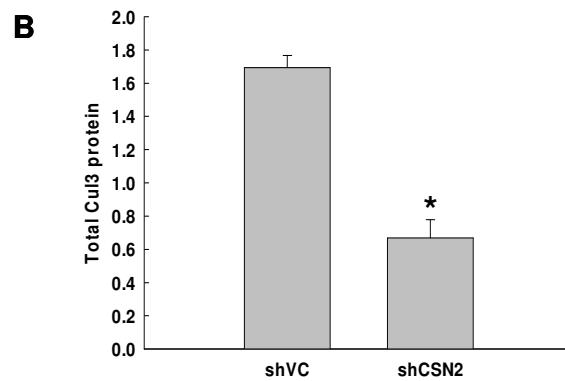
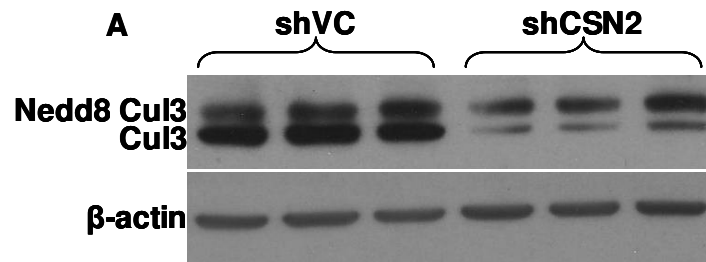


Figure 20. CSN2 knockdown results in a significant decrease in the Cul3:Nedd8 Cul3 ratio and loss of Cul3 protein.

A, Transfected cells were harvested day 6 post transfection, protein extracted and Cul3 protein levels in vector control and CSN2 knockdown cell extracts determined by western blot. Even loading was determined by β -actin western blot. The image shown is of three independent vector control and CSN2 knockdown transfections. Densitometry was carried out on the Cul3 western blot and the total Cul3 protein (**B**) and the Cul3 to neddylated Cul3 ratio (**C**) of vector control and CSN2 knockdown cells calculated. Data shown is the average of n=3 transfections \pm SEM. * indicates $p < 0.05$.

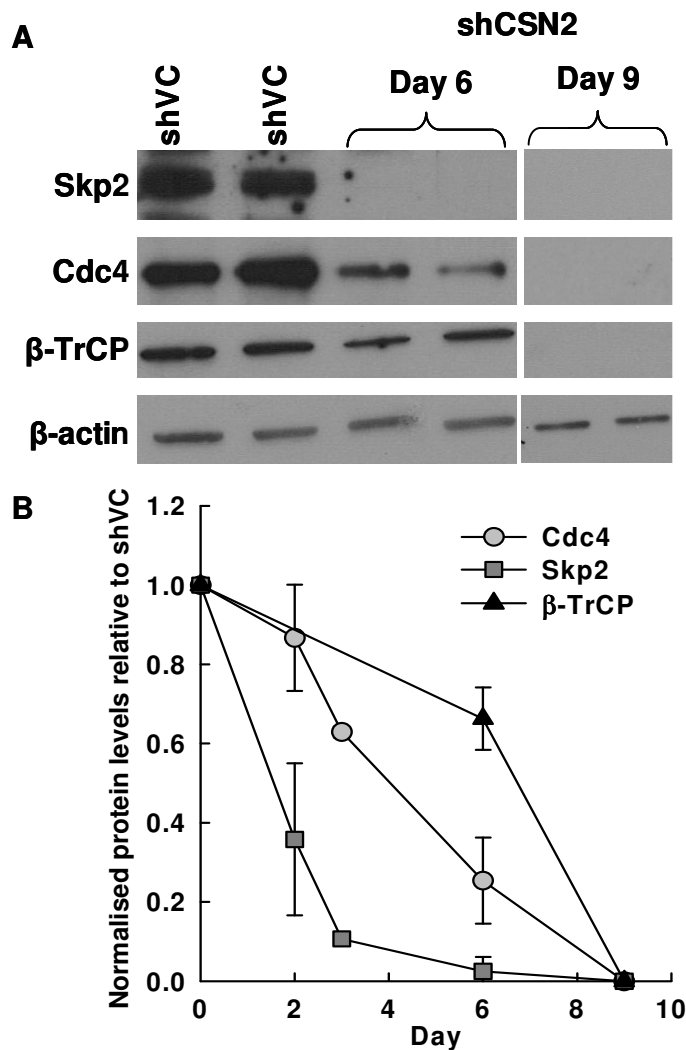


Figure 21. CSN2 knockdown results in the sequential loss of F-box proteins.

A, Transfected cells were harvested day 6 and day 9 post-transfection, protein extracted and Skp2, Cdc4 and β -TrCP protein levels in vector control and CSN2 knockdown cell extracts determined by western blot. Even loading was determined by β -actin western blot. **B**, Transfected cells were harvested day 2, 3, 6 and 9 post-transfection, protein extracted and Skp2, Cdc4 and β -TrCP protein levels in vector control and CSN2 knockdown cell extracts determined by western blot. Densitometry was used to determine the level of each of the proteins, normalised for loading using β -actin, in CSN2 knockdowns at each time point. Data was normalised to protein levels in vector control cells and the data plotted as the mean \pm SEM.

at all time points assessed, with normalization to β -actin signal for loading correction. Values obtained for CSN2 knockdown samples were normalized to vector control values and the data plotted as a line graph \pm the standard error of the mean (figure 21B). Skp2 protein was reduced by ~60% by day 2 and over 90% by day 6, whereas Cdc4 was lost at a slower rate with 30-40% lost by day 3 increasing to ~70% by day 6 post transfection (Figure 21B). Loss of β -TrCP was still more retarded with ~70% protein remaining at day 6 (Figure 21B). Importantly, treatment of shCSN2 cells with the proteasome inhibitor MG132 (10 μ M; (Naujokat et al., 2000, Su et al., 2008)) resulted in the rescue of F-box protein levels in these cells relative to vector controls (figure 22). This data suggests that these F-box proteins are, at least in part, degraded by the 26S proteasome in the absence of CSN2; degradation which is most likely mediated by the autocatalytic degradation mechanism reported previously (Wee et al., 2005, Galan and Peter, 1999).

3.2.8 Assessment of the effect of CSN2 knockdown on F-box protein mRNA

Although proteasome inhibition rescued F-box proteins in CSN2 knockdown cells, rescue was only partial, suggesting that CSN2 loss may also affect F-box protein expression as well as degradation. The effect of CSN2 knockdown on the level of F-box protein mRNA was therefore investigated. Vector control and shCSN2 cells were harvested at the time points indicated and Skp2, Cdc4 and β -TrCP mRNA measured by QRT-PCR. Skp2 mRNA was significantly reduced at all time points studied, whilst Cdc4 and β -TrCP mRNA were significantly increased at day 3 and day 6 post transfection, respectively (figure 23). These data suggest that both decreased transcription and increased protein

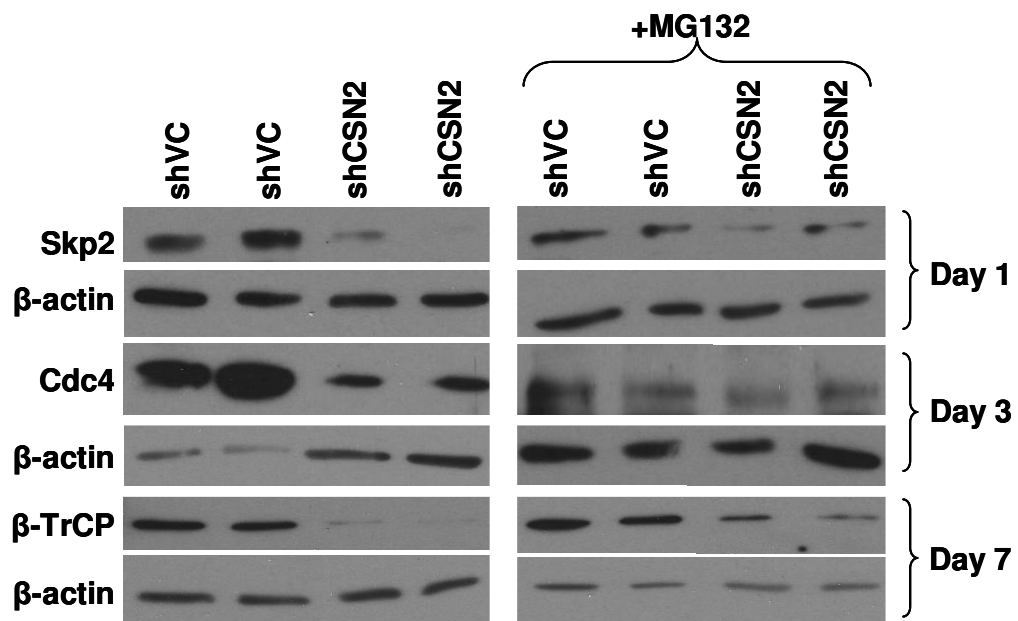


Figure 22. F-box protein loss in CSN2 knockdowns is rescued with the addition of the proteasome inhibitor MG132.

Transfected cells were treated with either DMSO (control) or 10 μ M MG132 for the final 18 hours of culturing and cells harvested, protein extracted and Skp2, Cdc4 and β -TrCP protein levels in cell extracts determined by western blot. Even loading was determined by β -actin western blot.

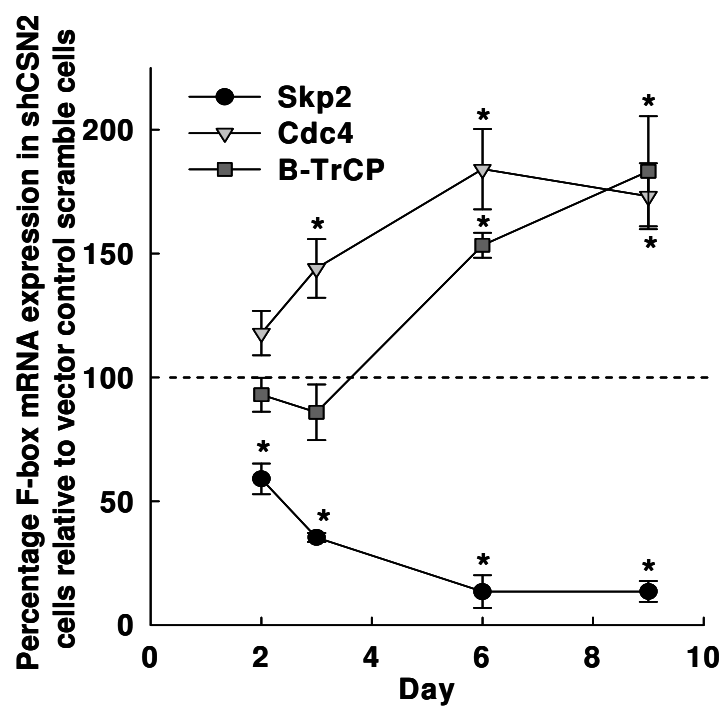


Figure 23. CSN2 knockdown results in significant alteration to the level of F-box mRNA.

The level of Skp2, Cdc4 and β -TrCP mRNA in shCSN2 cells was determined at each time point post transfection relative to expression in vector control scramble cells by QRT-PCR. Data shown is the mean \pm SEM of n=3 transfections. * indicates significant difference to vector controls with p<0.05.

degradation contribute to the reduced Skp2 protein level in CSN2 knockdown cells, whilst indicating that loss of Cdc4 and β -TrCP protein is not attributable to altered transcription. Finally, these data suggest a role, either direct or indirect, for the CSN complex in the regulation of F-box protein expression.

3.2.9 Assessment of the effect of CSN2 knockdown on cell growth and cell death

In order to determine the effects of CSN2 loss on cell growth and viability, cell counts were taken day 2-7 and day 9 post transfection, the cumulative cell growth for both vector control and CSN2 knockdown cells was calculated and the data plotted \pm the standard error of the mean of n=3 transfections. Knockdown of CSN2 caused dramatically reduced cell growth followed by loss of cell numbers mediated by loss of cell viability (Figure 24). The proliferation of cells lacking CSN2 was significantly less than that of shVC by day 4 post transfection (Figure 24, $P=0.034$), as determined using the t-test. These findings were corroborated by thymidine incorporation data. At day 3 post-transfection, there was no significant difference in the incorporation of tritiated thymidine into cellular DNA between shVC and CSN2 knockdown cells (Figure 25; $P=0.195$). However, by day 5 the CSN2 knockdown cells demonstrated a significant decrease in thymidine incorporation ($P=0.007$) which decreased even further by day 7 post transfection (Figure 25; $P=1.1 \times 10^{-5}$).

The cumulative growth profile of CSN2 knockdown cells (figure 24. Insert) suggests that the absence of CSN2 results in either slower passage through the cell cycle or cell cycle

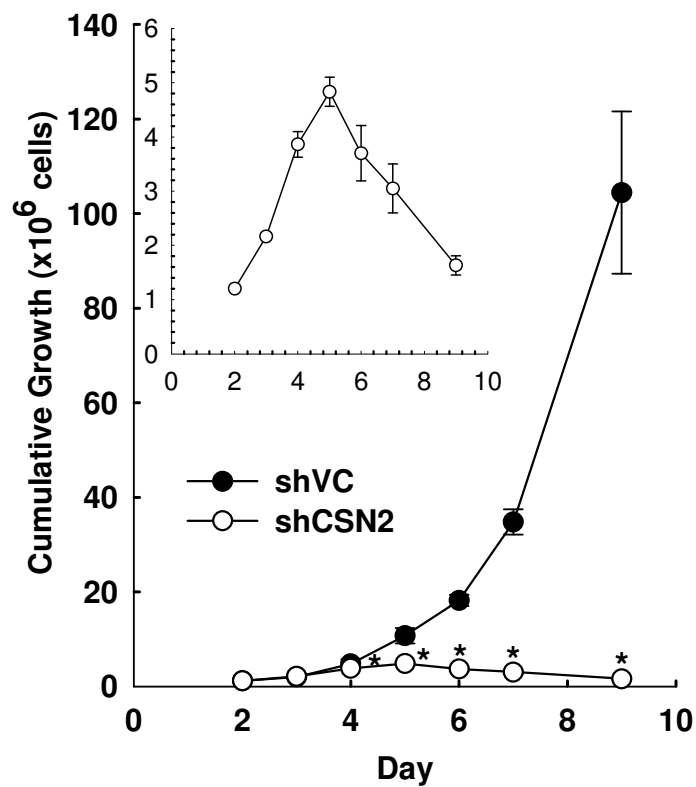


Figure 24. CSN2 knockdown results in significantly reduced cell growth.

Cell counts were taken daily and the cumulative growth calculated. The cumulative growth of CSN2 knockdowns and vector controls is shown. The insert shows the CSN2 knockdown cumulative growth profile in the absence of vector control data. Data shown are the mean \pm SEM of n=3. * indicates a significant difference to vector control cell growth with $p < 0.05$.

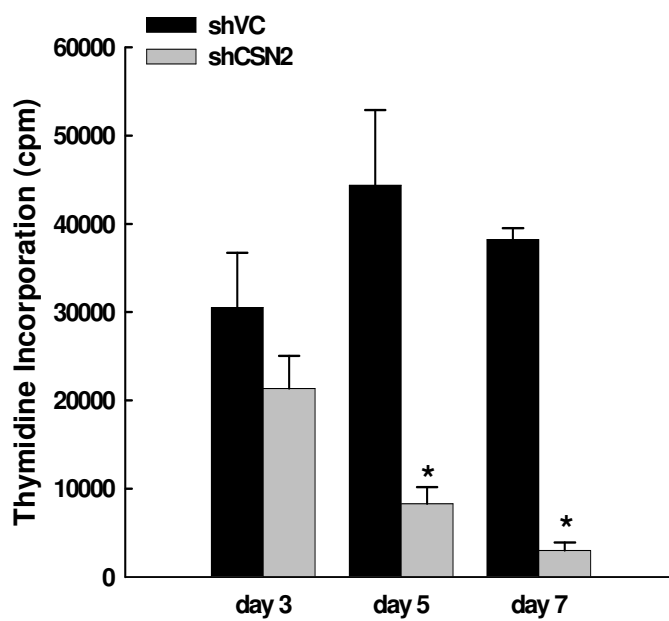


Figure 25. CSN2 knockdown results in significantly reduced thymidine incorporation into cellular DNA.

Thymidine incorporation in shCSN2 and vector control cells was measured day 3, 5 and 7 post transfection. Data shown are the mean \pm SEM of n=3 transfections. * indicates $p < 0.05$.

inhibition. In order to discern between these two possibilities, the cell cycle profiles of both vector control cells and cells lacking CSN2 were determined day 6 post transfection (figure 26). The percentage of cells in subG1, G1, S, and G2M in vector control and CSN2 knockdown cells was determined using flow cytometry and plotted as pie charts. Data shown is the mean \pm the standard error of the mean of n=3 transfections. The significance of any differences was determined using the t-test. As can be seen in figure 26, the cell cycle profiles of vector control and CSN2 knockdown cells were relatively similar, with no significant differences detected in the G1, S or G2M phases of the cell cycle. However, an approximately twofold increase in subG1 cells relative to vector control cells was observed (figure 26B; P=0.0003). As accumulation of cells in subG1 is indicative of cell death, this finding is in accordance with the onset of cell death at day 6 post transfection observed from the cumulative growth data. Together, the cumulative growth, thymidine incorporation and cell cycle flow cytometry data suggest that loss of CSN2 results in a slowed cell proliferation rate of K562s followed by cell death.

3.2.10 Determination of the mechanism of CSN2 knockdown induced cell death

In order to determine whether the loss of viability in CSN2 knockdown cells was due to apoptosis, vector control and CSN2 knockdown cells were harvested day 6 post transfection, protein extracted and caspase-9 cleavage determined by western blot analysis. As can be seen in figure 27, equivalent amounts of caspase-9 were present in vector control and CSN2 knockdown cells, and no caspase-9 cleavage product was detected. As a second measure of apoptosis, cells were co-analysed for annexin V

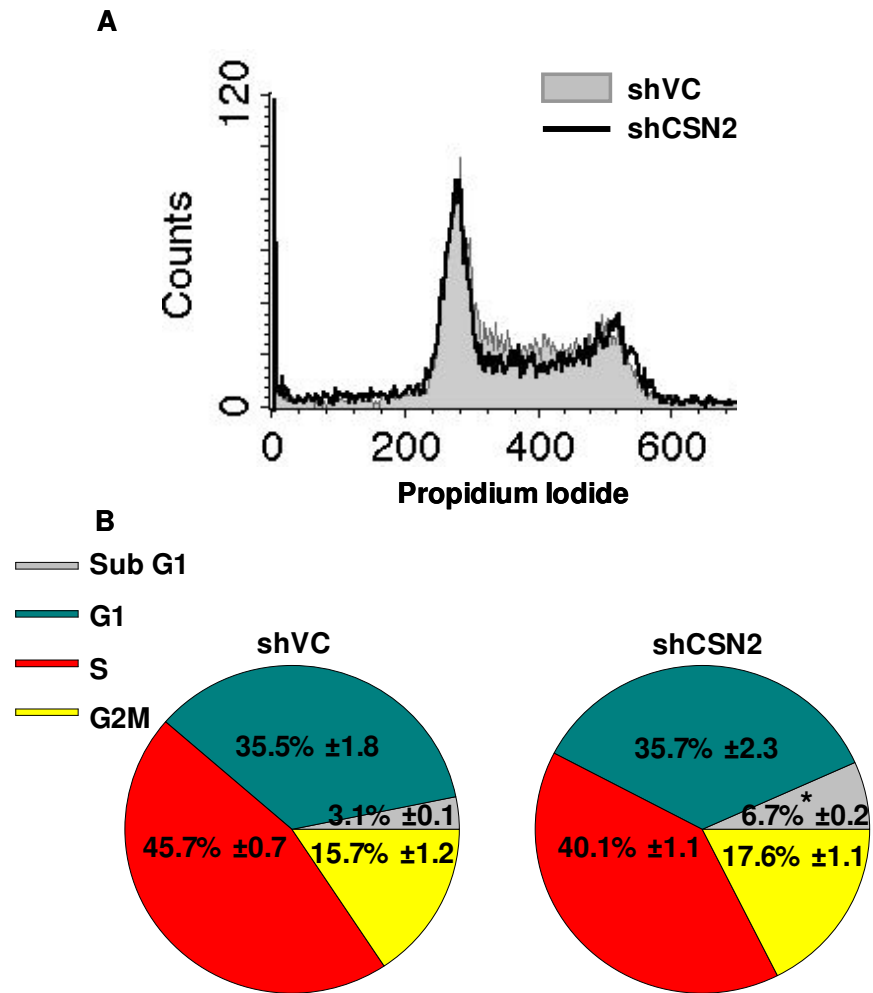


Figure 26. CSN2 knockdown has no significant effect on the cell cycle.

A, A representative image of CSN2 knockdown (black line) cell cycle profiles day 6 post transfection relative to vector control (light grey in fill). **B**, Statistical analysis of cell cycle data is shown as pie charts. Data shown are the mean \pm SEM of $n=3$. * indicates $p<0.05$.

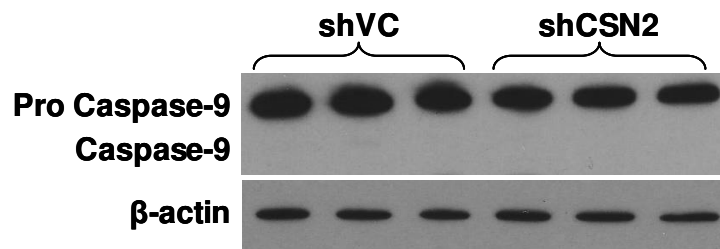


Figure 27. CSN2 knockdown has no effect on caspase-9 activation.

Transfected cells were harvested day 6 post transfection, protein extracted and caspase-9 protein levels in vector control and CSN2 knockdown cell extracts determined by western blot. Even loading was determined by β -actin western blot. The image shown is of three independent vector control and CSN2 knockdown transfections.

staining and propidium iodide uptake day 7 and day 9 post transfection (Figure 28). Annexin V binds phosphatidylserine, a phospholipid which is translocated from the inner to the outer leaflet of the plasma membrane during apoptosis; annexin V staining is therefore a measure of apoptosis. Propidium iodide is taken up by all cells but is efficiently effluxed by viable cells, whereas dead/dying cells remain PI-positive. In K562 cells, knockdown of CSN2 led to an increase in late apoptotic (annexin V^{+ve}:PI^{+ve}) cells (12.5%±0.9; P=0.023) compared to shVC cells (5.5%±2.2; figure 28A) day 7 post transfection, and resulted in no change in the proportion of early apoptotic (annexin V^{+ve}:PI^{-ve}) cells relative to vector control cells (5.5%±0.8 and 5.9%±1.9, respectively, P=0.826; figure 28A). However, by day 9 post transfection over two thirds of cells lacking CSN2 were annexin V positive (52%±2.4 annexin V^{+ve}:PI^{+ve}; P=4.1x10⁻⁵, and 16.8±1.8 annexin V^{+ve}:PI^{-ve}; P=0.001), indicative of significant apoptosis in these cells relative to vector control cells (7.2%±1.5 late apoptotic and 5%±0.2 early apoptotic, figure 28B). Although CSN2 loss resulted in a dramatic increase in the proportion of apoptotic cells by day 9 post transfection, the cell death apparent in CSN2 knockdown cells between days 5 and 7 (37.2%±6.6; P=0.015, figure 24) cannot be adequately accounted for by increased apoptosis during this time as measured by caspase-9 western and annexin V staining (figures 27 & 28A). Together, these data suggest that the cell death which ensues as a consequence of CSN2 loss involves a mix of both apoptotic and non-apoptotic cell death.

Annexin V and propidium iodide staining of CSN2 knockdown cells demonstrated that there was a significant shift to greater PI positivity in annexin V negative cells resulting

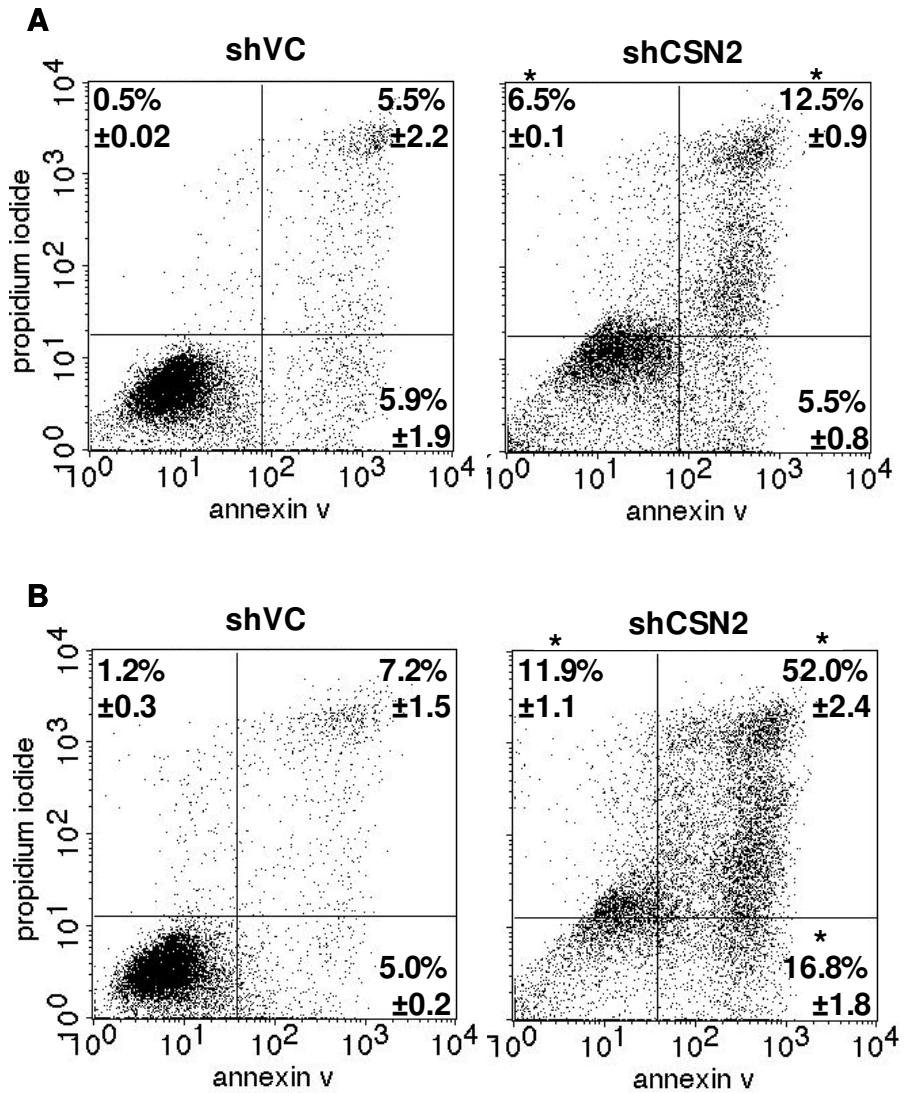


Figure 28. CSN2 knockdown results in a significant increase in annexin V positivity.

Binding of Annexin V and uptake of propidium iodide in vector control (left) and CSN2 knockdown (right) cells day 7 (**A**) and day 9 (**B**) post transfection was analysed by flow cytometry. The lower left quadrant encompasses the viable population of cells, the lower right quadrant contains early apoptotic cells, the upper right quadrant contains late apoptotic cells and the upper left quadrant contains the necrotic cell population. Dot plots shown are representative of n=3 transfections. The mean of three data sets was taken and the values shown in the corresponding quadrant \pm SEM. * indicates significance with $p < 0.05$.

in a significant increase in cells arising in the upper left quadrant relative to vector controls day 7 post transfection (6.5%±0.1 in CSN2 knockdowns compared to 0.5%±0.02 in vector controls, P=0.0018; figure 28A). This shift was also observed day 9 post transfection (figure 28B). These data are better displayed as a histogram of cell count against propidium iodide, in which only the annexin V negative population is considered. This analysis demonstrates that over 25% of annexin V negative CSN2 knockdown cells were propidium iodide positive by day 7 post transfection (figure 29A; P=3.3x10⁻⁵). This shift increased by day 9 post transfection, with over half of annexin V negative CSN2 knockdown cells retaining propidium iodide (figure 29B; P=5.5x10⁻⁶). CSN2 knockdown cells were also associated with the formation of large vacuoles (see below) which raised the possibility that the accumulation of propidium iodide (PI) positive cells in a population lacking CSN2 was an artifact of PI retention within vacuoles. However, visualization of PI stained shCSN2 cells demonstrated there was no PI retention within vacuoles (figure 29C). These data are further indicative of the occurrence of both non-apoptotic and apoptotic cell death in cells lacking CSN2.

3.2.11 Morphological analyses of CSN2 knock down in K562 cells

Both vector control and CSN2 knockdown cell cytopspins were stained with Jenner-Giemsa in order to observe cell morphology. This staining identified large vacuoles in a significant proportion of CSN2 knockdown cells which were not present in vector control cells (figure 30A). It was considered that these vacuoles may be autophagosomes. To test this, cells were stained with the autophagosome marker monodansylcadaverine (MDC).

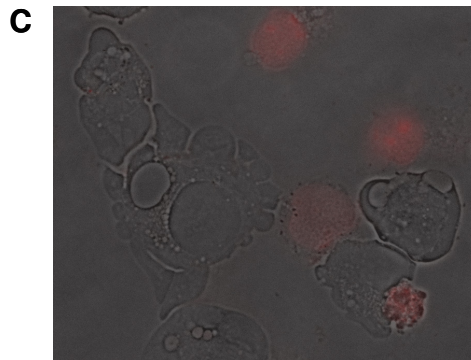
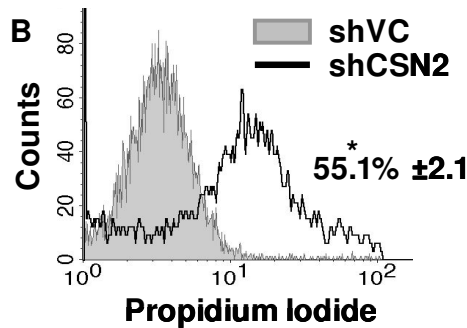
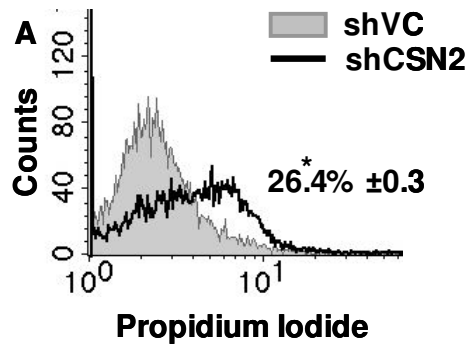


Figure 29. CSN2 knockdown results in a significant increase in the proportion of propidium iodide^{+ve}:annexin V^{-ve} cells, not caused by propidium iodide retention within vacuoles.

The histograms shown are representative of the propidium iodide^{+ve}:annexin V^{-ve} staining of n=3 vector controls (light grey in fill) and CSN2 knockdowns (black line) day 6 (A) and day 9 (B) post transfection. The mean percentage of propidium iodide positive staining in annexin V^{-ve} shCSN2 cells is shown \pm SEM. * indicates $p < 0.05$. C, shCSN2 cells were stained with propidium iodide and cytopins made to determine any retention of the stain within the vacuoles of shCSN2 cells day 6 post transfection. The image shown is representative of n=3 transfections.

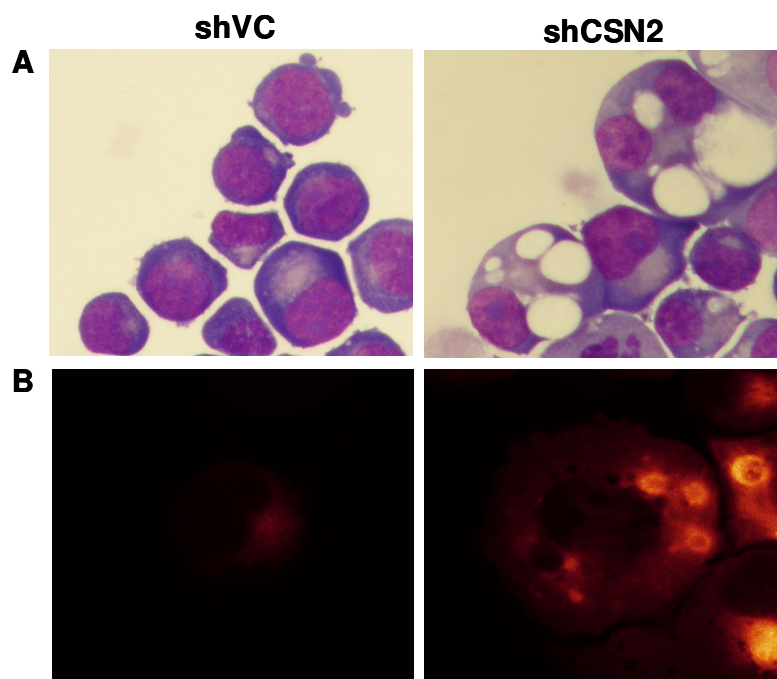


Figure 30. CSN2 knockdown cells contain autophagosomes.

A, Cytopspins were stained with Jenner-Giemsa for visualisation of vector control and shCSN2 cell morphology day 6 post transfection. **B**, Vector control and shCSN2 cells were stained with the autophagosome marker monodansylcadaverine day 6 post transfection and cytopspins made for the visualisation of autophagosomes. All images shown are representative of n=3 transfections.

MDC staining and DIC imaging identified these vacuoles as autophagosomes, whilst the staining of vector control cells with MDC was minimal (figure 30B). To further validate the association of autophagy with CSN2 knockdown cells, both vector control and CSN2 knockdown cells were harvested day 6 post transfection, protein extracted and the level of the autophagy marker protein light chain 3-II (LC3-II) determined by western blot analysis. As shown in figure 31, there was a highly significant accumulation of LC3-II protein in cells deficient in CSN2 relative to vector control cells. Thus, CSN2 knockdown cells were associated with autophagy.

3.2.12 Autophagy inhibition recapitulates shCSN2 cell growth, morphology and LC3-II accumulation

Although the observed significant loss of cell viability, MDC^{+ve} vacuolar morphology and LC3-II accumulation in CSN2 knockdowns suggests that these cells were undergoing autophagic cell death, current literature indicates that the large vacuoles and LC3-II accumulation observed in shCSN2 cells could be attributable to either autophagy induction or inhibition (Mizushima and Yoshimori, 2007, Klionsky et al., 2008). Autophagy inhibitors (3-methyl adenine, 3-MA; Bafilomycin A1, Baf A1) and an inducer (rapamycin) were therefore used in order to provide insight into the phenotype observed in shCSN2 cells.

The concentration of 3-MA used was determined from associated literature (Yan et al., 2006). Surprisingly, treatment of vector control cells with the early stage autophagy

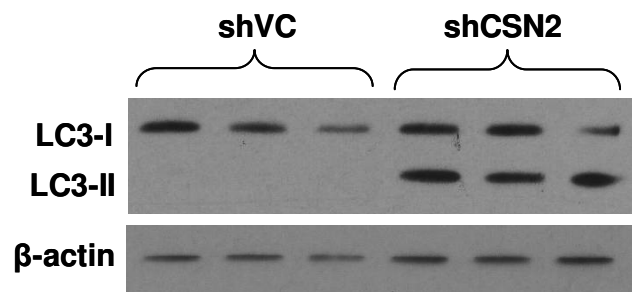


Figure 31. CSN2 knockdown results in accumulation of the autophagy marker protein LC3-II.

Transfected cells were harvested day 6 post transfection, protein extracted and LC3-II protein levels in vector control and CSN2 knockdown cell extracts determined by western blot. Even loading was determined by β -actin western blot. The image shown is representative of three sets of $n=3$ transfections.

inhibitor 3-MA recapitulated the cumulative cell growth kinetics of shCSN2 cells, whilst having a relatively small effect on the growth of shCSN2 cells (figure 32). These findings suggested that CSN2 loss may result in autophagy inhibition. For this to be consistent with the occurrence of large vacuoles in shCSN2 cells, such autophagy inhibition would have to be occurring at a late stage. The late stage autophagy inhibitor Baf A1 was thus used to further investigate the possibility of late stage autophagy inhibition in shCSN2 cells. The concentration of Baf A1 to be used had to first be determined experimentally due to variation in the literature (Fader et al., 2008, Jones et al., 1999, Savina et al., 2003, Shacka et al., 2006). Treatment of wild-type K562 cells for 48 hours with either 10nM, 100nM or 1 μ M Baf A1 resulted in a significant amount of apoptotic cell death at this time point (figure 33A) with a significant reduction in cell number (figure 33B), most likely attributable to the associated toxicity of the compound. It was therefore concluded that, rather than a time course, a 48 hour treatment would be optimal. Interestingly, it was observed during dose titration experiments that treatment of wild-type K562 cells for 48 hours with 1 μ M Baf A1 resulted in a dramatic accumulation of LC3-II protein (figure 33C) and the formation of large vacuoles (figure 33D). This finding was also confirmed in vector control cells, with treatment of shVC cells with 1 μ M Baf A1 for 48 hours also recapitulating both the vacuolar morphology (figure 34A) and the LC3-II protein accumulation (figure 34B) observed in shCSN2 cells. Cumulatively, autophagy inhibitor data suggests that cells lacking CSN2 undergo autophagy inhibition at a late stage.

For further indication of the effect of CSN2 loss on autophagy, the autophagy inducer rapamycin was also used. Cells were treated with three different concentrations of

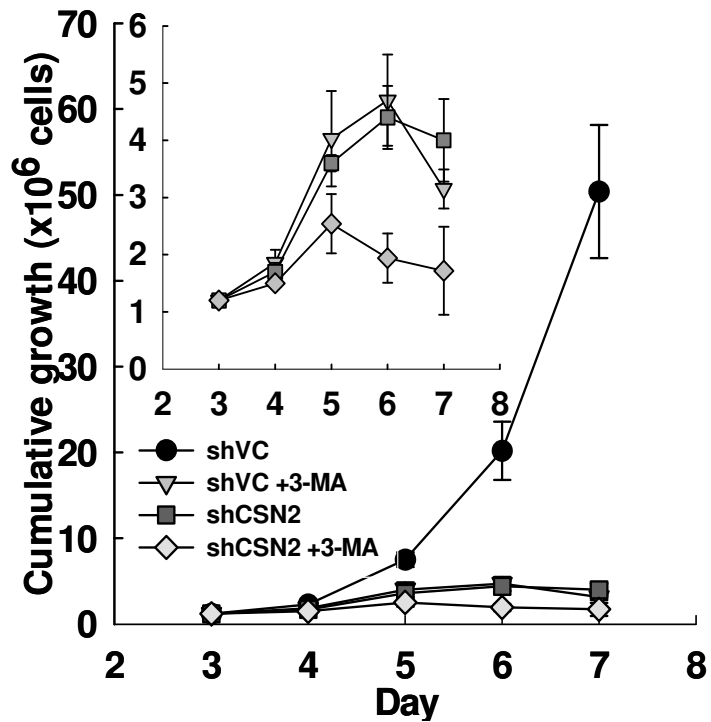


Figure 32. Treatment of vector control cells with 3-methyladenine recapitulates the cell growth pattern of CSN2 knockdown cells, whilst having little effect on cells lacking CSN2.

Cell counts were taken daily and the cumulative growth calculated. The cumulative growth of vector controls and CSN2 knockdowns treated with either DMSO (control) or the autophagy inhibitor 3-ma is shown. The insert has had the DMSO treated vector control data removed. Data shown are the mean \pm SEM of n=3.

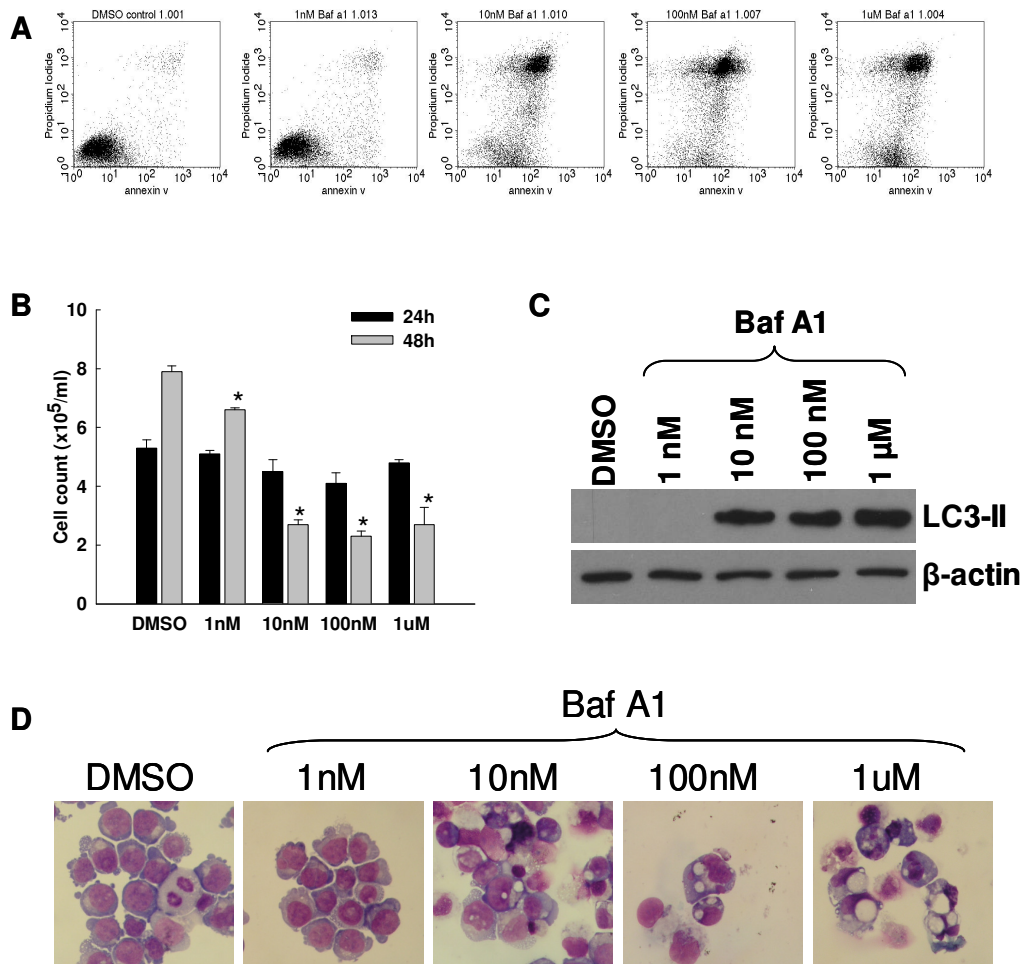


Figure 33. Dose titration of bafilomycin A1.

K562 cells were treated for 48 hours with either DMSO (control) or bafilomycin A1 and Annexin V flow cytometry (**A**), cell counts (**B**) LC3-II western blotting (**C**) and Jenner-Giemsa staining (**D**) carried out. Data shown is representative of n=3. * indicates $p < 0.05$.

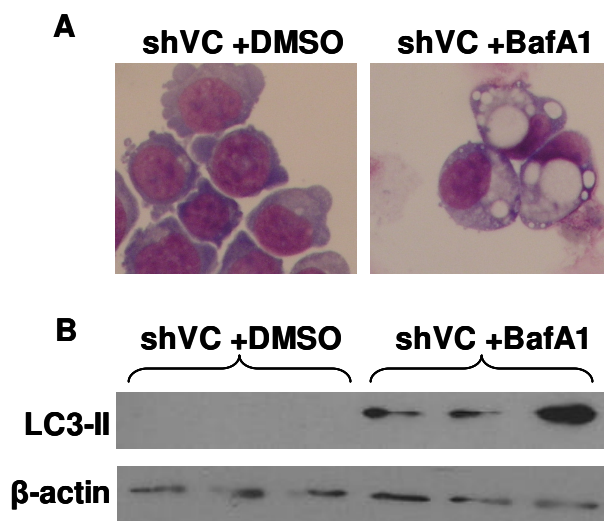


Figure 34. Treatment of vector control cells with bafilomycin A1 recapitulates the vacuolar morphology and LC3-II accumulation observed in shCSN2 cells.

A, Jenner-Giemsa staining of shVC +/- 48 hour 1 μ M bafilomycin A1 treatment. Images shown are representative of n=3 transfections. **B**, Vector control cells treated with either DMSO (control) or the autophagy inhibitor bafilomycin A1 for 48 hours were harvested and the level of LC3-II and β -actin protein determined by western blot.

rapamycin for 6 days and the level of LC3 protein determined by western blot. The data demonstrates that no accumulation of LC3-II occurs with rapamycin treatment (figure 35). However, a dose dependent increase in the LC3-II precursor protein LC3-I was observed, demonstrating that the compound is functional with respect to autophagy induction (figure 35). Collectively, these data imply strongly that CSN2 knockdown results in autophagy inhibition followed by apoptotic or non-apoptotic cell death.

It was hypothesized that the inhibition of autophagy in CSN2 knockdown cells may result in the accumulation of cellular protein, particularly in the absence of functional CRL complexes. To test this hypothesis, vector control and CSN2 knockdown cells were harvested day 6 post transfection and the amount of protein per cell calculated. Data was plotted as the average of n=3 transfections \pm the standard error of the mean and the significance of any changes determined using the t-test (figure 36). As can be seen in figure 36, there was a significant increase in the amount of cellular protein in cells lacking CSN2 compared to vector control cells (P=0.017).

3.2.13 Analysis of the effect of a vector control scramble sequence

The use of interfering RNA has been associated with off target effects (Fedorov *et al*, 2006). In order to demonstrate that the knockdowns generated here are due to the presence of a specific shRNA sequence, a vector control scramble sequence which encodes a non-targeting shRNA was generated, cloned into pcDNA3.1-H1 and co-transfected into cells together with HKK. Figure 37A demonstrates that there is no effect

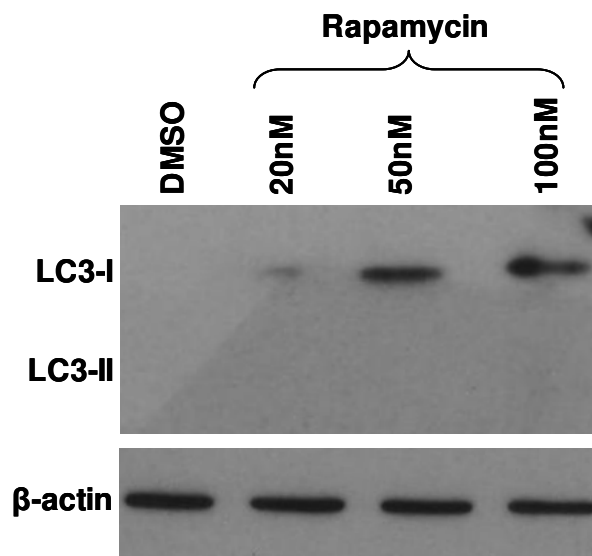


Figure 35. Treatment of K562 cells with the autophagy inducer rapamycin does not recapitulate the LC3-II accumulation observed in shCSN2 cells.

K562 cells were treated with either DMSO (control) or the autophagy inducer rapamycin for 6 days and the level of LC3-I, LC3-II and β -actin protein determined by western blot.

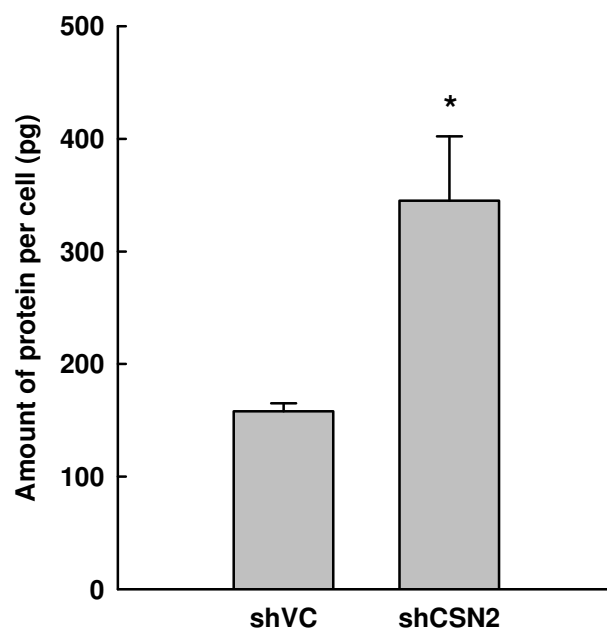


Figure 36. CSN2 knockdown results in a significant increase in total cellular protein.

Transfected cells were counted, harvested day 6 post transfection and protein extracted and quantified. The amount of protein per cell in both vector control and CSN2 knockdown cells was determined. Data shown is the mean \pm SEM of n=3 transfections. * indicates $p < 0.05$.

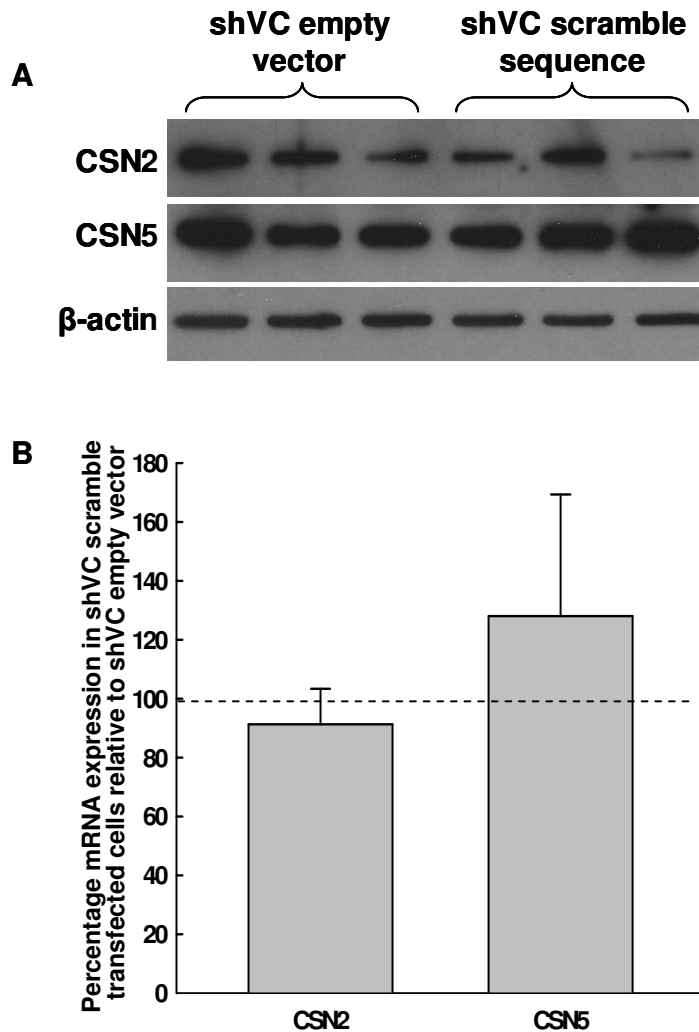


Figure 37. A vector control scramble sequence has no significant effect on the level of CSN2 or CSN5 protein or mRNA.

A, Transfected cells were harvested day 9 post transfection, protein extracted and CSN2 and CSN5 protein levels in empty vector and vector control scramble cell extracts determined by western blot. Even loading was determined by β -actin western blot. The image shown is of three independent empty vector and vector control scramble transfections. **B**, Empty vector and vector control scramble transfected cells were harvested day 9 post transfection, RNA extracted, cDNA generated and QRT-PCR carried out. CSN2 and CSN5 mRNA expression in vector control scramble cells relative to empty vector transfected cells is shown. Data is the mean of $n=3$ transfections \pm SEM.

on the level of CSN2 or CSN5 protein in vector control scramble cells relative to empty vector, determined by western blot. Furthermore, relative to empty vector, no significant effect is seen on CSN2 or CSN5 mRNA levels in vector control scramble cells as measured by QRT-PCR (figure 37B; P=0.826 and 0.684 respectively). These data clearly show that the high level of CSN2 and CSN5 protein and mRNA knockdown generated here are the result of the presence of a specific shRNA and not due to off target effects.

It was also important to assess any effect of non-targeting scramble sequence on K562 cell growth and death, and SCF activity, relative to empty vector control. Cell counts of empty vector and vector control scramble transfected cells were taken daily (day 3-9 post transfection) and the cumulative growth calculated. The data was plotted as a line graph \pm the standard error of the mean of n=3 transfections (figure 38). As can be seen in figure 38, there was no significant difference between the cumulative cell growth of empty vector and vector control scramble transfected cells, indicating that a non-targeting shRNA had no effect on cell growth or death.

In order to determine any effect of non-targeting shRNA on CRL activity, transfected cells were harvested day 9 post transfection, protein extracted and the level of Cull1, Skp2, p27 and protein determined by western blotting. Figure 39 demonstrates that the introduction of a non-targeting shRNA into K562 cells had no significant effect on the levels of these proteins. Conversely to CSN subunit targeting shRNA, the vector control scramble sequence did not increase the level of neddylated Cull1 and did not result in reduction of Skp2 or accumulation of p27 protein (figure 39). These data indicate that the

findings made following knockdown of CSN subunits in K562 cells are attributable to CSN subunit deficiency in these cells, and are not mediated by off target effects of the shRNA.

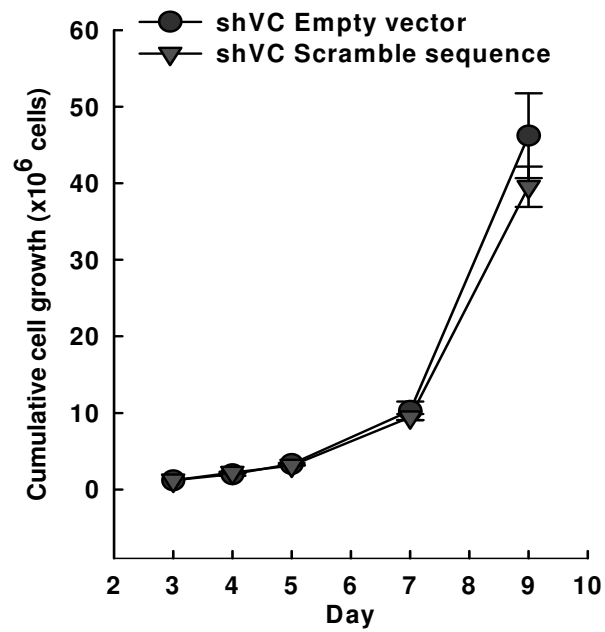


Figure 38. A vector control scramble sequence has no significant effect on cell growth.

Cell counts were taken daily and the cumulative growth calculated. The cumulative growth of empty vector and vector control scramble sequence transfected cells is shown. Data shown are the mean \pm SEM of n=3 transfections.

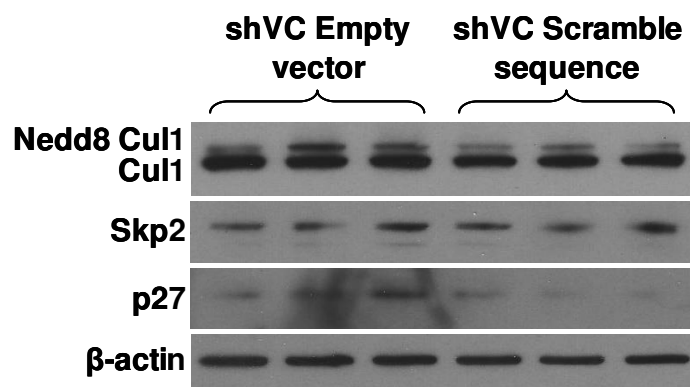


Figure 39. A vector control scramble sequence has no effect on the SCF or the SCF target p27.

Transfected cells were harvested day 9 post transfection, protein extracted and Cul1, Skp2, and p27 protein levels in empty vector and vector control scramble cell extracts determined by western blot. Even loading was determined by β -actin western blot. The image shown is of three independent empty vector and vector control scramble transfections.

Chapter 4.0:

**Analysis of the molecular and cellular
effects of CSN5 knockdown**

4.1 Introduction

Although the loss of CSN deneddylase activity was confirmed in shCSN2 cells, it was possible that the cellular phenotype of these cells was not attributable to the loss of cullin deneddylation. Indeed, although both resulting in defective cullin deneddylation, a *S. pombe* CSN2 null mutant does not share the same phenotype as a CSN5 null mutant (Mundt et al., 2002). It was thus important to determine whether loss of CSN5, which contains the cullin deneddylase activity of the CSN (Cope et al., 2002), resulted in the same phenotype as that observed in shCSN2 cells. To this end, CSN5 was targeted in K562 cells and the same analyses carried out as in the previous chapter.

4.2 Results

4.2.1 Assessment of target mRNA knockdown

In order to determine CSN5 mRNA levels in mock, vector control and shCSN5 cells, transfected cells were harvested day 4 post transfection, RNA extracted, quantified and cDNA produced using 1µg RNA. Once the quality of the sample cDNA was determined and the QRT-PCR protocol optimised (see 3.2.3), CSN5 expression was then determined. As shown in figure 40A, co-transfection of cells with HKK and empty vector had no significant effect on the expression of CSN5 relative to expression in mock transfected cells. However, co-transfection with HKK and shCSN5 resulted in only 5% CSN5 mRNA remaining relative to mock transfected cells (figure 40A; $P=3.12 \times 10^{-5}$).

4.2.2 Assessment of target protein knockdown

In order to determine CSN5 protein knockdown, vector control and shCSN5 cells were harvested day 4 post transfection, protein extracted, quantified, and 20µg protein used in western blot analyses. K562 cells co-transfected with HKK and shCSN5 plasmids had significantly less CSN5 protein than HKK and vector control plasmid transfected cells, with CSN5 protein undetectable in CSN5 knockdown cells (figure 40B). These data indicate a highly efficient knockdown at the protein level.

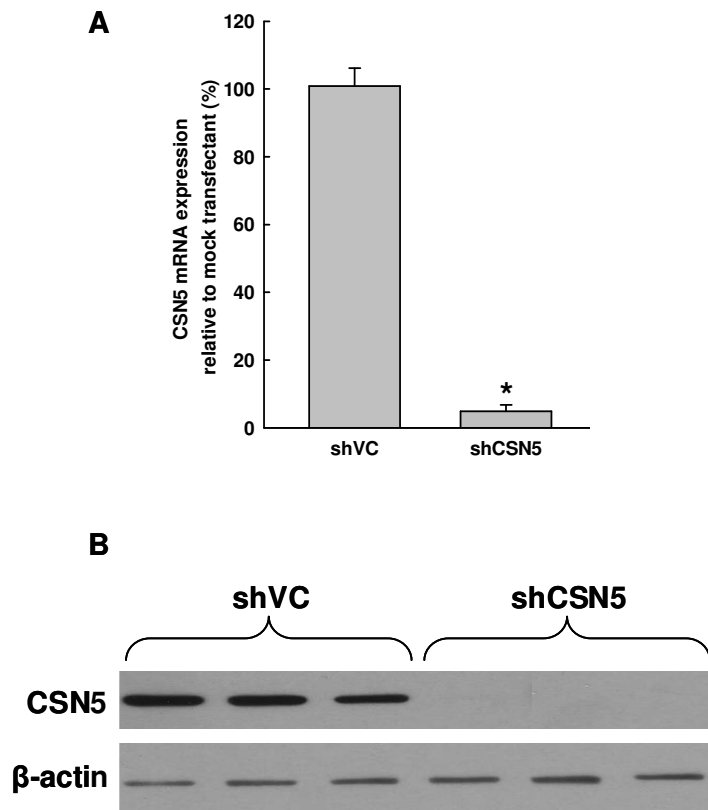


Figure 40. Determination of CSN5 mRNA and protein knockdown.

A, Mock, vector control and CSN5 knockdown transfected cells were harvested day 4 post transfection, RNA extracted, cDNA generated and used in QRT-PCR. Data shown is the mean CSN5 mRNA expression relative to mock transfected cells of $n=3$ transfections \pm SEM. * indicates $p<0.05$. **B**, Transfected cells were harvested day 4 post transfection, protein extracted and CSN5 protein levels in vector control and CSN5 knockdown cell extracts determined by western blot. Even loading was determined by β -actin western blot. The image shown is representative of three sets of $n=3$ transfections.

4.2.3 Assessment of the effect of CSN5 knockdown on SCF components and activity

In order to determine the effect of CSN5 loss on the level of Cul1, Skp2 and p27 proteins, vector control and CSN5 knockdown cells were harvested day 4 post transfection, protein extracted and the level of proteins in these samples determined by western blot analysis. As seen in figure 41A, knockdown of CSN5 resulted in an increase in neddylated Cul1 relative to vector control cells, at the expense of the deneddylated form of Cul1. This was confirmed by densitometry which demonstrated that the Cul1:Neddylated Cul1 ratio in cells lacking CSN5 was significantly less than that of vector controls (P=0.010; figure 41B).

Western blot analysis of Skp2 protein levels showed a complete loss of detectable Skp2 in cells lacking CSN5 (figure 41C), whilst p27 western blot analysis demonstrated significant p27 accumulation in CSN5 knockdown cells relative to vector control cells (figure 41D). As seen in CSN2 knockdowns, this data suggests that loss of CSN5 in K562 cells also results in deregulation of Cul1 neddylation and therefore, aberrant SCF^{Skp2} activity in K562 cells.

The effect of CSN5 loss on Cul3 protein was also investigated. CSN5 knockdown resulted in the marked accumulation of neddylated Cul3 protein relative to vector control cells (figure 42A). Quantitative analysis of this data demonstrated a significant reduction in the Cul3:Neddylated Cul3 ratio in cells lacking CSN5 (figure 42B; P=0.012). Furthermore, densitometric analysis also revealed a relatively small but significant loss of

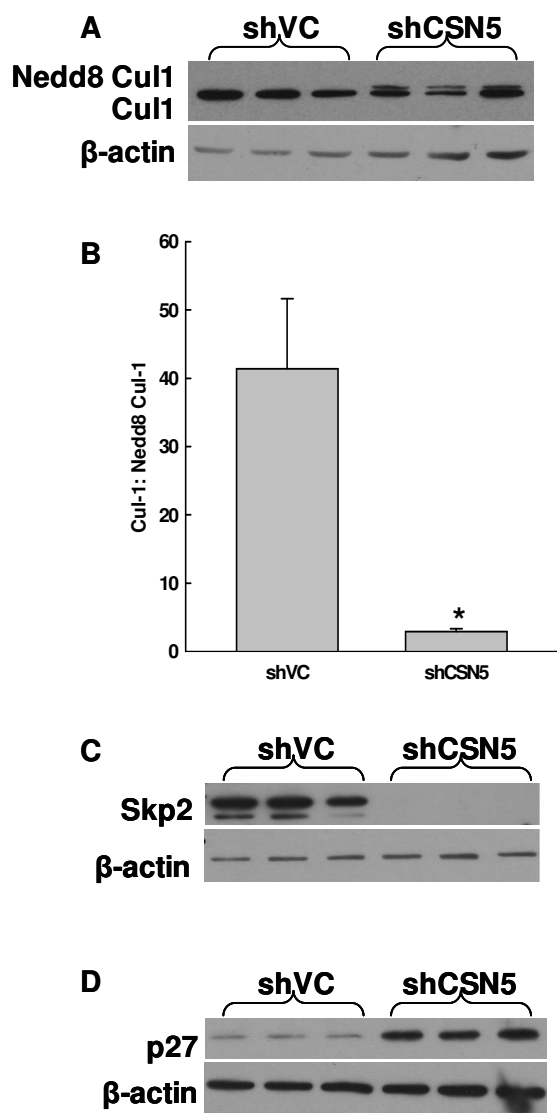


Figure 41. CSN5 knockdown results in accumulation of neddylated Cul1, loss of Skp2 and accumulation of p27.

Transfected cells were harvested day 4 post transfection, protein extracted and Cul1 (A), Skp2 (C) and p27 (D) protein levels in vector control and CSN5 knockdown cell extracts determined by western blot. Even loading was determined by β -actin western blot. The images shown are representative of three sets of n=3 transfections. B, Densitometry was carried out on the Cul-1 western blot and the Cul-1 to neddylated Cul-1 ratios of vector control and CSN5 knockdown cells calculated. Data shown is the average of n=3 transfections \pm SEM. * indicates $p < 0.05$.

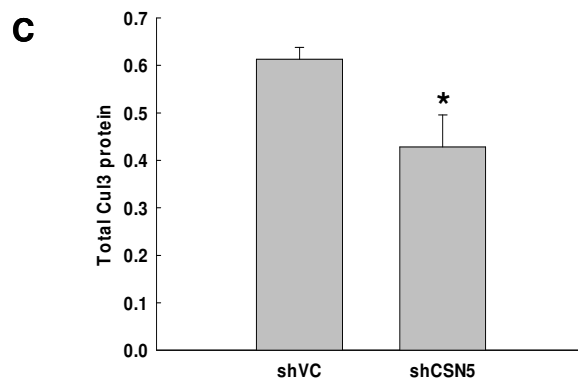
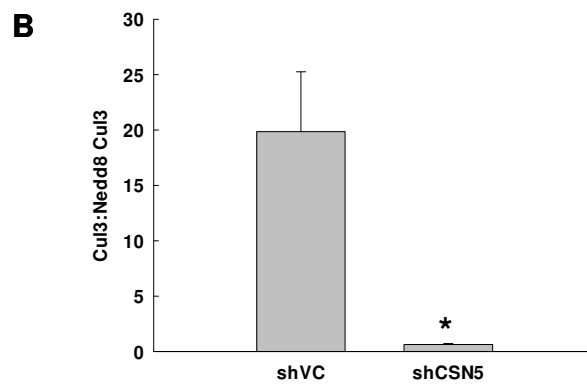
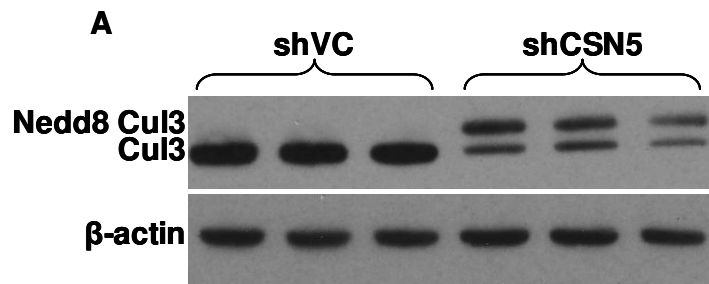


Figure 42. CSN5 knockdown results in the significant accumulation of neddylated Cul3 protein and loss of Cul3 protein.

A, Transfected cells were harvested day 4 post transfection, protein extracted and Cul3 protein levels in vector control and CSN5 knockdown cell extracts determined by western blot. Even loading was determined by β -actin western blot. The image shown is of three independent vector control and CSN5 knockdown transfections. Densitometry was carried out on the Cul3 western blot and the Cul3 to neddylated Cul3 ratios (**B**) and total Cul3 protein (**C**) of vector control and CSN5 knockdown cells calculated. Data shown is the average of $n=3$ transfections \pm SEM. * indicates $p<0.05$.

total Cul3 protein in shCSN5 cells (figure 42C; P=0.035). Collectively, these data suggest that, as in CSN2 knockdown cells, CSN5 loss results in the defective deneddylation of cullins, thus potentially altering the activity of multiple CRLs and therefore the degradation of many proteins. It is also important to note that the similar results obtained with CSN2 and CSN5 knockdowns with respect to CRL activity suggests that both knockdowns have the same effect on CSN deneddylase activity.

4.2.4 Assessment of the effect of CSN5 knockdown on the level of F-box proteins

In order to assess the effect of CSN5 knockdown on the level of multiple F-box proteins, protein levels of Skp2, Cdc4 and β -TrCP were determined day 4 post transfection. Figure 43 demonstrates the differential loss of F-box proteins in CSN5 knockdowns relative to vector control cells. At day 4 post transfection, Skp2 protein was undetectable in cells lacking CSN5 whilst Cdc4 protein was reduced by an average of 82%, as determined by densitometry. Furthermore, no significant effect on the level of β -TrCP protein was observed at this time point (figure 43). Addition of the proteasome inhibitor MG132 to cells at a time point at which these F-box proteins were found to be reduced restored the level of these proteins at least partially (figure 44; For Skp2, Cdc4 and β -TrCP protein rescue experiments vector control and CSN5 knockdown cells were treated with 10 μ M MG132 for 18 hours day 1, 3 and 6, respectively). These data suggest, in accordance with the CSN2 knockdown data, that F-box proteins are degraded in K562 cells in the absence of CSN deneddylase activity.

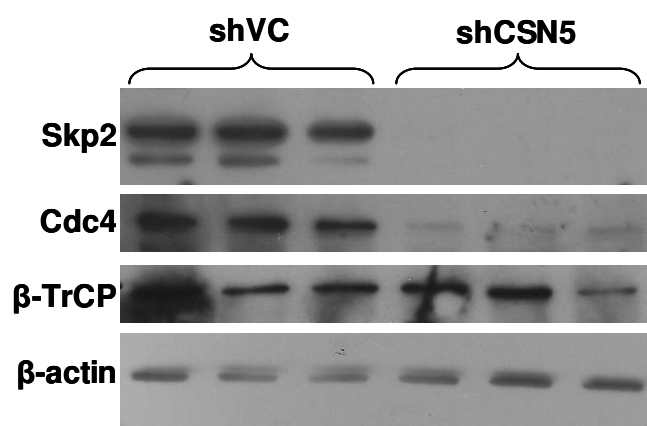


Figure 43. CSN5 knockdown results in the sequential loss of F-box proteins.

Transfected cells were harvested day 4 post-transfection, protein extracted and Skp2, Cdc4 and β -TrCP protein levels in vector control and CSN5 knockdown cell extracts determined by western blot. Even loading was determined by β -actin western blot. The image shown is of three independent vector control and CSN5 knockdown transfections.

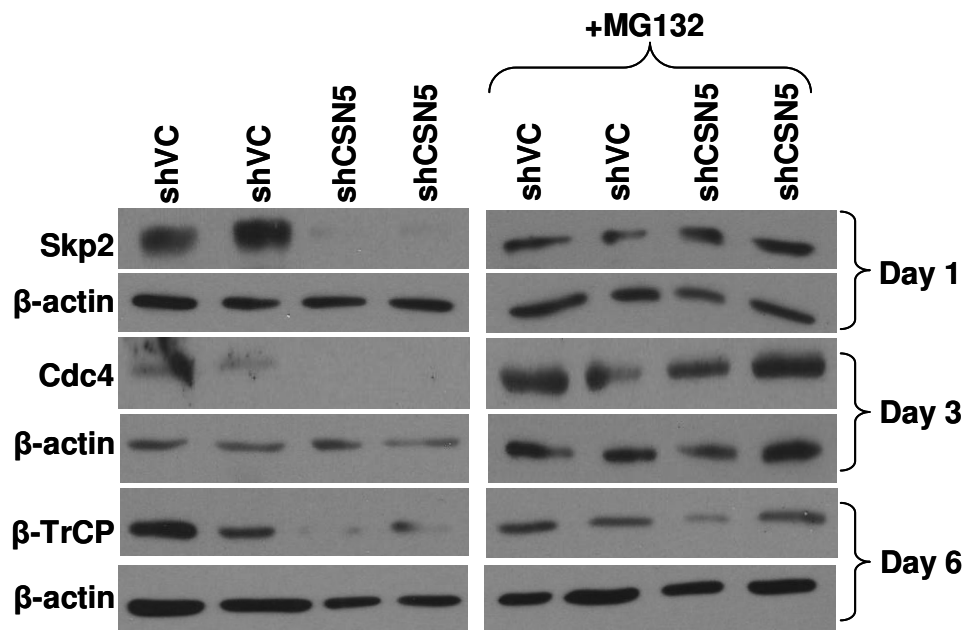


Figure 44. F-box protein loss in CSN5 knockdowns is rescued with the addition of the proteasome inhibitor MG132.

Transfected cells were treated with either DMSO (control) or 10 μ M MG132 for the final 18 hours of culturing. For Skp2, Cdc4 and β -TrCP protein rescue experiments vector control and CSN5 knockdown cells were treated day 1, 3 and 6, respectively. Cells were harvested, protein extracted and Skp2, Cdc4 and β -TrCP protein levels in cell extracts determined by western blot. Even loading was determined by β -actin western blot.

4.2.5 Assessment of the effect of CSN5 knockdown on F-box mRNA

Recently, a novel function of the CSN complex in the regulation of transcription has been suggested (Su et al., 2008, Ullah et al., 2007). The effect of CSN5 knockdown on the level of F-box protein mRNA was therefore investigated. Vector control and shCSN5 cells were harvested days 2, 3 and 6 and Skp2, Cdc4 and β -TrCP mRNA measured by QRT-PCR. β -TrCP mRNA was significantly reduced at all time points studied (figure 45; $P= 0.015$, 0.027 and 0.015 for day 2, 3 and 6, respectively) even though no difference in β -TrCP protein was observed by day 4 (figure 43), whilst Skp2 and Cdc4 mRNA were significantly reduced at day 6 post transfection (figure 45; $P=0.009$ and $P=0.044$, respectively). These data suggest that reduced F-box mRNA expression may in part account for the observed reduction in F-box proteins in CSN5 knockdown cells, and further implicate CSN5 or indeed the CSN complex in the regulation of F-box protein expression.

4.2.6 Assessment of the effect of CSN5 knockdown on cell growth and cell death

In order to determine the effects of CSN5 loss on cell growth and viability, cell counts were taken day 2-7 post transfection, the cumulative cell growth for both vector control and CSN5 knockdown cells was calculated and the data plotted \pm the standard error of the mean of $n=3$ transfections. The results demonstrate that knockdown of CSN5 resulted in the substantial reduction of cell growth followed by loss of cell viability (Figure 46). Analysis of cumulative growth demonstrated that proliferation of cells lacking CSN5 was

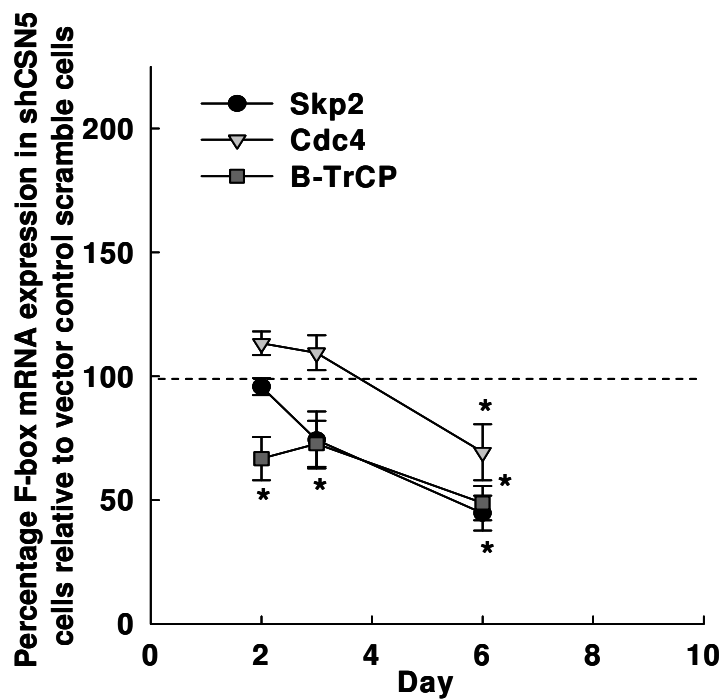


Figure 45. CSN5 knockdown results in significant alteration to the level of F-box mRNA.

The level of Skp2, Cdc4 and β -TrCP mRNA in shCSN5 cells was determined at each time point post transfection relative to expression in vector control scramble cells by QRT-PCR. Data shown is the mean \pm SEM of n=3 transfections. * indicates a significant difference to vector controls with p<0.05.

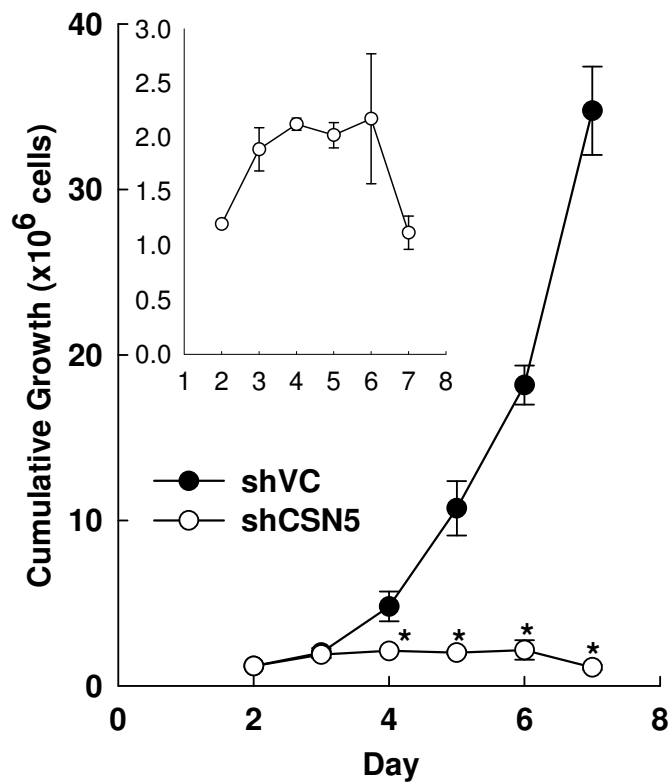


Figure 46. CSN5 knockdown results in significantly reduced cell growth.

Cell counts were taken daily and the cumulative growth calculated. The cumulative growth of CSN5 knockdowns and vector controls is shown. The insert shows a close up of the CSN5 knockdown cumulative growth profile in the absence of vector control data. Data shown are the mean \pm SEM of n=3. * indicates a significant difference to vector control cell growth with $p < 0.05$.

significantly less than that of shVC by day 4 post transfection (Figure 46, $P=0.0002$), as determined using the t-test. This data was corroborated by thymidine incorporation data which shows that, at day 3 post-transfection, there was a significant reduction in the incorporation of tritiated thymidine into cellular DNA between shVC and CSN5 knockdown cells ($P=0.001$), which decreased even further by day 4 post transfection (Figure 47; $P=0.007$).

The cell cycle profiles of both vector control cells and cells lacking CSN5 were determined day 4 post transfection (figure 48). The percentage of cells in subG1, G1, S, and G2M in vector control and CSN5 knockdown cells was calculated, plotted as pie charts and the significance of any differences determined using the t-test. As can be seen in figure 48, the cell cycle profile of CSN5 knockdown cells differed significantly to that of vector control cells in all phases. Differences included an increase in the subG1 fraction ($P=0.0005$), a significant reduction in the proportion of cells in the G1 and S phases of the cell cycle in CSN5 knockdowns ($P=0.004$ and 3.4×10^{-6} , respectively) and an accumulation of CSN5 knockdown cells in G2M ($P=0.001$; figure 48). This data suggests that cells deficient in CSN5 are subject to a block in mitosis, thereby corroborating the cumulative growth data. Furthermore, the cumulative growth profile and subG1 accumulation of CSN5 knockdown cells indicates reduced viability of CSN5 cells, which may potentially ensue as a consequence of the observed mitotic block.

In order to investigate the apparent mitotic block in CSN5 knockdown cells further, vector control and CSN5 knockdown cell cytopspins were Jenner-Giemsa stained to

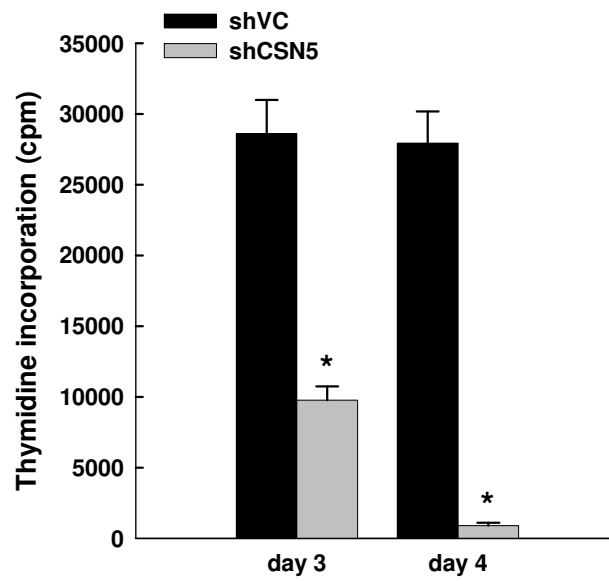


Figure 47. CSN5 knockdown results in significantly reduced thymidine incorporation into cellular DNA.

Thymidine incorporation in shCSN5 and vector control cells was measured day 3 and 4 post transfection. Data shown are the mean \pm SEM of n=3. * indicates $p < 0.05$.

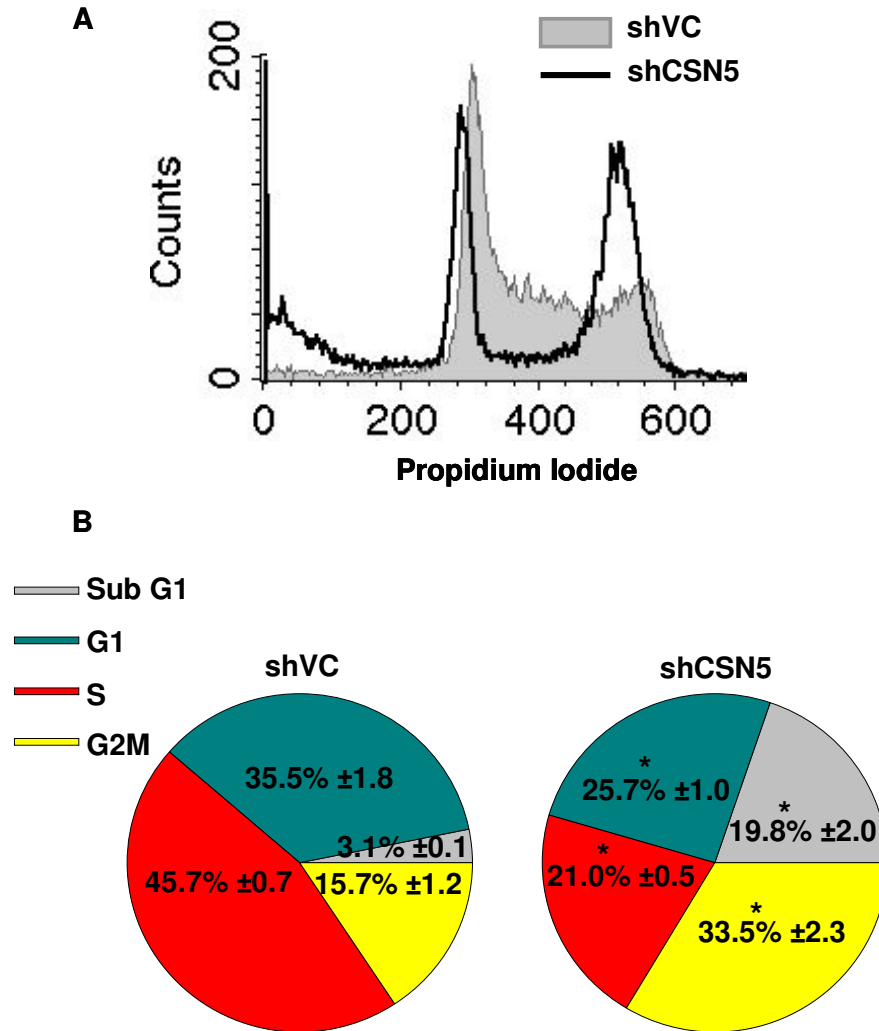


Figure 48. CSN5 knockdown results in significant changes in cell cycle.

A, A representative image of CSN5 knockdown (black line) cell cycle profiles day 4 post transfection relative to vector control (light grey in fill). **B**, Statistical analysis of cell cycle data is also shown as pie charts. Data shown are the mean \pm SEM of n=3 transfections. * indicates $p < 0.05$.

observe cell morphology. This staining clearly shows a significant number of cells in the CSN5 knockdown population which contained condensed, misaligned chromosomes, which were not present in the vector control population (figure 49A). To investigate this phenomenon further, vector control and CSN5 knockdown cells were immunostained for tubulin. As can be seen in figure 49B, shVC cells retained the ability to form a mitotic spindle and correctly aligned chromosomes at various stages of mitosis were observed. In contrast, the majority of cells lacking CSN5 demonstrated either aberrant or absent microtubule structures. In these cells, the condensed chromatids appeared to be either misaligned or indeed not associated with the spindle structures at all (figure 49B). The substantial numbers of cells showing this morphology are consistent with cell cycle arrest at G2/M. Altogether, this data suggests that loss of CSN5 in K562 cells results in reduced cell proliferation and subsequent cell death as a consequence of a mitotic block, possibly caused by aberrant mitotic spindle formation.

4.2.7 Determination of the mechanism of CSN5 knockdown induced cell death

To assess whether cell death in CSN5 knockdowns occurred via an apoptotic mechanism, vector control and CSN5 knockdown cells were harvested day 4 post transfection, protein extracted and caspase-9 protein levels determined by western blot analysis. As shown in figure 50, the caspase-9 cleavage product (indicative of apoptosis) is readily detectable in CSN5 knockdown cell extracts, the production of which occurs at the expense of the uncleaved form, whereas no caspase-9 cleavage is detectable in vector control cells (figure 50). To further validate apoptosis as the mechanism of CSN5 deficient cell death,

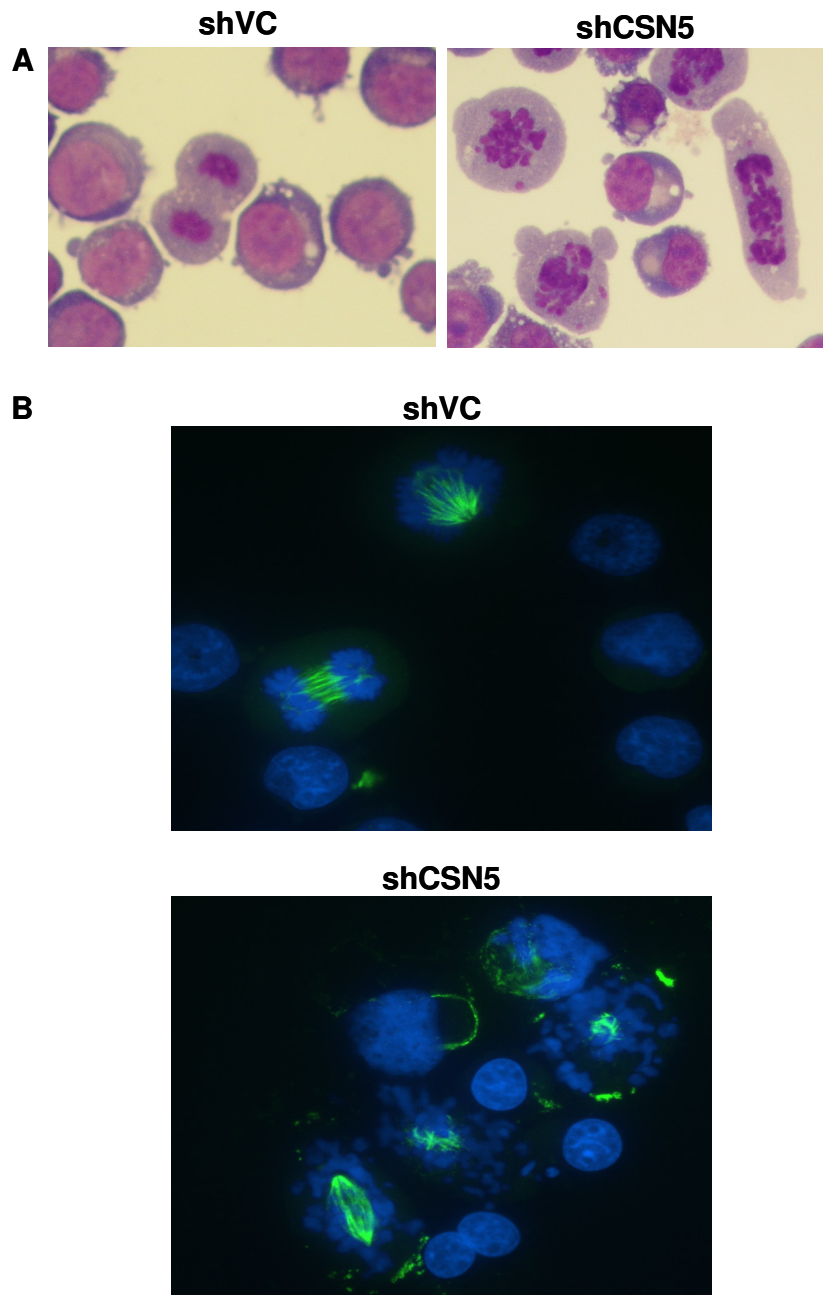


Figure 49. CSN5 knockdown results in altered cell morphology and aberrant mitotic spindle formation.

A, Cytopins were stained by Jenner-Giemsa for visualisation of vector control and shCSN5 cell morphology day 4 post transfection. **B,** Cytopins were stained with mouse anti-tubulin primary antibody, anti-mouse FITC secondary antibody and Hoescht for visualisation of both tubulin and DNA in vector control and shCSN5 cells day 4 post transfection. All images shown are representative of n=3 transfections.

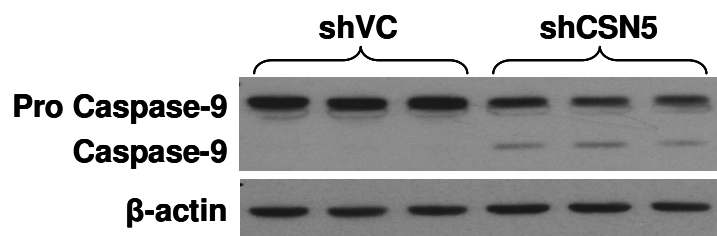


Figure 50. CSN5 knockdown results in caspase-9 activation.

Transfected cells were harvested day 4 post transfection, protein extracted and caspase-9 protein levels in vector control and CSN5 knockdown cell extracts determined by western blot. Even loading was determined by β -actin western blot. The image shown is of three independent vector control and CSN5 knockdown transfections.

cells were co-analysed for annexin V staining and propidium iodide uptake day 6 post transfection (Figure 51). CSN5 knockdown resulted in a large and highly significant increase in both early (annexin V^{+ve}:PI^{-ve}) and late (annexin V^{+ve}:PI^{+ve}) apoptotic cells relative to vector control cells (P=0.0015 and 0.0006, respectively; figure 51). Altogether, these data indicate that K562 cells lacking CSN5 die by apoptosis.

Annexin V and propidium iodide staining of CSN5 knockdown cells demonstrated that, contrary to the observations made in CSN2 knockdown cells, there was no shift to greater PI positivity in the annexin V negative cell population (figure 51). These data are better displayed as a histogram of cell count against propidium iodide, in which only the annexin V negative population is considered (figure 52). To further demonstrate the distinction between the phenotypes which occurred as a result of CSN2 and CSN5 knockdown, LC3-II protein levels day 4 post transfection were determined in vector control and CSN5 knockdown cells. Indeed, there was no accumulation of the autophagy marker protein LC3-II in CSN5 knockdown cells compared to vector controls (figure 53). It is important to note that the exposure time in figure 53 is 12 hours, compared to an exposure time of 1 minute in figure 31. Conversely to CSN2 knockdown cells (figure 31), an exposure time of 1 minute detected no LC3-II protein in CSN5 knockdown cells (data not shown). A longer exposure was therefore carried out in order to determine that there was no accumulation of LC3-II in shCSN5 cells relative to vector controls (figure 53). Cumulatively, these data indicate that, conversely to CSN2 knockdown cells, cells lacking CSN5 are not associated with autophagy and do not undergo non-apoptotic cell death but are instead subject to a mitotic block and die by apoptosis.

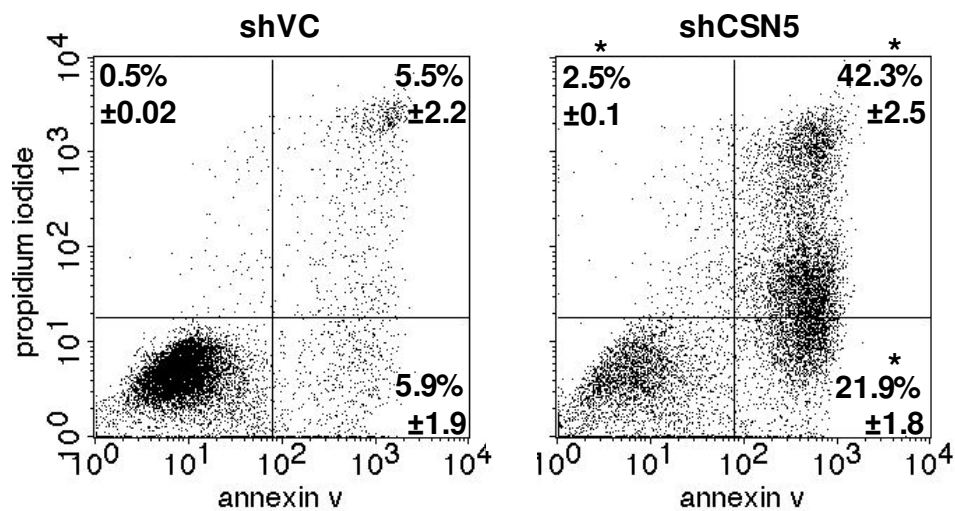


Figure 51. CSN5 knockdown results in a significant increase in annexin V positivity.

Binding of Annexin V and uptake of propidium iodide in vector control (left) and CSN5 knockdown (right) cells day 6 post transfection was analysed by flow cytometry. The lower left quadrant encompasses the viable population of cells, the lower right quadrant contains early apoptotic cells, the upper right quadrant contains late apoptotic cells and the upper left quadrant contains the necrotic cell population. Dot plots shown are representative of n=3 transfections. The mean of three data sets was taken and the values shown in the corresponding quadrant \pm SEM. * indicates significance with $p < 0.05$.

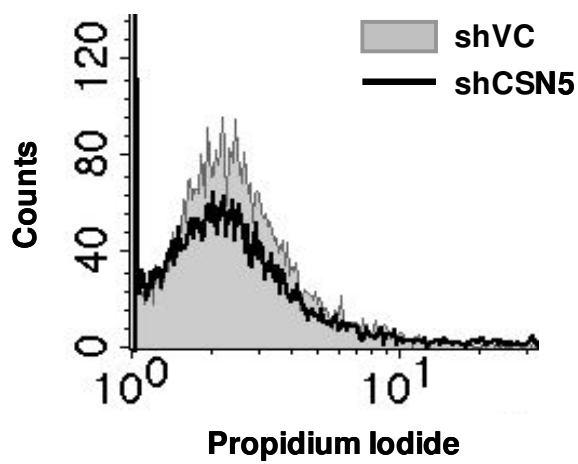


Figure 52. CSN5 knockdown has no significant effect on propidium iodide^{+ve}:annexin V^{-ve} staining.

The histogram shown is representative of the propidium iodide staining within the annexin V negative fraction of n=3 vector controls (light grey in fill) and CSN5 knockdowns (black line) day 6 post transfection.

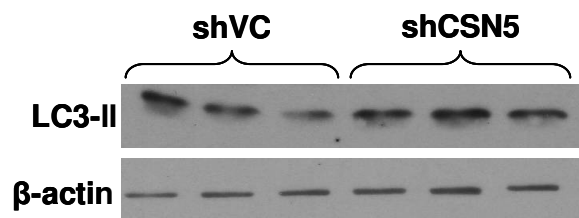


Figure 53. CSN5 knockdown has no effect on the level of the autophagy marker protein LC3-II.

Transfected cells were harvested day 4 post transfection, protein extracted and LC3-II protein levels in vector control and CSN5 knockdown cell extracts determined by western blot. Even loading was determined by β -actin western blot. The image shown is of three independent vector control and CSN5 knockdown transfections. Note that the exposure time used to generate figure 31 was 1 minute whilst the exposure time used here was much longer (12 hours). This longer exposure time was used here to permit detection of LC3-II in both vector control and CSN5 knockdown cells, whilst the short exposure time was used previously in figure 31 to show the clear accumulation of LC3-II in shCSN2 cells.

Chapter 5.0:
Analysis of the effect of CSN2 and CSN5
knockdown on CSN complex integrity

5.1 Introduction

The knockdown of CSN2 and CSN5 in K562 cells produced distinct phenotypes despite having comparable effects on cullin deneddylation. Similar findings have been reported previously in organisms such as *S. pombe* (Mundt et al., 2002) and *Drosophila* (Oron et al., 2002). The authors of these manuscripts suggested that the divergent phenotypes may be attributable to the fact that CSN subunits may function in distinct subcomplexes (Mundt et al., 2002) or may be due to the activity of a retained CSN complex (lacking CSN5) in the absence of CSN5 (Oron et al., 2002). In order to assess this possibility in K562 cells, a 2-dimensional gel technique was optimised for the study of the intact CSN complex and any CSN subcomplexes in shCSN2 and shCSN5 cells. A CSN subcomplex was identified in cells lacking CSN2 whilst shCSN5 cells were shown to retain the CSN complex and lose only monomeric CSN5. The contribution of these identified complexes to the phenotype of shCSN2 and shCSN5 cells was assessed by CSN2/CSN5 double knockdown experiments.

5.2 Results

5.2.1 Optimisation of the 2-Dimensional NativePAGE/SDS-PAGE gel electrophoresis protocol

A 2-D gel analysis technique was developed, in which proteins were separated in their native, complexed state in the first dimension, to enable assessment of the effect of CSN subunit knockdown on CSN complex integrity. In order to ensure that any variation in 2-D gel analysis was minimal, it was important to determine the effect of freezing either a cell pellet or protein extract prior to use in 2-D gel analysis, relative to the use of fresh cell lysate. To this end, three aliquots of K562 cells were harvested and, from one pellet, native proteins were extracted (fresh lysate, figure 54), whilst the second pellet was frozen for two weeks and then native proteins extracted from the thawed pellet (frozen pellet, figure 54). Finally, protein was extracted from the third pellet and the lysate frozen for a two week period (frozen lysate, figure 54). The distribution of CSN5 containing protein complexes within these samples was then analysed by 2-D gel analysis and CSN5 western blot analysis (figure 54). From these analyses it was determined that, at this exposure time of 10 minutes, CSN5 occurred only in complexes of approximately 550kDa and greater in the fresh lysate and frozen pellet samples, whereas CSN5 occurred in smaller complexes (<480kDa) in the frozen lysate (figure 54). This data indicates that the use of cell lysate from a frozen cell pellet has no significant effect on native protein complexes relative to fresh lysate. However, the process of freezing and thawing cell lysate results in the significant degradation of protein complexes. Therefore, in order to

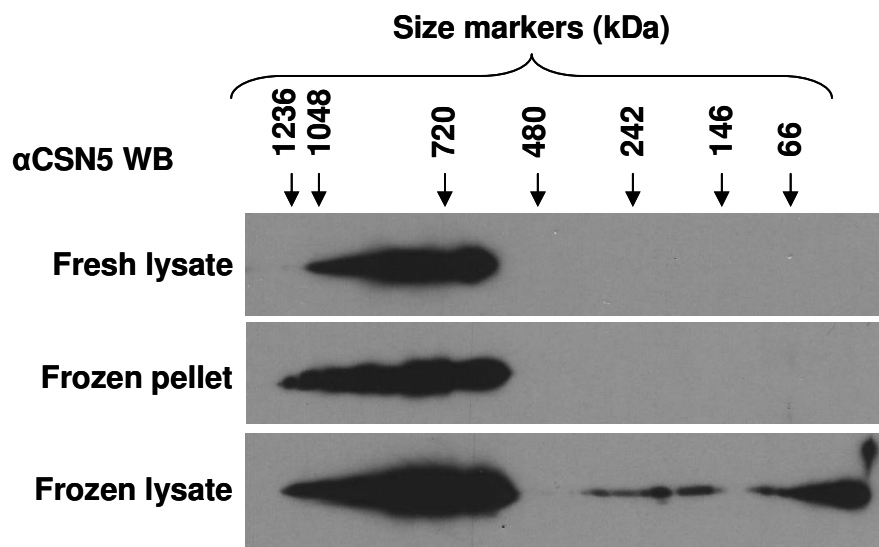


Figure 54. Optimisation of the 2-Dimensional NativePAGE gel protocol.

Three aliquots of 1×10^6 K562 cells were harvested. Native protein was extracted from the first pellet for immediate use (top panel). The second pellet was snap frozen in liquid nitrogen and native protein extracted from the thawed pellet two weeks later for immediate use (middle panel). Native protein was extracted from the third pellet immediately, the protein frozen and then thawed two weeks later for use (lower panel). CSN5 distribution in these samples was determined by 2-Dimensional Native-PAGE/SDS-PAGE and western blot analysis.

minimise any sample variation which may potentially have occurred frozen lysates were not used for native gel analysis.

5.2.2 Determination of the effect of CSN2 knockdown on CSN complex integrity

In order to determine the effect of CSN2 knockdown on CSN complex integrity, vector control and CSN2 knockdown cells were harvested day 3 post transfection, native proteins extracted and the distribution of CSN2 amongst cellular protein complexes determined by 2-D gel and western blot analysis. Figure 55 demonstrates that in CSN2 knockdown cells there was significant loss of CSN2 from the CSN complex (~500kDa) and super complexes (~700kDa) relative to vector controls. Therefore, to study CSN complex formation in the absence of CSN2, the distribution of CSN5 containing complexes was assessed in vector control and CSN2 knockdown cell extracts. CSN5 protein was also lost from the CSN complex in CSN2 knockdowns (figure 56), indicating the loss of the intact CSN complex in the absence of CSN2.

As the loss of CSN5 protein from the CSN complex did not result in a concomitant increase in monomeric CSN5 (figure 56), the possibility of an effect of CSN2 loss on the level of CSN5 was investigated. Cells were harvested day 6 post transfection, protein extracted and CSN5 western blot carried out. Figure 57A shows that cells lacking CSN2 have significantly less CSN5 protein relative to vector control cells. Densitometry was used to determine that on average cells lacking CSN2 had only $10.4 \pm 2.9\%$ CSN5 relative to vector control cells ($P=0.0001$). This loss was also determined at the level of mRNA.

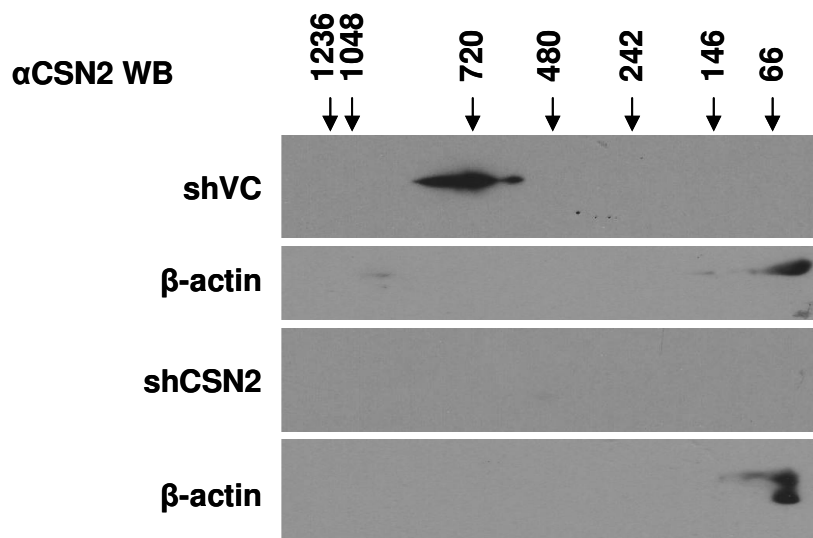


Figure 55. CSN2 knockdown results in a significant loss of CSN2 from the CSN complex.

Transfected cells were harvested day 3 post transfection and CSN2 distribution in vector control and CSN2 knockdown cells determined by 2-Dimensional Native-PAGE/SDS-PAGE and western blot analysis. Data shown is representative of $n=3$ transfections. β -actin loading controls are also shown.

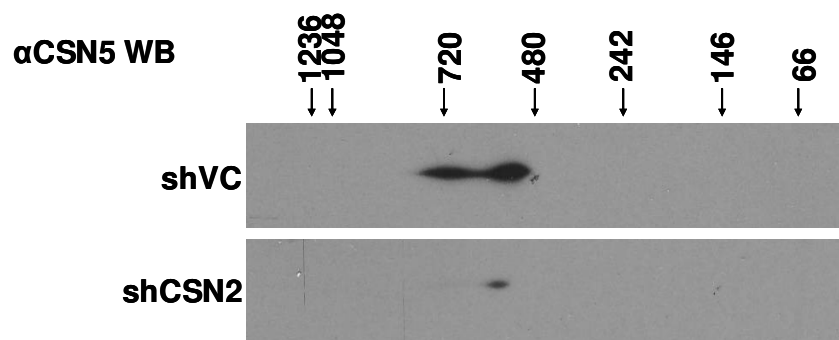


Figure 56. CSN2 knockdown results in a significant loss of CSN5 from the CSN complex.

Transfected cells were harvested day 3 post transfection and CSN5 distribution in vector control and CSN2 knockdown cells determined by 2-Dimensional Native-PAGE/SDS-PAGE and western blot analysis. Data shown is representative of n=3 transfections.

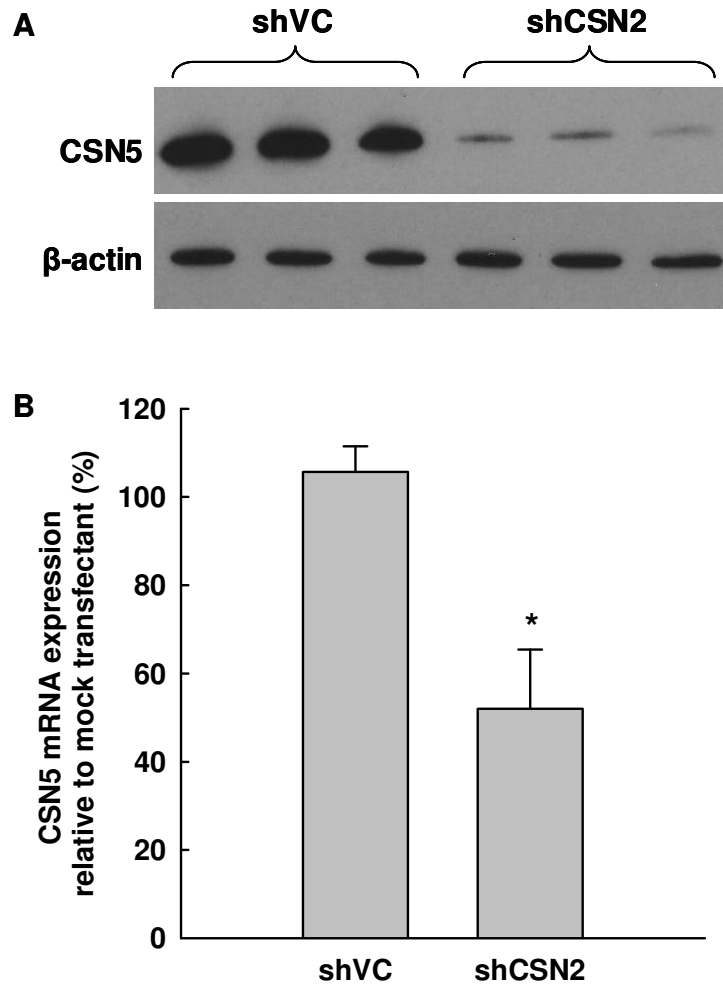


Figure 57. CSN2 knockdown results in a significant reduction of both CSN5 protein and mRNA.

A, Transfected cells were harvested day 6 post transfection, protein extracted and CSN5 protein levels in vector control and CSN2 knockdown cells determined by western blot. Even western blot loading was determined by β -actin western blot. The image shown is of three independent vector control and CSN2 knockdown transfections. **B**, Mock, vector control and CSN2 knockdown transfected cells were harvested day 6 post transfection, RNA extracted, cDNA generated and QRT-PCR carried out. Data shown is the mean CSN5 mRNA expression relative to mock transfected cells of n=3 transfections \pm SEM. * indicates $p < 0.05$.

The level of CSN5 mRNA in vector control cells did not differ from that of mock transfected cells, whereas CSN2 knockdown cells had a significant reduction in CSN5 mRNA of ~50% (P=0.011) relative to vector control transfected cells (figure 57B).

Interestingly, a longer exposure of the western blot in figure 56 demonstrated the formation of a CSN5 containing subcomplex (~242kDa) in cells lacking CSN2, which was not apparent in vector control cells (figure 58). Cumulatively, these data suggest that the loss of CSN2 results in the loss of the intact CSN complex, formation of a CSN5 containing CSN subcomplex, and loss of CSN5. Thus, these data are indicative of a role for CSN2 in CSN complex integrity.

5.2.3 Assessment of the effect of CSN2/5 double knockdown on CSN subcomplex formation and the occurrence of autophagy

The occurrence of a CSN5 containing subcomplex in the absence of CSN2 raised the possibility that the difference between the phenotypes of CSN2 and CSN5 knockdown cells is a consequence of the activity of this subcomplex in cells lacking CSN2. If this were the case, then loss of both CSN2 and CSN5 should not be associated with autophagy. To investigate this possibility, CSN2/CSN5 double knockdown was attempted in K562 cells by triple transfection of cells with HKK, shCSN2 and shCSN5 plasmids. Efficient double knockdown was confirmed by QRT-PCR which demonstrated 97.2% loss of CSN2 mRNA (P=0.001; figure 59) and 87.1% loss of CSN5 mRNA (P=0.005; figure 59) relative to vector controls.

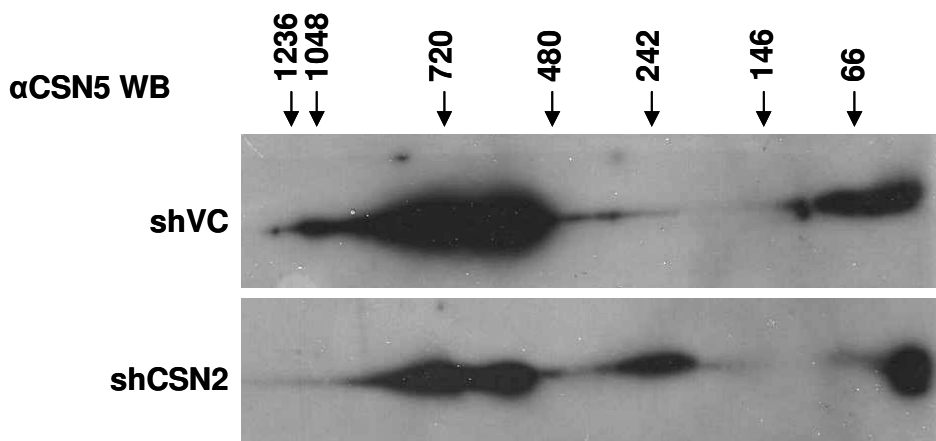


Figure 58. CSN2 knockdown results in the formation of a CSN5 containing CSN subcomplex.

Transfected cells were harvested day 3 post transfection and CSN5 distribution in vector control and CSN2 knockdown cells determined by 2-Dimensional Native-PAGE/SDS-PAGE and western blot analysis. Data shown is representative of n=3 transfections. This is the same blot as in figure 56. However, the exposure time in figure 56 was 30 minutes whilst the exposure time here was 12 hours.

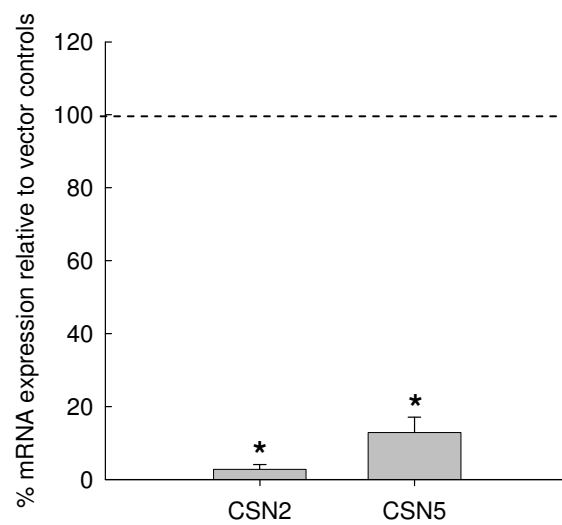


Figure 59. Determination of CSN2 and CSN5 mRNA knockdown in double knockdown cells.

Vector control and CSN2/CSN5 double knockdown transfected cells were harvested day 6 post transfection, RNA extracted, cDNA generated and QRT-PCR carried out. Data shown is the mean CSN2/CSN5 mRNA expression relative to vector control transfected cells of n=3 transfections \pm SEM. * indicates $p < 0.05$.

The distribution of CSN5 in double knockdown cells was determined by 2-D gel and western blot analysis of native proteins extracted from vector control and double knockdown cells harvested day 3 post transfection. As observed in CSN2 knockdown cells, a significant reduction in the amount of the intact CSN complex was observed in double knockdown cells relative to vector control cells (figure 60A). However, a CSN5 containing subcomplex could not be detected in double knockdown cells (figure 60A). This finding was made with a 12 hour film exposure time as used to detect subcomplex formation in cells lacking CSN2 (figure 58). These data imply that, unlike CSN2 knockdown cells, cells lacking both CSN2 and CSN5 do not form a CSN5 containing subcomplex.

In order to determine the effect of CSN2/5 double knockdown on cell morphology, double knockdown cell cytopins were made day 6 post transfection and Jenner-Giemsa stained. Interestingly, this analysis demonstrated a vesicular morphology of a proportion of double knockdown cells (figure 60B); a morphology comparable to that of CSN2 knockdown cells (figure 30A). This data suggests that the morphology associated with the loss of CSN2 is not a consequence of the activity of a CSN5 containing subcomplex. It should also be noted that within the double knockdown population a subset of cells also have what appears to be the same morphology as CSN5 knockdown cells (figure 60B).

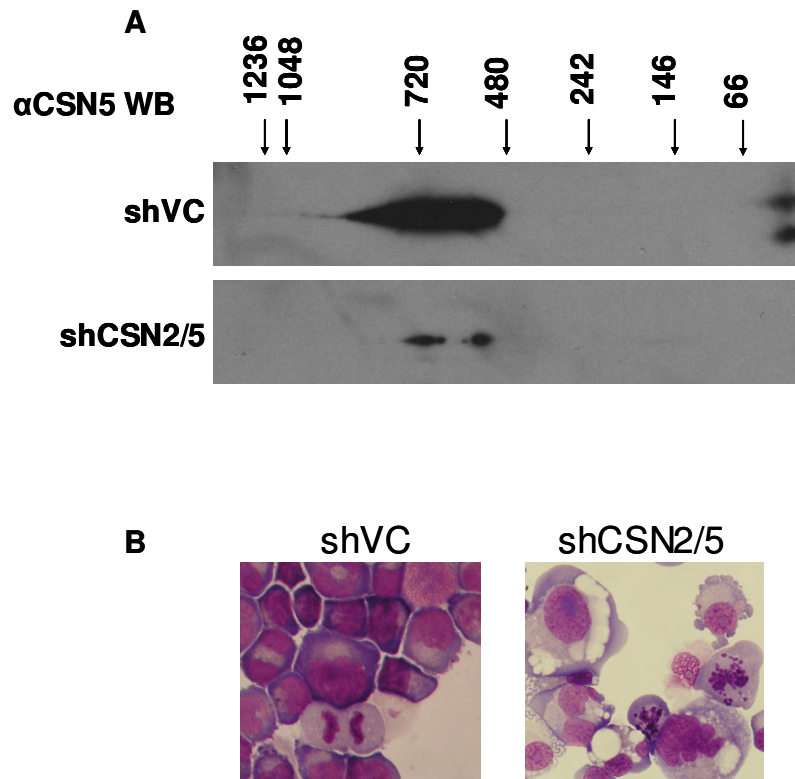


Figure 60. Cells lacking both CSN2 and CSN5 do not form CSN5 containing subcomplexes but do have a mixed phenotype associated with the loss of these subunits.

A, Transfected cells were harvested day 3 post transfection and CSN5 distribution in vector control and double knockdown cells determined by 2-Dimensional Native-PAGE/SDS-PAGE and western blot analysis. Data shown is representative of n=3 transfections. **B**, Cytopins were stained by Jenner-Giemsa for visualisation of vector control and double knockdown cell morphology day 6 post transfection. The images shown are representative of n=3 transfections.

5.2.4 Determination of the effect of CSN5 knockdown on CSN complex integrity

In order to determine the effect of CSN5 knockdown on CSN complex integrity, vector control and CSN5 knockdown cells were harvested day 3 post transfection, native proteins extracted and the distribution of CSN5 amongst cellular protein complexes determined by 2-D gel and western blot analysis. Surprisingly, this analysis demonstrated that CSN5 knockdown had no significant effect on the level of CSN5 within the intact CSN complex (figure 61). Indeed, quantitative analysis of 2-D gels investigating the distribution of CSN5 in CSN2 and CSN5 knockdowns relative to vector controls indicates significant loss of the intact CSN complex in cells lacking CSN2 ($P=0.015$), whilst also demonstrating that CSN5 loss had no significant impact on the intact CSN complex (figure 62; $P=0.619$). However, interestingly CSN5 knockdown resulted in the significant loss of the free form of CSN5 (37kDa; figure 63). These observations were surprising given the finding of apparent complete CSN5 protein loss by SDS-PAGE western blot (figure 40). This finding raised the possibility that the RIPA buffer extraction used for SDS-PAGE failed to extract the entire cellular pool of CSN5. To investigate this possibility, vector control and shCSN5 transfected cells were harvested day 3 post transfection and proteins extracted using either the RIPA buffer extraction protocol or by directly boiling the harvested cell pellet in SDS gel loading buffer. Determination of the level of CSN5 protein in these samples by western blot analysis demonstrated that RIPA buffer does not appear to extract the entire cellular pool of CSN5 (figure 64). Together, these data suggest that only the monomeric form of CSN5 may be present in RIPA buffer protein extractions.

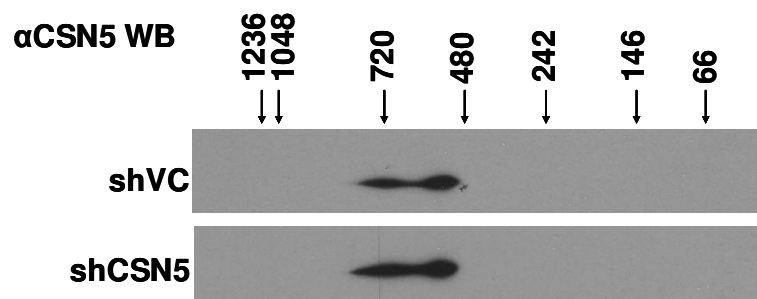


Figure 61. CSN5 knockdown has no significant effect on CSN5 within the intact CSN complex.

Transfected cells were harvested day 3 post transfection and CSN5 distribution in vector control and CSN5 knockdown cells determined by 2-Dimensional Native-PAGE/SDS-PAGE and western blot analysis. Data shown is representative of n=3 transfections.

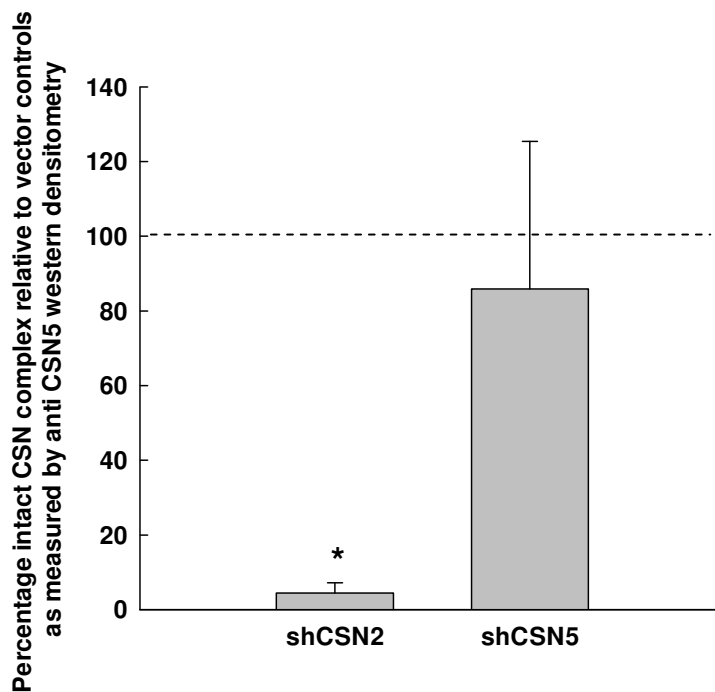


Figure 62. CSN2 knockdown results in a significant reduction of the intact CSN complex, whilst CSN5 knockdown has no significant effect on the intact CSN complex.

Transfected cells were harvested day 3 post transfection and CSN5 distribution in vector control, CSN2 knockdown and CSN5 knockdown cells determined by 2-Dimensional Native-PAGE/SDS-PAGE and western blot analysis. Densitometry was carried out on these membranes and data plotted as average percentage of intact CSN complex relative to vector control \pm SEM. * indicates $p < 0.05$. Data shown is representative of $n=3$ transfections.

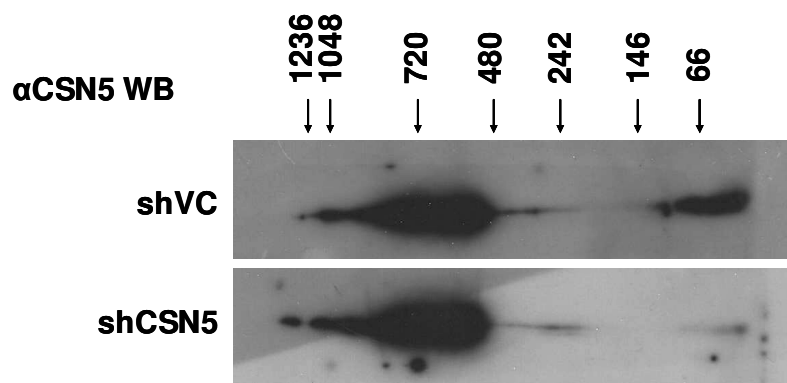


Figure 63. CSN5 knockdown results in loss of the free form of CSN5.

Transfected cells were harvested day 3 post transfection and CSN5 distribution in vector control and CSN5 knockdown cells determined by 2-Dimensional Native-PAGE/SDS-PAGE and western blot analysis. Data shown is representative of n=3 transfections.

CSN complex formation in CSN5 knockdown cells was further studied by assessment of CSN2 integration into the CSN complex in the absence of CSN5. There appears to be no significant difference in CSN2 incorporation into either the CSN complex or supercomplexes in CSN5 knockdown cells relative to vector controls (figure 65). Furthermore, conversely to the observation regarding CSN5 loss in CSN2 knockdown cells, there appeared to be no effect on the level of CSN2 protein in CSN5 knockdown cells. This was confirmed by western blot analysis. Cells were harvested day 4 post transfection, protein extracted and CSN2 levels determined by western blot. Figure 66A demonstrates that vector control cells and CSN5 knockdown cells contained similar amounts of CSN2 protein, with densitometry confirming that there was indeed no significant difference in the level of CSN2 protein in vector control and shCSN5 cell lysates ($P=0.587$). In addition, determination of the level of CSN2 mRNA by QRT-PCR in vector control and CSN5 knockdown cells demonstrated that there was no significant effect of CSN5 loss on the quantity of CSN2 mRNA in cells lacking CSN5 relative to vector controls (figure 66B; $P=0.861$).

Collectively, 2-D gel analyses of CSN2 and CSN5 knockdown samples demonstrated that loss of these subunits differentially affects CSN complex and CSN subunit stability, and that the half life of monomeric CSN5 protein is significantly shorter than that of CSN complex bound CSN5 protein.

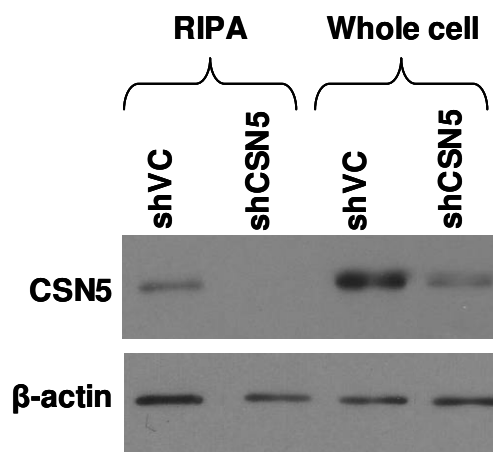


Figure 64. RIPA buffer does not extract the entire cellular CSN5 pool.

Transfected cells were harvested day 3 post transfection and protein extracted using either RIPA buffer extraction or by boiling the cell pellet in gel loading buffer. The level of CSN5 protein in these samples was determined by western blot and even gel loading determined by β -actin western blot.

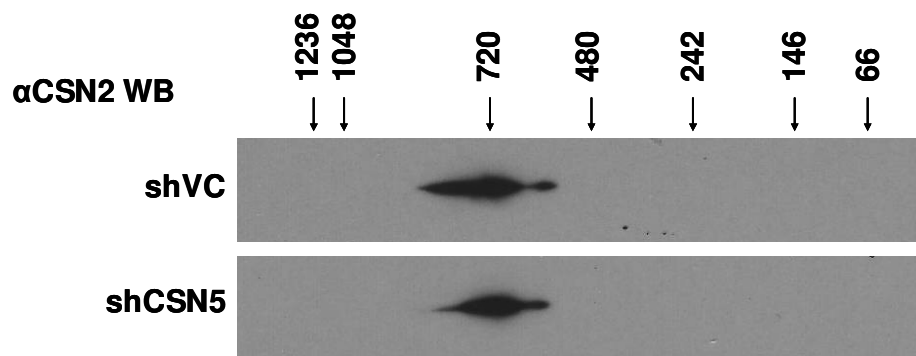


Figure 65. CSN5 knockdown has no significant effect on CSN2 integration into the CSN complex.

Transfected cells were harvested day 3 post transfection and CSN2 distribution in vector control and CSN5 knockdown cells determined by 2-Dimensional Native-PAGE/SDS-PAGE and western blot analysis. Data shown is representative of n=3 transfections.

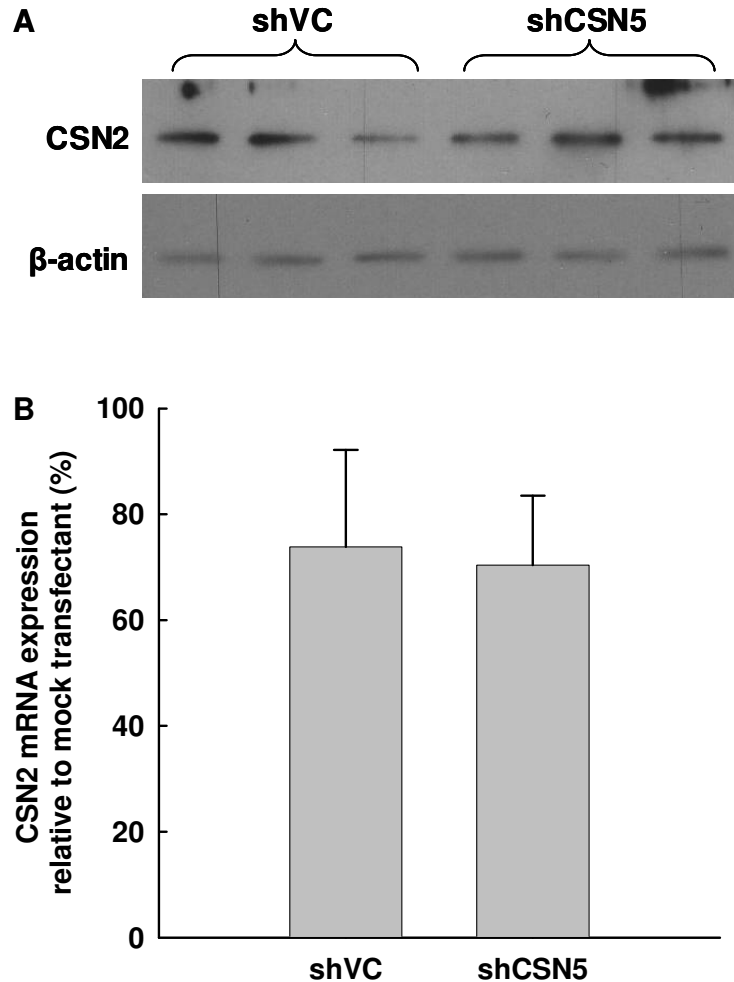


Figure 66. CSN5 knockdown has no significant effect on the level of CSN2 protein or mRNA.

A, Transfected cells were harvested day 4 post transfection, protein extracted and CSN2 protein levels in vector control and CSN5 knockdown cells determined by western blot. Even western blot loading was determined by β -actin western blot. The image shown is of three independent vector control and CSN5 knockdown transfections. **B**, Mock, vector control and CSN5 knockdown transfected cells were harvested day 4 post transfection, RNA extracted, cDNA generated and QRT-PCR carried out. Data shown is the mean CSN2 mRNA expression relative to mock transfected cells of n=3 transfections \pm SEM.

Chapter 6.0:

**Expression of wild-type and
deneddylase dead CSN5 in shCSN5
expressing cells**

6.1 Introduction

The results of the double knockdown study clearly indicated that the shCSN2 and shCSN5 associated phenotypes cannot be explained by the activity of a CSN5 containing subcomplex or remnant CSN complex, respectively. However, the findings of the 2-D gel analyses suggested that the CSN5 associated phenotype may occur as a result of the loss of monomeric CSN5 function. If this were the case then re-expression of deneddylase dead CSN5 which retains monomeric function would rescue the shCSN5 cell phenotype to the same extent as wild-type CSN5. In order to test this hypothesis, both wild-type and deneddylase dead CSN5 were re-expressed in a shCSN5 background and the rescue of the shCSN5 cell phenotype assessed. Unfortunately, due to time constraints, these experiments are only n=1, but they do provide interesting preliminary insights into the potential basis of the shCSN5 cell phenotype.

6.2 Results

6.2.1 Preparation of plasmids

The entire CSN5 protein coding sequence was amplified (figure 67) using CSN5 primers designed to include a BamHI and EcoRI restriction site, along with a GCAG cap, at the 5' end of the forward and reverse primers, respectively. The CSN5 coding sequence PCR product was purified, and this insert and pcDNA3.1 (+) vector digested with the restriction enzymes BamHI and EcoRI, the digestion products ligated and the ligation verified (figure 68A). The ligation reaction product was transformed into dh5 α and plated onto ampicillin containing agar plates. Colonies were screened by BamHI/EcoRI digestion of miniprep plasmid DNA and separation of digestion products by electrophoresis (figure 68B). Correct insertion of CSN5 coding sequence was verified by sequencing of plasmid DNA (figure 68C).

Site-directed mutagenesis was used to incorporate four silent mutations into the shRNA target sequence in the CSN5 coding sequence in pcDNA3.1-CSN5. This resulted in a mutated CSN5 expression plasmid which produces CSN5 mRNA which is not targeted for degradation by the CSN5 targeting shRNA, but also produces CSN5 protein with unaltered amino acid sequence. The mutation of four bases within the shRNA sequence was confirmed by plasmid sequencing (figure 69A). This plasmid was then used in a second round of plasmid mutation with a set of primers designed to generate a point mutation which resulted in aspartic acid 151 replacement with asparagine, culminating in

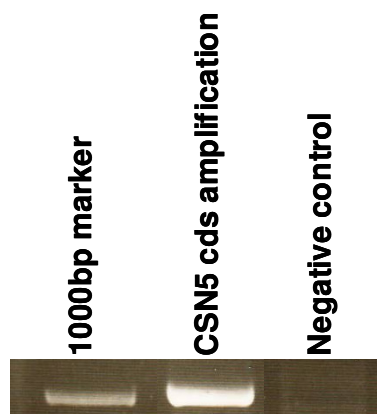


Figure 67. Amplification of CSN5 coding sequence.

The whole coding sequence (1004 bases) of CSN5 was amplified from Oligo dT cDNA using pre-designed primers and Accuzyme.

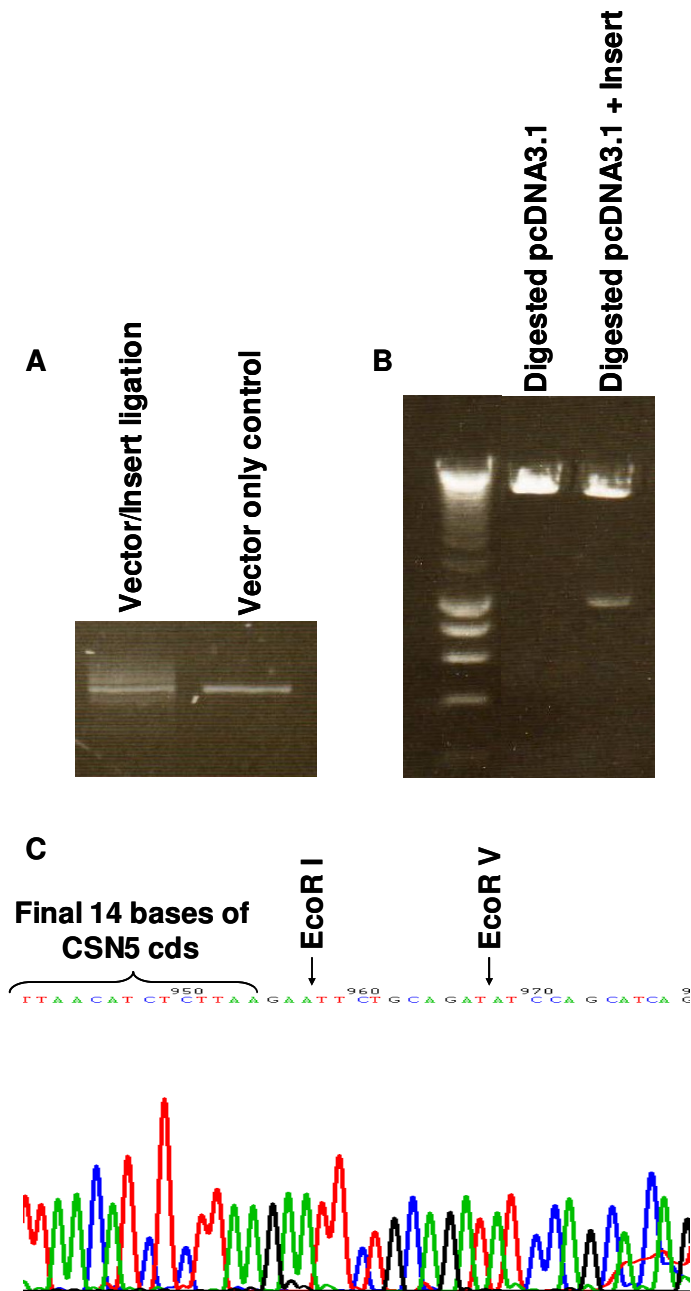


Figure 68. CSN5 re-expression plasmid preparation and validation.

(A) BamHI and EcoRI digested pcDNA3.1 vector and CSN5 coding sequence were ligated and the products separated by electrophoresis on a 1% agarose gel along with a vector only negative control to determine ligation. (B) Empty pcDNA3.1 and pcDNA3.1 plus insert were digested with BamHI and EcoRI and products separated by electrophoresis on a 1% agarose gel to determine plasmid insertion. (C) pcDNA3.1 plus insert was sequenced to determine the correct insertion.

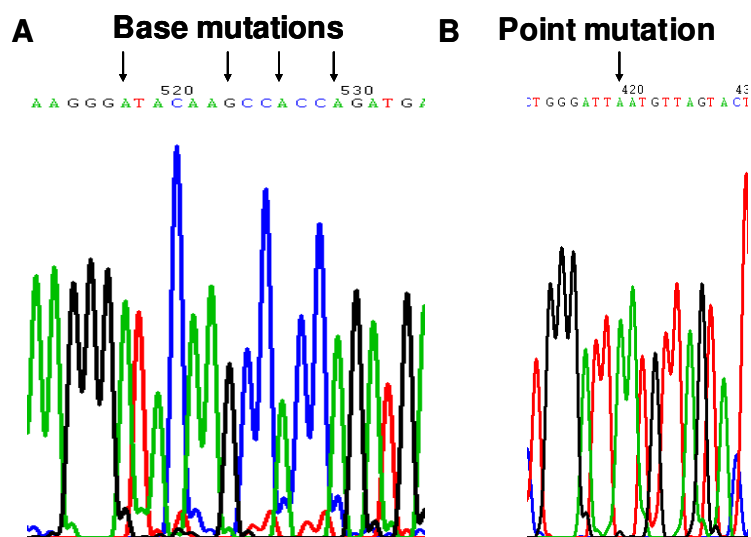


Figure 69. Determination of CSN5 re-expression plasmid shRNA sequence and deneddylation dead mutations.

Plasmid sequencing was carried out in order to determine that the required mutations of the CSN5 shRNA sequence (A) and the D151N mutation (B) were achieved.

the production of CSN5 protein lacking deneddylase activity. This point mutation was confirmed by plasmid sequencing (figure 69B).

6.2.2 Assessment of CSN5 protein levels

In order to determine the CSN5 protein level in vector control, CSN5 knockdown and either wild-type (WT) or deneddylase dead (dd) CSN5 expressing cells, transfected cells were harvested day 7 post transfection, protein extracted and quantified and CSN5 protein level assessed by western blot. The level of CSN5 protein was reduced in CSN5 knockdown cells, whilst transfection of cells with shCSN5 plasmid plus either wild-type or deneddylase dead CSN5 expression plasmid rescued the level of CSN5 protein (figure 70A). Quantitative analysis of this western blot demonstrated greater than 80% CSN5 protein loss in shCSN5 cells and restoration of CSN5 protein level to a level comparable to that seen in vector control cells in both wild-type and deneddylase dead CSN5 re-expressing cells (figure 70B).

6.2.3 Assessment of the cumulative growth of cells expressing CSN5 in a shCSN5 background

Transfected cells were counted daily, the cumulative growth calculated and the data plotted as a line and dot plot. Expression of neither wild-type nor deneddylase dead CSN5 in shCSN5 expressing cells restored the cumulative growth to that of vector control cells (figure 71A). However, cells expressing either wild-type or deneddylase

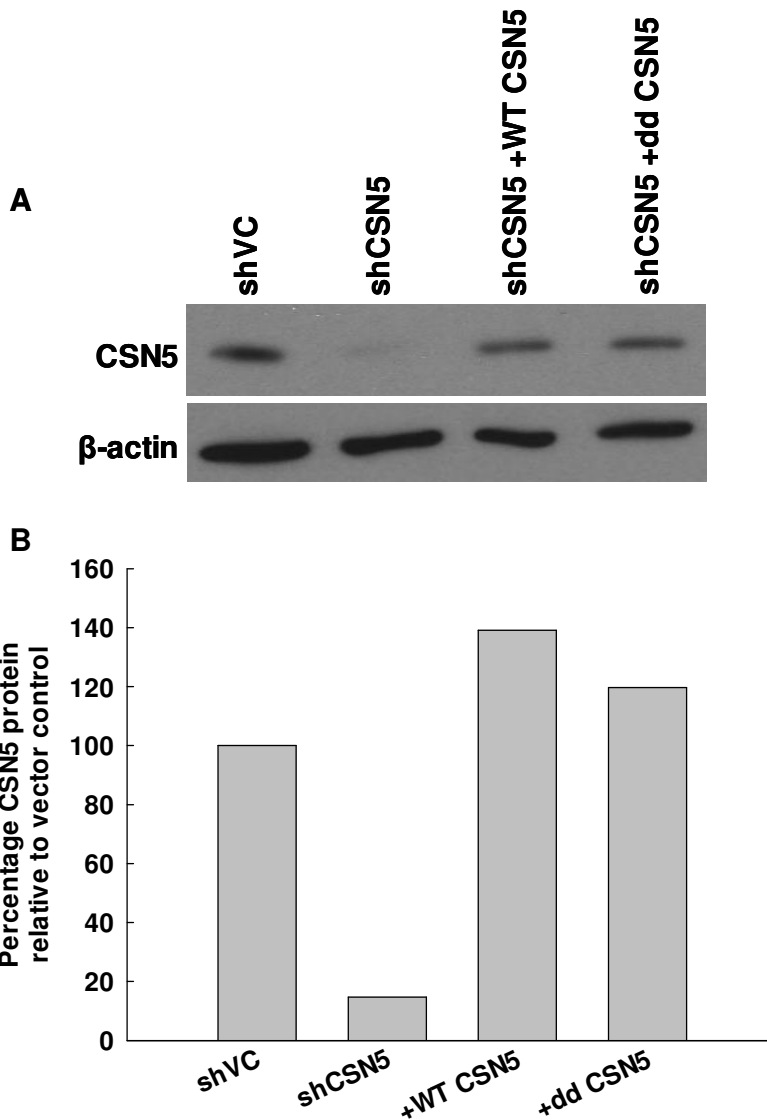


Figure 70. CSN5 protein expression in a shCSN5 background.

(A) Transfected cells were harvested day 7 post transfection, protein extracted and CSN5 protein levels in vector control, CSN5 knockdown and both wild-type (+WT) and deneddylase dead (+dd) CSN5 re-expression cell extracts determined by western blot. Even loading was determined by β -actin western blot. (B) Densitometry was carried out on the CSN5 western blot and the percentage of CSN5 in CSN5 knockdown, WT CSN5 expressing and dd CSN5 expressing cells relative to vector control cells calculated and plotted.

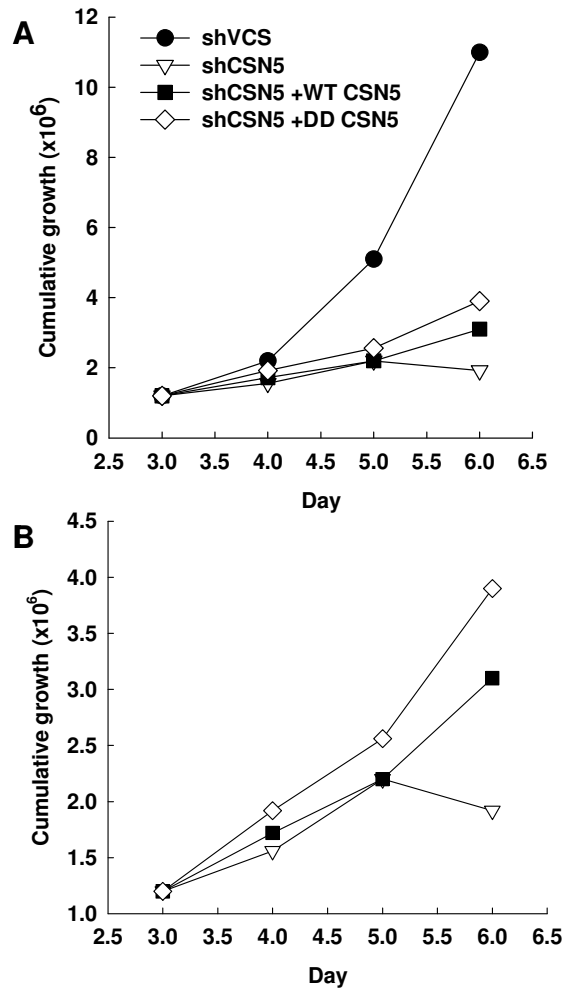


Figure 71. Expression of either wild-type or deneddylase dead CSN5 partially rescues cell growth.

Cell counts were taken daily and the cumulative growth calculated. The cumulative growth of wild-type CSN5 expressing and deneddylase dead CSN5 expressing cells is shown relative to CSN5 knockdown cumulative cell growth in the presence (A) or absence (B) of the vector control cell cumulative growth curve.

dead CSN5 had a greater cumulative growth than that of shCSN5 cells at the latest time point investigated (day 6 post transfection; figure 71B). Given that this data is n=1 these findings should be interpreted with caution, and it is possible that this difference may hold no significance. Alternatively, the expression of either wild-type or deneddylase dead CSN5 in a shCSN5 background may have partially rescued cumulative cell growth relative to CSN5 knockdown cells by day 6 post transfection (figure 71B). If this were the case, the deneddylase dead form of CSN5 would appear to rescue the cumulative cell growth to the same extent as wild-type CSN5 (figure 71B). Importantly, the partial rescue of cell growth upon re-expression of either form of CSN5 is supported by the observations made regarding the morphology of cells in which either wild-type or deneddylase dead CSN5 is re-expressed (see below).

6.2.4 Assessment of the morphology of cells expressing CSN5 in a shCSN5 background

In order to compare the morphology of cells lacking CSN5 with cells expressing either wild-type or deneddylase dead CSN5, cytopins were made of transfected cells day 4 post transfection and these cytopins Jenner-Giemsa stained. Visualisation of this staining suggested that there may be fewer cells containing disorganised, fragmented DNA in cells expressing either form of CSN5 compared to shCSN5 cells (figure 72A). In order to confirm this initial observation, cell counts were taken from six fields of each slide and the average percentage of cells with aberrant nuclear staining calculated and plotted \pm SEM. Less than 1% of vector control cells had aberrant nuclear staining, whilst almost 20% of cells lacking CSN5 contained fragmented, disorganized DNA (figure 72B);

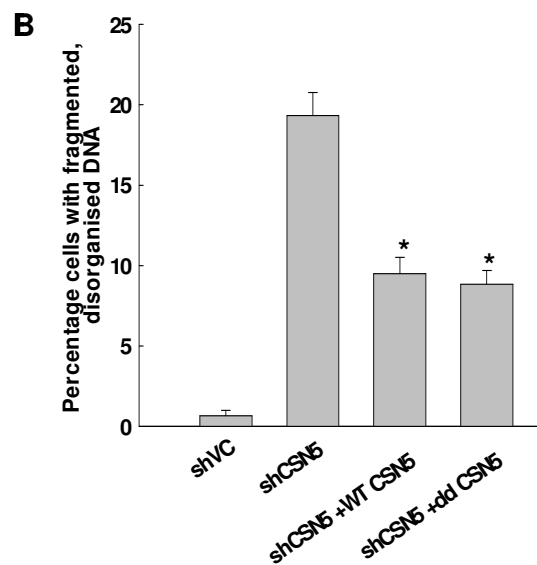
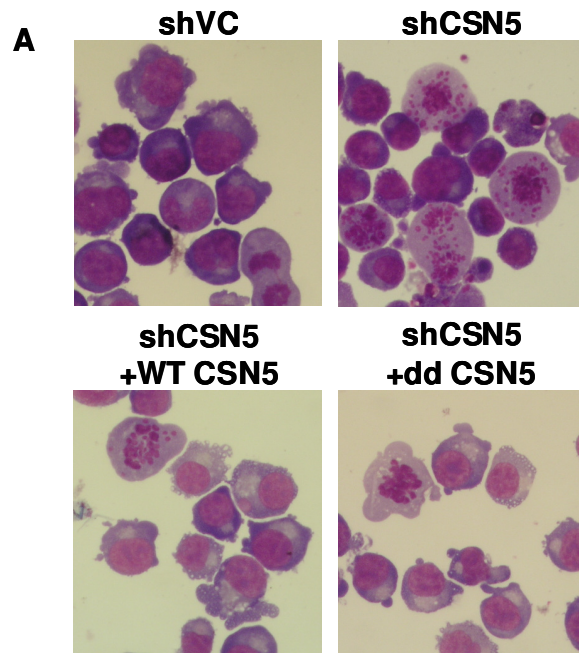


Figure 72. Expression of either wild-type or deneddylase dead CSN5 reduces the proportion of cells with disorganised, fragmented DNA.

(A) Cytopins were stained by Jenner-Giemsa for visualisation of cell morphology day 4 post transfection. (B) Counts were taken from Jenner-Giemsa stained cytopins of the number of cells containing aberrant nuclear staining per 100 cells. The data shown is the average count of 6 fields per slide \pm SEM. * indicates $p < 0.05$.

$P=1.69 \times 10^{-7}$). Expression of either wild-type or deneddylase dead CSN5 resulted in a significant reduction of cells with aberrant nuclear staining (9.5% $P=0.0002$ and 8.8% $P=9.3 \times 10^{-5}$, respectively), although, in accordance with the partial rescue of cell growth, neither wild-type nor deneddylase dead CSN5 rescued this phenotype completely (figure 72B).

6.2.5 Assessment of the effect of CSN5 protein expression in a shCSN5 background on SCF^{Skp2} activity

In order to determine the effect on SCF^{Skp2} activity of wild-type and deneddylase dead CSN5 expression in a shCSN5 background, vector control, CSN5 knockdown and either wild-type or deneddylase dead CSN5 expressing cells were harvested, protein extracted and quantified and Nedd8, Skp2 and p27 protein levels assessed by western blot. CSN5 knockdown resulted in the accumulation of a Nedd8 bound protein which migrated at a rate corresponding to that of neddylated Cul1 (figure 73A). Expression of wild-type CSN5 restored the level of what was predicted to be neddylated Cul1 to a level comparable to that of vector control cells (figure 73A). However, as would have been predicted, expression of deneddylase dead CSN5 failed to reduce the level of neddylated protein (figure 73A). Quantitative analysis of this western blot demonstrated a 4 fold increase in the level of supposed neddylated Cul1, which is restored by wild-type, but not deneddylase dead, CSN5 (figure 73B).

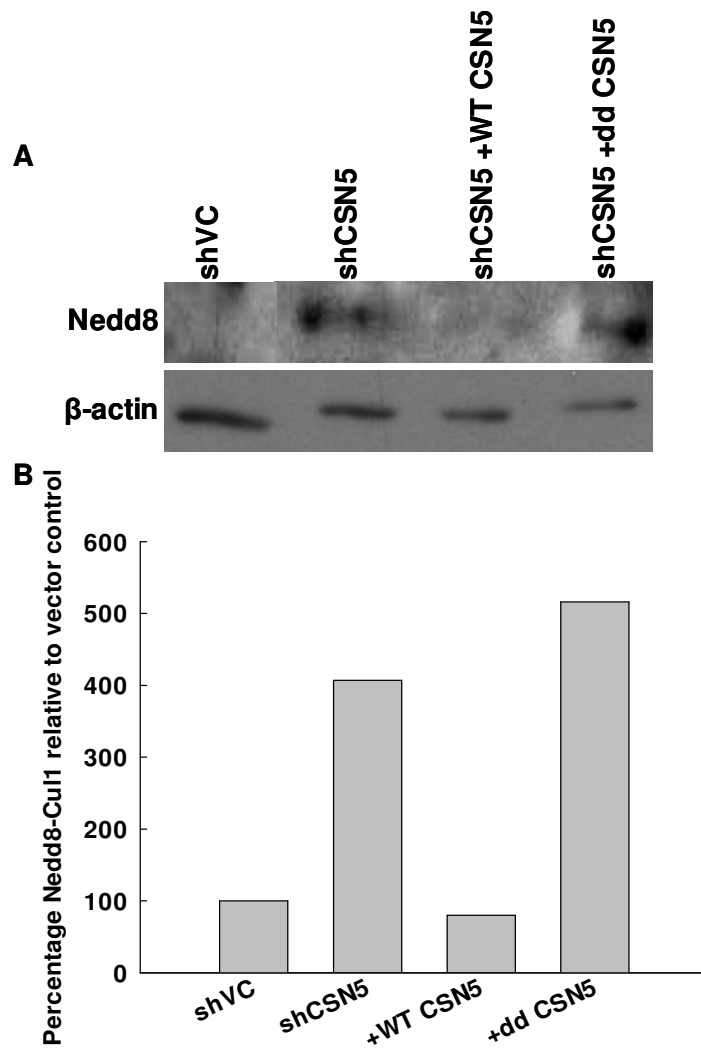


Figure 73. Expression of wild-type CSN5, but not deneddylase dead CSN5, restores Cul1 deneddylation.

(A) Transfected cells were harvested day 3 post transfection, protein extracted and Nedd8-Cul1 protein levels in vector control, CSN5 knockdown and both wild-type (+WT) and deneddylase dead (+dd) CSN5 re-expression cell extracts determined by western blot. β -actin western blot was used as a loading control.

(B) Densitometry was carried out on the Nedd8 western blot and the percentage of Nedd8-Cul1 in CSN5 knockdown, WT CSN5 expressing and dd CSN5 expressing cells relative to vector control cells calculated and plotted.

The level of Skp2 protein in vector control, shCSN5 and either wild-type or deneddylase dead CSN5 re-expressing cells was then determined by western blot. At an earlier time point, day 3 post transfection, both wild-type and deneddylase dead CSN5 protein expression rescued the Skp2 protein loss observed in CSN5 knockdown cells (figure 74). However, by day 7 post transfection, rescue of Skp2 protein was only observed in wild-type CSN5 expressing cells, with deneddylase dead CSN5 expressing cells having a Skp2 protein level comparable to that of CSN5 knockdown cells (figure 75). Finally, the level of p27 was determined by western blot. As determined previously, CSN5 knockdown resulted in the accumulation of p27 protein (figure 76). Interestingly, by day 7 post transfection, expression of neither wild-type nor deneddylase dead CSN5 reduced the level of p27 protein to that of vector control cells (figure 76).

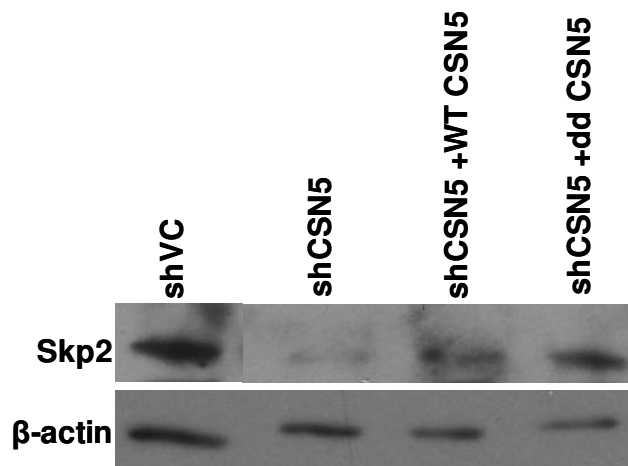


Figure 74. Expression of either wild-type or deneddylase dead CSN5 rescues Skp2 protein day 3 post transfection.

Transfected cells were harvested day 3 post transfection, protein extracted and the level of Skp2 protein in vector control, CSN5 knockdown and both wild-type (+WT) and deneddylase dead (+dd) CSN5 re-expression cell extracts determined by western blot. β -actin western blot was used as a loading control.

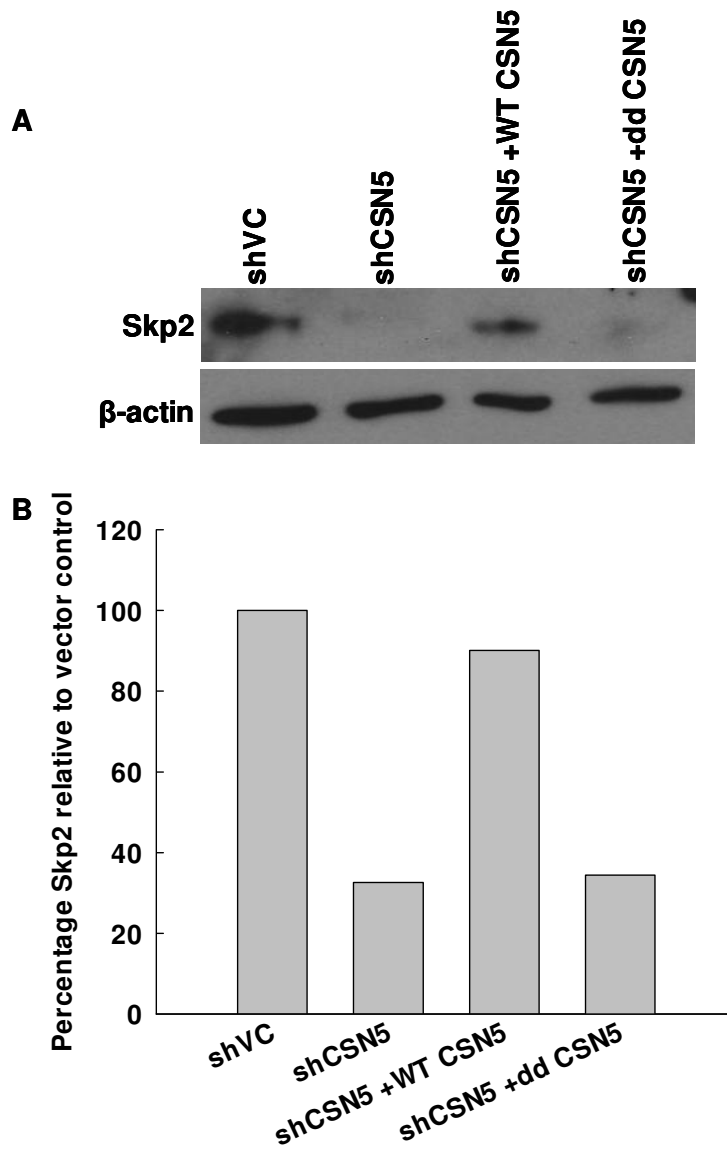


Figure 75. Expression of wild-type, but not deneddylase dead, CSN5 rescues Skp2 protein day 7 post transfection.

(A) Transfected cells were harvested day 7 post transfection, protein extracted and the level of Skp2 protein in vector control, CSN5 knockdown and both wild-type (+WT) and deneddylase dead (+dd) CSN5 re-expression cell extracts determined by western blot. β -actin western blot was used as a loading control.

(B) Densitometry was carried out on the Skp2 western blot and the percentage of Skp2 in CSN5 knockdown, WT CSN5 expressing and dd CSN5 expressing cells relative to vector control cells calculated and plotted.

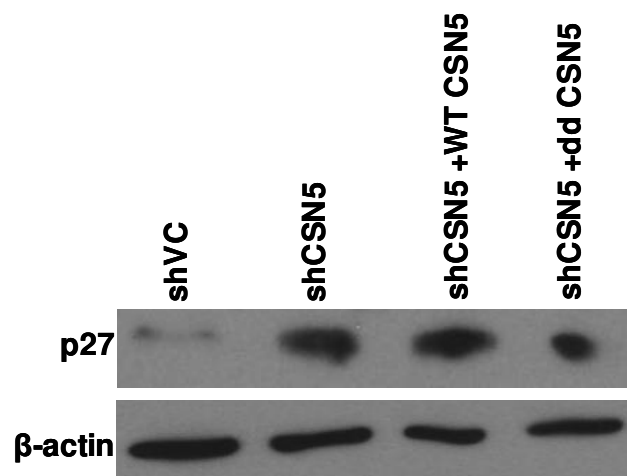


Figure 76. Expression of either wild-type or deneddylase dead CSN5 fails to restore the basal level of p27 protein.

Transfected cells were harvested day 7 post transfection, protein extracted and the level of p27 protein in vector control, CSN5 knockdown and both wild-type (+WT) and deneddylase dead (+dd) CSN5 re-expression cell extracts determined by western blot. β -actin western blot was used as a loading control.

Chapter 7.0:
General discussion

This study investigated the function and potential regulation of the CSN in the haematopoietic cell line and CML model, K562. Highly efficient knockdown of CSN2 and CSN5 was achieved, with both knockdowns resulting in aberrant CRL activity and the sequential loss of F-box proteins. However, the phenotypes of the knockdowns were distinct. CSN2 loss resulted in autophagy inhibition and non-apoptotic cell death, whilst loss of CSN5 resulted in a mitotic block, aberrant mitotic spindle formation and apoptotic cell death. The intact CSN complex was shown to be lost in cells lacking CSN2, and a CSN5 containing subcomplex formed. The possible dependence of the CSN2 knockdown associated phenotype on the activity of this subcomplex was ruled out. Conversely, the intact CSN complex was shown to persist in CSN5 knockdown cells, with loss of only monomeric CSN5. Re-expression of either wild-type or deneddylase dead CSN5 in shCSN5 cells partially rescued the CSN5 knockdown associated phenotype.

7.1 CSN subunit knockdown results in aberrant CRL activity

The achievement of almost complete CSN2 and CSN5 knockdown in this study has provided a powerful tool to study the function of these subunits and the CSN complex in K562 cells. At the molecular level, CSN2 and CSN5 knockdowns resulted in identical aberrant SCF activity. This complements another report in which CSN4 and CSN5 knockdown also resulted in increased neddylation of Cul-1 with a concomitant loss of Skp2 and increase in p27 protein in human epithelial cell lines rather than haemopoietic cells (Denti et al., 2006). Similar cullin hyperneddylation and aberrant CRL activity as a result of CSN subunit loss has also been observed in other organisms such as mice

(Lykke-Andersen et al., 2003), *A. thaliana* (Stuttman et al., 2009) and *S. pombe* (Wee et al., 2005). The instability of cullin proteins has also been demonstrated in other organisms including *Drosophila* (Wu et al., 2005) and *Neurospora* (He et al., 2005). Thus it appears that the CSN complex has CRL regulatory activities which are conserved between organisms and across cells from different cell lineages, and that disruption of the complex by loss of any subunit causes derangement of CRL activity.

7.2 Targeting the CSN results in the sequential loss of F-box proteins

The finding that F-box protein levels were at least partially restored in both knockdowns upon treatment with the proteasome inhibitor MG132 are in accordance with the finding that F-box proteins are autocatalytically degraded in the presence of hyperneddylated Cul-1 (Cope and Deshaies, 2006). However, this study has been the first to identify the sequential loss of F-box proteins following knockdown of CSN subunits. This is of great interest as it may explain published results which document the loss of particular F-box proteins at a specific time point post CSN manipulation, but no reduction in other F-box proteins (Cope and Deshaies, 2006, Su et al., 2008).

There are at least two explanations for the sequential loss of F-box proteins. First, given that binding of F-box proteins to the SCF has been suggested to be competitive (Patton et al., 1998, Bosu and Kipreos, 2008), it is possible that the rapid loss of Skp2 reflects high Skp2 expression in K562 cells and therefore preferential binding of Skp2 to the SCF. In support of this, the level of Skp2 mRNA in K562 was found to be greater than that of

Cdc4 and β -TrCP (data not shown). This finding was not surprising given that the fusion protein associated with CML, BCR-ABL, has been shown to induce Skp2 expression (Andreu et al., 2005). On the other hand, Cdc4 and β -TrCP were found to be expressed at the same level in K562 (data not shown). The disparate rates of Cdc4 and β -TrCP protein loss may be attributable to the potentially different affinities of these F-box proteins for the SCF. However, an alternative explanation is that some F-box proteins, such as β -TrCP, may not be as susceptible to autocatalytic degradation. Recently, a similar hypothesis has been put forward regarding the *Drosophila* β -TrCP homolog, Slimb (Knowles et al., 2009). In favour of this is the finding herein that whilst β -TrCP mRNA was reduced day 4 post transfection in CSN5 knockdown cells the level of β -TrCP protein was unaltered, suggesting that this protein is relatively stable. If this were the case then it is possible that SCF ^{β -TrCP} activity is retained in CSN subunit knockdowns, as presented by E.Bianchi at the recent Zomes symposium (Pick and Pintard, 2009), at early time points post transfection. Although further work would be necessary to test this hypothesis, the findings to date give rise to the possibility that the CSN may function in determining SCF target specificity in human cells, as has been postulated in *Drosophila* (Doronkin et al., 2003, Harari-Steinberg et al., 2007, Knowles et al., 2009).

7.3 The CSN and F-box protein/CSN subunit transcription

Both CSN2 and CSN5 knockdown resulted in temporal alterations to F-box protein mRNA. Further, CSN2 knockdown was associated with a significant loss of CSN5 mRNA. Together with other recent reports (Su et al., 2008, Ullah et al., 2007), these data

suggest that the CSN complex may have a direct role in the transcriptional regulation of CSN subunits and F-box proteins, independent of CSN deneddylase activity. For instance, it is possible from the findings regarding Skp2 mRNA levels in both CSN2 and CSN5 knockdown cells that the intact CSN complex functions directly in the transcriptional activation of Skp2. In support of this, the identical effect of CSN2 and CSN5 loss on SCF^{Skp2} activity suggests that the different rates of Skp2 mRNA reduction observed between the knockdowns most likely results from the loss of a deneddylase independent function of the CSN complex. The same can also be said for the alterations in Cdc4 and β -TrCP mRNA levels. In addition, the slower rate of Skp2 mRNA loss in shCSN5 cells relative to shCSN2 cells may reflect a delayed loss of the intact CSN complex in these cells. Although this would further implicate the CSN in the deneddylase independent regulation of transcription, the stability of the intact CSN complex in shCSN5 cells at a later time point (such as day 6 post transfection) remains to be experimentally determined.

It is important to note that the altered mRNA levels observed may be an indirect result of the aberrant degradation of proteins which may occur upon loss of other CSN functions such as protein phosphorylation and deubiquitination. In addition, the contribution of CSN subcomplexes or the CSN independent functions of CSN2 and CSN5 to the altered mRNA levels of Skp2, Cdc4 and β -TrCP cannot be ruled out. To further investigate the possibility that the CSN complex directly regulates CSN subunit and F-box protein transcription, chromatin immunoprecipitation (ChIP) could be used to determine promoter binding. MG132 and curcumin, which inhibit the proteasome and CSN

associated kinases respectively, could also be used to assess any contribution of aberrant protein degradation or CSN associated protein phosphorylation to altered CSN subunit or F-box protein mRNA levels.

7.4 CSN2 knockdown

This is the first study to show an association between the CSN complex and autophagy. The phenotype of K562 cells in which CSN2 had been knocked down included features of autophagy, and treatment of K562 cells with autophagy inhibitors recapitulated this phenotype. These findings suggest that CSN2 knockdown in K562 cells causes an arrested autophagic process resulting ultimately in cell death.

The autophagy inhibition and mitotic defects which arose from the loss of CSN2 and CSN5, respectively, raised the question of why knockdown of two subunits of the same complex should result in divergent phenotypes? It was predicted that the disparate consequences of CSN2 and CSN5 knockdown may be attributable to the effect of the knockdowns on the intact CSN complex, as has been postulated for the divergent phenotypes observed in *Drosophila* CSN4 and CSN5 mutations (Oron et al., 2002, Oron et al., 2007). Initially, CSN2 knockdown was shown to result in significant loss of the intact CSN complex and CSN5 protein. Interestingly, cells lacking CSN2 were also shown to be associated with the formation of a CSN5 containing subcomplex. It was thus postulated that the phenotype of shCSN2 cells may arise as a result of aberrant CSN5 activity within this subcomplex. However, a significant number of double knockdown

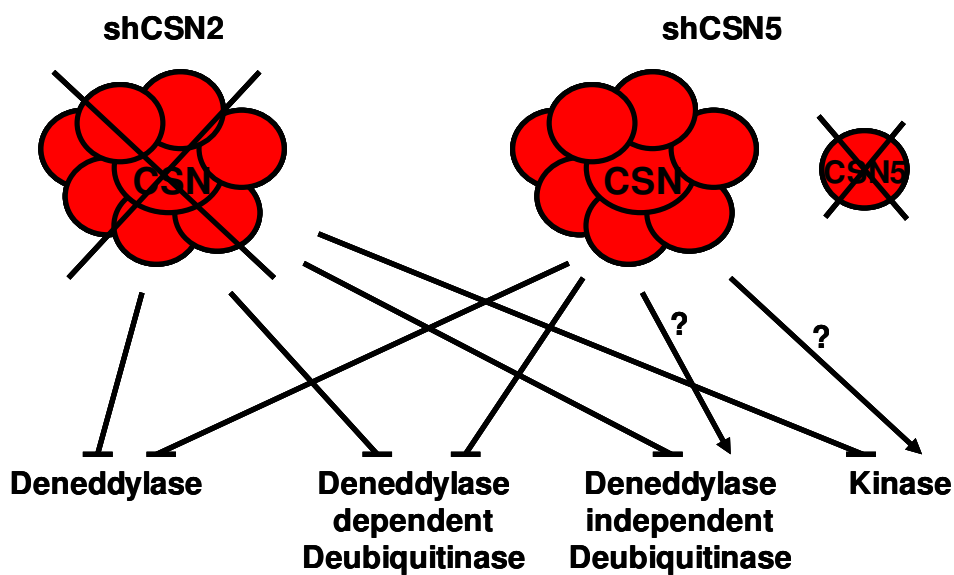


Figure 77. Diagram depicting the possible consequences of CSN2 or CSN5 loss for the functions of the intact CSN complex.

Diagram to show that in CSN2 knockdown cells, in which the CSN complex is lost, all functions of the intact CSN are likely to be lost. Further, CSN5 knockdown cells, which retain the intact CSN complex until at least day 3 post transfection but lose monomeric CSN5, may retain both deneddylase independent deubiquitinase and CSN associated kinase functions. It is thus postulated here that the inhibition of autophagy occurs as a result of the loss of a deneddylase independent function of the CSN, whilst the CSN5 associated phenotype is mediated by loss of a CSN independent function of CSN5.

cells lacking both CSN2 and CSN5, in which this subcomplex was not detected, demonstrated a vacuolar morphology comparable to that of shCSN2 cells. These findings indicate that the phenotype of shCSN2 cells is not attributable to the function of this CSN5 containing subcomplex.

As the intact CSN complex was lost in CSN2 targeted cells, it is possible that the CSN2 knockdown phenotype is attributable to the loss of a function of the intact CSN complex. However, as both CSN2 and CSN5 knockdowns appear to have the same affect on CRL activity it seems unlikely that the shCSN2 associated phenotype occurs as a result of the loss of cullin deneddylation. Rather, autophagy inhibition may occur due to the loss of a deneddylase independent function of the intact CSN complex such as protein phosphorylation or deubiquitination (figure 77). These functions are possibly retained in shCSN5 cells with the retention of the intact CSN complex until at least day 3 post transfection (figure 77), thus potentially giving rise to the divergent phenotypes observed. Alternatively, the inhibition of autophagy may be a consequence of the loss of CSN2 monomer function. In order to discern between these two possibilities, CSN2 re-expression studies should be carried out.

7.5 CSN5 knockdown

Previous studies in *Drosophila* (Oron et al., 2002), *Arabidopsis* (Dohmann et al., 2005) and HeLa cells (Peth et al., 2007a) have demonstrated the retention of a high molecular weight complex in the absence of CSN5. However, this is the first study to demonstrate

the longevity of the intact CSN complex including CSN5 in CSN5 knockdown cells. Initially, these data suggested that the shCSN5 associated phenotype may occur as a result of an activity of the surviving CSN complex. However, this was proven to be unlikely with the finding that a proportion of double knockdown cells, which lack the intact CSN complex, demonstrated a morphology comparable to that of shCSN5 cells.

Although the level of CSN complex bound CSN5 was unaltered in shCSN5 cells at day 3 post transfection, a significant proportion of monomeric CSN5 was lost. This indicates that complex bound and monomeric CSN5 have different half lives, with CSN5 potentially being protected from degradation when bound to the CSN complex. This finding also led to the hypothesis that the phenotype of CSN5 targeted K562 cells is mediated by the loss of a CSN complex independent function of CSN5. In support of this, Tomoda and colleagues demonstrated that a 22% CSN5 protein knockdown in K562 cells, which did not affect the level of the intact CSN, resulted in a similar cell cycle profile to that reported here, with loss of cells from the S phase of the cell cycle and an accumulation of cells in the G2M phase (Tomoda et al., 2005). In order to test this hypothesis both wild-type and deneddylase dead CSN5 were expressed in a shCSN5 background. Although performed only once, the cumulative growth and cell morphology data together suggest that re-expression of either WT or dd CSN5 rescues the CSN5 knockdown phenotype to the same extent, independently of their ability to restore cullin deneddylation and rescue Skp2 protein. Together with the finding that shCSN5 cells retain the intact CSN complex and thus potentially the deneddylase independent functions associated with the CSN, these results suggest that the shCSN5 associated

phenotype most likely occurs as a result of the loss of a CSN independent function of CSN5.

CSN5 knockdown was associated with reduced cell proliferation and apoptosis. These data complement previous studies demonstrating that CSN5 loss inhibits proliferation and induces apoptosis (Panattoni et al., 2008, Fukumoto et al., 2006). Closer analysis of CSN5 knockdown cells identified a G2/M cell cycle arrest and abnormal mitotic spindles. Microtubule stability (Peth et al., 2007b, Pintard et al., 2003) and progression through the G2/M phase of the cell cycle (Dohmann et al., 2008, Li et al., 2009) have been shown to be dependent on CSN deneddylase activity (Dohmann et al., 2008, Pintard et al., 2003) or CSN associated kinase activity (Li et al., 2009, Peth et al., 2007b). However, as the phenotype associated with the loss of CSN5 is most probably attributable to the loss of monomeric CSN5 function the precise mechanism accounting for the observed phenotype remains to be determined.

It is important to note that both CSN2 and CSN5 have been shown to function in distinct subcomplexes (Mundt et al., 2002, Tomoda et al., 2002) and that CSN5 has been shown to function within a CSN subcomplex in K562 (Tomoda et al., 2005). Although such subcomplexes were not consistently detected in the NativePAGE/SDS-PAGE studies, the possible contribution of either the CSN independent function of CSN2 or CSN subcomplexes to the phenotypic differences observed between the knockdowns cannot be ruled out. Indeed, Tomoda and colleagues have published data to suggest that the loss of a CSN subcomplex in K562 cells results in a similar cell cycle profile to that

demonstrated here for shCSN5 K562 cells (Tomoda et al., 2005). However, importantly this study does not document the effect of CSN5 knockdown on monomeric CSN5 and thus does not rule out the possible contribution of monomeric CSN5 function to this cell cycle profile.

7.6 CSN5 re-expression results in partial rescue of the shCSN5 phenotype

It should be noted that expression of neither WT nor dd CSN5 rescued the shCSN5 phenotype fully, even though the CSN5 protein level was comparable to that of vector control day 7 post transfection. This could be explained if CSN5 protein was found to be initially lost relatively rapidly in response to shRNA expression whereas vector-driven CSN5 re-expression only fully restored CSN5 protein at a later time point. In favour of this possibility, only partial rescue of Skp2 was observed day 3 post transfection, and although Skp2 protein was rescued day 7 post transfection, CSN5 re-expression failed to rescue p27 protein at this time point. However, further work would be needed to test this hypothesis. Such work may include earlier time point analysis of CSN5 protein, and an extended time course to confirm whether the re-expression of CSN5 restores p27 protein level and continues to rescue cumulative cell growth and cell morphology at later time points at which shCSN5 knockdown is lethal.

7.7 ddCSN5 expression rescues Skp2 protein levels

It is interesting to note that dd CSN5 expression was also found to rescue Skp2 protein levels. Although the incorporation of dd CSN5 into the CSN complex has not been demonstrated here, the incorporation of mutant CSN5 into the CSN complex has been described previously (Cope et al., 2002). It is thus possible that the expression of dd CSN5 resulted in increased deneddylase independent CSN associated deubiquitinase activity. Such an activity may reverse Skp2 autoubiquitination within the SCF and thus prevent the autocatalytic degradation of Skp2, thereby rescuing Skp2 protein. However, the deneddylase independent deubiquitination of Skp2 by the CSN would have to be demonstrated in order to verify this possibility.

7.8 A novel mechanism of CSN deneddylase activity regulation?

An important observation made here is that although the intact CSN complex was retained in shCSN5 cells until at least day 3 post transfection, SCF^{Skp2} activity was found to be aberrant at this time point. Intriguingly, this data suggests that the sustained deneddylase activity of the CSN complex may be dependent on the availability of monomeric CSN5. This finding gives rise to a novel potential mechanism of CSN deneddylase activity regulation in which CSN5 subunit refreshment may be required for continued cullin deneddylation. If this were the case, the absence of monomeric CSN5 would inhibit the deneddylase activity of the CSN, as is suggested by the findings of this study. However, in order to directly test this hypothesis the deneddylase activities of both

the shCSN5 and vector control CSN complex should be compared both in the presence and absence of recombinant CSN5.

7.9 The CSN and CML

Overall, the data presented here suggest that the CSN complex/CSN subunits may be viable targets in the treatment of CML. For instance, as ectopic CSN5 expression results in a myeloproliferative disorder resembling CML (Mori et al., 2008), the finding of a lethal phenotype of shCSN5 K562 cells implies that CSN5 may be a novel target in CML treatment. The modulation of autophagy in combination with imatinib as a possible CML treatment has been reported (Bellodi et al., 2009, Burchert et al., 2005, Dengler et al., 2005). In particular, imatinib treatment of both CML cell lines and primary CML cells has been shown to induce BCR-ABL dependent autophagy as a survival mechanism. Autophagy inhibition was subsequently shown to potentiate imatinib induced cell death in CML cell lines, primary CML cells and importantly, the CML stem cell population (Bellodi et al., 2009). This study together with the finding of CSN2 knockdown induced autophagy inhibition suggest that targeting CSN activity in combination with imatinib treatment may represent a novel treatment in CML. However, a significant amount of work would be required in order to verify the CSN as a novel target in CML, including studies into the effect of CSN subunit knockdown on primary CML cells and their non-malignant counterparts. Further, it would be of interest to determine the precise mechanism of autophagy inhibition in shCSN2 cells and mitotic defects in shCSN5 cells in order to allow more specific targeting of CSN function in CML.

References

- ADLER, A. S., LITTLEPAGE, L. E., LIN, M., KAWAHARA, T. L., WONG, D. J., WERB, Z. & CHANG, H. Y. (2008) CSN5 isopeptidase activity links COP9 signalosome activation to breast cancer progression. *Cancer Res*, 68, 506-15.
- ALBERTS, B. (2002) *Molecular biology of the cell*, New York, Garland Science.
- ALTINCICEK, B., TENBAUM, S. P., DRESSEL, U., THORMEYER, D., RENKAWITZ, R. & BANIAHMAD, A. (2000) Interaction of the corepressor Alien with DAX-1 is abrogated by mutations of DAX-1 involved in adrenal hypoplasia congenita. *J Biol Chem*, 275, 7662-7.
- ANDREU, E. J., LLEDO, E., POCH, E., IVORRA, C., ALBERO, M. P., MARTINEZ-CLIMENT, J. A., MONTIEL-DUARTE, C., RIFON, J., PEREZ-CALVO, J., ARBONA, C., PROSPER, F. & PEREZ-ROGER, I. (2005) BCR-ABL induces the expression of Skp2 through the PI3K pathway to promote p27Kip1 degradation and proliferation of chronic myelogenous leukemia cells. *Cancer Res*, 65, 3264-72.
- ANGERS, S., LI, T., YI, X., MACCOSS, M. J., MOON, R. T. & ZHENG, N. (2006) Molecular architecture and assembly of the DDB1-CUL4A ubiquitin ligase machinery. *Nature*, 443, 590-3.
- BECH-OTSCHIR, D., KRAFT, R., HUANG, X., HENKLEIN, P., KAPELARI, B., POLLMANN, C. & DUBIEL, W. (2001) COP9 signalosome-specific phosphorylation targets p53 to degradation by the ubiquitin system. *EMBO J*, 20, 1630-9.
- BELLODI, C., LIDONNICI, M. R., HAMILTON, A., HELGASON, G. V., SOLIERA, A. R., RONCHETTI, M., GALAVOTTI, S., YOUNG, K. W., SELMI, T., YACOBI, R., VAN ETTEN, R. A., DONATO, N., HUNTER, A., DINSDALE, D., TIRRO, E., VIGNERI, P., NICOTERA, P., DYER, M. J., HOLYOAKE, T., SALOMONI, P. & CALABRETTA, B. (2009) Targeting autophagy potentiates tyrosine kinase inhibitor-induced cell death in Philadelphia chromosome-positive cells, including primary CML stem cells. *J Clin Invest*, 119, 1109-23.
- BIANCHI, E., DENTI, S., GRANATA, A., BOSSI, G., GEGINAT, J., VILLA, A., ROGGE, L. & PARDI, R. (2000) Integrin LFA-1 interacts with the transcriptional co-activator JAB1 to modulate AP-1 activity. *Nature*, 404, 617-21.
- BORNSTEIN, G., GANOTH, D. & HERSHKO, A. (2006) Regulation of neddylation and deneddylation of cullin1 in SCFSkp2 ubiquitin ligase by F-box protein and substrate. *Proc Natl Acad Sci U S A*, 103, 11515-20.
- BOSU, D. R. & KIPREOS, E. T. (2008) Cullin-RING ubiquitin ligases: global regulation and activation cycles. *Cell Div*, 3, 7.
- BURCHERT, A., WANG, Y., CAI, D., VON BUBNOFF, N., PASCHKA, P., MULLER-BRUSSELBACH, S., OTTMANN, O. G., DUYSER, J., HOCHHAUS, A. & NEUBAUER, A. (2005) Compensatory PI3-kinase/Akt/mTor activation regulates imatinib resistance development. *Leukemia*, 19, 1774-82.
- BUSCH, S., ECKERT, S. E., KRAPPMANN, S. & BRAUS, G. H. (2003) The COP9 signalosome is an essential regulator of development in the filamentous fungus *Aspergillus nidulans*. *Mol Microbiol*, 49, 717-30.

- BUSCH, S., SCHWIER, E. U., NAHLIK, K., BAYRAM, O., HELMSTAEDT, K., DRAHT, O. W., KRAPPMANN, S., VALERIUS, O., LIPSCOMB, W. N. & BRAUS, G. H. (2007) An eight-subunit COP9 signalosome with an intact JAMM motif is required for fungal fruit body formation. *Proc Natl Acad Sci U S A*, 104, 8089-94.
- CALLIGE, M., KIEFFER, I. & RICHARD-FOY, H. (2005) CSN5/Jab1 is involved in ligand-dependent degradation of estrogen receptor {alpha} by the proteasome. *Mol Cell Biol*, 25, 4349-58.
- CHAMOVITZ, D. A. (2009) Revisiting the COP9 signalosome as a transcriptional regulator. *EMBO Rep*, 10, 352-8.
- CHAMOVITZ, D. A., WEI, N., OSTERLUND, M. T., VON ARNIM, A. G., STAUB, J. M., MATSUI, M. & DENG, X. W. (1996) The COP9 complex, a novel multisubunit nuclear regulator involved in light control of a plant developmental switch. *Cell*, 86, 115-21.
- CHAUCHEREAU, A., GEORGIAKAKI, M., PERRIN-WOLFF, M., MILGROM, E. & LOOSFELT, H. (2000) JAB1 interacts with both the progesterone receptor and SRC-1. *J Biol Chem*, 275, 8540-8.
- CIECHANOVER, A., HELLER, H., ELIAS, S., HAAS, A. L. & HERSHKO, A. (1980) ATP-dependent conjugation of reticulocyte proteins with the polypeptide required for protein degradation. *Proc Natl Acad Sci U S A*, 77, 1365-8.
- CIECHANOVER, A., HELLER, H., KATZ-ETZION, R. & HERSHKO, A. (1981) Activation of the heat-stable polypeptide of the ATP-dependent proteolytic system. *Proc Natl Acad Sci U S A*, 78, 761-5.
- CIECHANOVER, A., HOD, Y. & HERSHKO, A. (1978) A heat-stable polypeptide component of an ATP-dependent proteolytic system from reticulocytes. *Biochem Biophys Res Commun*, 81, 1100-5.
- CLARET, F. X., HIBI, M., DHUT, S., TODA, T. & KARIN, M. (1996) A new group of conserved coactivators that increase the specificity of AP-1 transcription factors. *Nature*, 383, 453-7.
- COHEN, H., AZRIEL, A., COHEN, T., MERARO, D., HASHMUELI, S., BECH-OTSCHIR, D., KRAFT, R., DUBIEL, W. & LEVI, B. Z. (2000) Interaction between interferon consensus sequence-binding protein and COP9/signalosome subunit CSN2 (Trip15). A possible link between interferon regulatory factor signaling and the COP9/signalosome. *J Biol Chem*, 275, 39081-9.
- COOPER, E. M., CUTCLIFFE, C., KRISTIANSEN, T. Z., PANDEY, A., PICKART, C. M. & COHEN, R. E. (2009) K63-specific deubiquitination by two JAMM/MPN+ complexes: BRISC-associated Brcc36 and proteasomal Poh1. *EMBO J*.
- COPE, G. A. & DESHAIES, R. J. (2003) COP9 signalosome: a multifunctional regulator of SCF and other cullin-based ubiquitin ligases. *Cell*, 114, 663-71.
- COPE, G. A. & DESHAIES, R. J. (2006) Targeted silencing of Jab1/Csn5 in human cells downregulates SCF activity through reduction of F-box protein levels. *BMC Biochem*, 7, 1.
- COPE, G. A., SUH, G. S., ARAVIND, L., SCHWARZ, S. E., ZIPURSKY, S. L., KOONIN, E. V. & DESHAIES, R. J. (2002) Role of predicted metalloprotease motif of Jab1/Csn5 in cleavage of Nedd8 from Cull1. *Science*, 298, 608-11.

- CULLINAN, S. B., GORDAN, J. D., JIN, J., HARPER, J. W. & DIEHL, J. A. (2004) The Keap1-BTB protein is an adaptor that bridges Nrf2 to a Cul3-based E3 ligase: oxidative stress sensing by a Cul3-Keap1 ligase. *Mol Cell Biol*, 24, 8477-86.
- DENG, X. W., DUBIEL, W., WEI, N., HOFMANN, K. & MUNDT, K. (2000a) Unified nomenclature for the COP9 signalosome and its subunits: an essential regulator of development. *Trends Genet*, 16, 289.
- DENG, X. W., DUBIEL, W., WEI, N., HOFMANN, K., MUNDT, K., COLICELLI, J., KATO, J., NAUMANN, M., SEGAL, D., SEEGER, M., CARR, A., GLICKMAN, M. & CHAMOVITZ, D. A. (2000b) Unified nomenclature for the COP9 signalosome and its subunits: an essential regulator of development. *Trends Genet*, 16, 202-3.
- DENGLER, J., VON BUBNOFF, N., DECKER, T., PESCHEL, C. & DUYSER, J. (2005) Combination of imatinib with rapamycin or RAD001 acts synergistically only in Bcr-Abl-positive cells with moderate resistance to imatinib. *Leukemia*, 19, 1835-8.
- DENTI, S., FERNANDEZ-SANCHEZ, M. E., ROGGE, L. & BIANCHI, E. (2006) The COP9 signalosome regulates Skp2 levels and proliferation of human cells. *J Biol Chem*, 281, 32188-96.
- DESSAU, M., HALIMI, Y., EREZ, T., CHOMSKY-HECHT, O., CHAMOVITZ, D. A. & HIRSCH, J. A. (2008) The Arabidopsis COP9 signalosome subunit 7 is a model PCI domain protein with subdomains involved in COP9 signalosome assembly. *Plant Cell*, 20, 2815-34.
- DIAS, D. C., DOLIOS, G., WANG, R. & PAN, Z. Q. (2002) CUL7: A DOC domain-containing cullin selectively binds Skp1.Fbx29 to form an SCF-like complex. *Proc Natl Acad Sci U S A*, 99, 16601-6.
- DOHERTY, F. J. & MAYER, R. J. (1992) *Intracellular protein degradation*, Oxford ; New York, IRL Press.
- DOHMANN, E. M., KUHNLE, C. & SCHWECHHEIMER, C. (2005) Loss of the CONSTITUTIVE PHOTOMORPHOGENIC9 signalosome subunit 5 is sufficient to cause the cop/det/fus mutant phenotype in Arabidopsis. *Plant Cell*, 17, 1967-78.
- DOHMANN, E. M., LEVESQUE, M. P., DE VEYLDER, L., REICHARDT, I., JURGENS, G., SCHMID, M. & SCHWECHHEIMER, C. (2008) The Arabidopsis COP9 signalosome is essential for G2 phase progression and genomic stability. *Development*, 135, 2013-22.
- DORONKIN, S., DJAGAEVA, I. & BECKENDORF, S. K. (2003) The COP9 signalosome promotes degradation of Cyclin E during early Drosophila oogenesis. *Dev Cell*, 4, 699-710.
- DRESSEL, U., THORMEYER, D., ALTINCICEK, B., PAULULAT, A., EGGERT, M., SCHNEIDER, S., TENBAUM, S. P., RENKAWITZ, R. & BANIAHMAD, A. (1999) Alien, a highly conserved protein with characteristics of a corepressor for members of the nuclear hormone receptor superfamily. *Mol Cell Biol*, 19, 3383-94.
- DUDA, D. M., BORG, L. A., SCOTT, D. C., HUNT, H. W., HAMMEL, M. & SCHULMAN, B. A. (2008) Structural insights into NEDD8 activation of cullin-RING ligases: conformational control of conjugation. *Cell*, 134, 995-1006.

- ECKEY, M., HONG, W., PAPAIOANNOU, M. & BANIAHMAD, A. (2007) The nucleosome assembly activity of NAP1 is enhanced by Alien. *Mol Cell Biol*, 27, 3557-68.
- FADER, C. M., SANCHEZ, D., FURLAN, M. & COLOMBO, M. I. (2008) Induction of autophagy promotes fusion of multivesicular bodies with autophagic vacuoles in k562 cells. *Traffic*, 9, 230-50.
- FANG, L., WANG, X., YAMOA, K., CHEN, P. L., PAN, Z. Q. & HUANG, L. (2008) Characterization of the human COP9 signalosome complex using affinity purification and mass spectrometry. *J Proteome Res*, 7, 4914-25.
- FENG, L., ALLEN, N. S., SIMO, S. & COOPER, J. A. (2007) Cullin 5 regulates Dab1 protein levels and neuron positioning during cortical development. *Genes Dev*, 21, 2717-30.
- FENG, S., MA, L., WANG, X., XIE, D., DINESH-KUMAR, S. P., WEI, N. & DENG, X. W. (2003) The COP9 signalosome interacts physically with SCF COI1 and modulates jasmonate responses. *Plant Cell*, 15, 1083-94.
- FREILICH, S., ORON, E., KAPP, Y., NEVO-CASPI, Y., ORGAD, S., SEGAL, D. & CHAMOVITZ, D. A. (1999) The COP9 signalosome is essential for development of *Drosophila melanogaster*. *Curr Biol*, 9, 1187-90.
- FUKUMOTO, A., TOMODA, K., KUBOTA, M., KATO, J. Y. & YONEDA-KATO, N. (2005) Small Jab1-containing subcomplex is regulated in an anchorage- and cell cycle-dependent manner, which is abrogated by ras transformation. *FEBS Lett*, 579, 1047-54.
- FUKUMOTO, A., TOMODA, K., YONEDA-KATO, N., NAKAJIMA, Y. & KATO, J. Y. (2006) Depletion of Jab1 inhibits proliferation of pancreatic cancer cell lines. *FEBS Lett*, 580, 5836-44.
- FURUKAWA, M. & XIONG, Y. (2005) BTB protein Keap1 targets antioxidant transcription factor Nrf2 for ubiquitination by the Cullin 3-Roc1 ligase. *Mol Cell Biol*, 25, 162-71.
- GALAN, J. M. & PETER, M. (1999) Ubiquitin-dependent degradation of multiple F-box proteins by an autocatalytic mechanism. *Proc Natl Acad Sci U S A*, 96, 9124-9.
- GATTO, S., SCAPPINI, B., PHAM, L., ONIDA, F., MILELLA, M., BALL, G., RICCI, C., DIVOKY, V., VERSTOVSEK, S., KANTARJIAN, H. M., KEATING, M. J., CORTES-FRANCO, J. E. & BERAN, M. (2003) The proteasome inhibitor PS-341 inhibits growth and induces apoptosis in Bcr/Abl-positive cell lines sensitive and resistant to imatinib mesylate. *Haematologica*, 88, 853-63.
- GEYER, R., WEE, S., ANDERSON, S., YATES, J. & WOLF, D. A. (2003) BTB/POZ domain proteins are putative substrate adaptors for cullin 3 ubiquitin ligases. *Mol Cell*, 12, 783-90.
- GLICKMAN, M. H., RUBIN, D. M., COUX, O., WEFES, I., PFEIFER, G., CJEKA, Z., BAUMEISTER, W., FRIED, V. A. & FINLEY, D. (1998) A subcomplex of the proteasome regulatory particle required for ubiquitin-conjugate degradation and related to the COP9-signalosome and eIF3. *Cell*, 94, 615-23.
- GOLDENBERG, S. J., CASCIO, T. C., SHUMWAY, S. D., GARBUTT, K. C., LIU, J., XIONG, Y. & ZHENG, N. (2004) Structure of the Cand1-Cul1-Roc1 complex reveals regulatory mechanisms for the assembly of the multisubunit cullin-dependent ubiquitin ligases. *Cell*, 119, 517-28.

- GONG, L. & YEH, E. T. (1999) Identification of the activating and conjugating enzymes of the NEDD8 conjugation pathway. *J Biol Chem*, 274, 12036-42.
- GORRE, M. E., MOHAMMED, M., ELLWOOD, K., HSU, N., PAQUETTE, R., RAO, P. N. & SAWYERS, C. L. (2001) Clinical resistance to STI-571 cancer therapy caused by BCR-ABL gene mutation or amplification. *Science*, 293, 876-80.
- GRAHAM, S. M., JORGENSEN, H. G., ALLAN, E., PEARSON, C., ALCORN, M. J., RICHMOND, L. & HOLYOAKE, T. L. (2002) Primitive, quiescent, Philadelphia-positive stem cells from patients with chronic myeloid leukemia are insensitive to STI571 in vitro. *Blood*, 99, 319-25.
- GROISMAN, R., POLANOWSKA, J., KURAOKA, I., SAWADA, J., SAIJO, M., DRAPKIN, R., KISSELEV, A. F., TANAKA, K. & NAKATANI, Y. (2003) The ubiquitin ligase activity in the DDB2 and CSA complexes is differentially regulated by the COP9 signalosome in response to DNA damage. *Cell*, 113, 357-67.
- GUSMAROLI, G., FIGUEROA, P., SERINO, G. & DENG, X. W. (2007) Role of the MPN subunits in COP9 signalosome assembly and activity, and their regulatory interaction with Arabidopsis Cullin3-based E3 ligases. *Plant Cell*, 19, 564-81.
- HAAS, A. L., WARMS, J. V., HERSHKO, A. & ROSE, I. A. (1982) Ubiquitin-activating enzyme. Mechanism and role in protein-ubiquitin conjugation. *J Biol Chem*, 257, 2543-8.
- HARARI-STEINBERG, O., CANTERA, R., DENTI, S., BIANCHI, E., ORON, E., SEGAL, D. & CHAMOVITZ, D. A. (2007) COP9 signalosome subunit 5 (CSN5/Jab1) regulates the development of the Drosophila immune system: effects on Cactus, Dorsal and hematopoiesis. *Genes Cells*, 12, 183-95.
- HE, Q., CHENG, P., HE, Q. & LIU, Y. (2005) The COP9 signalosome regulates the Neurospora circadian clock by controlling the stability of the SCFFWD-1 complex. *Genes Dev*, 19, 1518-31.
- HE, Y. J., MCCALL, C. M., HU, J., ZENG, Y. & XIONG, Y. (2006) DDB1 functions as a linker to recruit receptor WD40 proteins to CUL4-ROC1 ubiquitin ligases. *Genes Dev*, 20, 2949-54.
- HEHLMANN, R., HOCHHAUS, A. & BACCARANI, M. (2007) Chronic myeloid leukaemia. *Lancet*, 370, 342-50.
- HENKE, W., FERRELL, K., BECH-OTSCHIR, D., SEEGER, M., SCHADE, R., JUNGBLUT, P., NAUMANN, M. & DUBIEL, W. (1999) Comparison of human COP9 signalosome and 26S proteasome lid'. *Mol Biol Rep*, 26, 29-34.
- HERSHKO, A., HELLER, H., ELIAS, S. & CIECHANOVER, A. (1983) Components of ubiquitin-protein ligase system. Resolution, affinity purification, and role in protein breakdown. *J Biol Chem*, 258, 8206-14.
- HERSHKO, A., HELLER, H., EYTAN, E. & REISS, Y. (1986) The protein substrate binding site of the ubiquitin-protein ligase system. *J Biol Chem*, 261, 11992-9.
- HERSHKO, A., LESHINSKY, E., GANOTH, D. & HELLER, H. (1984) ATP-dependent degradation of ubiquitin-protein conjugates. *Proc Natl Acad Sci U S A*, 81, 1619-23.
- HETFELD, B. K., HELFRICH, A., KAPELARI, B., SCHEEL, H., HOFMANN, K., GUTERMAN, A., GLICKMAN, M., SCHADE, R., KLOETZEL, P. M. &

- DUBIEL, W. (2005) The zinc finger of the CSN-associated deubiquitinating enzyme USP15 is essential to rescue the E3 ligase Rbx1. *Curr Biol*, 15, 1217-21.
- HETFELD, B. K., PETH, A., SUN, X. M., HENKLEIN, P., COHEN, G. M. & DUBIEL, W. (2008) The COP9 signalosome-mediated deneddylation is stimulated by caspases during apoptosis. *Apoptosis*, 13, 187-95.
- HORI, T., OSAKA, F., CHIBA, T., MIYAMOTO, C., OKABAYASHI, K., SHIMBARA, N., KATO, S. & TANAKA, K. (1999) Covalent modification of all members of human cullin family proteins by NEDD8. *Oncogene*, 18, 6829-34.
- HUANG, D. T., AYRAULT, O., HUNT, H. W., TAHERBHOY, A. M., DUDA, D. M., SCOTT, D. C., BORG, L. A., NEALE, G., MURRAY, P. J., ROUSSEL, M. F. & SCHULMAN, B. A. (2009) E2-RING expansion of the NEDD8 cascade confers specificity to cullin modification. *Mol Cell*, 33, 483-95.
- HUANG, X., HETFELD, B. K., SEIFERT, U., KAHNE, T., KLOETZEL, P. M., NAUMANN, M., BECH-OTSCHIR, D. & DUBIEL, W. (2005) Consequences of COP9 signalosome and 26S proteasome interaction. *FEBS J*, 272, 3909-17.
- JIN, J., CARDOZO, T., LOVERING, R. C., ELLEDGE, S. J., PAGANO, M. & HARPER, J. W. (2004) Systematic analysis and nomenclature of mammalian F-box proteins. *Genes Dev*, 18, 2573-80.
- JONES, A. T., SPIRO, D. J., KIRCHHAUSEN, T., MELANCON, P. & WESSLING-RESNICK, M. (1999) Studies on the inhibition of endosome fusion by GTPgammaS-bound ARF. *J Cell Sci*, 112 (Pt 20), 3477-85.
- KAMURA, T., KOEPP, D. M., CONRAD, M. N., SKOWYRA, D., MORELAND, R. J., ILIOPOULOS, O., LANE, W. S., KAELIN, W. G., JR., ELLEDGE, S. J., CONAWAY, R. C., HARPER, J. W. & CONAWAY, J. W. (1999) Rbx1, a component of the VHL tumor suppressor complex and SCF ubiquitin ligase. *Science*, 284, 657-61.
- KAMURA, T., MAENAKA, K., KOTOSHIBA, S., MATSUMOTO, M., KOHDA, D., CONAWAY, R. C., CONAWAY, J. W. & NAKAYAMA, K. I. (2004) VHL-box and SOCS-box domains determine binding specificity for Cul2-Rbx1 and Cul5-Rbx2 modules of ubiquitin ligases. *Genes Dev*, 18, 3055-65.
- KAPELARI, B., BECH-OTSCHIR, D., HEGERL, R., SCHADE, R., DUMDEY, R. & DUBIEL, W. (2000) Electron microscopy and subunit-subunit interaction studies reveal a first architecture of COP9 signalosome. *J Mol Biol*, 300, 1169-78.
- KAWAKAMI, T., CHIBA, T., SUZUKI, T., IWAI, K., YAMANAKA, K., MINATO, N., SUZUKI, H., SHIMBARA, N., HIDAKA, Y., OSAKA, F., OMATA, M. & TANAKA, K. (2001) NEDD8 recruits E2-ubiquitin to SCF E3 ligase. *Embo J*, 20, 4003-12.
- KIM, B. C., LEE, H. J., PARK, S. H., LEE, S. R., KARPOVA, T. S., MCNALLY, J. G., FELICI, A., LEE, D. K. & KIM, S. J. (2004) Jab1/CSN5, a component of the COP9 signalosome, regulates transforming growth factor beta signaling by binding to Smad7 and promoting its degradation. *Mol Cell Biol*, 24, 2251-62.
- KLEEMANN, R., HAUSSER, A., GEIGER, G., MISCHKE, R., BURGER-KENTISCHER, A., FLIEGER, O., JOHANNES, F. J., ROGER, T., CALANDRA, T., KAPURNIOTU, A., GRELL, M., FINKELMEIER, D., BRUNNER, H. & BERNHAGEN, J. (2000) Intracellular action of the cytokine

- MIF to modulate AP-1 activity and the cell cycle through Jab1. *Nature*, 408, 211-6.
- KLIONSKY, D. J., ABELIOVICH, H., AGOSTINIS, P., AGRAWAL, D. K., ALIEV, G., ASKEW, D. S., BABA, M., BAEHRECKE, E. H., BAHR, B. A., BALLABIO, A., BAMBER, B. A., BASSHAM, D. C., BERGAMINI, E., BI, X., BIARD-PIECHACZYK, M., BLUM, J. S., BREDESEN, D. E., BRODSKY, J. L., BRUMELL, J. H., BRUNK, U. T., BURSCH, W., CAMOUGRAND, N., CEBOLLERO, E., CECCONI, F., CHEN, Y., CHIN, L. S., CHOI, A., CHU, C. T., CHUNG, J., CLARKE, P. G., CLARK, R. S., CLARKE, S. G., CLAVE, C., CLEVELAND, J. L., CODOGNO, P., COLOMBO, M. I., COTO-MONTES, A., CREGG, J. M., CUERVO, A. M., DEBNATH, J., DEMARCHI, F., DENNIS, P. B., DENNIS, P. A., DERETIC, V., DEVENISH, R. J., DI SANO, F., DICE, J. F., DIFIGLIA, M., DINESH-KUMAR, S., DISTELHORST, C. W., DJAVAHERIMERGNY, M., DORSEY, F. C., DROGE, W., DRON, M., DUNN, W. A., JR., DUSZENKO, M., EISSLER, N. T., ELAZAR, Z., ESCLATINE, A., ESKELINEN, E. L., FESUS, L., FINLEY, K. D., FUENTES, J. M., FUEYO, J., FUJISAKI, K., GALLIOT, B., GAO, F. B., GEWIRTZ, D. A., GIBSON, S. B., GOHLA, A., GOLDBERG, A. L., GONZALEZ, R., GONZALEZ-ESTEVEZ, C., GORSKI, S., GOTTLIEB, R. A., HAUSSINGER, D., HE, Y. W., HEIDENREICH, K., HILL, J. A., HOYER-HANSEN, M., HU, X., HUANG, W. P., IWASAKI, A., JAATTELA, M., JACKSON, W. T., JIANG, X., JIN, S., JOHANSEN, T., JUNG, J. U., KADOWAKI, M., KANG, C., KELEKAR, A., KESSEL, D. H., KIEL, J. A., KIM, H. P., KIMCHI, A., KINSELLA, T. J., KISELYOV, K., KITAMOTO, K., KNECHT, E., et al. (2008) Guidelines for the use and interpretation of assays for monitoring autophagy in higher eukaryotes. *Autophagy*, 4, 151-75.
- KNOWLES, A., KOH, K., WU, J. T., CHIEN, C. T., CHAMOVITZ, D. A. & BLAU, J. (2009) The COP9 signalosome is required for light-dependent timeless degradation and *Drosophila* clock resetting. *J Neurosci*, 29, 1152-62.
- KOBAYASHI, A., KANG, M. I., OKAWA, H., OHTSUJI, M., ZENKE, Y., CHIBA, T., IGARASHI, K. & YAMAMOTO, M. (2004) Oxidative stress sensor Keap1 functions as an adaptor for Cul3-based E3 ligase to regulate proteasomal degradation of Nrf2. *Mol Cell Biol*, 24, 7130-9.
- KOEPP, D. M., SCHAEFER, L. K., YE, X., KEYOMARSI, K., CHU, C., HARPER, J. W. & ELLEDGE, S. J. (2001) Phosphorylation-dependent ubiquitination of cyclin E by the SCFFbw7 ubiquitin ligase. *Science*, 294, 173-7.
- KUNATH, T., GISH, G., LICKERT, H., JONES, N., PAWSON, T. & ROSSANT, J. (2003) Transgenic RNA interference in ES cell-derived embryos recapitulates a genetic null phenotype. *Nat Biotechnol*, 21, 559-61.
- KURZ, T., CHOU, Y. C., WILLEMS, A. R., MEYER-SCHALLER, N., HECHT, M. L., TYERS, M., PETER, M. & SICHERI, F. (2008) Dcn1 functions as a scaffold-type E3 ligase for cullin neddylation. *Mol Cell*, 29, 23-35.
- KURZ, T., OZLU, N., RUDOLF, F., O'ROURKE, S. M., LUKE, B., HOFMANN, K., HYMAN, A. A., BOWERMAN, B. & PETER, M. (2005) The conserved protein DCN-1/Dcn1p is required for cullin neddylation in *C. elegans* and *S. cerevisiae*. *Nature*, 435, 1257-61.

- KWOK, S. F., SOLANO, R., TSUGE, T., CHAMOVITZ, D. A., ECKER, J. R., MATSUI, M. & DENG, X. W. (1998) Arabidopsis homologs of a c-Jun coactivator are present both in monomeric form and in the COP9 complex, and their abundance is differentially affected by the pleiotropic cop/det/fus mutations. *Plant Cell*, 10, 1779-90.
- LEUNG, S. K. & OHH, M. (2002) Playing Tag with HIF: The VHL Story. *J Biomed Biotechnol*, 2, 131-135.
- LEVINE, B. & KLIONSKY, D. J. (2004) Development by self-digestion: molecular mechanisms and biological functions of autophagy. *Dev Cell*, 6, 463-77.
- LI, J., WANG, Y., YANG, C., WANG, P., OELSCHLAGER, D. K., ZHENG, Y., TIAN, D. A., GRIZZLE, W. E., BUCHSBAUM, D. J. & WAN, M. (2009) Polyethylene glycosylated curcumin conjugate inhibits pancreatic cancer cell growth through inactivation of Jab1. *Mol Pharmacol*, 76, 81-90.
- LI, L. & DENG, X. W. (2003) The COP9 signalosome: an alternative lid for the 26S proteasome? *Trends Cell Biol*, 13, 507-9.
- LI, S., LIU, X. & ASCOLI, M. (2000) p38JAB1 binds to the intracellular precursor of the lutropin/choriogonadotropin receptor and promotes its degradation. *J Biol Chem*, 275, 13386-93.
- LIAKOPOULOS, D., DOENGES, G., MATUSCHEWSKI, K. & JENTSCH, S. (1998) A novel protein modification pathway related to the ubiquitin system. *Embo J*, 17, 2208-14.
- LIU, J., FURUKAWA, M., MATSUMOTO, T. & XIONG, Y. (2002) NEDD8 modification of CUL1 dissociates p120(CAND1), an inhibitor of CUL1-SKP1 binding and SCF ligases. *Mol Cell*, 10, 1511-8.
- LIU, Y., SHAH, S. V., XIANG, X., WANG, J., DENG, Z. B., LIU, C., ZHANG, L., WU, J., EDMONDS, T., JAMBOR, C., KAPPES, J. C. & ZHANG, H. G. (2009) COP9-Associated CSN5 Regulates Exosomal Protein Deubiquitination and Sorting. *Am J Pathol*.
- LOZZIO, C. B. & LOZZIO, B. B. (1975) Human chronic myelogenous leukemia cell-line with positive Philadelphia chromosome. *Blood*, 45, 321-34.
- LYAPINA, S., COPE, G., SHEVCHENKO, A., SERINO, G., TSUGE, T., ZHOU, C., WOLF, D. A., WEI, N., SHEVCHENKO, A. & DESHAIES, R. J. (2001) Promotion of NEDD-CUL1 conjugate cleavage by COP9 signalosome. *Science*, 292, 1382-5.
- LYKKE-ANDERSEN, K., SCHAEFER, L., MENON, S., DENG, X. W., MILLER, J. B. & WEI, N. (2003) Disruption of the COP9 signalosome Csn2 subunit in mice causes deficient cell proliferation, accumulation of p53 and cyclin E, and early embryonic death. *Mol Cell Biol*, 23, 6790-7.
- MANIATIS, T. (1999) A ubiquitin ligase complex essential for the NF-kappaB, Wnt/Wingless, and Hedgehog signaling pathways. *Genes Dev*, 13, 505-10.
- MCCALL, C. M., HU, J. & XIONG, Y. (2005) Recruiting substrates to cullin 4-dependent ubiquitin ligases by DDB1. *Cell Cycle*, 4, 27-9.
- MENON, S., CHI, H., ZHANG, H., DENG, X. W., FLAVELL, R. A. & WEI, N. (2007) COP9 signalosome subunit 8 is essential for peripheral T cell homeostasis and antigen receptor-induced entry into the cell cycle from quiescence. *Nat Immunol*, 8, 1236-45.

- MIN, K. W., HWANG, J. W., LEE, J. S., PARK, Y., TAMURA, T. A. & YOON, J. B. (2003) TIP120A associates with cullins and modulates ubiquitin ligase activity. *J Biol Chem*, 278, 15905-10.
- MIYAUCHI, Y., KATO, M., TOKUNAGA, F. & IWAI, K. (2008) The COP9/signalosome increases the efficiency of von Hippel-Lindau protein ubiquitin ligase-mediated hypoxia-inducible factor- α ubiquitination. *J Biol Chem*, 283, 16622-31.
- MIZUSHIMA, N. & YOSHIMORI, T. (2007) How to interpret LC3 immunoblotting. *Autophagy*, 3, 542-5.
- MOEHREN, U., DRESSEL, U., REEB, C. A., VAISANEN, S., DUNLOP, T. W., CARLBERG, C. & BANIAHMAD, A. (2004) The highly conserved region of the co-repressor Sin3A functionally interacts with the co-repressor Alien. *Nucleic Acids Res*, 32, 2995-3004.
- MOEHREN, U., PAPAIOANNOU, M., REEB, C. A., HONG, W. & BANIAHMAD, A. (2007) Alien interacts with the human androgen receptor and inhibits prostate cancer cell growth. *Mol Endocrinol*, 21, 1039-48.
- MORI, M., YONEDA-KATO, N., YOSHIDA, A. & KATO, J. Y. (2008) Stable form of JAB1 enhances proliferation and maintenance of hematopoietic progenitors. *J Biol Chem*, 283, 29011-21.
- MORIMOTO, M., NISHIDA, T., HONDA, R. & YASUDA, H. (2000) Modification of cullin-1 by ubiquitin-like protein Nedd8 enhances the activity of SCF(skp2) toward p27(kip1). *Biochem Biophys Res Commun*, 270, 1093-6.
- MUNDT, K. E., LIU, C. & CARR, A. M. (2002) Deletion mutants in COP9/signalosome subunits in fission yeast *Schizosaccharomyces pombe* display distinct phenotypes. *Mol Biol Cell*, 13, 493-502.
- MUNDT, K. E., PORTE, J., MURRAY, J. M., BRIKOS, C., CHRISTENSEN, P. U., CASPARI, T., HAGAN, I. M., MILLAR, J. B., SIMANIS, V., HOFMANN, K. & CARR, A. M. (1999) The COP9/signalosome complex is conserved in fission yeast and has a role in S phase. *Curr Biol*, 9, 1427-30.
- NAUJOKAT, C., SEZER, O., ZINKE, H., LECLERE, A., HAUPTMANN, S. & POSSINGER, K. (2000) Proteasome inhibitors induced caspase-dependent apoptosis and accumulation of p21WAF1/Cip1 in human immature leukemic cells. *Eur J Haematol*, 65, 221-36.
- NAUMANN, M., BECH-OTSCHIR, D., HUANG, X., FERRELL, K. & DUBIEL, W. (1999) COP9 signalosome-directed c-Jun activation/stabilization is independent of JNK. *J Biol Chem*, 274, 35297-300.
- NAYAK, S., SANTIAGO, F. E., JIN, H., LIN, D., SCHEDL, T. & KIPREOS, E. T. (2002) The *Caenorhabditis elegans* Skp1-related gene family: diverse functions in cell proliferation, morphogenesis, and meiosis. *Curr Biol*, 12, 277-87.
- OH, W., LEE, E. W., SUNG, Y. H., YANG, M. R., GHIM, J., LEE, H. W. & SONG, J. (2006a) Jab1 induces the cytoplasmic localization and degradation of p53 in coordination with Hdm2. *J Biol Chem*, 281, 17457-65.
- OH, W., YANG, M. R., LEE, E. W., PARK, K. M., PYO, S., YANG, J. S., LEE, H. W. & SONG, J. (2006b) Jab1 mediates cytoplasmic localization and degradation of West Nile virus capsid protein. *J Biol Chem*, 281, 30166-74.

- OHH, M., KIM, W. Y., MOSLEHI, J. J., CHEN, Y., CHAU, V., READ, M. A. & KAELIN, W. G., JR. (2002) An intact NEDD8 pathway is required for Cullin-dependent ubiquitylation in mammalian cells. *EMBO Rep*, 3, 177-82.
- OREN-GILADI, P., KRIEGER, O., EDGAR, B. A., CHAMOVITZ, D. A. & SEGAL, D. (2008) Cop9 signalosome subunit 8 (CSN8) is essential for Drosophila development. *Genes Cells*, 13, 221-31.
- ORON, E., MANNERVIK, M., RENCUS, S., HARARI-STEINBERG, O., NEUMAN-SILBERBERG, S., SEGAL, D. & CHAMOVITZ, D. A. (2002) COP9 signalosome subunits 4 and 5 regulate multiple pleiotropic pathways in Drosophila melanogaster. *Development*, 129, 4399-409.
- ORON, E., TULLER, T., LI, L., ROZOVSKY, N., YEKUTIELI, D., RENCUS-LAZAR, S., SEGAL, D., CHOR, B., EDGAR, B. A. & CHAMOVITZ, D. A. (2007) Genomic analysis of COP9 signalosome function in Drosophila melanogaster reveals a role in temporal regulation of gene expression. *Mol Syst Biol*, 3, 108.
- PANATTONI, M., SANVITO, F., BASSO, V., DOGLIONI, C., CASORATI, G., MONTINI, E., BENDER, J. R., MONDINO, A. & PARDI, R. (2008) Targeted inactivation of the COP9 signalosome impairs multiple stages of T cell development. *J Exp Med*, 205, 465-77.
- PAPAIOANNOU, M., MELLE, C. & BANIAHMAD, A. (2007) The coregulator Alien. *Nucl Recept Signal*, 5, e008.
- PATIL, M. A., GUTGEMANN, I., ZHANG, J., HO, C., CHEUNG, S. T., GINZINGER, D., LI, R., DYKEMA, K. J., SO, S., FAN, S. T., KAKAR, S., FURGE, K. A., BUTTNER, R. & CHEN, X. (2005) Array-based comparative genomic hybridization reveals recurrent chromosomal aberrations and Jab1 as a potential target for 8q gain in hepatocellular carcinoma. *Carcinogenesis*, 26, 2050-7.
- PATTON, E. E., WILLEMS, A. R., SA, D., KURAS, L., THOMAS, D., CRAIG, K. L. & TYERS, M. (1998) Cdc53 is a scaffold protein for multiple Cdc34/Skp1/F-box protein complexes that regulate cell division and methionine biosynthesis in yeast. *Genes Dev*, 12, 692-705.
- PAUSE, A., LEE, S., WORRELL, R. A., CHEN, D. Y., BURGESS, W. H., LINEHAN, W. M. & KLAUSNER, R. D. (1997) The von Hippel-Lindau tumor-suppressor gene product forms a stable complex with human CUL-2, a member of the Cdc53 family of proteins. *Proc Natl Acad Sci U S A*, 94, 2156-61.
- PAUSE, A., PETERSON, B., SCHAFFAR, G., STEARMAN, R. & KLAUSNER, R. D. (1999) Studying interactions of four proteins in the yeast two-hybrid system: structural resemblance of the pVHL/elongin BC/hCUL-2 complex with the ubiquitin ligase complex SKP1/cullin/F-box protein. *Proc Natl Acad Sci U S A*, 96, 9533-8.
- PENG, Z., SHEN, Y., FENG, S., WANG, X., CHITTETI, B. N., VIERSTRA, R. D. & DENG, X. W. (2003) Evidence for a physical association of the COP9 signalosome, the proteasome, and specific SCF E3 ligases in vivo. *Curr Biol*, 13, R504-5.
- PETH, A., BERNDT, C., HENKE, W. & DUBIEL, W. (2007a) Downregulation of COP9 signalosome subunits differentially affects the CSN complex and target protein stability. *BMC Biochem*, 8, 27.

- PETH, A., BOETTCHER, J. P. & DUBIEL, W. (2007b) Ubiquitin-dependent proteolysis of the microtubule end-binding protein 1, EB1, is controlled by the COP9 signalosome: possible consequences for microtubule filament stability. *J Mol Biol*, 368, 550-63.
- PETROSKI, M. D. & DESHAIES, R. J. (2003) Context of multiubiquitin chain attachment influences the rate of Sic1 degradation. *Mol Cell*, 11, 1435-44.
- PETROSKI, M. D. & DESHAIES, R. J. (2005) Function and regulation of cullin-RING ubiquitin ligases. *Nat Rev Mol Cell Biol*, 6, 9-20.
- PICK, E. & PINTARD, L. (2009) In the land of the rising sun with the COP9 signalosome and related Zomes. Symposium on the COP9 signalosome, Proteasome and eIF3. *EMBO Rep*, 10, 343-8.
- PICKART, C. M. (2004) Back to the future with ubiquitin. *Cell*, 116, 181-90.
- PINTARD, L., KURZ, T., GLASER, S., WILLIS, J. H., PETER, M. & BOWERMAN, B. (2003) Neddylation and deneddylation of CUL-3 is required to target MEI-1/Katanin for degradation at the meiosis-to-mitosis transition in *C. elegans*. *Curr Biol*, 13, 911-21.
- PINTARD, L., WILLEMS, A. & PETER, M. (2004) Cullin-based ubiquitin ligases: Cul3-BTB complexes join the family. *Embo J*, 23, 1681-7.
- PODUST, V. N., BROWNELL, J. E., GLADYSHEVA, T. B., LUO, R. S., WANG, C., COGGINS, M. B., PIERCE, J. W., LIGHTCAP, E. S. & CHAU, V. (2000) A Nedd8 conjugation pathway is essential for proteolytic targeting of p27Kip1 by ubiquitination. *Proc Natl Acad Sci U S A*, 97, 4579-84.
- POLLY, P., HERDICK, M., MOEHREN, U., BANIAHMAD, A., HEINZEL, T. & CARLBERG, C. (2000) VDR-Alien: a novel, DNA-selective vitamin D(3) receptor-corepressor partnership. *FASEB J*, 14, 1455-63.
- QI, C. F., XIANG, S., SHIN, M. S., HAO, X., LEE, C. H., ZHOU, J. X., TORREY, T. A., HARTLEY, J. W., FREDRICKSON, T. N. & MORSE, H. C., 3RD (2006) Expression of the cyclin-dependent kinase inhibitor p27 and its deregulation in mouse B cell lymphomas. *Leuk Res*, 30, 153-63.
- QIN, Z. X., CHEN, Q. J., TONG, Z. & WANG, X. C. (2005) The Arabidopsis inositol 1,3,4-trisphosphate 5/6 kinase, AtItpk-1, is involved in plant photomorphogenesis under red light conditions, possibly via interaction with COP9 signalosome. *Plant Physiol Biochem*, 43, 947-54.
- RAIMONDI, S. C., DUBE, I. D., VALENTINE, M. B., MIRRO, J., JR., WATT, H. J., LARSON, R. A., BITTER, M. A., LE BEAU, M. M. & ROWLEY, J. D. (1989) Clinicopathologic manifestations and breakpoints of the t(3;5) in patients with acute nonlymphocytic leukemia. *Leukemia*, 3, 42-7.
- READ, M. A., BROWNELL, J. E., GLADYSHEVA, T. B., HOTTELET, M., PARENT, L. A., COGGINS, M. B., PIERCE, J. W., PODUST, V. N., LUO, R. S., CHAU, V. & PALOMBELLA, V. J. (2000) Nedd8 modification of cul-1 activates SCF(beta(TrCP))-dependent ubiquitination of IkappaBalpha. *Mol Cell Biol*, 20, 2326-33.
- RICHARDSON, K. S. & ZUNDEL, W. (2005) The emerging role of the COP9 signalosome in cancer. *Mol Cancer Res*, 3, 645-53.
- ROSEL, D. & KIMMEL, A. R. (2006) The COP9 signalosome regulates cell proliferation of Dictyostelium discoideum. *Eur J Cell Biol*, 85, 1023-34.

- ROWLEY, J. D. (1980) Ph1-positive leukaemia, including chronic myelogenous leukaemia. *Clin Haematol*, 9, 55-86.
- SAKATA, E., YAMAGUCHI, Y., MIYAUCHI, Y., IWAI, K., CHIBA, T., SAEKI, Y., MATSUDA, N., TANAKA, K. & KATO, K. (2007) Direct interactions between NEDD8 and ubiquitin E2 conjugating enzymes upregulate cullin-based E3 ligase activity. *Nat Struct Mol Biol*, 14, 167-8.
- SAVINA, A., FURLAN, M., VIDAL, M. & COLOMBO, M. I. (2003) Exosome release is regulated by a calcium-dependent mechanism in K562 cells. *J Biol Chem*, 278, 20083-90.
- SAWYERS, C. L., HOCHHAUS, A., FELDMAN, E., GOLDMAN, J. M., MILLER, C. B., OTTMANN, O. G., SCHIFFER, C. A., TALPAZ, M., GUILHOT, F., DEININGER, M. W., FISCHER, T., O'BRIEN, S. G., STONE, R. M., GAMBACORTI-PASSERINI, C. B., RUSSELL, N. H., REIFFERS, J. J., SHEA, T. C., CHAPUIS, B., COUTRE, S., TURA, S., MORRA, E., LARSON, R. A., SAVEN, A., PESCHEL, C., GRATWOHL, A., MANDELLI, F., BEN-AM, M., GATHMANN, I., CAPDEVILLE, R., PAQUETTE, R. L. & DRUKER, B. J. (2002) Imatinib induces hematologic and cytogenetic responses in patients with chronic myelogenous leukemia in myeloid blast crisis: results of a phase II study. *Blood*, 99, 3530-9.
- SCHWECHHEIMER, C. (2004) The COP9 signalosome (CSN): an evolutionary conserved proteolysis regulator in eukaryotic development. *Biochim Biophys Acta*, 1695, 45-54.
- SCHWECHHEIMER, C., SERINO, G., CALLIS, J., CROSBY, W. L., LYAPINA, S., DESHAIES, R. J., GRAY, W. M., ESTELLE, M. & DENG, X. W. (2001) Interactions of the COP9 signalosome with the E3 ubiquitin ligase SCFTIR1 in mediating auxin response. *Science*, 292, 1379-82.
- SCHWEITZER, K., BOZKO, P. M., DUBIEL, W. & NAUMANN, M. (2007) CSN controls NF-kappaB by deubiquitylation of Ikbalpha. *EMBO J*, 26, 1532-41.
- SEEGER, M., KRAFT, R., FERRELL, K., BECH-OTSCHIR, D., DUMDEY, R., SCHADE, R., GORDON, C., NAUMANN, M. & DUBIEL, W. (1998) A novel protein complex involved in signal transduction possessing similarities to 26S proteasome subunits. *FASEB J*, 12, 469-78.
- SHACKA, J. J., KLOCKE, B. J., SHIBATA, M., UCHIYAMA, Y., DATTA, G., SCHMIDT, R. E. & ROTH, K. A. (2006) Bafilomycin A1 inhibits chloroquine-induced death of cerebellar granule neurons. *Mol Pharmacol*, 69, 1125-36.
- SHARON, M., MAO, H., BOERI ERBA, E., STEPHENS, E., ZHENG, N. & ROBINSON, C. V. (2009) Symmetrical modularity of the COP9 signalosome complex suggests its multifunctionality. *Structure*, 17, 31-40.
- SHIRAISHI, S., ZHOU, C., AOKI, T., SATO, N., CHIBA, T., TANAKA, K., YOSHIDA, S., NABESHIMA, Y., NABESHIMA, Y. & TAMURA, T. A. (2007) TBP-interacting protein 120B (TIP120B)/cullin-associated and neddylation-dissociated 2 (CAND2) inhibits SCF-dependent ubiquitination of myogenin and accelerates myogenic differentiation. *J Biol Chem*, 282, 9017-28.
- SIMPSON, M. V. (1953) The release of labeled amino acids from the proteins of rat liver slices. *J Biol Chem*, 201, 143-54.

- SMITH, P., LEUNG-CHIU, W. M., MONTGOMERY, R., ORSBORN, A., KUZNICKI, K., GRESSMAN-COBERLY, E., MUTAPCIC, L. & BENNETT, K. (2002) The GLH proteins, *Caenorhabditis elegans* P granule components, associate with CSN-5 and KGB-1, proteins necessary for fertility, and with ZYX-1, a predicted cytoskeletal protein. *Dev Biol*, 251, 333-47.
- STUTTMANN, J., LECHNER, E., GUEROIS, R., PARKER, J. E., NUSSAUME, L., GENSHIK, P. & NOEL, L. D. (2009) COP9 signalosome- and 26S Proteasome-dependent regulation of SCFTIR1 accumulation in Arabidopsis. *J Biol Chem*.
- SU, H., HUANG, W. & WANG, X. (2008) The COP9 signalosome negatively regulates proteasome proteolytic function and is essential to transcription. *Int J Biochem Cell Biol*.
- SU, H., HUANG, W. & WANG, X. (2009) The COP9 signalosome negatively regulates proteasome proteolytic function and is essential to transcription. *Int J Biochem Cell Biol*, 41, 615-24.
- SUMARA, I., QUADRONI, M., FREI, C., OLMA, M. H., SUMARA, G., RICCI, R. & PETER, M. (2007) A Cul3-based E3 ligase removes Aurora B from mitotic chromosomes, regulating mitotic progression and completion of cytokinesis in human cells. *Dev Cell*, 12, 887-900.
- SUN, Y., WILSON, M. P. & MAJERUS, P. W. (2002) Inositol 1,3,4-trisphosphate 5/6-kinase associates with the COP9 signalosome by binding to CSN1. *J Biol Chem*, 277, 45759-64.
- TENBAUM, S. P., JUENEMANN, S., SCHLITT, T., BERNAL, J., RENKAWITZ, R., MUNOZ, A. & BANIAHMAD, A. (2003) Alien/CSN2 gene expression is regulated by thyroid hormone in rat brain. *Dev Biol*, 254, 149-60.
- TENBAUM, S. P., PAPAIOANNOU, M., REEB, C. A., GOEMAN, F., ESCHER, N., KOB, R., VON EGGELING, F., MELLE, C. & BANIAHMAD, A. (2007) Alien inhibits E2F1 gene expression and cell proliferation. *Biochim Biophys Acta*, 1773, 1447-54.
- TOMODA, K., KATO, J. Y., TATSUMI, E., TAKAHASHI, T., MATSUO, Y. & YONEDA-KATO, N. (2005) The Jab1/COP9 signalosome subcomplex is a downstream mediator of Bcr-Abl kinase activity and facilitates cell-cycle progression. *Blood*, 105, 775-83.
- TOMODA, K., KUBOTA, Y., ARATA, Y., MORI, S., MAEDA, M., TANAKA, T., YOSHIDA, M., YONEDA-KATO, N. & KATO, J. Y. (2002) The cytoplasmic shuttling and subsequent degradation of p27Kip1 mediated by Jab1/CSN5 and the COP9 signalosome complex. *J Biol Chem*, 277, 2302-10.
- TOMODA, K., KUBOTA, Y. & KATO, J. (1999) Degradation of the cyclin-dependent-kinase inhibitor p27Kip1 is instigated by Jab1. *Nature*, 398, 160-5.
- TOMODA, K., YONEDA-KATO, N., FUKUMOTO, A., YAMANAKA, S. & KATO, J. Y. (2004) Multiple functions of Jab1 are required for early embryonic development and growth potential in mice. *J Biol Chem*, 279, 43013-8.
- TSUNEMATSU, R., NISHIYAMA, M., KOTOSHIBA, S., SAIGA, T., KAMURA, T. & NAKAYAMA, K. I. (2006) Fbxw8 is essential for Cul1-Cul7 complex formation and for placental development. *Mol Cell Biol*, 26, 6157-69.

- TSVETKOV, L. M., YEH, K. H., LEE, S. J., SUN, H. & ZHANG, H. (1999) p27(Kip1) ubiquitination and degradation is regulated by the SCF(Skp2) complex through phosphorylated Thr187 in p27. *Curr Biol*, 9, 661-4.
- UHLE, S., MEDALIA, O., WALDRON, R., DUMDEY, R., HENKLEIN, P., BECH-OTSCHIR, D., HUANG, X., BERSE, M., SPERLING, J., SCHADE, R. & DUBIEL, W. (2003) Protein kinase CK2 and protein kinase D are associated with the COP9 signalosome. *EMBO J*, 22, 1302-12.
- ULLAH, Z., BUCKLEY, M. S., ARNOSTI, D. N. & HENRY, R. W. (2007) Retinoblastoma protein regulation by the COP9 signalosome. *Mol Biol Cell*, 18, 1179-86.
- VERMA, R., ARAVIND, L., OANIA, R., MCDONALD, W. H., YATES, J. R., 3RD, KOONIN, E. V. & DESHAIES, R. J. (2002) Role of Rpn11 metalloprotease in deubiquitination and degradation by the 26S proteasome. *Science*, 298, 611-5.
- WANG, X., FENG, S., NAKAYAMA, N., CROSBY, W. L., IRISH, V., DENG, X. W. & WEI, N. (2003) The COP9 signalosome interacts with SCF UFO and participates in Arabidopsis flower development. *Plant Cell*, 15, 1071-82.
- WANG, X., KANG, D., FENG, S., SERINO, G., SCHWECHHEIMER, C. & WEI, N. (2002) CSN1 N-terminal-dependent activity is required for Arabidopsis development but not for Rub1/Nedd8 deconjugation of cullins: a structure-function study of CSN1 subunit of COP9 signalosome. *Mol Biol Cell*, 13, 646-55.
- WANG, Y., FEI, M., CHENG, C., ZHANG, D., LU, J., HE, S., ZHAO, Y., WANG, Y. & SHEN, A. (2008) Jun activation domain-binding protein 1 negatively regulate p27(kip1) in non-Hodgkin's lymphomas. *Cancer Biol Ther*, 7, 1-8.
- WANG, Y., LU, C., WEI, H., WANG, N., CHEN, X., ZHANG, L., ZHAI, Y., ZHU, Y., LU, Y. & HE, F. (2004) Hepatopoietin interacts directly with COP9 signalosome and regulates AP-1 activity. *FEBS Lett*, 572, 85-91.
- WEE, S., GEYER, R. K., TODA, T. & WOLF, D. A. (2005) CSN facilitates Cullin-RING ubiquitin ligase function by counteracting autocatalytic adapter instability. *Nat Cell Biol*, 7, 387-91.
- WEI, N., CHAMOVITZ, D. A. & DENG, X. W. (1994) Arabidopsis COP9 is a component of a novel signaling complex mediating light control of development. *Cell*, 78, 117-24.
- WEI, N. & DENG, X. W. (1992) COP9: a new genetic locus involved in light-regulated development and gene expression in arabidopsis. *Plant Cell*, 4, 1507-18.
- WEI, N. & DENG, X. W. (2003) The COP9 signalosome. *Annu Rev Cell Dev Biol*, 19, 261-86.
- WEISBERG, E., MANLEY, P. W., COWAN-JACOB, S. W., HOCHHAUS, A. & GRIFFIN, J. D. (2007) Second generation inhibitors of BCR-ABL for the treatment of imatinib-resistant chronic myeloid leukaemia. *Nat Rev Cancer*, 7, 345-56.
- WILKINSON, K. D., URBAN, M. K. & HAAS, A. L. (1980) Ubiquitin is the ATP-dependent proteolysis factor I of rabbit reticulocytes. *J Biol Chem*, 255, 7529-32.
- WILSON, M. P., SUN, Y., CAO, L. & MAJERUS, P. W. (2001) Inositol 1,3,4-trisphosphate 5/6-kinase is a protein kinase that phosphorylates the transcription factors c-Jun and ATF-2. *J Biol Chem*, 276, 40998-1004.

- WU, J. T., LIN, H. C., HU, Y. C. & CHIEN, C. T. (2005) Neddylation and deneddylation regulate Cul1 and Cul3 protein accumulation. *Nat Cell Biol*, 7, 1014-20.
- WU, K., CHEN, A. & PAN, Z. Q. (2000) Conjugation of Nedd8 to CUL1 enhances the ability of the ROC1-CUL1 complex to promote ubiquitin polymerization. *J Biol Chem*, 275, 32317-24.
- XU, L., WEI, Y., REBOUL, J., VAGLIO, P., SHIN, T. H., VIDAL, M., ELLEDGE, S. J. & HARPER, J. W. (2003) BTB proteins are substrate-specific adaptors in an SCF-like modular ubiquitin ligase containing CUL-3. *Nature*, 425, 316-21.
- YADA, M., HATAKEYAMA, S., KAMURA, T., NISHIYAMA, M., TSUNEMATSU, R., IMAKI, H., ISHIDA, N., OKUMURA, F., NAKAYAMA, K. & NAKAYAMA, K. I. (2004) Phosphorylation-dependent degradation of c-Myc is mediated by the F-box protein Fbw7. *Embo J*, 23, 2116-25.
- YAN, C. H., LIANG, Z. Q., GU, Z. L., YANG, Y. P., REID, P. & QIN, Z. H. (2006) Contributions of autophagic and apoptotic mechanisms to CrTX-induced death of K562 cells. *Toxicol*, 47, 521-30.
- YAN, J., WALZ, K., NAKAMURA, H., CARATTINI-RIVERA, S., ZHAO, Q., VOGEL, H., WEI, N., JUSTICE, M. J., BRADLEY, A. & LUPSKI, J. R. (2003) COP9 signalosome subunit 3 is essential for maintenance of cell proliferation in the mouse embryonic epiblast. *Mol Cell Biol*, 23, 6798-808.
- YAN, T., WUNDER, J. S., GOKGOZ, N., GILL, M., ESKANDARIAN, S., PARKES, R. K., BULL, S. B., BELL, R. S. & ANDRULIS, I. L. (2007) COPS3 amplification and clinical outcome in osteosarcoma. *Cancer*, 109, 1870-6.
- YANG, X., MENON, S., LYKKE-ANDERSEN, K., TSUGE, T., DI, X., WANG, X., RODRIGUEZ-SUAREZ, R. J., ZHANG, H. & WEI, N. (2002) The COP9 signalosome inhibits p27(kip1) degradation and impedes G1-S phase progression via deneddylation of SCF Cul1. *Curr Biol*, 12, 667-72.
- YARON, A., HATZUBAI, A., DAVIS, M., LAVON, I., AMIT, S., MANNING, A. M., ANDERSEN, J. S., MANN, M., MERCURIO, F. & BEN-NERIAH, Y. (1998) Identification of the receptor component of the IkappaBalpha-ubiquitin ligase. *Nature*, 396, 590-4.
- YONEDA-KATO, N., LOOK, A. T., KIRSTEIN, M. N., VALENTINE, M. B., RAIMONDI, S. C., COHEN, K. J., CARROLL, A. J. & MORRIS, S. W. (1996) The t(3;5)(q25.1;q34) of myelodysplastic syndrome and acute myeloid leukemia produces a novel fusion gene, NPM-MLF1. *Oncogene*, 12, 265-75.
- YONEDA-KATO, N., TOMODA, K., UMEHARA, M., ARATA, Y. & KATO, J. Y. (2005) Myeloid leukemia factor 1 regulates p53 by suppressing COP1 via COP9 signalosome subunit 3. *Embo J*, 24, 1739-49.
- YU, Z. K., GERVAIS, J. L. & ZHANG, H. (1998) Human CUL-1 associates with the SKP1/SKP2 complex and regulates p21(CIP1/WAF1) and cyclin D proteins. *Proc Natl Acad Sci U S A*, 95, 11324-9.
- ZHANG, D. D., LO, S. C., CROSS, J. V., TEMPLETON, D. J. & HANNINK, M. (2004) Keap1 is a redox-regulated substrate adaptor protein for a Cul3-dependent ubiquitin ligase complex. *Mol Cell Biol*, 24, 10941-53.
- ZHENG, J., YANG, X., HARRELL, J. M., RYZHIKOV, S., SHIM, E. H., LYKKE-ANDERSEN, K., WEI, N., SUN, H., KOBAYASHI, R. & ZHANG, H. (2002a)

- CAND1 binds to unneddylated CUL1 and regulates the formation of SCF ubiquitin E3 ligase complex. *Mol Cell*, 10, 1519-26.
- ZHENG, N., SCHULMAN, B. A., SONG, L., MILLER, J. J., JEFFREY, P. D., WANG, P., CHU, C., KOEPP, D. M., ELLEDGE, S. J., PAGANO, M., CONAWAY, R. C., CONAWAY, J. W., HARPER, J. W. & PAVLETICH, N. P. (2002b) Structure of the Cul1-Rbx1-Skp1-F boxSkp2 SCF ubiquitin ligase complex. *Nature*, 416, 703-9.
- ZHOU, C., WEE, S., RHEE, E., NAUMANN, M., DUBIEL, W. & WOLF, D. A. (2003) Fission yeast COP9/signalosome suppresses cullin activity through recruitment of the deubiquitylating enzyme Ubp12p. *Mol Cell*, 11, 927-38.

Research article

Open Access

Analysis of the role of COP9 Signalosome (CSN) subunits in K562; the first link between CSN and autophagy

Claire Pearce, Rachel E Hayden, Christopher M Bunce and Farhat L Khanim*

Address: College of Life and Environmental Sciences, School of Biosciences, University of Birmingham, Edgbaston, Birmingham, B15 2TT, UK

Email: Claire Pearce - CXP263@bham.ac.uk; Rachel E Hayden - R.E.Hayden@bham.ac.uk; Christopher M Bunce - C.M.Bunce@bham.ac.uk; Farhat L Khanim* - F.L.Khanim@bham.ac.uk

* Corresponding author

Published: 28 April 2009

Received: 8 July 2008

BMC Cell Biology 2009, 10:31 doi:10.1186/1471-2121-10-31

Accepted: 28 April 2009

This article is available from: <http://www.biomedcentral.com/1471-2121/10/31>

© 2009 Pearce et al; licensee BioMed Central Ltd.

This is an Open Access article distributed under the terms of the Creative Commons Attribution License (<http://creativecommons.org/licenses/by/2.0>), which permits unrestricted use, distribution, and reproduction in any medium, provided the original work is properly cited.

Abstract

Background: The COP9/signalosome (CSN) is a highly conserved eight subunit complex that, by deneddylating cullins in cullin-based E3 ubiquitin ligases, regulates protein degradation. Although studied in model human cell lines such as HeLa, very little is known about the role of the CSN in haemopoietic cells.

Results: Greater than 95% knockdown of the non-catalytic subunit CSN2 and the deneddylating subunit CSN5 of the CSN was achieved in the human myeloid progenitor cell line K562. CSN2 knockdown led to a reduction of both CSN5 protein and mRNA whilst CSN5 knockdown had little effect on CSN2. Both knockdowns inhibited CSN deneddylase function as demonstrated by accumulation of neddylated Cull. Furthermore, both knockdowns resulted in the sequential loss of Skp2, Cdc4 and β -TrCP F-box proteins. These proteins were rescued by the proteasome inhibitor MG132, indicating the autocatalytic degradation of F-box proteins upon loss of CSN2 or CSN5. Interestingly, altered F-box protein gene expression was also observed in CSN2 and CSN5 knockdowns, suggesting a potential role of the CSN in regulating F-box protein transcription.

Loss of either CSN subunit dramatically reduced cell growth but resulted in distinct patterns of cell death. CSN5 knockdown caused mitotic defects, G2/M arrest and apoptotic cell death. CSN2 knockdown resulted in non-apoptotic cell death associated with accumulation of both the autophagy marker LC3-II and autophagic vacuoles. Treatment of vector control K562 cells with the autophagy inhibitors 3-methyladenine and bafilomycin A1 recapitulated the growth kinetics, vacuolar morphology and LC3-II accumulation of CSN2 knockdown cells indicating that the cellular phenotype of CSN2 cells arises from autophagy inhibition. Finally, loss of CSN2 was associated with the formation of a CSN5 containing subcomplex.

Conclusion: We conclude that CSN2 is required for CSN integrity and the stability of individual CSN subunits, and postulate that CSN2 loss results in a phenotype distinct from that of cells lacking CSN5 possibly as a consequence of altered CSN5 activity within a resultant CSN subcomplex. Our data present the first evidence for the sequential loss of F-box proteins upon CSN manipulation and are the first to identify a potential link between CSN function and autophagy.

Background

The regulated expression and degradation of proteins are critical to all aspects of cell development and proliferation. The two main routes for eukaryotic intracellular protein clearance are the ubiquitin-proteasome system (UPS) and the autophagy-lysosome pathway. A key component involved in regulating degradation of proteins by the UPS is the COP9 signalosome (CSN). The CSN is an eight-subunit (CSN1-8) protein complex, highly conserved amongst eukaryotes [1-5] originally identified in *Arabidopsis* as a negative regulator of photomorphogenesis [6]. Through its function in the regulation of the UPS, the CSN has been implicated in the regulation of biological processes as diverse as DNA replication and repair, cell-cycle progression and cell development [7-9].

Degradation of cellular proteins by the 26S proteasome [10-13] is preceded by ubiquitination of target proteins [14], a process mediated by three enzyme complexes; a ubiquitin activating enzyme (E1), a ubiquitin conjugating enzyme (E2) and a ubiquitin ligase (E3) [15]. The E3 ligase interacts with the protein substrate and thus confers the specificity of the UPS [16]. The largest known class of E3 ubiquitin ligases comprises the Cullin-RING ligases (CRLs) of which the best studied is the SCF (Skp1, Cul1, F-box protein) complex [16]. The cullin subunit (Cul1) of the SCF forms a scaffold to recruit and bring into close proximity the E2 and its substrate, thereby facilitating ubiquitin transfer from the E2 to target proteins (SCF structure reviewed in [16]). The RING protein (Hrt1/Roc1/Rbx1) is the fourth subunit of the SCF and is responsible for E2 recruitment, whilst the variable F-box protein subunit, recruited to the SCF complex via the adaptor protein Skp1, binds substrates selectively [17-19]. In yeast, over 19 F-box proteins are known, over 400 in *A. thaliana*, and ~70 in humans [16]. Since each cullin (Cul1-5) forms complexes with a variable substrate recognition subunit (SRS) (F-box proteins for Cul1 as above, VHL box proteins for Cul2, BTB proteins for Cul3, WD40 proteins for Cul4 and SOCS box proteins for Cul5, reviewed in [20]) specificity in CRL target protein recruitment is achieved by the large number of variable SRS containing CRLs. It is thought that, altogether, the human genome may have the capacity to code for as many as 350 different CRLs.

Given the potential number and diversity of target proteins requiring CRL mediated ubiquitination for degradation, dynamic regulation of the CRL complex repertoire in a cell at any given time is essential. All cullins studied (Cul1-5) have been shown to be modified by neddylation [21], which facilitates their ubiquitin ligase activity [22] possibly via increased E2 affinity [23,24]. The deneddylation of cullins is mediated by the CSN complex [25]. Although initial studies indicated a negative role for deneddylation, further studies have implicated dened-

dylation in the positive regulation of CRL activity [3,4,26]. It has since been proposed by several groups that optimal CRL activity requires the cyclic neddylation and deneddylation of the cullin subunit [4,7,27]. Although the exact mechanisms are not fully understood, it is thought that F-box proteins themselves are targeted for degradation in part by autoubiquitination within the SCF complex [28]. The deneddylation of cullins by the CSN is believed to regulate the autoubiquitination of SRSs [28,29], thereby modulating CRL composition and activity. Furthermore, the CSN has been shown to be associated with a deubiquitinase activity which may further stabilize autoubiquitinated SRSs [27,29]. The CSN complex is therefore an integral regulator of CRL activity and subsequent protein degradation.

In this present study we have investigated the effects of knocking down CSN2 and CSN5 in the model K562 cell line, a model of human erythrocyte and megakaryocyte progenitors [30,31]. Whilst knockdown of either CSN2 or CSN5 resulted in common changes including the sequential loss of F-box proteins Skp2, Cdc4 and β -TrCP other important differences occurred. For example CSN5 knockdown resulted in apoptotic cell death associated with aberrant mitosis, whereas CSN2 knockdown cells underwent non-apoptotic cell death that was associated with both inhibition of autophagy and the formation of a novel CSN5 containing CSN subcomplex.

Results

CSN2 and CSN5 knockdown and resulting aberrant SCF activity

Plasmids encoding short hairpin RNA (shRNA) to either CSN2 or CSN5 were electroporated into K562 cells together with H-2K^k plasmid and transfected cells sorted by anti- H-2K^k magnetic beads. Three days post transfection, neither CSN2 nor CSN5 protein could be detected by western blot analysis in their respective knockdown protein extracts (Fig. 1A). Furthermore, CSN2 knockdown of over 99% and CSN5 knockdown of over 95% was achieved at the mRNA level relative to mock transfectants as measured by quantitative real-time PCR (QRT-PCR) (Fig. 1B). This level of knockdown was maintained throughout the time course of the experiments (data not shown). Transfection with either the H-2K^k plasmid alone or co-transfection with H-2K^k plasmid and empty vector (shVC) had no effect on the level of CSN2 or CSN5 mRNA or protein relative to mock transfected cells (Fig. 1A & 1B and data not shown). Co-transfections with H-2K^k and a vector encoding a control scrambled shRNA sequence had no effect on the level of CSN2 or CSN5 mRNA or protein relative to cells co-transfected with empty vector (Additional file 1), demonstrating that the results were specific and not due to off-target effects.

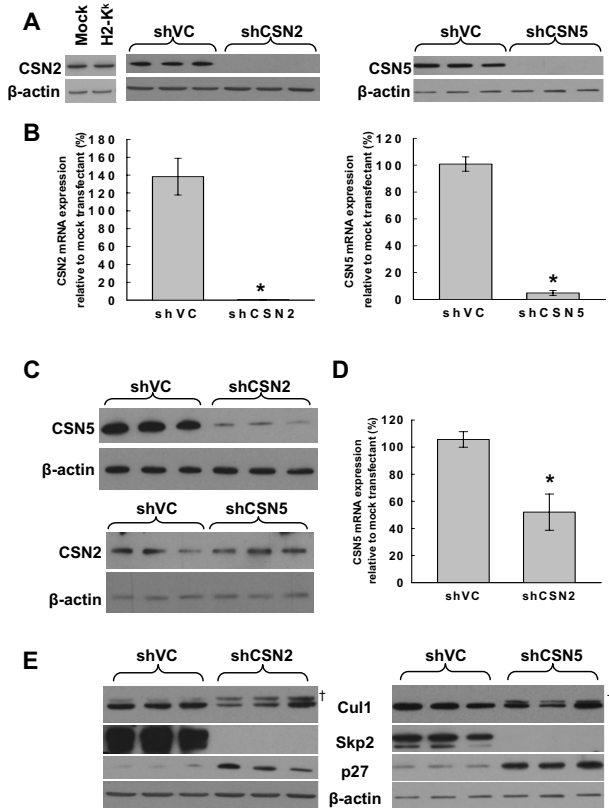


Figure 1
CSN2 and CSN5 knockdowns result in Cul-1 hyper-neddylation, loss of Skp-2 and accumulation of p27. K562 cells were transiently transfected in the absence of plasmid DNA (mock), with pMACS K^k.II plasmid alone (HKK) or transiently co-transfected with HKK plasmid together with either vector control (shVC), CSN2 knockdown (shCSN2) or CSN5 knockdown (shCSN5) plasmid. HKK positive cells were sorted 24 hours post-transfection, re-cultured and harvested for analysis. (A) CSN2 (left) and CSN5 (right) protein knockdown was determined by western blot in three independent transfectants. (B) mRNA levels in vector control and knockdown cells were determined by QRT-PCR (CSN2, left, $P = 0.0012$; CSN5, right, $P = 0.000031$). Data represents 3 independent sets of triplicate transfections. (C) CSN5 and CSN2 protein levels were determined by western blot in $n = 3$ CSN2 (top) and CSN5 (bottom) knockdowns, respectively. (D) CSN5 mRNA levels in $n = 3$ vector control and CSN2 knockdown cells were determined by QRT-PCR ($P = 0.011$). (E) The level of Cul1 neddylation (top panels, † indicates neddylated Cul-1), Skp2 protein (second panels) and p27 protein (third panels) was determined in $n = 3$ shCSN2 (left) and shCSN5 (right) samples by western blot. Even gel loading was determined by β -actin signal. Graphical data indicates the mean \pm s.e.m. * indicates significance with a p value of less than 0.05.

The instability of particular CSN subunits in the absence of another subunit has been reported previously. For example, CSN8 knockdown has been shown to result in the loss of CSN3, CSN5 and CSN7 protein [32]. We therefore determined CSN5 and CSN2 protein levels in CSN2 and CSN5 knockdown cells, respectively, by western blotting. A significant reduction in CSN5 protein was observed in cells lacking CSN2, whilst depletion of CSN5 had no effect on CSN2 protein or mRNA levels relative to vector control cells (Fig. 1C and data not shown). Interestingly, CSN2 knockdown not only resulted in loss of CSN5 protein, but also in the significant reduction of CSN5 mRNA as determined by QRT-PCR (Fig. 1D, $P = 0.011$).

Consistent with previous studies of CSN deregulation [28,33], both CSN2 and CSN5 knockdowns were associated with accumulation of neddylated Cul1 (Fig. 1E) indicating functional dysregulation of the CSN following knockdown of either subunit. Studies demonstrating Cul1 hyperneddylation in CSN deficient cells have also demonstrated degradation of the F-box protein Skp2 [28,33]. In agreement with these observations, complete loss of Skp2 protein was observed in both the CSN2 and CSN5 knockdown cells (Fig. 1E). Skp2 binds to and mediates the ubiquitination of multiple proteins, including the cyclin dependent kinase inhibitor p27^{kip1} [34]. Consistent with loss of Skp2, knockdown of CSN2 and CSN5 resulted in the accumulation of p27 (Fig. 1E).

Loss of CSN2 and CSN5 results in the sequential loss of F-box proteins

Skp2 is one of many F-box proteins that can bind to the Cul1/Roc1/Skp1 complex, thereby altering the substrate specificity of the SCF (F-box proteins reviewed in [19]). Analysis of three such F-box proteins, Skp2, Cdc4 and β -TrCP revealed a sequential loss of protein in CSN2 and CSN5 knockdown cells (Fig. 2A & 2B and Additional file 1, part D). In CSN2 knockdown cells, Skp2 protein was reduced by $\sim 60\%$ by day 2 and over 90% by day 6, whereas Cdc4 was lost at a slower rate with 30–40% lost by day 3 increasing to $\sim 70\%$ by day 6 (Fig. 2B). Loss of β -TrCP was still more retarded with $\sim 70\%$ protein remaining at day 6 (Fig. 2B). By day 9, all three F-box proteins were undetectable in CSN2 knockdown cells (Fig. 2A). Similar sequential loss of F-box proteins was observed in CSN5 knockdown cells. At day 4 post transfection Skp2 protein could not be detected, Cdc4 protein was greatly reduced but remained detectable, and β -TrCP was largely unaffected (Additional file 1, part D).

In order to determine the mechanism of F-box protein loss in both CSN2 and CSN5 knockdown cells, we investigated the rescue of F-box proteins by the proteasome

inhibitor MG132 (Fig. 2C) and measured the levels of F-box mRNA over time (Fig. 2D & 2E). Treatment of both CSN2 and CSN5 knockdown cells with MG132 resulted in Skp2, Cdc4 and β -TrCP protein rescue (Fig. 2C), indicating involvement of the proteasome in the loss of these F-box proteins. However the strength of the observed rescue varied. Importantly, CSN subunit depletion also affected levels of F-box mRNA. CSN2 knockdown resulted in a significant reduction of Skp2 mRNA by day 2 post transfection. Thus it is likely that transcriptional changes also contribute to loss of Skp2 protein in these cells. In contrast Cdc4 and β -TrCP mRNAs were significantly increased following CSN2 knockdown despite clear loss of protein (Fig. 2D). CSN5 depletion resulted in a modest reduction of all three F-box protein mRNAs but not enough to account for the observed loss of protein (Fig. 2E). Collectively these data indicate that, with the possible exception of Skp2 in CSN2 knockdown cells, proteasomal degradation rather than transcriptional repression was the main driver of F-box protein loss in CSN2 and CSN5 knockdown K562 cells.

Both CSN2 and CSN5 knockdowns result in reduced cell growth and cell death

Knockdown of either CSN2 or CSN5 dramatically diminished cell proliferation, followed by loss of cell viability (Fig. 3A). Analysis of cumulative growth demonstrated that proliferation of cells lacking CSN2 was significantly reduced when compared to that of shVC cells by day 4 post transfection (Fig. 3A, $P = 0.034$), whilst loss of proliferation following CSN5 knockdown was even more marked (Fig. 3A insert, $P = 0.0023$). This difference in diminished proliferation was corroborated by measurement of thymidine incorporation. At day 3 post-transfection, there was no significant difference in the incorporation of tritiated thymidine into cellular DNA between shVC and CSN2 knockdown (Fig. 3B) whereas the CSN5 knockdown cells already had markedly reduced thymidine incorporation (Fig. 3C, $P = 0.0012$). However, by day 5 the CSN2 knockdown cells also had a significant decrease in thymidine incorporation (Fig. 3B, $P = 0.0072$) which decreased even further by day 7 ($P = 1.1 \times 10^{-5}$). Thus, although the changes in Cul1 neddylation and F-box protein levels are very similar between the CSN2 and CSN5 knockdowns, differences were apparent in the growth kinetics of the cells.

Knockdown of CSN5 but not CSN2 is associated with cell cycle arrest and defects in mitotic spindle formation

Cell cycle analyses revealed striking differences between the profiles of CSN2 and CSN5 knockdown cells. Despite leading to significantly reduced cell proliferation, loss of CSN2 did not affect the cell cycle distribution of K562 cells as compared to shVC K562 cells by day 6 post transfection (Fig. 4A). Given the significantly reduced cell numbers in CSN2 knockdown by day 6, this would sug-

gest that these cells are growing more slowly, rather than arresting at any stage in the cell cycle. In contrast, CSN5 knockdown resulted in a reduction in cells in G1 (25.7% compared to shVC 35.5%, $P = 0.0044$), loss of cells from S phase (21% compared to shVC 45.7%, $P = 3.4 \times 10^{-5}$) and accumulation in G2/M (33.5% compared to shVC 15.7%, $P = 0.0011$) by day 4 post transfection (Fig. 4A). Morphological analysis of Jenner-Giemsa stained CSN5 knockdown cells identified a significant number of large cells which appeared to be arrested in late mitosis with chaotically organized condensed chromosomes (Fig. 4B). Cells of these morphologies were not observed in either shVC (Fig. 4B) or CSN2 knockdown (Fig. Six A) cells. To investigate this morphology further, shCSN5 cells were immunostained for tubulin. As can be seen in Fig. 4C, shVC cells retained the ability to form a mitotic spindle and correctly aligned chromosomes at various stages of mitosis were observed. In striking contrast, cells lacking CSN5 demonstrated either aberrant or absent microtubule structures. In these cells, the condensed chromatids appeared to be either misaligned or indeed not associated with the spindle structures at all (Fig. 4C). This aberrant cellular phenotype is in accordance with cell cycle arrest at G2/M.

Knockdown of CSN5 but not CSN2 results in apoptotic cell death

In order to determine whether the subsequent loss of viability in CSN2 and CSN5 knockdown cells was due to apoptosis, cells were co-analysed for annexin V staining and propidium iodide uptake day 7 and day 6 post transfection, respectively (Fig. 5A). Annexin V binds phosphatidylserine, a phospholipid which is translocated from the inner to the outer leaflet of the plasma membrane during early apoptosis. Propidium iodide is taken up by all cells but is efficiently effluxed by viable cells, whereas dead/dying cells remain PI-positive. In accordance with the marked increase in the sub-G1 fraction of shCSN5 cells (Fig. 4A), knockdown of CSN5 lead to significant increases in both early apoptotic (annexin V⁺PI^{-ve}) ($21.9 \pm 1.8\%$, $P = 0.0015$) and late apoptotic (annexin V⁺PI⁺) cells ($42.3 \pm 2.5\%$, $P = 0.0006$) compared to shVC cells ($5.9 \pm 1.9\%$ and $5.5 \pm 2.2\%$, respectively; Fig. 5A). Furthermore, CSN5 knockdown cells demonstrated cleavage of caspase 9 (Fig. 5B), consistent with death by apoptosis in these cells. In marked contrast, CSN2 knockdown showed only a relatively small increase in annexin V positive cells ($5.5 \pm 0.8\%$ and $12.5 \pm 0.9\%$, respectively; Fig. 5A) and no caspase 9 activation (Fig. 5B). Instead, the CSN2 knockdown cells demonstrated increased retention of PI in the annexin V^{-ve} cell population (Fig. 5C, $P = 3.3 \times 10^{-5}$). This large shift in PI single-positivity relative to shVCs was not observed in CSN5 knockdown cells (Fig. 5A & 5C). Thus knockdown of CSN2 in K562 cells did not result in overt apoptosis. Taken together these data indicate that knockdown in K562 cells of CSN5, but not

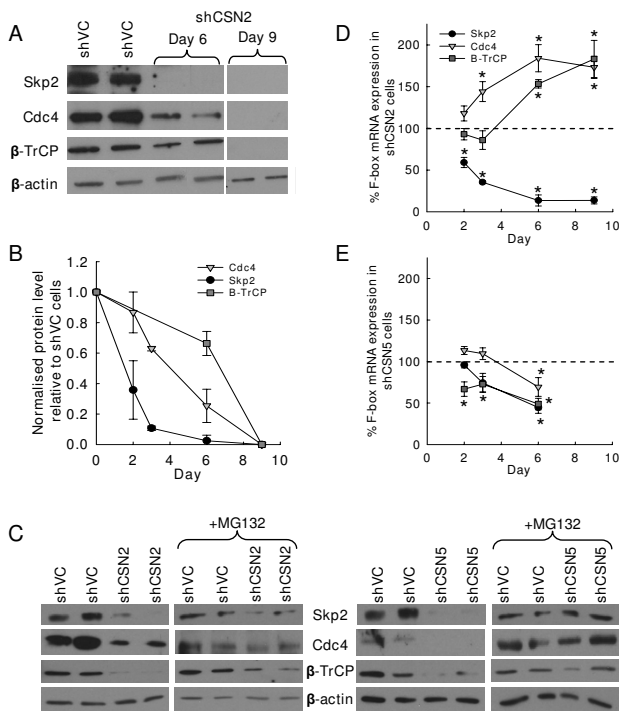


Figure 2
Loss of CSN2 and CSN5 results in sequential loss of F-box proteins. K562 cells were transiently co-transfected with HKK plasmid together with either shVC, shCSN2 or shCSN5 plasmid. HKK positive cells were sorted 24 hours post-transfection and cells re-cultured. (A) shVC and shCSN2 cells were harvested day 6 and 9 post transfection and the level of Skp2, Cdc4, β -TrCP and β -actin protein determined by western blot. (B) The level of Skp2, Cdc4 and β -TrCP proteins (normalised for loading using β -actin) in shCSN2 at each time point was normalised to expression in shVC cells and the data plotted as the mean \pm s.e.m. (C) shVC, shCSN2 and shCSN5 cells were treated with DMSO (control) or the proteasome inhibitor MG132 (10 μ M) for the final 18 hours of culturing and the level of Skp-2, Cdc4, β -TrCP and β -actin protein determined by western blot. (D, E) The level of Skp2, Cdc4 and β -TrCP mRNA in shCSN2 (D) and shCSN5 (E) cells was determined at each time point post transfection relative to expression in vector control scramble cells by QRT-PCR. Data shown is the mean \pm s.e.m of n = 3 transfections. * indicates a significant difference to vector controls with a p value of less than 0.05.

CSN2, resulted in apoptotic cell death and that loss of cell viability in the CSN2 knockdowns was likely to be by a non-apoptotic mechanism.

CSN2 but not CSN5 knockdown is associated with autophagy

Whilst culturing the transfectants, marked differences in cell morphology were noted in the CSN2 knockdown cells. Jenner-Giemsa staining of cytopspins identified large

vacuoles in a significant proportion of CSN2 knockdown cells which were not present in either shVC or shCSN5 cells (Fig. 6A). Staining with the autophagosome/autophagic vacuole marker monodansylcadaverine (MDC, [35]) identified these large vacuoles as autophagic bodies (Fig. 6B). Moreover, western blotting identified a highly significant accumulation of the autophagy associated LC3-II protein [36] in CSN2 knockdown cells relative to shVC cells (Fig. 6C). In contrast, no increase of LC3-II was detected in CSN5 knockdown cells. To demonstrate this we used a prolonged exposure (12 hours) of autoradiographs that allowed detection of basal expression of LC3-II in shVC cells and demonstrated that this was not increased in shCSN5 knockdown cells (Fig. 6C). Thus, knockdown of CSN2, but not CSN5, appeared strongly associated with autophagy. However, LC3-II accumulation can occur as a result of either enhanced autophagy or inhibition of autophagy dependant LC3-II degradation [37]. Indeed, treatment of vector control cells with the autophagy inhibitor 3-methyladenine (3-MA) resulted in a growth pattern almost identical to that of shCSN2 cells, whilst having a relatively small additional effect on shCSN2 cells (Fig. 6D). Furthermore, treatment of vector control cells with the late stage autophagy inhibitor bafilomycin A1 recapitulated both the vacuolar morphology (Fig. 6E) and the LC3-II protein accumulation (Fig. 6F) observed in cells lacking CSN2 (Fig. 6A & 6C). These observations suggest that CSN2 knockdown is associated with the inhibition of autophagy.

Loss of CSN2 results in the formation of an alternative CSN5 containing complex

The above data indicate that knockdown of CSN2 or CSN5 in K562 cells results in common derangement of SCF activity as measured by accumulation of hypernedylated Cul1, accumulation of p27 and the sequential loss of Skp-2, cdc4 and β -TrCP. However, the cellular responses to CSN2 or CSN5 knockdown were markedly different. Since it has previously been shown that depletion of individual subunits can destabilize the CSN holocomplex [38-40] we reasoned that one explanation for the differences between CSN2 and CSN5 knockdown cellular responses may be due to the generation, in CSN2 knockdowns, of CSN5 containing CSN subcomplexes with altered activities. To investigate this, 2-dimensional native gel electrophoresis was performed on knockdown cells day 3 post transfection (Fig. 7).

Immunoblotting of extracts from shVC cells with either CSN2 or CSN5 antibody identified 2 major complexes, one of approximately 500 KDa, correlating in size with the CSN holocomplex, and the second of 750 KDa (Fig. 7A & 7B). A multitude of proteins have been shown to associate with CSN subunits [41] and larger complexes have previously been observed. Monomeric CSN2 and CSN5 were also observed in the shVC cell extracts (Fig. 7C

and data not shown). Following knockdown of CSN2, CSN2 protein was no longer detectable (Fig. 7A). CSN5 protein, as also shown in Fig. 1C, was greatly reduced in cells lacking CSN2, with significant loss of the CSN complex relative to vector controls (Fig. 7B). Interestingly, a longer exposure of the autoradiograph identified a CSN5 containing subcomplex of ~242 KDa in cells lacking CSN2 (Fig. 7C).

Discussion

The achievement of almost complete CSN2 and CSN5 knockdown in this study has provided a powerful tool to study the function of these CSN subunits more closely. At the molecular level, CSN2 and CSN5 knockdowns resulted in aberrant SCF activity, with the accumulation of neddylated Cul-1, loss of the F-box protein Skp2 and an increase in the Skp2 target protein, p27. This complements another report in which CSN4 and CSN5 knockdown also resulted in increased neddylation of Cul-1 with a concomitant loss of Skp2 and increase in p27 protein in human epithelial cell lines rather than haemopoietic cells [33]. Thus it appears that the CSN complex has highly conserved activities across cells from different cell lineages and that disruption of the complex by loss of any subunit causes derangement of these activities.

It was also observed that CSN2 knockdown not only results in loss of CSN5 protein but also results in a significant reduction of CSN5 mRNA. Moreover, both CSN2 and CSN5 knockdown resulted in temporal alterations of F-box protein mRNA. Together with other recent reports [32,42], this data suggests that CSN subunits or the CSN complex as a whole may have a direct role in transcriptional regulation of CSN subunits and F-box proteins. However, it is also possible that the altered mRNA levels observed are due to secondary effects of aberrant CRL mediated protein degradation such as accumulation of proteins involved in transcriptional regulation.

Here we show for the first time sequential loss of F-box proteins following knockdown of CSN subunits. Moreover, protein levels were at least partially restored in both knockdowns upon treatment with the proteasome inhibitor MG132. These observations are in accordance with the finding that F-box proteins are autocatalytically degraded in the presence of hyperneddylated Cul-1 [28]. However, the three F-box proteins studied were each lost at a different rate, with the loss of Skp2 protein being the most rapid. The sequential loss of F-box proteins is of great interest as it may explain published results which document the loss of particular F-box proteins at a specific time point post CSN manipulation, but no reduction in other F-box proteins [28,32].

The CSN5 knockdown cultures contained aberrantly large cells and were associated with G2/M arrest and apoptosis.

This data complements previous studies demonstrating that CSN5 loss inhibits proliferation and induces apoptosis [43-45]. Closer analysis of CSN5 knockdown cells identified disorganized condensed chromatids and abnormal mitotic spindles in the large cells. A recent report described stabilization of the microtubule end-binding protein 1 (EB1) by the CSN complex in human cells [46]. EB1, which is a master regulator of microtubule dynamics, was shown to bind the CSN via CSN5, and was also shown to be reduced in cells lacking CSN1 or CSN3 [46]. EB1 has recently been shown to directly interact with and regulate the activity of Aurora B, one essential component of the chromosomal passenger complex that is required for correct chromosomal alignment and spindle assembly checkpoint [47,48]. Furthermore, the dynamic behaviour of Aurora B on mitotic chromosomes has been shown to be regulated by a Cul3 E3 ligase [48]. Given that we observed hyperneddylated Cul3 in the CSN5 knockdown cells (data not shown), our data suggests that CSN5/the CSN complex is integral to the regulation of multiple components of the mitotic machinery.

K562 cells in which CSN2 had been knocked down did not display apoptosis markers as in CSN5 knockdown cells, but were instead associated with features of autophagy. Interestingly, autophagy inhibitors recapitulated the cell growth kinetics, vacuolar morphology and LC3-II accumulation of cells lacking CSN2, whilst treatment of CSN2 knockdown cells with one of these inhibitors (3-MA) had a comparatively mild effect on cell growth. These findings suggest that CSN2 knockdown K562 cells undergo autophagy inhibition resulting in non-apoptotic cell death. This is the first data to show an association between the CSN complex and autophagy.

The distinct phenotypes observed between CSN2 and CSN5 knockdowns may arise as a result of aberrant CSN5 activity within the observed CSN subcomplex in cells lacking CSN2. However, it is important to note that both the CSN subunits studied here have CSN independent functions [49-54], and that CSN5 has been shown to function within a CSN subcomplex in K562 [55]. Therefore, we cannot rule out the possible contribution of the independent functions of CSN2 and CSN5 to the phenotypic differences observed between the knockdowns. It is also noteworthy that the subcomplex observed in this study may be a result of CSN complex breakdown in the absence of CSN2 [54], rather than a functional complex contributing to the observed phenotypic differences between knockdowns. Moreover, as we see no effect of CSN5 loss on the level of CSN2 protein, one possibility not investigated here is the formation of a CSN2 containing subcomplex in the absence of CSN5. This is an intriguing possibility, particularly given the recent findings of Su et al who demonstrated an increase in the proportion of CSN2 residing in mini-complexes upon CSN8 knock-

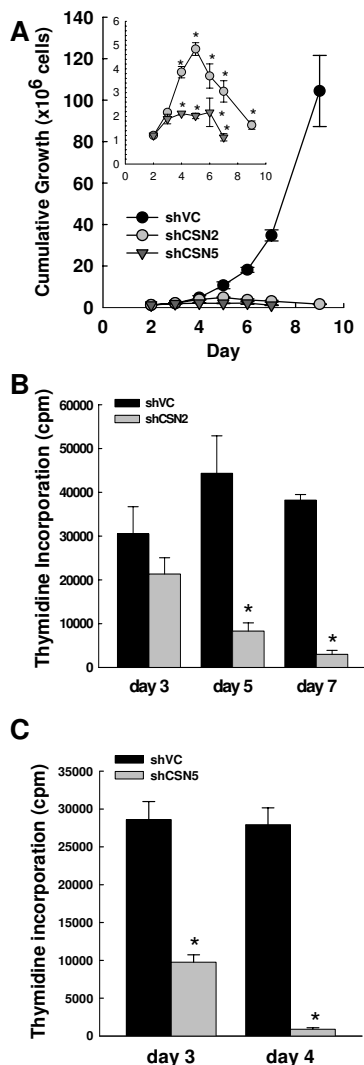


Figure 3
Both CSN2 and CSN5 knockdowns result in reduced cell growth. K562 cells were transiently co-transfected with HKK plasmid together with either shVC, shCSN2 or shCSN5 plasmid. HKK positive cells were sorted 24 hours post-transfection and cells re-cultured. (A) Cell counts were taken daily and the cumulative growth calculated. The cumulative growth of shCSN2 and shCSN5 cells is shown relative to shVC. The insert graph has a different Y scale to highlight the differences between shCSN2 and shCSN5 cumulative growth profiles. Data shown are the mean \pm s.e.m. of $n = 3$. * indicates a significant difference to shVC cell growth with a p value of less than 0.05. (B) Thymidine incorporation in shCSN2 cells relative to shVC cells was measured day 3, 5 and 7 post transfection. Data shown are the mean \pm s.e.m. of $n = 3$. (C) Thymidine incorporation in shCSN5 cells relative to shVC cells was measured day 3 and 4 post transfection. Data shown are the mean \pm s.e.m. of $n = 3$. * indicates significance with a p value of less than 0.05.

down [32]. It will be of great interest to determine the precise mechanism accounting for the divergent phenotypes encountered here, and is something which is currently under investigation.

Conclusion

In conclusion, we have shown that loss of either CSN2 or CSN5 in human K562 cells results in significant loss of viability but by very different mechanisms, potentially attributable to the formation of a CSN5 containing sub-complex in the absence of CSN2. Furthermore, we have provided data to suggest a possible function of the CSN complex in the transcriptional regulation of both its own components and CRL subunits. Finally, we have demonstrated here for the first time the sequential loss of F-box proteins in the absence of the CSN complex and have provided the first evidence of a link between the CSN complex and autophagy.

Methods

Cell culture and treatments

K562 cells were cultured in RPMI 1640 supplemented with 100 U/ml penicillin, 100 μ g/ml streptomycin and 10% v/v foetal bovine serum (Invitrogen, Gibco) and maintained at 37°C with 5% CO₂. For proteasome inhibition, cells were treated with 10 μ M MG132 for the final 18 hours of culturing. For autophagy inhibition, cells were treated in culture with either 10 mM 3-methyladenine from day 3-day 7 post transfection or 1 μ M bafilomycin A1 for 48 hours day 5-day 7 post transfection.

shRNA constructs

The shRNA vector used was a modified pcDNA3.1 vector (pcDNA3.1-H1) developed by Heiko Lickert [56] (kind gift from Heiner Schrewe) in which the CMV promoter has been replaced by the human RNase P RNA H1 promoter [56]. CSN2 and CSN5 silencing sequences were selected using a siRNA design tool available on http://www1.qiagen.com/products/genesilencing/custom_siRNA/siRNA_designer.aspx and cloned into the Asp718 and XbaI restriction enzyme sites of pcDNA3.1-H1. The target sequences are as follows:

CSN2 knockdown 5'AAGCGGCATTAAGCAGTTTCC3'

CSN5 knockdown – 5'AAGGGCTACAAACCTCCTGAT3'

shRNA scramble control – 5'AAGCGG GATTCAGTAGT TACG3'

Transfections and cell sorting

Transfection efficiencies in K562 cells vary between 20–50%. Therefore, to allow enrichment of transfected cells, 5×10^6 K562 cells were electroporated in Nucleofector kit V solution (Amaxa) using a Nucleofector I (Amaxa) and

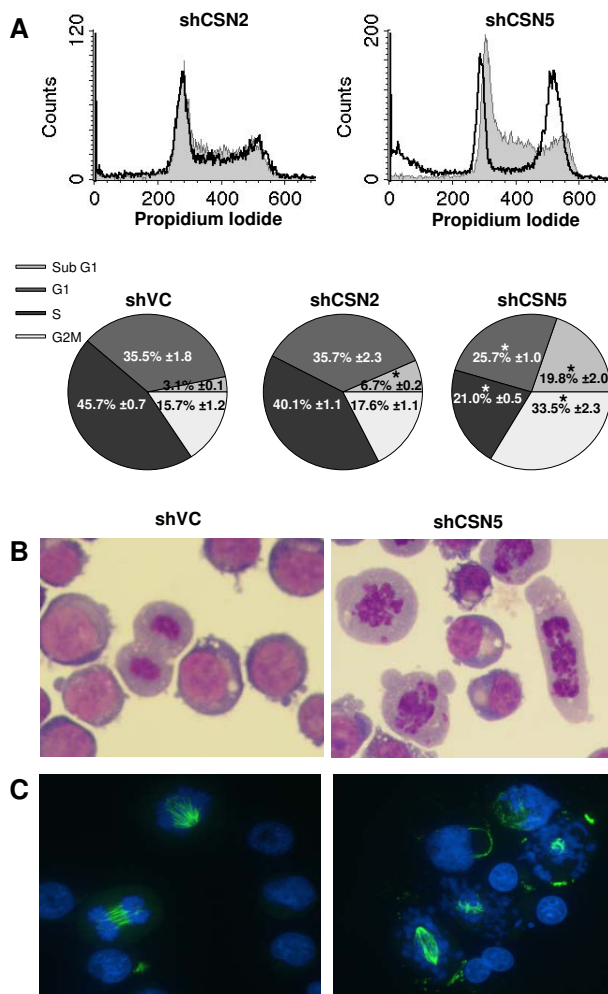


Figure 4
Cell cycle arrest in CSN5 knockdowns is associated with mitotic defects. K562 cells were transiently co-transfected with HKK plasmid together with shVC, shCSN2 or shCSN5 plasmid. HKK positive cells were sorted 24 hours post-transfection and cells re-cultured. (A) Representative images of shCSN2 (left, dark grey line) and shCSN5 (right, dark grey line) cell cycle profiles relative to shVC cells (light grey fill). Pie charts show data as the mean \pm s.e.m. of $n = 3$. * indicates significance with a p value of less than 0.05. (B) Cytopins of shVC and shCSN5 cells were stained by Jenner-Giemsa day 4 post transfection. (C) Cytopins were immunostained for tubulin (FITC) and Hoescht (blue) for visualisation of DNA in shVC and shCSN5 cells day 4 post transfection. All images shown are representative of $n = 3$ transfections.

file T16, with 5 μ g pMACS K^k.II and 10 μ g of the relevant knockdown pcDNA3.1-H1 plasmid according to manufacturer guidelines. The pMACS K^k.II produces a truncated murine MHC class I cell surface protein, H-2K^k, which lacks the cytoplasmic domain and is transiently expressed on the cell surface of transfected cells between 6 and 48

hours post-transfection. Transfected cells were sorted 24 hours post transfection using anti-H-2K^k antibody conjugated to magnetic beads, MACS MS columns and a MACS magnet (Miltenyi Biotec) according to manufacturer instructions. Post sorting, cells were set at 3×10^5 /ml daily and cells harvested for protein and mRNA analysis as indicated in results.

Thymidine incorporation assay

2×10^4 cells were pulsed with 2 μ Ci/ml ³H-thymidine (Amersham) for the final 18 hours of culture leading up to each time point. Samples were transferred to a filter mat (Wallac) using a Skatron cell harvester (Skatron Instruments) and read using a beta-plate scintillation counter (Skatron Instruments).

Immunofluorescence and Jenner-Giemsa staining

Cytopins were made with 5×10^4 cells in 80 μ l, using a Shandon cytopsin 3 (Shandon). For immunofluorescence staining, cytopins were fixed in 4% paraformaldehyde and stained using anti- β -tubulin antibody (Sigma, 1/500 dilution) followed by FITC labelled secondary antibody (Jackson Laboratories, 1/500 dilution). DNA was counterstained using Hoescht 33342 (Sigma, 1/1000 dilution). All reagents were diluted in PBS and slides mounted using Mowiol (6 g glycerol, 2.4 g Mowiol-4-88 (Sigma), 12 ml 0.2 M Tris HCl pH8.5, anti-fade crystal (Sigma), 6 ml distilled water). Slides were viewed using an Axioskop2 microscope (Zeiss) and images captured with a Q-imaging 12-bit QICAM (Media Cybernetics) and Openlab software (Improvision).

For Jenner-Giemsa staining, cytopins were air-dried, methanol fixed and stained; First with Jenner staining solution (VWR, UK) diluted 1/3 in 1 mM sodium phosphate buffer pH5.6 (5 mins) and second with Giemsa stain (VWR, UK) diluted 1/20 in 1 mM sodium phosphate buffer pH5.6 (10 mins). Slides were dried and then mounted onto coverslips using DePex (VWR, UK). Slides were viewed with an Olympus BX40 microscope (Olympus) and images captured using an Olympus Chameleon digital SLR (Olympus).

Staining of autophagosomes

For visualisation of autophagic vacuoles, 5×10^4 cells were incubated with 0.05 mM monodansylcadaverine (MDC, Sigma) in 0.5 ml PBS for 10 minutes at 37°C. Cells were washed four times with PBS, cytopins made as above and cells viewed immediately using a Leica DMIRE2 system.

Fluorescence flow cytometry

For Annexin V labelling, 1×10^5 cells were stained using Annexin V-FITC Apoptosis Detection Kit I (BD Biosciences) according to manufacturer instructions, and staining analysed within 1 hour by flow cytometry. For cell cycle analysis 1×10^5 cells were resuspended in cell

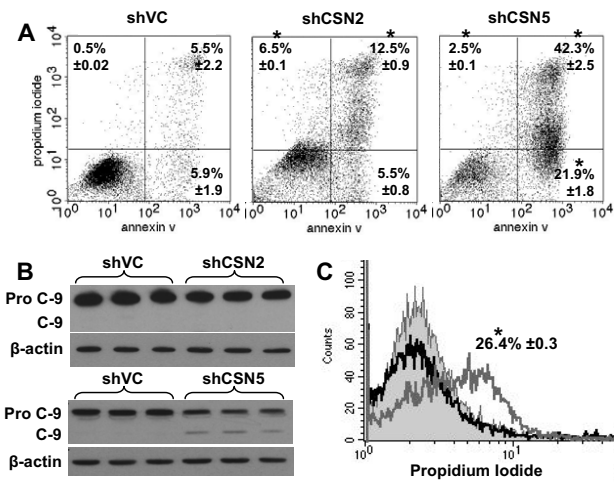


Figure 5
CSN5, but not CSN2, knockdown results in apoptotic cell death. K562 cells were transiently co-transfected with HKK plasmid together with either shVC, shCSN2 or shCSN5 plasmid. HKK positive cells were sorted 24 hours post-transfection and re-cultured. (A) Binding of Annexin V and uptake of propidium iodide were analysed by flow cytometry. The lower left quadrant encompasses the viable population of cells, the lower right quadrant contains early apoptotic cells, the upper right quadrant contains late apoptotic cells and the upper left quadrant contains the necrotic cell population. Dot plots shown are representative of n = 3 transfections. The mean of three data sets was taken and the values shown in the corresponding quadrant ± s.e.m. * indicates significance with a p value of less than 0.05. (B) Cells were harvested day 6 (shCSN2, top panels) or day 4 (shCSN5, bottom panels) post transfection and the level of caspase-9 cleavage determined by western blot. (C) Propidium iodide uptake was determined day 6 post transfection. The histogram shown is representative of n = 3 shVC (light grey in fill), shCSN2 (dark grey line) and shCSN5 (black line). The significant shift in propidium iodide staining in shCSN2 cells is shown ± s.e.m. * indicates significance with a p value of less than 0.05.

cycle buffer (10 µg/ml propidium iodide, 0.1 mM sodium chloride, 1% Triton X100) and samples analysed within 24 hours by flow cytometry. All staining was analysed using a FACS Calibur (Becton Dickinson) and the data evaluated using Cell Quest Pro software (Becton Dickinson).

Western blot analysis

Whole cell lysates were prepared using RIPA buffer (1% v/v NP40, 0.5% w/v sodium deoxycholate, 0.1% w/v 10% SDS, in distilled water) and protein quantified using the D_c protein assay according to manufacturer instructions (Bio-Rad). Forty micrograms of protein were boiled for 10 minutes in 1× SDS gel loading buffer (15.6 mM Tris HCl pH6.8, 6.25% v/v glycerol, 0.5% SDS, 1.25% v/v 2-mer-

captoethanol, Bromophenol Blue, in distilled water). Proteins were separated by SDS-PAGE and transferred to PVDF membrane (Millipore). For western blot analysis, the following antibodies were used at 1:1000 dilution: CSN2 (Bethyl), CSN5 (Bethyl), Cul-1 (Zymed), Skp2 (Zymed), p27 (Santa Cruz), caspase-9 (Cell Signalling), LC-3 (Novus Biologicals) and β-actin (Sigma). Proteins recognized by these antibodies were detected using anti-mouse (Sigma, 1/1000 dilution) or anti-rabbit (Pierce, 1/1000 dilution) HRP conjugated secondary antibody followed by enhanced chemiluminescence (SuperSignal West Pico Chemiluminescent Substrate, Pierce) and autoradiography (Kodak X-Omat LS film, Sigma). Quantitative analysis of western blots was carried out using ImageJ software <http://rsb.info.nih.gov/ij/download.html> and protein levels normalized by comparison to β-actin signals on the same membrane.

2-Dimensional gel analysis

Native protein extracts were obtained from 2.5 × 10⁵ cells by resuspending cells in 50 µl mild lysis buffer (25% 4× NativePAGE sample buffer (Invitrogen), 1% digitonin, 10% 10× protease inhibitor, in distilled water). Extracts were separated out in the first dimension using a NativePAGE Novex Bis-Tris Gel System (Invitrogen) according to manufacturer instructions. The gel was then cut into individual lanes, proteins denatured by incubation in 1× SDS gel loading buffer and resolved in the second dimension by electrophoresis through 12.5% SDS-polyacrylamide gels. Proteins were transferred to PVDF membrane (Millipore) and immunoblotting performed as above.

Quantitative real-time PCR analysis (QRT-PCR)

RNA was extracted using the Qiagen RNeasy kit according to manufacturer instructions and cDNA generated using 1 µg RNA, random hexamers (Promega) and Superscript II reverse transcriptase (Invitrogen). Quantitative real-time PCR was carried out using either TAQMAM or SYBR-Green based assays. For TAQMAM assays, QRT-PCR was carried out in duplicate 20 µl reactions containing 1× qPCR Mastermix Plus (Eurogentec), 20–40 ng cDNA, 18 pmoles each primer and 2.5 pmoles FAM/TAMRA dual labeled probes. For SYBR-Green assays, QRT-PCR was carried out in duplicate 25 µl reactions containing 1× Sensimix (Quantace), 20–40 ng cDNA, 9 pmoles each primer, 1× SYBR-Green solution (Quantace), 4 mM MgCl₂ and 0.5 units UNG (Quantace). QRT-PCR was carried out on an ABI Prism 7000 sequence detector (Applied Biosystems). The following primers (Sigma Genosys) and FAM/TAMRA labeled probes (Eurogentec) were used:

CSN2, 5'-CCTCATCCACTGATTATGGGAGT-3' (forward),
 5'-CATCATAATTCTTGAAGGCTTCAAAA-3' (reverse),

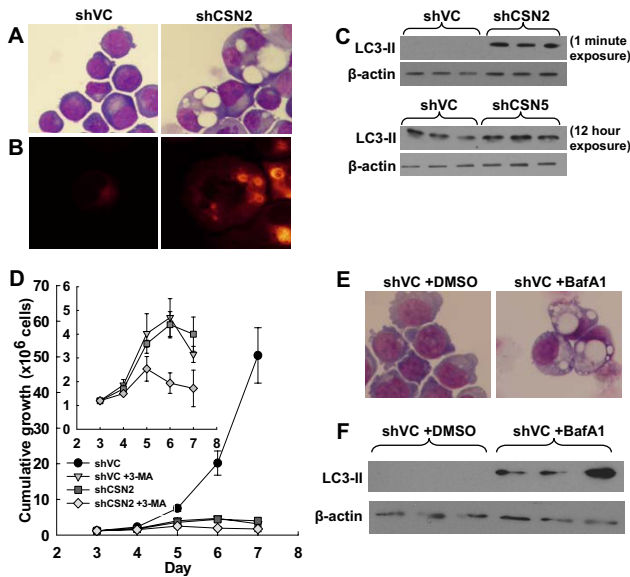


Figure 6
Cells lacking CSN2, but not CSN5, are associated with autophagy. K562 cells were transiently co-transfected with HKK plasmid together with either shVC, shCSN2 or shCSN5 plasmid. HKK positive cells were sorted 24 hours post-transfection and re-cultured. (A) Jenner-Giemsa staining of shVC and shCSN2 cytopins day 6 post transfection. (B) shVC and shCSN2 cells were stained with the autophagosome marker monodansylcadaverine day 6 post transfection. All images shown are representative of n = 3 transfections. (C) Cells were harvested day 6 (shCSN2, top panels) or day 4 (shCSN5, bottom panels) post transfection and the level of LC3-II protein determined by western blot. Even loading was determined by β -actin signal. (D) Cell counts were taken daily and the cumulative growth of shVC cells and shCSN2 cells +/- 3-MA calculated. The insert has had the untreated shVC data removed in order to demonstrate the similarity between the shVC +3-MA and shCSN2 cumulative growth profiles. Data shown is the mean of n = 3 \pm s.e.m. (E) Jenner-Giemsa staining of shVC +/- 1 μ M bafilomycin A1 cytopins day 7 post transfection. Images shown are representative of n = 3 transfections. (F) Cells were harvested day 7 post transfection and the level of LC3-II and β -actin protein determined by western blot.

5'-CCCTCAAGTGCATTTTACCACCACATTCTCT-3'
 (probe);

CSN5, 5'-ATATCCGCAGGAAAG-3' (forward),

5'-GGTCCITTCATCAGGAGTTTGT-3' (reverse),

5'-TGGCGCCTTTAGGACATACCCAAAGG-3' (probe);

Skp2, 5'-CGCTGCCACGATCATT-3' (forward),

5'-CCATGTGCTGTACACGAAAAGG-3' (reverse);

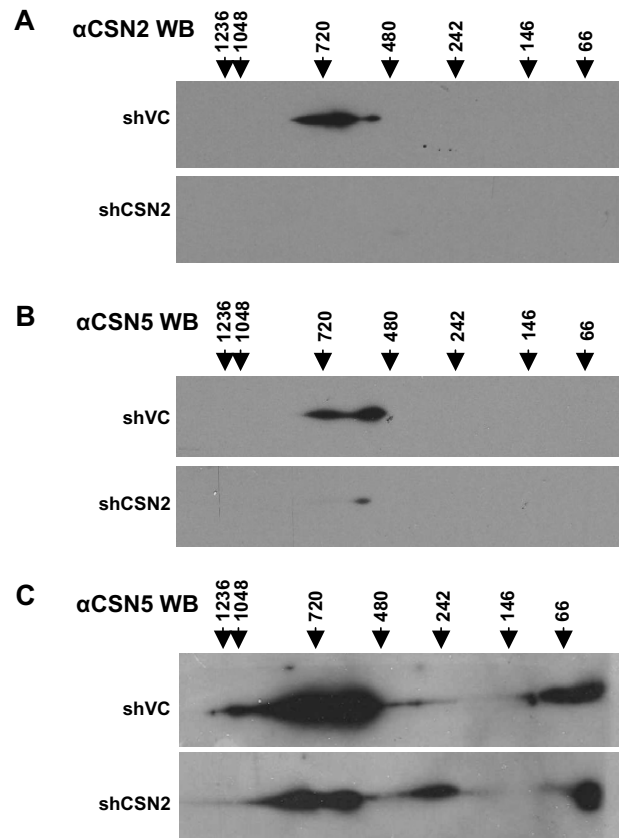


Figure 7
Loss of CSN2 results in the formation of CSN5 containing CSN subcomplexes. K562 cells were transiently co-transfected with HKK plasmid together with either shVC or shCSN2 plasmid. HKK positive cells were sorted 24 hours post-transfection, re-cultured and harvested day 3 post transfection. Both CSN2 (A) and CSN5 (B, short exposure; C, long exposure) distribution in shVC and shCSN2 cells was determined by 2-Dimensional Native-PAGE/SDS-PAGE and western blot analysis. All data shown is representative of n = 3 transfections.

Cdc4, 5'-ACGACGCCGAATTACATCTGT-3' (forward),

5'-ACTCCAGCTCTGAAACATTTTTAGC-3' (reverse);

β -Trcp, 5'-GAGGCATTGCCTGTTTGCA-3' (forward)

5'-TGTCCATAATCTGATAGTGTGCA-3' (reverse)

18S, 5'-GCCGCTAGAGGTGAAATTCTTG-3' (forward),

5'-CATTCTTGGCAAATGCCTTCG-3' (reverse).

Preoptimised primers and probes to 18S ribosomal RNA were used as internal standards in TAQMAN QRT-PCR (Applied Biosystems). Cycle threshold (Ct) values were

obtained graphically for test genes and 18S internal standards. Δ Ct values were calculated by subtracting 18S Ct from test gene Ct, and average Δ Ct values obtained from duplicates. Relative mRNA levels were determined by subtraction of mock transfection Δ Ct values from shVC/shCSN2/shCSN5 Δ Ct values to give a $\Delta\Delta$ Ct value and conversion through $2^{-\Delta\Delta\text{Ct}}$.

Authors' contributions

CP conceived of and designed the study, carried out all laboratory experimentation except for that carried out by REH and FLK, and drafted the manuscript. REH harvested thymidine plates, generated the propidium iodide flow cytometry data and assisted in the analysis of all flow cytometry data. CMB and FLK conceived of and designed the study and drafted the manuscript. FLK designed the shRNA sequence and generated the plasmid for CSN2 knockdown. All authors read and approved the manuscript.

Additional material

Additional file 1

Vector control scramble sequence has no effect on protein levels, mRNA expression or cell growth, whilst CSN5 knockdown resulted in the sequential loss of F-box proteins. K562 cells were transiently co-transfected with HKK plasmid together with either empty vector or vector control scramble plasmid. HKK positive cells were sorted 24 hours post-transfection, re-cultured and harvested day 9 post transfection. (A) The levels of CSN2, CSN5, Cull1, Skp2, p27, LC3-II and caspase-9 protein was determined by western blot. (B) CSN2 and CSN5 mRNA levels in vector control scramble cells relative to empty vector transfected cells were determined by QRT-PCR. Data is the mean of $n = 3$ transfections \pm s.e.m. The dashed line indicates mRNA expression in empty vector transfected cells. (C) Cell counts were taken daily and the cumulative growth calculated. The cumulative growth of shVC scramble cells is shown relative to empty vector transfected cells. Data shown are the mean \pm s.e.m. of $n = 3$. (D) shVC and shCSN5 cells were harvested day 4 post transfection and the level of Skp-2, Cdc4, β -TrCP and β -actin protein determined by western blot.

Click here for file

[<http://www.biomedcentral.com/content/supplementary/1471-2121-10-31-S1.pdf>]

Acknowledgements

We would like to acknowledge Heiner Schrewe (MPI, Berlin), Debbie Cunningham (Univ of Birmingham, UK) and Simon Johnston (Univ of Birmingham, UK) for technical assistance. CP is funded by a grant from the BBSRC (UK) and REH and FLK are funded by a Leukaemia Research (UK) grant.

References

- Wei N, Deng XW: **Characterization and purification of the mammalian COP9 complex, a conserved nuclear regulator initially identified as a repressor of photomorphogenesis in higher plants.** *Photochemistry and photobiology* 1998, **68(2)**:237-241.
- Mundt KE, Porte J, Murray JM, Brikos C, Christensen PU, Caspari T, Hagan IM, Millar JB, Simanis V, Hofmann K, et al.: **The COP9/signosome complex is conserved in fission yeast and has a role in S phase.** *Curr Biol* 1999, **9(23)**:1427-1430.
- Doronkin S, Djagaeva I, Beckendorf SK: **The COP9 signalosome promotes degradation of Cyclin E during early Drosophila oogenesis.** *Developmental cell* 2003, **4(5)**:699-710.
- Pintard L, Kurz T, Glaser S, Willis JH, Peter M, Bowerman B: **Neddylation and deneddylation of CUL-3 is required to target MEI-1/Katanin for degradation at the meiosis-to-mitosis transition in C. elegans.** *Curr Biol* 2003, **13(11)**:911-921.
- Rosel D, Kimmel AR: **The COP9 signalosome regulates cell proliferation of Dictyostelium discoideum.** *European journal of cell biology* 2006, **85(9-10)**:1023-1034.
- Chamovitz DA, Wei N, Osterlund MT, von Arnim AG, Staub JM, Matsui M, Deng XW: **The COP9 complex, a novel multisubunit nuclear regulator involved in light control of a plant developmental switch.** *Cell* 1996, **86(1)**:115-121.
- Cope GA, Deshaies RJ: **COP9 signalosome: a multifunctional regulator of SCF and other cullin-based ubiquitin ligases.** *Cell* 2003, **114(6)**:663-671.
- Nielsen O: **COP9 signalosome: a provider of DNA building blocks.** *Curr Biol* 2003, **13(14)**:R565-567.
- Groisman R, Polanowska J, Kuraoka I, Sawada J, Saijo M, Drapkin R, Kisselev AF, Tanaka K, Nakatani Y: **The ubiquitin ligase activity in the DDB2 and CSA complexes is differentially regulated by the COP9 signalosome in response to DNA damage.** *Cell* 2003, **113(3)**:357-367.
- Hough R, Pratt G, Rechsteiner M: **Ubiquitin-lysozyme conjugates. Identification and characterization of an ATP-dependent protease from rabbit reticulocyte lysates.** *The Journal of biological chemistry* 1986, **261(5)**:2400-2408.
- Peters JM: **Proteasomes: protein degradation machines of the cell.** *Trends in biochemical sciences* 1994, **19(9)**:377-382.
- Rubin DM, Finley D: **Proteolysis. The proteasome: a protein-degrading organelle?** *Curr Biol* 1995, **5(8)**:854-858.
- Voges D, Zwickl P, Baumeister W: **The 26S proteasome: a molecular machine designed for controlled proteolysis.** *Annual review of biochemistry* 1999, **68**:1015-1068.
- Chau V, Tobias JW, Bachmair A, Marriott D, Ecker DJ, Gonda DK, Varshavsky A: **A multiubiquitin chain is confined to specific lysine in a targeted short-lived protein.** *Science* 1989, **243(4898)**:1576-1583.
- Hershko A, Heller H, Elias S, Ciechanover A: **Components of ubiquitin-protein ligase system. Resolution, affinity purification, and role in protein breakdown.** *The Journal of biological chemistry* 1983, **258(13)**:8206-8214.
- Petroski MD, Deshaies RJ: **Function and regulation of cullin-RING ubiquitin ligases.** *Nature reviews* 2005, **6(1)**:9-20.
- Bai C, Sen P, Hofmann K, Ma L, Goebel M, Harper JW, Elledge SJ: **SKP1 connects cell cycle regulators to the ubiquitin proteolysis machinery through a novel motif, the F-box.** *Cell* 1996, **86(2)**:263-274.
- Skowyra D, Craig KL, Tyers M, Elledge SJ, Harper JW: **F-box proteins are receptors that recruit phosphorylated substrates to the SCF ubiquitin-ligase complex.** *Cell* 1997, **91(2)**:209-219.
- Ho MS, Tsai PI, Chien CT: **F-box proteins: the key to protein degradation.** *Journal of biomedical science* 2006, **13(2)**:181-191.
- Bosu DR, Kipreos ET: **Cullin-RING ubiquitin ligases: global regulation and activation cycles.** *Cell division* 2008, **3**:7.
- Hori T, Osaka F, Chiba T, Miyamoto C, Okabayashi K, Shimbara N, Kato S, Tanaka K: **Covalent modification of all members of human cullin family proteins by NEDD8.** *Oncogene* 1999, **18(48)**:6829-6834.
- Ohh M, Kim WY, Moslehi JJ, Chen Y, Chau V, Read MA, Kaelin WG Jr: **An intact NEDD8 pathway is required for Cullin-dependent ubiquitylation in mammalian cells.** *EMBO reports* 2002, **3(2)**:177-182.
- Kawakami T, Chiba T, Suzuki T, Iwai K, Yamanaka K, Minato N, Suzuki H, Shimbara N, Hidaka Y, Osaka F, et al.: **NEDD8 recruits E2-ubiquitin to SCF E3 ligase.** *The EMBO journal* 2001, **20(15)**:4003-4012.
- Sakata E, Yamaguchi Y, Miyauchi Y, Iwai K, Chiba T, Saeki Y, Matsuda N, Tanaka K, Kato K: **Direct interactions between NEDD8 and ubiquitin E2 conjugating enzymes upregulate cullin-based E3 ligase activity.** *Nature structural & molecular biology* 2007, **14(2)**:167-168.
- Lyapina S, Cope G, Shevchenko A, Serino G, Tsuge T, Zhou C, Wolf DA, Wei N, Shevchenko A, Deshaies RJ: **Promotion of NEDD-**

- CUL1 conjugate cleavage by COP9 signalosome.** *Science* 2001, **292(5520)**:1382-1385.
26. Cope GA, Suh GS, Aravind L, Schwarz SE, Zipursky SL, Koonin EV, Deshaies RJ: **Role of predicted metalloprotease motif of Jab1/Csn5 in cleavage of Nedd8 from Cull1.** *Science* 2002, **298(5593)**:608-611.
 27. Wu JT, Chan YR, Chien CT: **Protection of cullin-RING E3 ligases by CSN-UBP12.** *Trends in cell biology* 2006, **16(7)**:362-369.
 28. Cope GA, Deshaies RJ: **Targeted silencing of Jab1/Csn5 in human cells downregulates SCF activity through reduction of F-box protein levels.** *BMC biochemistry* 2006, **7**:1.
 29. Wee S, Geyer RK, Toda T, Wolf DA: **CSN facilitates Cullin-RING ubiquitin ligase function by counteracting autocatalytic adapter instability.** *Nature cell biology* 2005, **7(4)**:387-391.
 30. Peng H, Du ZW, Zhang JW: **Identification and characterization of a novel zinc finger protein (HZF1) gene and its function in erythroid and megakaryocytic differentiation of K562 cells.** *Leukemia* 2006, **20(6)**:1109-1116.
 31. Jacquelin A, Herrant M, Defamie V, Belhacene N, Colosetti P, Marchetti S, Legros L, Deckert M, Mari B, Cassuto JP, et al.: **A survey of the signaling pathways involved in megakaryocytic differentiation of the human K562 leukemia cell line by molecular and c-DNA array analysis.** *Oncogene* 2006, **25(5)**:781-794.
 32. Su H, Huang W, Wang X: **The COP9 signalosome negatively regulates proteasome proteolytic function and is essential to transcription.** *The international journal of biochemistry & cell biology* 2009, **41(3)**:615-624.
 33. Denti S, Fernandez-Sanchez ME, Rogge L, Bianchi E: **The COP9 signalosome regulates Skp2 levels and proliferation of human cells.** *The journal of biological chemistry* 2006, **281(43)**:32188-32196.
 34. Tsvetkov LM, Yeh KH, Lee SJ, Sun H, Zhang H: **p27(Kip1) ubiquitination and degradation is regulated by the SCF(Skp2) complex through phosphorylated Thr187 in p27.** *Curr Biol* 1999, **9(12)**:661-664.
 35. Biederbick A, Kern HF, Elsasser HP: **Monodansylcadaverine (MDC) is a specific in vivo marker for autophagic vacuoles.** *European journal of cell biology* 1995, **66(1)**:3-14.
 36. Kabeya Y, Mizushima N, Ueno T, Yamamoto A, Kirisako T, Noda T, Kominami E, Ohsumi Y, Yoshimori T: **LC3, a mammalian homologue of yeast Apg8p, is localized in autophagosome membranes after processing.** *The EMBO journal* 2000, **19(21)**:5720-5728.
 37. Mizushima N, Yoshimori T: **How to interpret LC3 immunoblotting.** *Autophagy* 2007, **3(6)**:542-545.
 38. Schwechheimer C: **The COP9 signalosome (CSN): an evolutionary conserved proteolysis regulator in eukaryotic development.** *Biochimica et biophysica acta* 2004, **1695(1-3)**:45-54.
 39. Oren-Giladi P, Krieger O, Edgar BA, Chamovitz DA, Segal D: **Cop9 signalosome subunit 8 (CSN8) is essential for Drosophila development.** *Genes Cells* 2008, **13(3)**:221-231.
 40. Peth A, Berndt C, Henke W, Dubiel W: **Downregulation of COP9 signalosome subunits differentially affects the CSN complex and target protein stability.** *BMC biochemistry* 2007, **8**:27.
 41. Bech-Otschir D, Seeger M, Dubiel W: **The COP9 signalosome: at the interface between signal transduction and ubiquitin-dependent proteolysis.** *Journal of cell science* 2002, **115(Pt 3)**:467-473.
 42. Ullah Z, Buckley MS, Arnosti DN, Henry RW: **Retinoblastoma protein regulation by the COP9 signalosome.** *Molecular biology of the cell* 2007, **18(4)**:1179-1186.
 43. Fukumoto A, Tomoda K, Yoneda-Kato N, Nakajima Y, Kato JY: **Depletion of Jab1 inhibits proliferation of pancreatic cancer cell lines.** *FEBS letters* 2006, **580(25)**:5836-5844.
 44. Panattoni M, Sanvito F, Basso V, Dogliani C, Casorati G, Montini E, Bender JR, Mondino A, Pardi R: **Targeted inactivation of the COP9 signalosome impairs multiple stages of T cell development.** *The journal of experimental medicine* 2008, **205(2)**:465-477.
 45. Dohmann EM, Levesque MP, De Veylder L, Reichardt I, Jurgens G, Schmid M, Schwechheimer C: **The Arabidopsis COP9 signalosome is essential for G2 phase progression and genomic stability.** *Development (Cambridge, England)* 2008, **135(11)**:2013-2022.
 46. Peth A, Boettcher JP, Dubiel W: **Ubiquitin-dependent proteolysis of the microtubule end-binding protein 1, EB1, is controlled by the COP9 signalosome: possible consequences for microtubule filament stability.** *Journal of molecular biology* 2007, **368(2)**:550-563.
 47. Sun L, Gao J, Dong X, Liu M, Li D, Shi X, Dong JT, Lu X, Liu C, Zhou J: **EB1 promotes Aurora-B kinase activity through blocking its inactivation by protein phosphatase 2A.** *Proceedings of the National Academy of Sciences of the United States of America* 2008, **105(20)**:7153-7158.
 48. Sumara I, Quadroni M, Frei C, Olma MH, Sumara G, Ricci R, Peter M: **A Cul3-based E3 ligase removes Aurora B from mitotic chromosomes, regulating mitotic progression and completion of cytokinesis in human cells.** *Developmental cell* 2007, **12(6)**:887-900.
 49. Chamovitz DA, Segal D: **JAB1/CSN5 and the COP9 signalosome. A complex situation.** *EMBO reports* 2001, **2(2)**:96-101.
 50. Claret FX, Hibi M, Dhut S, Toda T, Karin M: **A new group of conserved coactivators that increase the specificity of AP-1 transcription factors.** *Nature* 1996, **383(6599)**:453-457.
 51. Lee JW, Choi HS, Gyuris J, Brent R, Moore DD: **Two classes of proteins dependent on either the presence or absence of thyroid hormone for interaction with the thyroid hormone receptor.** *Molecular endocrinology (Baltimore, Md)* 1995, **9(2)**:243-254.
 52. Papaioannou M, Melle C, Baniahmad A: **The coregulator Alien.** *Nuclear receptor signaling* 2007, **5**:e008.
 53. Tanguy G, Drevillon L, Arous N, Hasnain A, Hinzpeter A, Fritsch J, Goossens M, Fanen P: **CSN5 binds to misfolded CFTR and promotes its degradation.** *Biochimica et biophysica acta* 2008, **1783(6)**:1189-1199.
 54. Wei N, Serino G, Deng XW: **The COP9 signalosome: more than a protease.** *Trends in biochemical sciences* 2008, **33(12)**:592-600.
 55. Tomoda K, Kato JY, Tatsumi E, Takahashi T, Matsuo Y, Yoneda-Kato N: **The Jab1/COP9 signalosome subcomplex is a downstream mediator of Bcr-Abl kinase activity and facilitates cell-cycle progression.** *Blood* 2005, **105(2)**:775-783.
 56. Kunath T, Gish G, Lickert H, Jones N, Pawson T, Rossant J: **Transgenic RNA interference in ES cell-derived embryos recapitulates a genetic null phenotype.** *Nature biotechnology* 2003, **21(5)**:559-561.

Publish with **BioMed Central** and every scientist can read your work free of charge

"BioMed Central will be the most significant development for disseminating the results of biomedical research in our lifetime."

Sir Paul Nurse, Cancer Research UK

Your research papers will be:

- available free of charge to the entire biomedical community
- peer reviewed and published immediately upon acceptance
- cited in PubMed and archived on PubMed Central
- yours — you keep the copyright

Submit your manuscript here:
http://www.biomedcentral.com/info/publishing_adv.asp

